

ROLE OF miRNAs IN MULTIPLE SCLEROSIS: STUDY OF miRNAs IN CEREBROSPINAL FLUID FOR DIFFERENT CLINICAL CONDITIONS

María Muñoz San Martín

Per citar o enllaçar aquest document:

Para citar o enlazar este documento:

Use this url to cite or link to this publication:

<http://hdl.handle.net/10803/672871>

ADVERTIMENT. L'accés als continguts d'aquesta tesi doctoral i la seva utilització ha de respectar els drets de la persona autora. Pot ser utilitzada per a consulta o estudi personal, així com en activitats o materials d'investigació i docència en els termes establerts a l'art. 32 del Text Refós de la Llei de Propietat Intel·lectual (RDL 1/1996). Per altres utilitzacions es requereix l'autorització prèvia i expressa de la persona autora. En qualsevol cas, en la utilització dels seus continguts caldrà indicar de forma clara el nom i cognoms de la persona autora i el títol de la tesi doctoral. No s'autoritza la seva reproducció o altres formes d'explotació efectuades amb finalitats de lucre ni la seva comunicació pública des d'un lloc aliè al servei TDX. Tampoc s'autoritza la presentació del seu contingut en una finestra o marc aliè a TDX (framing). Aquesta reserva de drets afecta tant als continguts de la tesi com als seus resums i índexs.

ADVERTENCIA. El acceso a los contenidos de esta tesis doctoral y su utilización debe respetar los derechos de la persona autora. Puede ser utilizada para consulta o estudio personal, así como en actividades o materiales de investigación y docencia en los términos establecidos en el art. 32 del Texto Refundido de la Ley de Propiedad Intelectual (RDL 1/1996). Para otros usos se requiere la autorización previa y expresa de la persona autora. En cualquier caso, en la utilización de sus contenidos se deberá indicar de forma clara el nombre y apellidos de la persona autora y el título de la tesis doctoral. No se autoriza su reproducción u otras formas de explotación efectuadas con fines lucrativos ni su comunicación pública desde un sitio ajeno al servicio TDR. Tampoco se autoriza la presentación de su contenido en una ventana o marco ajeno a TDR (framing). Esta reserva de derechos afecta tanto al contenido de la tesis como a sus resúmenes e índices.

WARNING. Access to the contents of this doctoral thesis and its use must respect the rights of the author. It can be used for reference or private study, as well as research and learning activities or materials in the terms established by the 32nd article of the Spanish Consolidated Copyright Act (RDL 1/1996). Express and previous authorization of the author is required for any other uses. In any case, when using its content, full name of the author and title of the thesis must be clearly indicated. Reproduction or other forms of for profit use or public communication from outside TDX service is not allowed. Presentation of its content in a window or frame external to TDX (framing) is not authorized either. These rights affect both the content of the thesis and its abstracts and indexes.



DOCTORAL THESIS

Role of miRNAs in multiple sclerosis:

**Study of miRNAs in cerebrospinal fluid for different
clinical conditions**

María Muñoz San Martín

2021



DOCTORAL THESIS

Role of miRNAs in multiple sclerosis:

**Study of miRNAs in cerebrospinal fluid for different
clinical conditions**

María Muñoz San Martín

2021

**Doctoral Programme in Molecular Biology,
Biomedicine and Health**

Supervised by:

Ester Quintana Camps, Ph. D

Lluís Ramió i Torrentà, Ph. D, M.D.

Tutor:

Elisabet Kádár García, Ph. D

Presented to obtain the degree of PhD at the University of
Girona

Ph.D candidate:

María Muñoz San Martín

Supervisors:

Ester Quintana Camps, Ph. D

Lluís Ramió i Torrentà, Ph. D, M.D.

Tutor:

Elisabet Kádár García, Ph. D



Dr **Lluís Ramió i Torrentà**, head of *Neurology Department at Dr. Josep Trueta University Hospital and Santa Caterina Hospital*; group leader of the *Girona Neuroimmunology and Multiple Sclerosis Unit (UNIEMTG)*; principal investigator of the *Neurodegeneration and Neuroinflammation Research Group at the Biomedical Research Institute of Girona (IDIBGI)*; and full Professor at *Medical Sciences Department at University of Girona*

Dr **Ester Quintana Camps**, postdoctoral researcher of the *Neurodegeneration and Neuroinflammation Research Group at the Biomedical Research Institute of Girona (IDIBGI)*; and Professor at *Medical Sciences Department at University of Girona*

WE DECLARE:

That the thesis entitled "**ROLE OF *miRNAs* IN MULTIPLE SCLEROSIS: STUDY OF *miRNAs* IN CEREBROSPINAL FLUID FOR DIFFERENT CLINICAL CONDITIONS**", presented by María Muñoz San Martín to obtain the doctoral degree in *Molecular Biology, Biomedicine and Health* by the UdG, has been completed under our supervision and fulfils all the requirements to qualify for an International Doctorate.

For all intents and purposes, we hereby sign this document.

Dr Lluís Ramió i Torrentà

Dr Ester Quintana Camps

Girona, 2021

La imaginación es la mitad de la enfermedad;

la tranquilidad es la mitad del remedio;

y la paciencia es el comienzo de la cura.

- Ibn Sina

No hay un solo tema científico

que no pueda ser explicado

a nivel popular.

- Carl Sagan

ACKNOWLEDGEMENTS

Hoy es 31 de diciembre de 2020, el último día de un año tan aciago y complicado para todos, el último día de un año que nos ha enseñado que el esfuerzo colectivo es la mejor manera de solventar cualquier obstáculo. Por eso, creo que hoy es el día más indicado para dar gracias a todas aquellas personas que me han acompañado durante el desarrollo de esta tesis doctoral. Podría definir estos últimos años como un periodo de evolución, ya que creo que la María que comenzó en junio de 2016 no es la misma que escribe estas palabras. A nivel profesional, esta oportunidad ha sido altamente gratificante y enriquecedora. A nivel personal, ha sido exigente y un desafío en ciertos momentos puntuales; pero el hecho de caminar acompañada te da el empuje necesario para continuar.

Por ello, y porque me gustan los espóileres, voy a comenzar por el final; dando las gracias a los pilares de mi día a día. No hay nada que me honre más que reconocer en mi fragmentos de cada uno de los miembros de mi familia. Por eso, esta tesis es de ellos, porque sin el trabajo duro, constancia y esfuerzo que han empleado a lo largo de sus vidas, yo no habría sabido luchar y esforzarme hasta el final. A mis padres, la base de todo lo que soy. A mi hermano, un modelo al que siempre intento emular pero siempre me quedo corta porque es excepcional. A mis abuelos, por acompañarme los cuatro juntos desde la infancia, haber trabajado duro por nosotros y ser el claro ejemplo del sacrificio que hay que hacer, a veces alejándonos de nuestro hogar, para prosperar. A mi tía Pitu, mi segunda madre. A mi tía Chari, que me inculcó interés por la rama sanitaria pero que, debido a mi miedo a las agujas, pude satisfacer en parte dedicándome a la investigación. A mis tíos Paco y Fernando, mis tías María Luisa y Elena y mis primos. Por supuesto, no me voy a olvidar de nuestra Trufi, miembro de pleno derecho de la familia, luchadora y cabezota como la que más. Aunque tenga que moverme e ir migrando de un sitio a otra para continuar con la aventura, todos vosotros sois mi hogar.

Carlos, tú llegaste a mitad de camino, cuando todo se empezaba a poner cuesta arriba y se iba volviendo más y más pindio. Mientras escribo esto estás entrenando, y ahora entiendo que necesitas mucha fuerza para haber aguantado mis crisis existenciales estos años y, sobre todo, estos últimos meses. No puedo prometer que a partir de ahora vaya a estar más relajada, pero voy a intentarlo. Gracias por aguantarme, hacerme llorar de la risa, ayudarme y no rendirme conmigo.

Ester, aunque tú no te acuerdes, el viernes 12 de febrero de 2016 me mandaste un email diciendo que tenías una noticia bomba porque una chica había renunciado y la beca pasaba a mi. Nos habíamos escrito un montón de emails y no nos habíamos visto ni por videollamada. Sin embargo, la buena impresión que me habías transmitido se magnificó cuando por fin nos conocimos. Voy a estar eternamente agradecida contigo por todo lo que me has enseñado, tanto a nivel profesional como personal. Has dejado el pabellón muy alto para mis futuros jefes. Gracias por haber contado conmigo, por haber escuchado y valorado mis opiniones y por haber creado este ambiente de trabajo que tanto voy a echar de menos. Espero haber absorbido lo máximo posible de todas tus cualidades y poder emplearlas para ser mejor profesional y persona.

Lluís, gràcies per haver confiat en mi i donar-me l'oportunitat de treballar al costat de l'Ester. Em sento molt afortunada de haver començat la meva carrera amb vosaltres i espero que els nostres camins es creuin de nou en un futur. Tens un equip increïble, m'he sentit com a casa des del primer dia. Moltes gràcies!

Imma, voy a echar mucho de menos desayunar, trabajar codo con codo y conocer nuevos lugares contigo. Eres la mejor compi de congresos que existe ¡Muchas gracias por estar siempre ahí! Ahora toca agradecer al resto de la UNIMTG. Miky y Marina, muchas gracias por intentar quitarme el miedo a las agujas, no sé a quién recurriré a partir de ahora para nuestras “operaciones quirúrgicas estéticas”; pero sobre todo, gracias por tener una sonrisa siempre preparada. Pepi y Cris, gracias por hacerme sentir una más desde el primer momento. Héctor, muchas gracias por tu ayuda y por estar siempre ahí cuando lo necesito. Judit, Claudia, gracias por los buenos ratos y por acompañarme en las crisis con los deadlines de los congresos. René, gracias por tus explicaciones y tu gran interés investigador. Gary, Jordi, Txell, Anna, Laura, Olga; muchas gracias a todos por acompañarme en este viaje. No voy a olvidarme de Júlia, que me acompañó durante mis primeros meses y se ilusionó conmigo con los miRNAs de EBV. Gracias, también, a los pacientes de la unidad por colaborar e interesarse por la investigación. Esta tesis es vuestra, ya que, sin la organización y la gestión de la Unidad, el diagnóstico, la donación y procesamiento de las muestras, esta hubiese sido imposible de desarrollar.

Moving to Ireland was a really enriching and exciting opportunity. I am really grateful to Dr Eva Jiménez Mateos and Dr Claire McCoy for hosting me in their laboratories during those three months. Your advice and experience have highly benefited my thesis and your figures have inspired my future aspirations. Claire, I would also like to thank you for your trust and your effort. You have a really great

team that welcomed me incredibly from the first day. Conor, thank you for teaching me such incredible things. Remsha, Chiara, Jen and Frances, thanks for being so kind and friendly.

Lo mejor que me llevo de Girona son los amigos tan maravillosos que he hecho y que sé que perdurarán a pesar de la distancia. Rocío, mi negri, gracias por estar siempre ahí. Aunque ya no pueda escribirte cada día por el chat el “buenos días amoor amoor amoor, ocho de la mañana”; siempre voy a estar para lo que necesites, incluyendo tarros de bonito y cotilleos. Gracias por ayudarme, acogerme y cuidarme (darme brócoli, entre otras cosas). Aini y Jess, mis fuafis, cuantos momentos hemos vivido juntas, sobre todo y los mejores, fuera del trabajo. Aunque ya no os vea cada día en el IdIBGi como venía ocurriendo desde hace años ya, seguís estando en mi día a día, escuchando, aconsejando y apoyando. Una de las primeras cosas que haré cuando la situación se normalice será coger un avión para poder celebrar con vosotras y unas cervezas y abrazaros con total tranquilidad. Marini, nunca pierdas esa sonrisa eterna e inspiradora. Gracias por alegrarme los momentos de trabajo, dejarme notitas y ser tan cariñosa.

Por el camino, he convivido con un montón de compañeros con lo que he compartido multitud de momentos inolvidables tanto dentro como fuera del IdIBGi. Ferri, Berta, Ari, Adri, Nuria, Anna; gracias por haber creado un ambiente increíble que voy a echar tanto de menos. Liss, Moni, Èric, Laia (compi de aniversario y series); gracias por acompañarme también. Bet, Carme, Sílvia, Sara, Marc, Paco; muchas gracias por vuestros consejos y experiencia. Esther, gracias por ser un ejemplo de fuerza, lucha y determinación. Gracias también al personal de IdIBGi que tanto me ha ayudado y apoyado, Maria Buxó, Nuria Chico, Josep Pairoli, Ferrán Pedro.

Y como no todo es el trabajo, muchas gracias a los que me han hecho desconectar. Albert, gracias por ser un compi de piso comprensivo, un compañero de cerves y, sobre todo, un amigo. Gracias a los qualiteros de Barcelona, por ofrecerme los mejores planes de fin de semana. A mis amigos de Santander, Manu, Cris, Fer, Lara, Mery, Ali, Vicky, Laurita, Marina, Olguis; sois los culpables de la morriña que siempre siento. Por último, Anita, Jone, Ali y Amy, gracias por estar siempre que os necesito.

Eva y Luzma, gracias por haber participado y haberme ayudado a mejorar y hacer más bonita esta tesis.

Pensaba que escribir los agradecimientos iba a ser bastante más fácil y no estoy del todo contenta con haber conseguido plasmar todo lo agradecida que estoy. ¡Muchísimas gracias a todos! ¡Esta tesis es vuestra!

LIST OF ORIGINAL PUBLICATIONS

1. Muñoz-San Martín M, Reverter G, Robles-Cedeño R, Buxó M, Ortega FJ, Gómez I, Tomàs-Roig J, Celarain N, Villar LM, Perkal H, Fernández-Real JM, Quintana E, Ramió-Torrentà L. **Analysis of miRNA signatures in CSF identifies upregulation of miR-21 and miR-146a/b in patients with multiple sclerosis and active lesions.** *J Neuroinflammation*. 2019;16(1):220. doi: 10.1186/s12974-019-1590-5.
2. Muñoz-San Martín M, Torras S, Robles-Cedeño R, Buxó M, Gómez I, Matute-Blanch C, Comabella M, Villar LM, Perkal H, Quintana H, Ramió-Torrentà L. **Radiologically isolated syndrome: targeting miRNAs as prognostic biomarkers.** *Epigenomics*. 2020;12(23):2065. doi: 10.2271/epi-2020-0172.

Articles attached in Annex II.

ABBREVIATIONS

25<RRMS<35	RRMS individuals whose age at onset was between 25 and 35 years old
AGO	Argonaute
AUC	Area under curve
BBB	Blood brain barrier
BCSFB	Blood-CSF barrier
C1	Cohort 1
C2	Cohort 2
cc-OA	Custom-configured TaqMan OpenArray Human Advanced microRNA plate
CDMS	Clinically definite multiple sclerosis
cDNA	Complementary DNA
circRNA	Circular RNA
CIS	Clinically isolated syndrome
CHI3L1	Chitinase-3-like protein 1
CMV	Cytomegalovirus
CNS	Central nervous system
Cq	PCR cycle number at which fluorescence level reaches the specified threshold in qPCR
CSF	Cerebrospinal fluid
CV	Coefficient of Variation score
DGCR8	DiGeorge syndrome critical region 8
DMTs	Disease-modifying therapies
DNA	Deoxyribonucleic acid
dR	de Ronde method for handling missing data
dsRNA	Double-stranded RNA
EAE	Experimental autoimmune encephalomyelitis
EBNA1	EBV nuclear antigen-1
EBV	Epstein-Barr virus
EDSS	Expanded Disability Status Scale
EGFR	Epidermal growth factor receptor
EN	Endogenous normalizers
EU	European Union
fc-OA	Fixed-content TaqMan OpenArray Human Advanced microRNA plate
Gd	Gadolinium
Gd+	Gd-enhancing lesions
Gd-	Absence of Gd-enhancing lesions
GDERD	Gross domestic expenditure on research and development

GM	Gray matter
GN	Global normalization
GN_All	GN using all available miRNA data
GN_70%	GN using analyzable miRNA data
GO	Gene ontology
HLA	Human leukocyte antigen
ICC	Intraclass correlation coefficient
IEF	Isoelectric focusing
IFN	Interferon- β
IgG	Immunoglobulin G
IgM	Immunoglobulin M
IRAK-1	Interleukin receptor-associated kinase 1
JCV	John Cunningham virus
lncRNA	Long ncRNA
LPC	Lysolecithin
LS_OCMB	Lipid-specific oligoclonal IgM bands
MaxCq	Maximum number of cycles run in the qPCR equipment
miR-Amp	miRNA-Amplification step
miRNA	microRNA
MRI	Magnetic resonance imaging
mRNA	Messenger RNA
MS	Multiple sclerosis
MS-E	MS individuals of European origin
MS-NA	MS individuals of North-African origin
MS-NA (<15)	MS individuals of North-African origin who were born in Europe or migrated before 15 years old
MS-NA (>15)	MS individuals of North-African origin who migrated after 15 years old
ncRNA	Non-coding RNA
NF-L	Neurofilament light chain
NF water	Nuclease-free water
NGS	Next Generation Sequencing
NoRep_CSF	CSF samples without replicates
OCGB	Oligoclonal IgG bands
OND	Other neurological diseases controls
PBMCs	Peripheral blood mononuclear cells
PCR	Polymerase chain reaction
piRNA	Piwi-interacting RNA
PML	Progressive multifocal leukoencephalopathy
PMS	Progressive forms of multiple sclerosis
PPMS	Primary progressive multiple sclerosis

Preamp	Preamplification
pre-miRNA	Precursor miRNA
pri-miRNA	Primary miRNA transcript
PW	Pairwise deletion method
Q1-Q3	First quartile-Third quartile
QN	Quantile normalization
qPCR	Quantitative real-time PCR
RCSI	Royal College of Surgeons in Ireland
R&D	Research and development
RD	Real dataset
RIN	Rank-invariant set normalization
RIS	Radiologically isolated syndrome
RIS-Conversion	RIS individuals who converted to CDMS after five years of follow-up
RIS-RIS	RIS individuals who remained as RIS after five years of follow-up
RISC	RNA-induced silencing complex
RNA	Ribonucleic acid
RNS	Reactive nitrogen species
ROC	Receiver-operating characteristics
ROS	Reactive oxygen species
RoT	Room temperature
RQ	Relative quantification
RRMS	Relapsing-remitting multiple sclerosis
RRMS<25	RRMS individuals whose age at onset was below 25 years old
RRMS>45	RRMS individuals whose age at onset was after 45 years old
r_s	Spearman's Rho coefficient
RT	Retrotranscription
SAS	Spinal anesthesia subjects
siRNA	Small interfering RNA
SPMS	Secondary progressive multiple sclerosis
SPSS	Statistical Package for the Social Sciences
SSS	Summarized Stability Score
TLDA	TaqMan Low-Density Array
Trip_CSF	CSF samples with triplicates
UTR	Untranslated region
WM	White matter
XPO5	Exportin-5

LIST OF FIGURES

Figure 1. Map of prevalence of MS worldwide	10
Figure 2. Clinical course of MS	17
Figure 3. Key neurodegenerative processes as a consequence of chronic inflammation	21
Figure 4. miRNA biogenesis and release of extracellular miRNAs	39
Figure 5. Canonical site types for miRNA:mRNA interaction	41
Figure 6. Scheme of Applied Biosystems™ TaqMan™ Advanced miRNA cDNA Synthesis kit workflow	65
Figure 7. Reaction mix components and thermal cycling conditions for Poly(A) tailing reaction	66
Figure 8. Reaction mix components and thermal cycling conditions for Adaptor ligation reaction	67
Figure 9. Reaction mix components and thermal cycling conditions for Reverse transcription reaction	67
Figure 10. Reaction mix components and thermal cycling conditions for miR-Amp reaction	68
Figure 11. Scheme of TaqMan™ Advanced miRNA assays workflow	70
Figure 12. Schematic disposition of an OpenArray plate	71
Figure 13. Reaction mix components and thermal cycling conditions for qPCR with Individual TaqMan Advanced hydrolysis probes	73
Figure 14. Reaction mix components and thermal cycling conditions for Reverse transcription reaction with Megaplex RT Primers pool	74
Figure 15. Reaction mix components and thermal cycling conditions for Reverse transcription reaction with custom RT Primers pool	75
Figure 16. Reaction mix components and thermal cycling conditions for preamplification reaction	76
Figure 17. Reaction mix components and thermal cycling conditions for qPCR with Individual First Generation TaqMan hydrolysis probes	77
Figure 18. Impact of initial CSF volume and number of cycles of miR-Amp reaction in C _q values distribution	86
Figure 19. miRNA detection in CSF and serum samples in TaqMan® OpenArray® Human Advanced microRNA panels	88
Figure 20. C _q values mean and count of valid C _q values for each sample in C1 (a) and C2 (b)	90

Figure 21. miRNA abundance in C1 and C2	93
Figure 22. Scatter plot of correlation between Amp Score/Cq Confidence/Mean Cq value and detectability for each miRNA in C1 and C2	94
Figure 23. CV of replicates measurements for different miRNAs	95
Figure 24. Correlation of Cq raw data values in OpenArray and Cq raw data values in individual qPCR	96
Figure 25. Correlation of stability scores obtained by three different algorithms for C1 and C2	98
Figure 26. Correlation of stability values for each employed algorithm between C1 and C2 data	99
Figure 27. Evaluation of the optimum number of reference miRNAs according to the geNorm software	101
Figure 28. Scheme of the four steps of the OpenArray analysis flowchart under comparison	102
Figure 29. Column graphs showing the valid number of Cq values detected in each sample	104
Figure 30. Column graphs showing the number of miRNAs detected in different percentages of samples for each handling replicates method	106
Figure 31. CV of technical replicates of analyzable miRNA for each method	107
Figure 32. Column graphs showing the number of miRNAs detected in different percentages of samples according to each quality parameters combination	110
Figure 33. Amp Score and Cq Confidence values for NoRep_CSF and Trip_CSF datasets	111
Figure 34. Colored schemes showing datasets behaviours and simulated recreations	113
Figure 35. CV distribution for RD, PW, MaxCq and dR methods in each dataset	114
Figure 36. Scatter plot showing association between the real mean miRNA value and recreated values	115
Figure 37. CV distribution for GN_All, GN_70%, QN and RIN normalization methods in each dataset	116
Figure 38. Scatter plot showing association between miRNA relative quantifications in Trip_CSF and NoRep_CSF datasets	117
Figure 39. Relative quantification of miRNA levels in CSF of RRMS and OND in individual and triplicates measurements in OpenArray analysis	119-120
Figure 40. Scheme of the four steps of the OpenArray analysis flowchart under comparison with the selected method for each dataset	122

Figure 41. Differentially expressed miRNAs in CSF in the screening phase of PPMS study	126
Figure 42. Differentially expressed miRNAs in CSF in the validation phase of PPMS study	128
Figure 43. Differentially expressed miRNAs in serum in the screening phase of PPMS study	131
Figure 44. Differentially expressed miRNAs in serum in the validation phase of PPMS study	133
Figure 45. Differentially expressed miRNAs in the validation phase in PPMS individuals according to the inflammatory activity	137
Figure 46. Volcano plots representing changes in miRNA expression in <i>ex vivo</i> cerebellar tissue culture during different conditions	139
Figure 47. Differentially expressed miRNAs during normal myelination, demyelination and remyelination	140
Figure 48. Volcano plots representing changes in miRNA expression in CSF samples for different clinical MS subtypes	142
Figure 49. Differentially expressed miRNAs in CSF samples of SAS, PPMS and RRMS individuals	143
Figure 50. Venn diagrams plot the number of decreased/increased miRNAs in different conditions	144
Figure 51. Dot plots of overlapped miRNAs with reduced levels among <i>ex vivo</i> cultures and human MS samples	146
Figure 52. Dot plots of overlapped miRNAs with increased levels among <i>ex vivo</i> cultures and human MS samples	147
Figure 53. Dot plots of normalized miR-143-3p levels in <i>ex vivo</i> cultures and human MS samples	148
Figure 54. Differentially expressed miRNAs in CSF in RIS study	152
Figure 55. Differentially expressed miRNAs in plasma in RIS study	154
Figure 56. Visualization of the significantly associated GO biological processes in CSF using REVIGO	157
Figure 57. Visualization of the significantly associated GO biological processes in plasma using REVIGO	158
Figure 58. Differentially expressed miRNAs in CSF from MS individuals with different ethnic origin	163
Figure 59. Correlation of normalized Ct values in CSF samples with radiological and clinical variables	164

Figure 60. Differentially expressed miRNAs in CSF from RRMS individuals with different ethnic origin and age of migration	165
Figure 61. Dot plot for normalized levels of let-7c-5p in CSF of RRMS individuals depending on age at onset.	171
Figure 62. Differentially expressed miRNAs in CSF from RRMS individuals with early and late MS onset	173
Figure 63. Differentially expressed miRNAs in CSF samples according to the absence or presence of Gd+ lesions	178
Figure 64. ROC analysis of individual and combined miRNAs to discriminate inflammatory activity	179
Figure 65. Differential expression of NF-L in CSF according to the absence or presence of Gd+ lesions	180
Figure 66. Scatter plot of correlation between NF-L in CSF and miRNA levels ...	180
Figure 67. Pathway and target analysis of miR-21, miR-146a and miR-146b	184
Figure 68. Target analysis of miR-21, miR-146a and miR-146b	185
Figure 69. Correlation analysis of deregulated miRNAs and candidate targets mRNA expression in publicly available datasets	186
Figure 70. Correlation of normalized Cq values between CSF and plasma samples	188
Figure 71. Normalized expression of ebv-miR-BART7-3p in plasma samples of OND and MS individuals	192
Figure 72. Normalized expression of ebv-miR-BART7-3p in plasma samples of CIS and RRMS individuals	192
Figure 73. Normalized expression of ebv-miR-BART7-3p in plasma samples of MS individuals according to the absence or presence of relapses in the next two years	193

LIST OF TABLES

Table 1. Lifestyle and environmental risk factors for MS and their interactions with <i>HLA</i> gene	15
Table 2. DMTs for multiple sclerosis approved by EMA	24
Table 3. Clinical trials targeting remyelination	25
Table 4. miRNA studies in CSF in MS	45
Table 5. miRNA studies in serum in MS	46
Table 6. miRNA studies in plasma in MS	47
Table 7. miRNA studies in urine in MS	47
Table 8. Summary of the methodology employed in each study	81
Table 9. Distribution of samples in C1 and C2 cohorts used to test OpenArray plates performance	89
Table 10. miRNA classification according to the detectability in C1	91
Table 11. miRNA classification according to the detectability in C2	92
Table 12. miRNA stability scores for geNorm, Normfinder and CV algorithms and SSS score for CSF samples	100
Table 13. Description of used methods to handle technical replicates in Trip_CSF dataset	105
Table 14. Description of methods to evaluate quality and reliability of Cq values in studied datasets	108
Table 15. Relative quantification of miRNA expression in RRMS vs OND in CSF samples in individual measurements or triplicate measurements analysis	118
Table 16. Demographic, clinical, radiological and genetic data of the studied cohorts in PPMS study.....	124
Table 17. Differential miRNA expression among groups in CSF samples in the screening phase of PPMS study	125
Table 18. Differential miRNA expression among groups in CSF samples in the validation phase of PPMS study	127
Table 19. Differential miRNA expression among groups in serum samples in the screening phase of PPMS study	129-130
Table 20. Differential miRNA expression among groups in serum samples in the validation phase of PPMS study	132
Table 21. Association of serum miRNA levels with radiological and clinical variables at sampling	134

Table 22. Differential miRNA expression between PPMS patients according to inflammatory activity in CSF samples in the screening phase	135
Table 23. Differential miRNA expression between PPMS patients according to inflammatory activity in serum samples in the screening phase	135
Table 24. Differential miRNA expression between PPMS patients according to inflammatory activity in CSF samples in the validation phase	136
Table 25. Differential miRNA expression between PPMS patients according to inflammatory activity in serum samples in the validation phase	136
Table 26. Demographic data of the studied cohort	141
Table 27. Demographic, clinical, radiological and genetic data of the studied RIS cohort	150
Table 28. Differential miRNA expression between groups in CSF samples in RIS study	152
Table 29. Differential miRNA expression between groups in plasma samples in RIS study	153
Table 30. List of strongly validated targets for CSF deregulated miRNAs in RIS study	155
Table 31. List of strongly validated targets for plasma deregulated miRNAs in RIS study	156
Table 32. Association of miRNA levels with number of T2 lesions, CHI3L1 and NF-L levels in RIS study	159
Table 33. Demographic, clinical, radiological and genetic data of the studied RRMS cohort with different ethnic origin	161
Table 34. Differential miRNA expression between MS individuals of different ethnic origin in CSF samples	162
Table 35. Association of CSF miRNA levels with number of T2 lesions, levels of Vitamin D and EDSS	164
Table 36. Clinical, radiological and miRNA data of the studied RRMS cohort	166-167
Table 37. Demographic, clinical, radiological and genetic data of the studied RRMS cohort with different ages at onset	170
Table 38. Median expression values of normalized let-7c-5p for each group.....	171
Table 39. Median expression values of miRNAs for RRMS<25 and RRMS>45...	172
Table 40. Demographic data of the study MS cohort according to the absence or presence of Gd+ lesions	175
Table 41. List of 28 analyzed miRNAs and percentage of detection for each miRNAs in CSF	176

Table 42. Differential miRNA expression between groups in CSF of MS patients depending on the absence or presence of Gd+ lesions	177
Table 43. Capacity of selected miRNAs to detect inflammatory activity in CNS	178
Table 44. Correlations between radiological and clinical data with miRNA expression levels in CSF	181
Table 45. Validated targets for miR-21-5p, miR-146a-5p and miR-146b-5p from miRTarBase	182-183
Table 46. Differential miRNA expression between groups in plasma samples ...	187
Table 47. Demographic, clinical and, genetic data of the studied cohort in EBV study	191
Table 48. ebv-miR-BART7-3p expression in plasma samples of OND and MS individuals	191
Table 49. Differential expression of ebv-miR-BART7-3p in plasma samples of the validation cohort	194
Table 50. Differential expression of ebv-miR-BART7-3p in plasma samples of the cohort from Lleida	194
Table 51. Differential expression of ebv-miR-BART7-3p in plasma samples of the cohort from Madrid	194
Table 52. Summary table of miRNA findings in this doctoral thesis	230
Table 53. Number of researchers and gross domestic expenditure on research and development per country in 2018	232

TABLE OF CONTENTS

ACKNOWLEDGEMENTS	i
LIST OF ORIGINAL PUBLICATIONS	v
ABBREVIATIONS	vii
LIST OF FIGURES	xi
LIST OF TABLES	xv
SUMMARY	1
RESUMEN	3
RESUM	5
1. INTRODUCTION	7
1.1. MULTIPLE SCLEROSIS	9
1.1.1 Definition of multiple sclerosis	9
1.1.2 Epidemiology of multiple sclerosis	9
1.1.3 Etiology and risk factors	11
1.1.3.1 Environmental factors	11
1.1.3.1.1 Epstein-Barr virus	11
1.1.3.1.2 Vitamin D levels and sun exposure.....	12
1.1.3.1.3 Smoking	13
1.1.3.1.4 Other environmental factors	13
1.1.3.2 Genetic factors	14
1.1.4 Clinical forms of multiple sclerosis	16
1.1.5 Pathogenesis of multiple sclerosis	18
1.1.6 Diagnosis and treatment	21
1.2 BIOMARKERS IN MS	26
1.2.1 Origin and function of CSF	26
1.2.2 Study of CSF biomarkers	27
1.2.3 Other biomarkers in MS	29
1.3 EPIGENETICS	30

1.3.1 Definition	30
1.3.2 Epigenetic mechanisms	31
1.3.3 Epigenetic studies in MS	33
1.4 microRNAs	36
1.4.1 Definition	36
1.4.2 miRNA biogenesis	37
1.4.3 miRNA function	40
1.4.4 Circulating miRNAs	42
1.4.5 Detection techniques	43
1.4.6 Methodological challenges	44
1.4.7 Circulating miRNAs and MS	45
1.4.7.1 miRNAs in CSF	45
1.4.7.2 miRNAs in other biological fluids	46
2. HYPOTHESIS AND OBJECTIVES	51
3. MATERIALS AND METHODS	57
3.1 STUDY POPULATION	59
3.1.1 Biological material	59
3.1.2 Study variables	60
3.2 BIOLOGICAL MATERIAL FROM MICE	61
3.3 ETHICAL CONSIDERATIONS	62
3.4 RNA EXTRACTION	62
3.4.1 RNA extraction from human samples	62
3.4.2 RNA extracion from mice samples	63
3.5 miRNA DETECTION WITH TaqMan™ ADVANCED miRNA ASSAYS	64
3.5.1 miRNA cDNA synthesis	64
3.5.1.1 Poly(A) tailing reaction	66
3.5.1.2 Adaptor ligation reaction	66
3.5.1.3 Reverse transcription reaction	67
3.5.1.4 miR-Amp reaction	68
3.5.2 miRNA DETECTION	68

3.5.2.1 miRNA profiling by TaqMan™ OpenArray™ Human Advanced microRNA panel	70
3.5.2.2 miRNA detection by quantitative real-time PCR with TaqMan™ Advanced microRNA assays	72
3.6 miRNA DETECTION WITH FIRST GENERATION TaqMan™ miRNA ASSAYS	73
3.6.1 miRNA cDNA synthesis	73
3.6.1.1 Reverse transcription reaction	74
3.6.1.2 Pre-amplification reaction	75
3.6.2 miRNA detection	76
3.6.2.1 miRNA detection by real-time PCR with TaqMan™ microRNA assays	76
3.7 miRNA EXPRESSION NORMALIZATION	77
3.7.1 Normalization of TaqMan™ OpenArray™ miRNA plates	77
3.7.2 Normalization of individual qPCR experiments	78
3.8 miRNA RELATIVE QUANTIFICATION	78
3.9 IN SILICO TOOLS	79
3.10 STATISTICAL ANALYSES	79
4. RESULTS	83
4.1 DESCRIPTION OF A PANEL OF CSF-ENRICHED miRNA USEFUL TO STUDY NEUROLOGICAL DISEASES	85
4.1.1 Optimization of TaqMan Advanced miRNA technology protocol for CSF samples	85
4.1.2 Platform format selection for the study of CSF miRNAs in OpenArray Human Advanced miRNA panels	87
4.1.3 Customized OpenArray plates performance	89
4.1.4 Variability of replicates measurements	95
4.1.5 Correlation between individual qPCR (22 cycles) and OpenArray performance	97
4.1.6 Search of suitable endogenous controls	97
4.1.7 Summary	101
4.2 CHOICE OF A SUITABLE FLOWCHART TO ANALYZE OpenArray miRNA DATA IN CSF SAMPLES	102
4.2.1 Samples	103

4.2.2 Technical replicates	105
4.2.3 Evaluation of quality and reliability of Cq values	108
4.2.4 Handling missing data	112
4.2.5 Normalization methods for OpenArray plates in CSF samples	115
4.2.6 Replicates vs individual measurements in OpenArray	116
4.2.7 Summary	121
4.3 STUDY OF THE CIRCULATING miRNA PROFILES IN PPMS PATIENTS	123
4.3.1 Samples: inclusion and exclusion criteria	123
4.3.2 Clinical characteristics of the studied cohort	123
4.3.3 To establish a characteristic miRNA signature in CSF of PPMS patients.....	125
4.3.4 To establish a characteristic miRNA signature in serum of PPMS patients	128
4.3.5 Correlation of deregulated miRNA expression with radiological and clinical variables	133
4.3.6 miRNA signature in PPMS according to the inflammatory activity.....	134
4.3.7 Summary	137
4.4 RELATION OF THE CSF miRNA PROFILE OF MS INDIVIDUALS WITH THE miRNA SIGNATURE DURING DEMYELINATION AND REMYELINATION IN CEREBELLAR ORGANOTYPIC CULTURE MODEL	138
4.4.1 To establish a characteristic miRNA signature in murine <i>ex vivo</i> cultures by OpenArray	138
4.4.2 Comparison of non-inflammatory PPMS and RRMS <i>vs</i> SAS	141
4.4.3 Cross-analysis of miRNA expression between murine <i>ex vivo</i> cultures and human CSF samples	144
4.4.4. Summary	148
4.5 STUDY OF THE CIRCULATING miRNA SIGNATURE IN RIS INDIVIDUALS	149
4.5.1 Clinical characteristics of the RIS patients	149
4.5.2 CHI3L1 and NF-L levels in CSF	151
4.5.3 miRNA profile in CSF	151
4.5.4 miRNA profile in plasma	153

4.5.5 Targets, pathways and cellular/tissue enriched sources analysis of selected miRNAs	154
4.5.6 Association of miRNA levels with CSF biochemical and radiological variables	159
4.5.7 Summary	159
4.6 STUDY OF CIRCULATING miRNA PROFILES IN CSF OF RRMS PATIENTS	160
4.6.1 Comparison of CSF miRNA profiles in MS patients according to their ethnic origin	160
4.6.1.1 Clinical characteristics of the studied patients	160
4.6.1.2 miRNA profile in CSF	162
4.6.1.3 Association of miRNA levels with other variables	163
4.6.1.4 Analysis depending on age of migration to Europe	165
4.6.1.5 Summary	168
4.6.2 Comparison of CSF miRNA profiles in RRMS patients depending on age at disease onset	169
4.6.2.1 Clinical characteristics of the studied patients	169
4.6.2.2 miRNA profile in CSF	171
4.6.2.3 miRNA CSF profile comparison between individuals of early and late onset	172
4.6.2.6 Summary	173
4.6.3 Comparison of active lesions-enriched miRNAs in CSF according to the presence of Gd ⁺ lesions in MRI	174
4.6.3.1 Clinical characteristics of patients	174
4.6.3.2 Detection of miRNAs in CSF	175
4.6.3.3 Differential miRNA values in CSF of MS patients with Gd ⁺ lesions	177
4.6.3.4 Correlation between deregulated miRNAs and CSF NF-L levels	179
4.6.3.5 Association of CSF miRNA expression with radiological and clinical variables	181
4.6.3.6 Target and pathway analysis of miR-21, miR-146a and miR-146b	181
4.6.3.7 Correlation analysis of miRNAs and mRNA expression in <i>in silico</i> datasets	185

4.6.3.8 Plasma expression of miR-21, miR-146a and miR-146b	187
4.6.3.9 Summary	188
4.7 STUDY OF CIRCULATING VIRUS-ENCODED miRNAs IN MS PATIENTS AND HEALTHY CONTROLS	189
4.7.1 Selection of EBV-encoded miRNA assays and detection in plasma samples	189
4.7.2 Demographic data of Girona cohort	190
4.7.3 Comparison of viral miRNA expression between MS patients and OND controls in Girona cohort	190
4.7.4 Comparison of viral miRNA expression between MS patients and OND controls in a bigger cohort	193
4.7.5 Summary	195
5. DISCUSSION	197
5.1 DESCRIPTION OF A PANEL OF CSF-ENRICHED miRNA USEFUL TO STUDY NEUROLOGICAL DISEASES	200
5.2 CHOICE OF A SUITABLE FLOWCHART TO ANALYZE OpenArray miRNA DATA IN CSF SAMPLES	204
5.3 STUDY OF THE CIRCULATING miRNA PROFILES IN PPMS PATIENTS	208
5.4 RELATION OF THE CSF miRNA PROFILE OF MS INDIVIDUALS WITH THE miRNA SIGNATURE DURING DEMYELINATION AND REMYELINATION IN CEREBELLAR ORGANOTYPIC CULTURE MODEL	212
5.5 STUDY OF THE CIRCULATING miRNA SIGNATURE IN RIS INDIVIDUALS	215
5.6 STUDY OF CIRCULATING miRNA PROFILES IN CSF OF RRMS PATIENTS	218
5.6.1 Comparison of CSF miRNA profiles in MS patients according to their ethnic origin	218
5.6.2 Comparison of CSF miRNA profiles in RRMS patients depending on age at disease onset	221
5.6.3 Comparison of active lesions-enriched miRNAs in CSF according to the presence of Gd+ lesions in MRI	223
5.7 STUDY OF CIRCULATING VIRUS-ENCODED miRNAs IN MS PATIENTS AND HEALTHY CONTROLS	226
5.8 GENERAL DISCUSSION	229

5.9 LIMITATIONS	231
5.10 FINAL CONSIDERATION	231
6. CONCLUSIONS	233
7. REFERENCES	237
8. ANNEX I	273
9. ANNEX II	281

SUMMARY

Multiple sclerosis (MS) is the most common non-traumatic neurological cause of disability in young individuals, affecting more than 1 million people in Europe. It is considered a chronic inflammatory and neurodegenerative disease, characterized by the existence of demyelinated areas in the white and gray substances of the central nervous system, infiltration of inflammatory cells in the brain parenchyma, gliosis and, axonal damage. The most common clinical subtype, known as relapsing-remitting MS (RRMS), is associated with an inflammatory burden, whereas 15% of individuals present primary progressive MS (PPMS), another clinical form characterized by demyelination and disability from the onset. The etiology is still unknown but it has been suggested that epigenetics is involved in the complex interaction between some genetic and environmental factors producing the pathology and the symptoms in MS. microRNAs (miRNAs), one of these epigenetic mechanisms, might regulate gene expression post-transcriptionally. They also present many properties to be considered as promising biomarkers for different pathological conditions as they could be released into biological fluids. Over the last years, miRNA studies in MS, mainly focused on RRMS, have gained tremendous attention through the study of different biological samples.

In this doctoral thesis, specific miRNA signatures in different clinical and pre-clinical forms of MS are described. OpenArray plates specifically directed to analyze cerebrospinal fluid (CSF)-enriched miRNAs have been designed and the most appropriate strategy for their analyses has been defined. Firstly, miRNA profiles in CSF and serum samples of PPMS individuals have been identified and the comparison of these clinical manifestations with an *ex vivo* demyelinating model has been proposed as an approach to further define the mechanisms involved in demyelinating and neurodegenerative processes. Secondly, the description of circulating miRNA profiles in CSF and plasma of radiologically isolated syndrome individuals has allowed to preliminary differentiate those who

SUMMARY

finally convert to MS. Thirdly, miRNA deregulation in RRMS depending on different clinical variables such as ethnicity, age at onset and disease activity has been studied in order to describe their potential role as informative biomarker. Finally, the expression of virus-encoded miRNAs in plasma samples of RRMS and control subjects has been explored.

Altogether, miR-21-5p, miR-20a-5p, miR-142-5p, miR-143-3p, miR-146a-5p and miR-448 are proposed as potential miRNA candidates involved in MS pathogenesis as their deregulation has been manifested in different sub-studies.

RESUMEN

La esclerosis múltiple (EM) es la primera causa de discapacidad de origen no traumático en adultos jóvenes, afectando a más de un millón de personas en Europa. Es considerada una enfermedad crónica, inflamatoria y neurodegenerativa, caracterizada por la existencia de áreas de desmielinización en las sustancias blanca y gris del sistema nervioso central, infiltración de células inflamatorias en el parénquima cerebral, gliosis y daño axonal. El subtipo clínico más común, conocido como EM remitente-recurrente (EMRR), se asocia con una carga inflamatoria; mientras que el 15% de los individuos presenta EM primaria progresiva (EMPP), otra forma clínica caracterizada por desmielinización y discapacidad desde el inicio. La etiología de la EM es aún desconocida, pero se cree que la epigenética influye en la compleja interacción entre factores genéticos y ambientales que producen la patología y los síntomas en la EM. Los microRNAs (miRNAs), cuya función es regular la expresión génica postranscripcionalmente, constituyen uno de estos mecanismos epigenéticos. Presentan, a su vez, muchas propiedades para ser considerados potenciales biomarcadores en diferentes condiciones patológicas, ya que pueden ser liberados en diferentes fluidos biológicos. En los últimos años, los estudios de miRNAs en EM, principalmente centrados en EMRR, han captado una gran atención a través del estudio de diferentes muestras biológicas. En esta tesis doctoral se describen perfiles de miRNAs específicos en diferentes formas clínicas y preclínicas de EM. Se han diseñado placas OpenArray específicamente dirigidas a analizar miRNAs enriquecidos en líquido cefalorraquídeo (LCR) y se ha definido la estrategia más adecuada para su análisis. En primer lugar, se han identificado perfiles de miRNAs en muestras de LCR y suero de individuos con EMPP y se ha propuesto la comparación de estas manifestaciones clínicas con un modelo desmielinizante *ex vivo* como un enfoque para definir mejor los mecanismos implicados en los procesos desmielinizantes y neurodegenerativos. En segundo lugar, la descripción de los perfiles de miRNAs circulantes en LCR y plasma de individuos con

RESUMEN

síndrome radiológicamente aislado ha permitido diferenciar preliminarmente a aquellos sujetos que finalmente convierten a EM. En tercer lugar, se ha estudiado la desregulación de miRNAs en LCR en EMRR en función de diferentes variables clínicas como el origen étnico, la edad de inicio y la actividad de la enfermedad para describir su papel como potencial biomarcador informativo. Finalmente, se ha explorado la expresión de miRNAs codificados por virus en muestras de plasma de EMRR y de sujetos control.

En resumen, miR-21-5p, miR-20a-5p, miR-142-5p, miR-143-3p, miR-146a-5p y miR-448 se proponen como posibles miRNAs candidatos a estar involucrados en la patogénesis de la EM ya que su desregulación se ha observado en diferentes subestudios.

RESUM

L'esclerosi múltiple (EM) és la primera causa de discapacitat d'origen no traumàtic en adults joves, afectant a més d'un milió de persones a Europa. És considerada una malaltia crònica, inflamatòria i neurodegenerativa, caracteritzada per l'existència d'àrees de desmielinització a les substàncies blanca i gris del sistema nerviós central, infiltració de cèl·lules inflamatòries en el parènquima cerebral, gliosi i dany axonal. El subtipus clínic més comú, conegut com EM remitent-recurrent (EMRR), s'associa amb una càrrega inflamatòria; mentre que el 15% dels individus presenta EM primària progressiva (EMPP), una altra forma clínic caracteritzada per desmielinització i discapacitat des de l'inici. L'etiologia de l'EM és encara desconeguda, però es creu que l'epigenètica influeix en la complexa interacció entre factors genètics i ambientals que produeixen la patologia i els símptomes en l'EM. Els microRNAs (miRNAs), la funció dels quals és regular l'expressió gènica postranscripcionalment, constitueixen un d'aquests mecanismes epigenètics. Presenten, al seu torn, moltes propietats per a ser considerats potencials biomarcadors en diferents condicions patològiques, ja que poden ser alliberats en diferents fluids biològics. En els últims anys, els estudis de miRNAs en EM, principalment centrats en EMRR, han sigut de gran interès a través de l'estudi de diferents mostres biològiques.

En aquesta tesi doctoral es descriuen perfils de miRNAs específics en diferents formes clíniques i preclíniques d'EM. S'han dissenyat plaques OpenArray específicament dirigides a analitzar miRNAs enriquits en líquid cefaloraquídi (LCR) i s'ha definit l'estratègia més adequada per al seu anàlisi. En primer lloc, s'han identificat perfils de miRNAs en mostres de LCR i sèrum d'individus amb EMPP i s'ha proposat la comparació d'aquestes manifestacions clíniques amb un model desmielinitzant *ex vivo* com un enfocament per definir millor els mecanismes implicats en els processos desmielinitzants i neurodegeneratius. En segon lloc, la descripció dels perfils de miRNAs circulants en LCR i plasma d'individus amb síndrome radiològicament aïllat ha permès diferenciar de forma

RESUM

preliminar a aquells subjectes que finalment converteixen a EM. En tercer lloc, s'ha estudiat la desregulació de miRNAs en LCR en EMRR en funció de diferents variables clíniques com l'origen ètnic, l'edat de debut i l'activitat de la malaltia per descriure el seu paper com a potencial biomarcador informatiu. Finalment, s'ha explorat l'expressió de miRNAs codificats per virus en mostres de plasma de EMRR i de subjectes control.

En resum, miR-21-5p, miR-20a-5p, miR-142-5p, miR-143-3p, miR-146a-5p i miR-448 es proposen com a possibles miRNAs candidats a estar involucrats en la patogènesi de l'EM ja que la seva desregulació s'observa en diferents subestudis.

1. Introduction

1.1 MULTIPLE SCLEROSIS

1.1.1 Definition of multiple sclerosis

Multiple sclerosis (MS) is a chronic inflammatory and neurodegenerative disease of the central nervous system (CNS), the etiology of which is still unknown [1]. It is known to have an autoimmune component that is characterized by the existence of demyelinated areas in the white matter (WM) and gray matter (GM) of the CNS, infiltration of inflammatory cells in the brain parenchyma, gliosis and, axonal damage [2].

The first detailed description of MS was made by Jean-Martin Charcot in 1868, indicating three indicators of disease: intention tremor, nystagmus and, scanning speech, which would be known as Charcot's triad [3]. He related the clinical and histopathological features of MS and described the lesions as "plaques" with focal demyelination, inflammation gliosis and, axonal loss [4].

1.1.2 Epidemiology of multiple sclerosis

MS is estimated to affect more than 1 million people in Europe and 2.8 million people worldwide [5]. Recent data have shown a significantly increase in the number of affected people in Europe, where the cases have increased from 700,000 in 2017 to more than one million in 2020, affecting 47,000 people in Spain [6,7]. The epidemiology of MS has been widely studied and its prevalence has been rising [8]. This increase has been related to several factors as the implementation of better counting methods, improved MS diagnosis criteria and health-care system or increased life expectancy in MS individuals [2]. However, the existence of a real increase in the risk of developing MS could not be discarded [5].

Several studies have linked the prevalence of MS with latitude [9] with a clear North-South gradient with people living in countries closer to the equator presenting lower MS risk than those living in countries further from the equator

INTRODUCTION

with greater risk [10], as it could be observed in Figure 1, where the prevalence of MS are depicted for countries. This differential distribution might be due to both genetic and environmental factors as sun exposure, vitamin D levels and/or hygiene of populations [2,5].

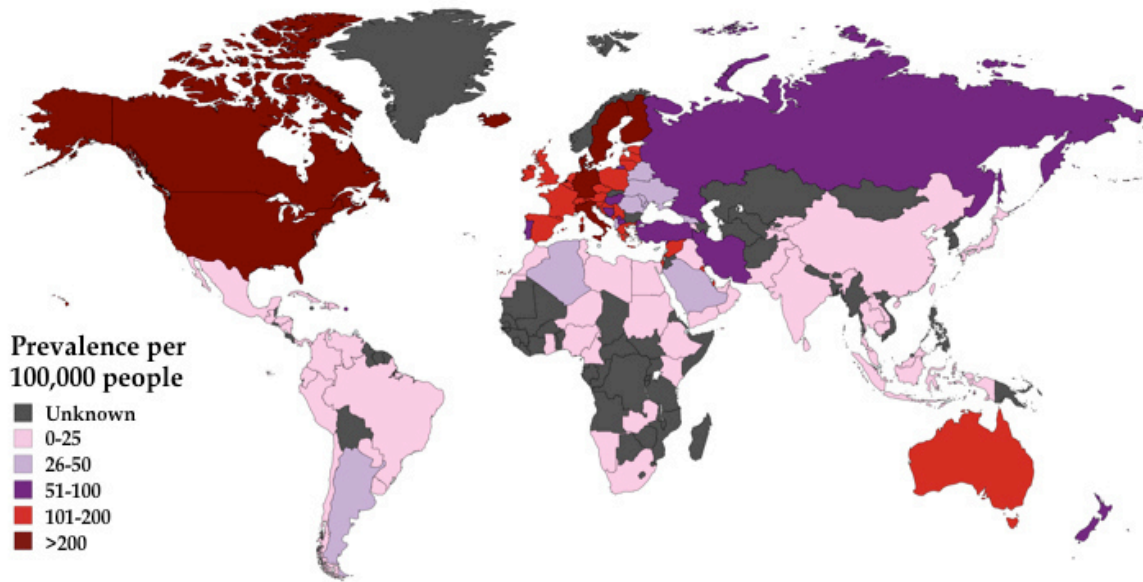


Figure 1. Map of prevalence of MS worldwide. Information retrieved from Atlas of MS 2020 [5].

MS is the most common non-traumatic neurological cause of disability in young population [11], which implies a great quality of life impact in patients and their families and a high health cost for the governments [12]. Although the average age of MS onset is 32 years old [5], there are individuals with early and late MS onset presenting distinct features and characteristics [13]. Although the diagnosis of MS in pediatric age is rare, recent studies have estimated that at least 30,000 MS individuals are under 18 years old [5], and surely it is still underdiagnosed. Aging might be considered a risk factor for MS progression as it diminishes the natural ability of the CNS of remyelination [14] and produces some changes in the immune system [15].

Usually, women are affected at a 3:1 ratio compared to men [16], showing the characteristic gender bias of autoimmune diseases [17]. Interestingly, the rate of disability accumulation is faster in male than female patients [18]. The reasons of this difference might be attributed to several factors as genetic and hormonal differences or social and environmental exposures [5]. However there is a MS phenotype, primary progressive MS (PPMS), whose sex ratio is 1:1 and the rate of disability accumulation is similar between male and female individuals [18].

1.1.3 Etiology and risk factors

Etiology of MS is still unknown but it has been suggested that the disease is the result of a complex interaction between both environmental and genetic factors that will produce the characteristic features and symptoms of MS through different pathogenic mechanisms [19].

1.1.3.1 Environmental factors

Some environmental factors involved in MS pathogenesis have been suggested during the last 30 years, some of which are Epstein-Barr virus (EBV), vitamin D levels, smoking, obesity during childhood and adolescence or microbiota.

1.1.3.1.1 Epstein-Barr virus

EBV is a deoxyribonucleic acid (DNA) lymphotropic herpesvirus that is highly prevalent in human population affecting more than 90% of people worldwide and it is the causative agent of infectious mononucleosis [20]. EBV has been also implicated in other conditions as different types of cancer, thyroid disorders, lymphoproliferative disorders, rheumatoid arthritis, MS and other autoimmune disorders [21]. The main way of viral transmission is through oral secretions and it could persist inside human B cells as latent [22].

INTRODUCTION

EBV has been related to MS susceptibility as EBV seronegative individuals present an extremely low risk for MS compared with those seropositive individuals [23]; only 3.3% MS subjects could present EBV nuclear antigen-1 (EBNA1) seronegativity compared to controls that is around 6%. However, one study performed by Dobson *et al.* confirmed that these percentages might be not real, suggesting the performance of serologic testing against multiple EBV antigens to discard false negatives [24]. Several prospective studies among healthy individuals have found a positive association between increased EBV immunoglobulin G (IgG) antibody titers and MS risk [25–30] and this humoral immune response against EBV has been related to disease activity on magnetic resonance imaging (MRI) [31]. In addition, it has also been described a significant increased risk of MS related to infectious mononucleosis history [32].

There are two main EBV genotypes distinguished by differences in *EBNA-2* gene [22]. Another important genes that have potential roles in different viral processes are *LMP-1*, *LMP-2a*, *LM BZLF1*, *EBNA-3A*, *-3B*, and *-3C* [33]. Moreover, the viral genome encodes 44 microRNAs (miRNAs) that regulate genes involved in different cellular processes such as cell apoptosis, antigen presentation and recognition or, B cell transformation [34]. Some of these viral miRNAs have been found deregulated in MS [35,36].

1.1.3.1.2 Vitamin D levels and sun exposure

Vitamin D is one of the environmental MS risk factors. It is a hormone that is on the skin and might be uptaken from diet. Vitamin D, after suffering some transformations in the organism, is capable of activating the nuclear vitamin D receptor, resulting in different immunoregulatory responses [37]. Low levels of vitamin D have been related to increased MS risk [38], relapse rate, MRI lesions, disability and progression [39–41].

The differential geographical distribution of MS prevalence previously explained has been attributed to genetic and environmental differences. One of this environmental factors is sun exposure through its effect on vitamin D levels [42]. This is due to the essential role of ultraviolet radiation in the conversion of 7-dehydrocholesterol into a previous form of vitamin D in the skin [37]. Lower MS risk has been associated with higher sun exposure during childhood and early adolescence [43]. It is thought that sun exposure might influence on MS not only by its effect on vitamin D levels but also by other immunomodulatory pathways [44].

1.1.3.1.3 Smoking

Several meta-analyses have been performed evaluating the influence of smoking on MS risk, all concluding the existence of an increased MS risk in consumers [45-47]. There are studies with contradictory results regarding the association of smoking with disease progression [48-50].

There is a strong evidence that smoking might play a role in MS as it could affect innate and cell-mediated immunity, produce systemic and local inflammation in the lungs and direct toxicity as well as contribute to genome-wide epigenetic modifications [51].

1.1.3.1.4 Other environmental factors

Some studies have related childhood and adolescence obesity with an increase risk of MS, mainly in females [52-54]. It has been observed the existence of a “proinflammatory state” in obese children [55], as obesity might induce the production of pro-inflammatory cytokines, promote Th1 responses and decrease the number of regulatory T cells [56].

Recent experimental evidences have suggested the existence of a microbial imbalance in the gut of MS individuals, with different studies trying to define

INTRODUCTION

microbiota composition in MS patients [57]. There are differences in specific taxa, promoting inflammatory cytokines and inflammation [58]. Animal models have been extremely valued in pointing out that gut microbiome adjustment might be a potential intervention for MS [59].

Night work, excessive alcohol or the consumption of caffeine have also been proposed as potential risk factors but more studies are required to establish their contribution [60].

1.1.3.2 Genetic factors

The study of the role of genetic factors on the susceptibility of developing MS is justified by the evidence that there is a higher risk of MS in individuals with biological relatives suffering MS [61]. The continuous advances in genetics and technology along with the establishment of collaborative research networks have allowed to describe up to 233 susceptibility genetic variants until now [62].

Different studies using microarrays or ImmunoChip genotyping arrays as well as genome wide association studies have identified several variants as heritable risk factors in MS. Some of them are really immunologically relevant genes particularly implicated in T cell activation and proliferation as *IL2* and *IL7R* [63–67]. The major histocompatibility complex on chromosome 6 is the greatest contributor to MS susceptibility with the allele for the human leukocyte antigen (HLA) *HLA-DRB1*15:01* strongly associated with MS risk [68]. Additional effects have been observed in class II risk alleles (*HLA-DRB1*03:01* and *HLA-DRB1*13:03*), whereas class I alleles as *HLA-A*02:01*, *HLA-B*44:02* and *HLA-B*38:01* could be considered protective [69].

Two of the last studies carried out by the International Multiple Sclerosis Genetics Consortium have described interesting findings. First, although 20% of MS risk heritability could be attributed to common genetic variants, coding low-frequency variants might explain almost another 5% of heritability [70]. Second, the creation

of a genetic and genomic map of MS susceptibility has highlighted the implication of multiple innate and adaptive immune pathways and an enrichment for MS gene expression in human microglia [62].

In conclusion, these studies support the idea that the overall genetic MS risk results from the contribution of multiple polymorphic genes with risk alleles that are common in the population.

However, the etiology of the disease is still unknown. These genetic factors are related to environmental factors in a complex way in order to determine disease susceptibility and its course [71]. As depicted in Table 1, certain factors interact with *HLA* MS risk genes, increasing substantially the risk in individuals who carry genes that predispose to MS [72].

Table 1. Lifestyle and environmental risk factors for MS and their interactions with *HLA* gene.

Risk factor	Odds ratio	<i>HLA</i> gene interaction	Combined odds ratio	Immune system implied
Smoking	~1.6	Yes	14	Yes
EBV infection	~3.6	Yes	~15	Yes
Vitamin D levels <50 mM	~1.4	No	NA	Yes
Adolescent obesity	~2	Yes	~15	Yes
Low sun exposure	~2	No	NA	Yes
Infectious mononucleosis	~2	Yes	7	Yes

MS: multiple sclerosis; *HLA*: human leukocyte antigen; EBV: Epstein-Barr virus. Adolescent obesity was determined by body mass index >27 at age 20 years. Table adapted from Olsson *et al.* (2016) [72].

INTRODUCTION

1.1.4 Clinical forms of multiple sclerosis

MS is clinically heterogeneous and the definition of four distinct clinical subtypes has been indispensable. The consistency of the definitions is critical to improve communication among clinicians and to standardize the inclusion of patients in clinical trials and demographic studies [73]. The two major subtypes can be distinguished according to the relapsing and progressive onset of the disease [74].

Approximately 85% of patients with MS are diagnosed with relapsing-remitting MS (RRMS), which is characterized by acute neurological deficits that are followed by complete or incomplete remission [75]. The different neurological symptoms that occur during relapses are associated with different areas of CNS inflammation [76]. The age of onset in RRMS individuals is around 32 years old with a significant predominance of women compared to men [74]. Natural history studies have shown that after around 15 years of relapsing-remitting course, the disease evolves into a progressive course with disability accumulation over time without remission in 65% of RRMS cases, which is called secondary progressive MS (SPMS) (Figure 2A) [73]. At this point, progression is persistent and usual therapies become ineffective [2,77]. SPMS is diagnosed retrospectively because there is no a clear defined criteria to determine the transition point between RRMS and SPMS [73].

The remaining 15% of patients are diagnosed with a progressive disease course from the onset without the presence of clinically evident relapses; it is PPMS phenotype (Figure 2B) [78]. PPMS represents a distinct pathologic form of MS than RRMS, which involves less peripheral inflammation [79]. It has been proposed that PPMS and SPMS could be further sub-classified depending on the clinical and radiological activity and the existence or absence of disability progression in order to better select patients for starting therapies [80]. Unlike what happens with RRMS, the age of onset in PPMS is around 42 years old and the sex ratio is almost balanced [74].

Clinically isolated syndrome (CIS) refers to the first clinical presentation of the disease, which shows characteristics of inflammatory demyelination but still has to fulfill criteria of dissemination in time [2]. CIS individuals might become clinically or radiologically active and be diagnosed with RRMS or remain as a single event [60]. The conversion rate is estimated in 60–70% within 20 years according to some prospective studies [81]. Clinical trials with disease-modifying therapies (DMTs) showed fewer conversion to MS and reduced MRI activity in CIS individuals [73]. The risk of conversion might be estimated using different epidemiological, clinical, biochemical, radiological and, immunogenetic factors [82].

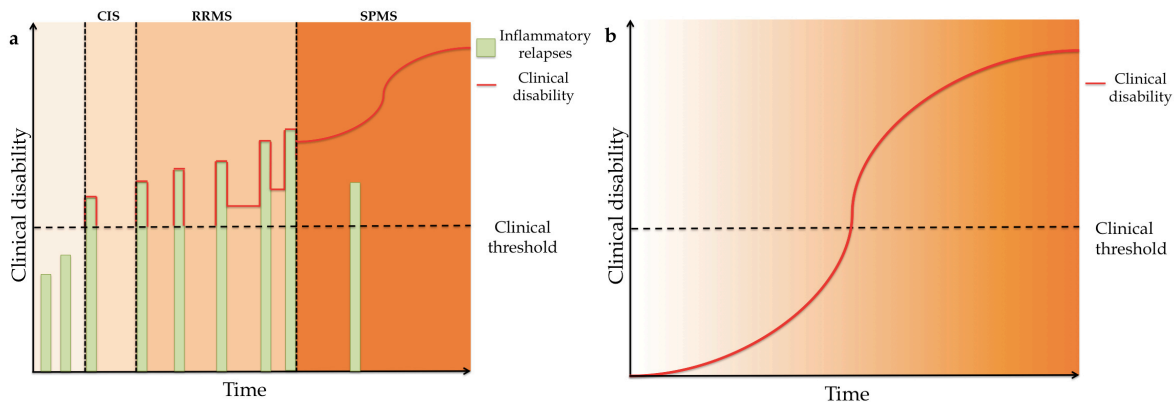


Figure 2. Clinical course of MS. CIS: clinically isolated syndrome; RRMS: relapsing-remitting multiple sclerosis; SPMS: secondary progressive multiple sclerosis; PPMS: primary progressive multiple sclerosis. (a) Clinical course of most MS individuals. First, a first clinical presentation with characteristics of inflammatory demyelination that does not fulfil its diagnostic criteria is observed, CIS. RRMS is characterized by the occurrence of relapses with complete or incomplete neurological recovery. Most patients will evolve into SPMS, characterized by the progressive, irreversible disability that occurs independently of the presence of relapses. (b) Clinical course of patients presenting PPMS, which is characterized by disease progression from the onset without relapses. Muñoz-San Martín (2021).

The incidental radiological finding of lesions suggestive of MS in asymptomatic individuals is known as radiologically isolated syndrome (RIS) [83]. One third of these individuals develops a symptomatic demyelinating event, CIS, and evolve toward clinically definite MS (CDMS) in 5 years time [84]. Since there are no clinical signs or symptoms, this group is not included in the MS subtypes. Some

INTRODUCTION

features have been described as risk factors for clinical conversion of RIS into CDMS: younger age, male sex, presence of Gadolinium (Gd)-enhancing lesions (Gd+), affected visual evoked potential, presence of spinal cord lesions and high levels of neurofilament light chain (NF-L) in cerebrospinal fluid (CSF) [85,86].

1.1.5 Pathogenesis of multiple sclerosis

MS is a very heterogeneous disease and its pathology might vary among patients and even in a single person over time [87]. It is defined as a chronic demyelinating and neurodegenerative disease, whose main pathological hallmark is the appearance of confluent demyelinated areas in WM and GM of the brain, spinal cord and optic nerve (lesions or plaques) with variable degrees of inflammation, gliosis and neurodegeneration [88]. These pathognomic inflammatory events boost some neurodegenerative processes that lead to the destruction of oligodendrocytes, axons and even neurons and might also be observed from the earliest stages of MS [89]. However, these lesions are unable to explain all the clinical disability observed in the progressive forms of MS (PMS) [87]. Different mechanisms that occur at different stages of MS might drive to axonal loss [60]. Although many pathologic features are shared and overlapped between RRMS and PMS, specific differentiations might be made [90].

It is suggested that two types of inflammation, which might be developed in parallel but independently, could be observed in MS individuals. On the one hand, the first type is mainly observed in acute and RRMS patients and it is characterized by peripheral inflammatory infiltrates of T and B lymphocytes with intense blood brain barrier (BBB) leakage [91]. BBB is formed by endothelial cells connected by tight junctions and its main function is to regulate the exchange of molecules and cells between the blood and the brain [92]. This acute inflammation predominantly affects WM forming active demyelinating lesions [60].

On the other hand, although already present in early stages of MS, the second type of inflammation is more pronounced in later stages of the disease. It has been suggested that a compartmentalized inflammation occurs in PMS as it has been observed the existence of lymphoid aggregates in the meninges, mainly formed by B lymphocytes, adjacent to an intact BBB [87]. This type of inflammation is associated with the existence of inactive and chronic active plaques. However, these lesions are unable to explain all the disability observed in PMS [87]. Some other processes such as the existence of slow expanding lesions in the WM, diffuse neurodegeneration in the normal appearing WM or GM and the formation of new cortical gray matter lesions have been proposed to have an important role in disability [60,87,91].

Other mechanisms, apart from the inflammatory processes just described, might explain all the constellation of characteristic pathological findings in MS (Figure 3). First, chronic inflammatory state in MS might increase the production of both reactive oxygen species (ROS) and reactive nitrogen species (RNS) by activated microglia found surrounding lesions in the cortex and in normal-appearing white matter [87,89]. This toxic environment produces direct oxidation of lipids, proteins and DNA and probably induces mitochondrial injury [93], with the subsequent metabolic stress, energy deficiency and loss of neuronal competence [89], which magnifies the existing inflammatory response by amplifying ROS production [94].

Second, the chronic inflammation and demyelination cause a redistribution of the ion channels in charge of creating electrochemical gradients in order to help to maintain ionic homeostasis [89]. These changes produce differences in energy demand and consumption and, mitochondria also begin to activate compensatory mechanisms as increasing their number or changing localization and shape in order to balance the situation [95]. This happens in parallel with ROS and RNS toxic environment that leads to a significant accumulative impairment in energy production by these organelles [95].

INTRODUCTION

Third, extracellular glutamate concentration increases due to neuronal injury and increased production by macrophages and microglia, causing excitotoxicity [87,96]. Glutamate excitotoxicity, ion channels redistribution and mitochondria impairment promote an ionic imbalance [89]. When ATP production is compromised, sodium is accumulated at high concentration inside the axon, which leads a transfer of calcium inside the cell. This accumulation of calcium activates calcium dependent proteases, which drives to axonal damage [95,97].

This axonal damage occurs during the entire MS disease course [98] and might be spread in an anterograde or retrograde manner from the initial site of axonal injury [89]. In addition, it might also promote trans-synaptic degeneration in distant neurons eventually leading to neuronal apoptosis or necrosis [87].

All these processes might occur in parallel and create a vicious cycle where chronic inflammatory state is perpetuated and mitochondria dysfunction and ionic imbalance result in the final outcome of axonal and neuronal damage. However, although neurons and axons have limited potential for regeneration, shadow plaques are the evidence that myelin could be repaired during remyelination [99].

Briefly, adult oligodendrocyte progenitors close to a plaque are activated in response to the demyelinating insult, expanded and they migrate to the damaged area, where they will undergo differentiation to be able to form new myelin sheaths. These new sheaths are often thinner than the ones formed during normal myelination in the development [100]. Remyelination typically fails in MS patients and it is not enough to compensate for the ongoing demyelination in MS [99]. As myelin is necessary for the metabolic axon support and allows the quick transmission of action potentials through the axon, remyelination therapies might limit the progressive degeneration and restore function [100].

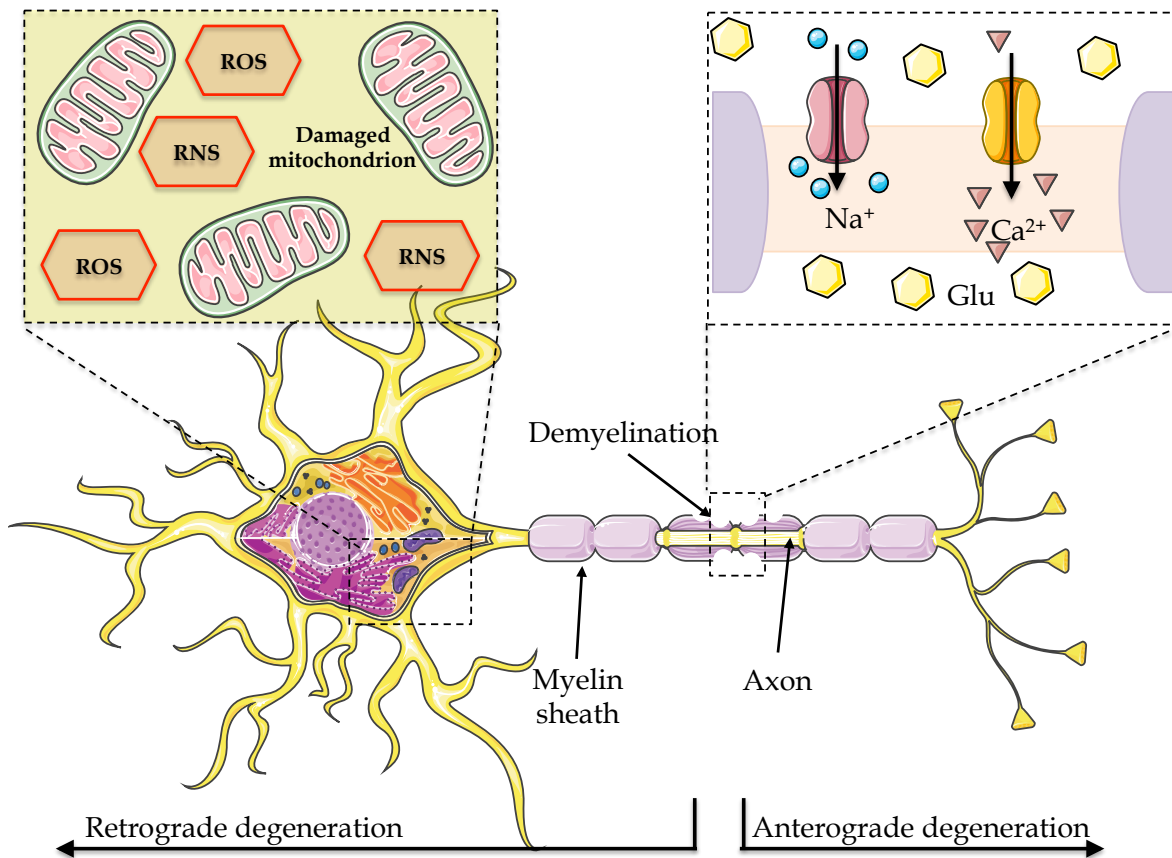


Figure 3. Key neurodegenerative processes as a consequence of chronic inflammation. Chronic inflammation in MS leads to the production of reactive oxygen species (ROS) and reactive nitrogen species (RNS), promoting damage in mitochondria. The redistribution of different ion channels in the axon, along with the excess of glutamate, promotes an ionic imbalance that drives to tissue damage perpetuation. In addition, these mechanisms might be propagated backwards towards the cell body or towards the axon terminal. Muñoz-San Martín (2021).

1.1.6 Diagnosis and treatment

Different clinical criteria have been continuously evolving since 1950 to make the diagnosis of MS, improving sensitivity and specificity until the definition of the current McDonald criteria 2017 [2]. However, in 2016, when samples employed in this doctoral thesis were categorized, the McDonald criteria 2010 were used by clinicians to diagnose MS. Some changes were introduced in the transition from 2010 to 2017 criteria: CIS patients with dissemination in space and positive

INTRODUCTION

oligoclonal IgG bands (OCGB) are diagnosed with MS and symptomatic and cortical lesions could be used to demonstrate dissemination in space [101].

MS diagnosis is mainly supported by medical history and neurological examination. It is based on the demonstration of the dissemination of lesions over time and located at different regions of CNS [60]. MS lesions present specific characteristics regarding MRI signal, shape and location and usually appear as multifocal areas of increased signal located in periventricular, juxtacortical and infratentorial regions of the brain and the spinal cord. The intravenous administration of an agent containing Gd is used to distinguish active from inactive MRI lesions as signal enhancement corresponds to areas with active inflammation [60]. Another important examination usually employed during MS diagnosis is the analysis of CSF. In addition, electrophysiological tests as visual evoked potentials and somatosensory evoked potentials might be used if necessary [4]. It is very important to rule out other immunological, infectious or neoplastic diseases to make a final diagnosis of MS.

Regarding therapeutic options, current treatments for MS are designed to: manage relapses, manage ongoing symptoms and modify the course of the disease [102]. On the one hand, the use of anti-inflammatory agents as steroids is the usual way to treat acute exacerbations or relapses [103]. These drugs enable a quicker functional recovery [60]. On the other hand, there is a multitude of different complex symptoms associated with MS that might affect the quality of life of the patients and their relatives [104]. There are some treatments aimed at relieving symptoms as walking capability, spasticity, pain, fatigue, paresthesia, sleep disturbances, loss of bowel and bladder control and neuropsychiatric symptoms, but their clinical efficacy is still weak [60,105].

Since the first approved DMT for MS in 1993, the number of drugs with different efficacy-risk profiles has exponentially increased in the recent decades [106]. MS is a complex disease with different pathological mechanisms contributing to the

disease course. Thus, each of these mechanisms could be therapeutically addressed. However, current DMTs act on the immune system, modulating or suppressing immune responses to reduce CNS inflammation, the number of relapses and new inflammatory lesions in MRI [107] (Table 2). In addition, most are indicated in the treatment of RRMS, showing none or little efficacy in PPMS and SPMS due to the lack of understanding of underlying mechanisms, inappropriateness of patients included in clinical trials and, failures in clinical and imaging outcomes [108].

However, some potential agents with neuroprotective and remyelinating effects have been identified and some of them are currently in Phase I-II-III clinical trials (Table 3) [60].

Table 2. DMTs for multiple sclerosis approved by EMA.

Generic name	Trade name	Administration	Mechanism of action	Indication	Approval year*
IFN β -1b	Betaferon®/Extavia®	SC	Immunoregulatory activity	RRMS/SPMS	1995/2008
IFN β -1a	Avonex®/Rebif®	IM/SC	Immunoregulatory activity	RMS	1997/1998
Mitoxantrone	Novantrone®	IV	Inhibition of lymphocyte proliferation	RMS	1998
Glatiramer acetate	Copaxone® 20/40 mg	SC	Immunomodulatory activity	RMS	2004/2015
Natalizumab	Tysabri®	IV	Binding to integrin α 4 β 1 expressed in lymphocytes, blocking the interaction with VCAM-1 and avoiding lymphocyte migration through BBB	RRMS	2006
Fingolimod	Gilenya®	Oral	Functional antagonist of S1P receptor in lymphocytes, blocking their ability to leave the lymph nodes	RRMS	2011
Teriflunomide	Aubagio®	Oral	Immunomodulatory activity	RRMS	2013
Dymethilfumarate	Tecfidera®	Oral	Immunomodulatory activity	RRMS	2014
Alemtuzumab	Lemtrada®	IV	Binding to CD52, present in lymphocytes, promoting antibody-dependent cellular cytolysis	RRMS	2013
PEG-IFN β -1b	Plegridy®	SC	Immunoregulatory activity	RRMS	2014
Cladribine	Mavenclad®	Oral	Nucleoside analog of deoxyadenosine, inducer of apoptosis	RMS	2017
Ocrelizumab	Ocrevus®	IV	Binding to CD20 lymphocytes, promoting antibody-dependent cellular cytolysis	RMS/PPMS	2018
Siponimod	Mayzent®	Oral	Functional antagonist of S1P receptor in lymphocytes, blocking their ability to leave the lymph nodes	SPMS	2020

EMA: European Medicines Agency; IFN: interferon; PEG: polyethylene glycol; SC: subcutaneous; IM: intramuscular; IV: intravenous; VCAM-1: vascular cell adhesion molecule-1; BBB: blood-brain barrier; RRMS: relapsing-remitting multiple sclerosis; RMS: relapsing multiple sclerosis; SPMS: secondary progressive multiple sclerosis; PPMS: primary progressive multiple sclerosis. * Approval year by EMA. Information was retrieved from the website of Medicine Online Information Center of the Spanish Agency for Medicines and Health Products (2020) [109].

Table 3. Clinical trials targeting remyelination.

Compound	Mechanism of action	Clinical trials	Results
Anti-Nogo-A antibody	Blocking inhibitory signals for neurite growth/differentiation	Phase I	Well tolerated
Olesoxime	Targeting mitochondrial permeability transition pore	Phase 1b	Well tolerated
rHIgM22	Promoting OPCs differentiation	Phase I	Well tolerated
Clemastine fumarate	Anti-histaminic, OPCs differentiation	Phase II	Reduced VEP latency
GSK239512	Histamine H3 receptor antagonist	Phase II	Small effect on MTR
Opicinumab	Anti-LINGO1 monoclonal antibody enhancing OPCs differentiation	Phase II	No significant difference in VEP latency, negative for clinical outcomes
Domperidone	Increasing serum prolactin	Phase II	Results pending
Bexarotene	Retinoid X receptor γ agonist in OPCs	Phase II	Results pending
GnbAC1	Monoclonal antibody against HERV	Phase II	Negative for primary MRI outcome
Fingolimod	Modulation of multiple neuroglial cell responses	Phase III	No assessment of remyelinating activity

OPCs: oligodendocyte precursor cells; HERV: human endogenous retrovirus; VEP: visual evoked potentials; MTR: magnetisation transfer ratio; MRI: magnetic resonance imaging. Table adapted from [110-112].

INTRODUCTION

1.2 BIOMARKERS IN MS

A biomarker is a measurable characteristic that might be used as an indicator of normal biological and pathogenic processes or biological responses to an exposure or intervention, including therapeutic interventions. Some molecular, histologic, radiographic or physiologic characteristics could be considered biomarkers [113]. There are several biomarker subtypes according to their assumed applications such as diagnostic, monitoring, pharmacodynamic/response, predictive, prognostic, safety or susceptibility/risk biomarkers [114].

One of the major challenges in the MS research field is to develop helpful biomarkers to offer a better disease handling for MS individuals [115]. There are some biomarkers such as OCB, MRI, John Cunningham virus (JCV) viral titers, neutralizing antibodies against interferon- β (IFN) or natalizumab that are currently used in the clinical practice [116].

1.2.1 Origin and function of CSF

CSF is an ultrafiltrate of plasma that is around and within the organs of the CNS. It has three main roles: mechanical and supportive, protective and metabolic function [117]. Regarding this last one, it maintains an appropriate chemical environment for the neural tissue. [118].

Adult CSF estimated volume is around 150 ml, with a continuous generation and reabsorption that supposes a complete renovation of CSF every 7.5 hours approximately [119]. Around 80-90% of CSF is secreted by the choroid plexus, whereas the remaining 10-20% is obtained via fluid transport across the BBB. The choroid plexus is composed by highly-vascularised epithelial cells in the ventricles of the brain and the ones surrounding the capillaries form the blood-CSF barrier (BCSFB) that controls its composition [92]. When the balance among secretion, circulation and resorption of the CSF is compromised, its accumulation might cause a condition known as hydrocephalia [120].

The performance of different cellular and biochemical mechanisms at several interfaces between the brain and periphery allows the restricted exchange of molecules between different compartments: the BBB, the BCSFB, the blood-arachnoid barrier and the CSF-brain barrier, which is only present during brain developmental stages [121]. Therefore, these barriers provide a relatively stable environment for CSF [118] that is mainly composed of water (99%) with 1% formed by proteins, ions, neurotransmitters or, glucose [122]. Most proteins, as albumin and IgG, are derived from the serum, passing across BBB and BCSFB; although up to 20% of total CSF protein might be produced by the choroid plexus or derived from CNS. In addition, CSF might contain a small number of T lymphocytes and monocytes with immunosurveillance functions derived from the blood [123].

1.2.2 Study of CSF biomarkers

In order to support the diagnosis of MS, the study of CSF might be employed. Although the obtention of CSF has some disadvantages as the invasiveness, low quantity and the difficulty to make serial measurements, some clinically useful biomarkers in CSF have already been proposed [124]. Besides a basic CSF biochemistry, microbiological test and cytopathological evaluation to rule out other pathologies, OCGB and IgG index are biomarkers that are routinely used to support MS diagnosis.

The existence of a pattern of OCGB in CSF different than in serum, which indicates intrathecal synthesis of OCGB, is found in almost 95% of MS patients [124]. Although they are not MS-specific, they support the diagnosis and have been recently introduced in the updated version of McDonald criteria 2017 [101]. CSF and serum samples are analyzed in parallel by isoelectrofocusing (IEF) to determine its intrathecal synthesis [125]. Intrathecal synthesis of IgG is associated with the conversion from CIS to MS [126] and Expanded disability status scale (EDSS) progression after four years [127].

INTRODUCTION

The IgG index is a calculation that describes the ratio between IgG and albumin in CSF and serum, and might be used to quantify intrathecal synthesis of IgG [128]. Approximately 70% of MS patients present an elevated IgG index [124].

Apart from these diagnostic biomarkers, JCV antibody titers and/or JCV DNA in CSF and blood are necessary for monitoring possible therapeutic side effects [124]. JCV is a human polyomavirus that usually infects to 70% to 90% of people during childhood and adolescence. In immune-compromised individuals, the virus might reactivate and migrate to the brain where it could cause a progressive multifocal leukoencephalopathy (PML), a severe infectious disease [129]. Some immunosuppressive therapies in MS might lead to viral reactivation. Natalizumab is the MS therapy with the higher risk of PML, whose frequency increases with treatment duration and previous immunosuppressive status [130]. Other DMTs, as fingolimod, dimethylfumarate, ocrelizumab among others, have been also associated with PML infection. Therefore, a careful monitoring of serum antibodies and viral DNA is required and, although it could be made in blood, some studies really encourage to perform CSF analysis due to lack of uniform correlation between serum and CSF titers [131].

There are other promising biomarkers that are not being used in routine clinical practice yet. CSF NF-L levels have been associated with disability and radiological markers of inflammation and CSF chitinase-3-like 1 (CHI3L1) levels have been related to neurological disability in RRMS [132]. Neurofilaments are components of the neuronal cytoskeleton and their detection in CSF and blood has been studied for years and related to neurodegeneration. In MS, NF-L, one of the elements forming neurofilaments, have been extensively examined as a diagnostic, disease activity and therapy response biomarker [128]. CHI3L1 is a glial activation marker predominantly expressed in reactive astrocytes. Its physiological role is unknown but increased CSF levels have been associated with conversion from CIS to MS and faster progression [129].

Lipid-specific oligoclonal immunoglobulin M (IgM) bands (LS_OCMB) in CSF are present in about 40% of MS patients [133]. They might predict a more adverse long-term outcome in MS patients [134] and be a biomarker for inflammatory PPMS patients [135]. In addition, they are associated with higher risk of conversion from CIS to MS [136,137] and future MRI activity [138–140].

Kappa free light chains and kappa free light chains index have been proven to be more sensitive but less specific than LS_OCGB for MS diagnosis. It has been proposed as a prognostic biomarker of CIS conversion to MS [128].

There are some other biomarkers in CSF that require further validation such as increased levels of nitric oxide metabolites, osteopontin, myelin basic protein, C-X-C motif ligand 13, matrix metalloproteinase-9, glial fibrillary acidic protein or, neuronal cell adhesion molecule for assuring disease activity [128] and MIP-1 α and CXCL10 for diagnosis [141].

1.2.3 Other biomarkers in MS

MRI is the most important established clinical tool for MS diagnosis, disease activity, monitoring treatment efficacy and recognition of adverse effects derived from the therapies [60]. MRI offers a wide range of parameters such as the existence of Gd⁺ or new T2 lesions that could be used to assure disease activity [129] or measurements of brain atrophy that have been correlated with long-term disability [60].

Another technique that could predict conversion of CIS individuals into MS is the optical coherence tomography, which generates high-resolution images from the retina [60].

The search of potential biomarkers in blood is a flourishing research area in MS. Its obtention is safer and easier than CSF, different timepoints could be easily analyzed and larger quantities can be obtained [124].

INTRODUCTION

Nowadays, there are some blood biomarkers that are routinely used in clinical practice. Neutralizing antibodies might be formed in response to the administration of some drugs and they can be measured in serum to identify poor therapy response. Specifically, neutralizing antibodies against IFN and natalizumab are molecular biomarkers associated with a reduced efficacy of the therapy [124]. In addition, as explained in previous section, measurements of JCV antibody titers could be also assessed in blood samples to monitor therapeutic side effects risk [129].

Due to the convenience of using blood and as long as sensitive technological platforms are being increasingly developed, the viability of identifying soluble biomarkers in blood has also bursted [141]. At this time, serum NF-L levels can be measured sensitively and reproducibly and could be considered a marker of neurodegeneration. Moreover, its concentration correlates with disability and MRI measures and might predict the course of the disease and the response to therapy [142].

1.3 EPIGENETICS

MS course is modulated by the relationship between environmental factors and genetic susceptibility. Epigenetics is the way of translating environmental signals into changes in gene expression [143]. The British biologist Conrad Waddington was the first in introducing the term in 1942 [144] and since then, many scientific advances have been made in this area, including the first approval of an epigenetic drug in 2004, 5-azacitidine [145].

1.3.1 Definition

Epigenetics could be defined as stable and heritable changes in gene expression without permanent modification of the DNA sequence [146,147]. Epigenetics mechanisms are vitally important for controlling normal physiological processes like cell cycle or the generation of the different cell types in the developing brain

[143]. Due to the fact that epigenetic changes are preserved during mitosis [146], epigenetic signatures are cell and tissue specific allowing to characterize cellular and functional specificity in each tissue in spite of sharing the same DNA sequence [143]. In addition, as epigenetic patterns can vary in different conditions, multitude of studies have been carried out to decipher changes associated with disease [148].

1.3.2 Epigenetic mechanisms

The major epigenetic mechanisms are DNA methylation, histone modifications and non-coding ribonucleic acids (RNA) (ncRNAs) [147].

One of the best-studied epigenetic modifications is DNA methylation, traditionally associated with transcriptional repression [143]. It was in 1975 when Riggs, Holliday and Pugh proposed that DNA methylation might act as an epigenetic mark [149,150].

This process consists in the addition of a methyl group to the 5-carbon of cytosine nucleotides by the action of enzymes known as DNA methyltransferases [147]. Usually this methylation occurs when a cytosine is followed by a guanine, a CpG site. These CpG sites can be found singly or in group of up to several hundred forming CpG islands that frequently occur at promoter regions of genes [146].

When DNA is unmethylated, transcription factors are able to bind to the DNA, which results in expression of that specific gene [147]. However, the methylation of CpG islands associated with a gene usually leads to transcriptional repression [146], as it interferes with sequence recognition by transcription factors [143]. Methyl-CpG binding domain proteins also bind to the methylated nucleotides, forming compact and inactive chromatin [147].

Stedman and Stedman suggested in 1950 that the histones might act repressing gene expression. Histones are proteins that are fundamental for chromatin packaging as they conform the scaffold of DNA [146]. There are 147 base pairs of

INTRODUCTION

DNA that wrap around an octamer of histones, formed by dimers of the histone proteins H2A, H2B, H3, and H4, shaping the nucleosome, the basic unit of chromatin [143].

Histones have areas with high content of lysine and arginine residues that might be subjected to different post-translational modifications. These modifications regulate the structure of chromatin and are associated with the activation or repression of nearby genes [146]. The addition or removal of an acetyl group to lysine mediated by the enzymes acetyl transferase or deacetylase, respectively, is the best characterized histone modification [146]. However, there are some other modifications such as methylation, citrullination, sumoylation, and ubiquitination [143,147].

Finally, the remaining epigenetic mechanism corresponds to ncRNAs, functional RNA molecules that are transcribed from almost every element of the genome and are not translated into proteins [151]. ncRNAs have a wide ability to modulate gene expression and have been related to brain development and neurological disorders [143]. The most studied type of ncRNAs are miRNAs, molecules whose origin, function and involvement in MS will be further explained in the next sections. Apart from miRNAs, other ncRNAs with regulatory roles include small interfering RNAs (siRNAs), Piwi-interacting RNAs (piRNAs), circular RNAs (circRNAs) and, long non-coding RNA (lncRNAs).

siRNA are RNA fragments of 19-24 nucleotides derived from long double-stranded RNA (dsRNA) molecules that might lead to transcriptional gene silencing [152]. piRNAs are a class of 26-31 nucleotide RNA molecules that bind to Piwi proteins under physiological conditions. They might have important roles in epigenetic regulation [152] and are thought to be indispensable for fertility as they are predominantly found in animal gonads [153]. circRNAs are a class of ncRNAs that are linked by a covalent bond forming a closed structure [154]. They have a unique ability to control several miRNAs by blocking their activity [155]. lncRNAs

are a group of transcripts exceeding 200 nucleotides in length, which are located in the nucleus or cytoplasm [152]. They could participate in several biological processes as transcription, splicing, protein localization, proliferation and apoptosis [156].

DNA methylation, histone modifications and ncRNAs might act coordinated to reinforce the regulation of gene expression. For instance, miRNA expression might be regulated by DNA methylation and histone modification in the same way that miRNA could directly target enzymes involved in DNA methylation and histone modification processes [157].

1.3.3 Epigenetic studies in MS

Epigenetics marks might have functional roles as biomarkers, providing information about metabolic pathways and/or new putative therapeutic targets. There are two major projects (ENCODE and Roadmap Epigenomics project), whose objectives are creating public catalogues with functional elements from human genome and epigenome in order to have reference datasets for future research [158,159]. In addition, there are plenty of individual studies trying to figure out specific epigenetic marks or modifications in the framework of MS.

DNA methylation patterns have been analyzed in some studies involving MS-discordant monozygotic twins. The first one carried out by Baranzini *et al.* in 2010 barely found differences in the methylation signatures that could explain the discrepancies in MS onset between siblings [160]. On the other hand, a more recent study identified and validated two MS-associated differentially methylated positions in peripheral blood mononuclear cells (PBMCs) and one in CD4 + T cells [161].

Some studies have reported differential DNA methylation pattern in CNS tissues. In pathology-free areas derived from human MS and control brains, genes regulating oligodendrocyte survival expressed at decreased levels in MS brains

INTRODUCTION

due to hypermethylation [162]. In addition, DNA methylation in MS hippocampus is causing altered gene expression [163]. As it was previously mentioned, epigenetic mechanisms are cell-specific and this was corroborated in the study of Maltby *et al.* where the methylation pattern in CD8⁺ T cells was found different from the one in CD4⁺ T cells [164]. Differential DNA methylation profiles could be detected in cell-free plasma DNA from MS patients (relapse and remission) and healthy volunteers, highlighting their role as non-invasive biomarker [165].

MS patients might exhibit an hypermethylation in repetitive elements as *LINE-1* compared to healthy controls with an association with the degree of EDSS score [166]. This finding has been validated in independent studies. Pinto-Medel *et al.* found an association between higher levels of *LINE-1* methylation and increased risk of developing MS or presenting clinical activity [167]. Another study confirmed that the methylation level in the *LINE-1* promoter is elevated in DNA from serum of RRMS patients compared to controls [168].

Another one performed by Castro *et al.* clearly showed the interaction between environmental factors and epigenetic mechanisms, as high body mass index, had a negative impact on MS course by modulating monocyte cell number through DNA methylation [169]. In addition, it might also affect genetic variants associated with MS risk as differential methylation profiles have been identified in an alternative promoter of the *VDR* gene [170] and *IL2RA* in PBMCs [171].

Epigenetic mechanisms work together to modulate gene expression. On the one hand, DNA methylation and histone modifications are crucial to initiate the differentiation of progenitors into mature myelin-forming oligodendrocytes and to elicit pro-inflammatory functions in immune cells [172]. On the other hand, two studies have related miR-21 levels in MS to DNA hypermethylation marks [173,174].

Several histone modifications have been shown to be involved in different biological processes related to MS pathogenesis such as regulation of CD4⁺ T cells and Th17 T cells differentiation or neurodegeneration [175]. In addition, a study made by Pedre *et al.* analyzed histone modifications in early and chronic MS lesions and, interestingly, they showed that histone deacetylation mainly occurs at the early stages of the disease whereas a shift toward acetylation could be observed in the white matter of aged subjects and chronic MS lesions [176].

Regarding ncRNAs, siRNAs might have potential in the future as therapeutic agents by repressing the expression of specific genes [177]. Specifically in MS, the down-regulation of TRIF by a specific siRNA could alleviate experimental autoimmune encephalomyelitis (EAE) severity decreasing the release of interleukin and cytokines [178].

As new evidences suggest that piRNAs might play roles in neurons and be involved in axon regeneration, behaviour or memory formation, new studies with the aim of deepening the knowledge of neuronal PIWI-piRNA pathways are required to potentially provide precise targets for therapeutic applications in neurodegenerative diseases as MS [179].

The first published study analysing circRNA in MS found an upregulated circRNA in the PBMCs of RRMS patients when alternative splicing abnormalities in *GSDMB* gene were studied [180]. Later, Iparraguirre *et al.* revealed the down-regulation of two different circRNAs in peripheral blood leukocytes from MS patients compared to healthy controls [181]. It is still unknown their role in MS pathology, but the data encourage their study as blood biomarkers [182]. Another study identified 18 circRNAs derived from MS-associated genes [183]. Finally, Zurawska *et al.* discovered differential expression of circRNAs in immune cells of RRMS patients compared to controls, highlighting a pathway involved in the polarization of the immune response toward Th17 and inflammatory-mediated demyelination [155].

INTRODUCTION

One interesting study carried out by Cardamone *et al.* joined observations of two types of ncRNAs, as they described an upregulation of the lncRNA MALAT1 in MS patients that produced backsplicing of circRNAs and splicing abnormalities of some MS-associated genes (IL7R, SP140) [184]. Different studies have analyzed the potential role of lncRNAs in MS as specific biomarkers for disease course or treatment response [182]. Santoro *et al.* identified three upregulated lncRNAs in the serum of RRMS patients [185]. Then, the presence of another three upregulated and three down-regulated lncRNAs in PBMCs of MS patients was described [186]. Eftekharian *et al.* also identified another three deregulated lncRNAs in the circulating blood cells of RRMS patients [187]. Four lncRNAs from a total of eight candidates were significantly differentially expressed, allowing the differentiation of phenotypic severity in MS [188]. Despite the lack of consensus on the results, their potential role as biomarkers is clearly demonstrated. In addition, several studies have also highlighted the involvement of lncRNAs in different MS processes as M2 polarization or remyelination [182].

1.4 microRNAs

1.4.1 Definition

miRNAs are small ncRNAs evolutionarily conserved whose mature and biologically active form comprises 18-25 nucleotides long [189-191]. miRNAs regulate gene expression posttranscriptionally through a mixture of translational inhibition and promotion of messenger RNA (mRNA) decay [192]. Approximately, miRNAs regulate 30% of the human protein-coding genome, controlling the expression of genes with important roles in different biologic processes such as apoptosis, differentiation or proliferation [193]. It has been shown that a single miRNA might regulate the expression of many different target genes [191].

In 1993, Lee *et al.* found that the transcript from *Caenorhabditis elegans* gene *lin-4* were not translated into an active protein and gave rise to a small RNA that was

processed from a longer hairpin precursor. This small RNA was involved in repressing the production of LIN-14 protein, an essential element for larval transition, via an antisense RNA-RNA interaction in the 3' UTR [194,195]. This model of regulating gene expression was first thought to be a nematode peculiarity [192], as another small RNA essential for the transition from larva to adult, let-7, was described in *C. elegans* in 2000 [196,197]. However, it was discovered the existence of homologues of this gene in other invertebrate and vertebrate organisms, including humans, and multiple different miRNAs were identified [198–200]. Since then, the identification of hundreds of small RNAs that derived from hairpin structures in plant and animal genomes have settled the foundation to the miRNA field [189,192].

The primary online miRNA repository was established in 2002 and offers information about potential miRNA sequences, annotation, nomenclature and, target prediction information [201]. The current release (version 22.1) updated in October 2018 contains 38,589 entries representing hairpin precursors that express 48,860 mature miRNAs in 271 organisms [202].

1.4.2 miRNA biogenesis

miRNA genes can be located in different sites in the genome. Half of them are estimated to be expressed from non-protein coding transcripts while the rest are mostly located in the introns of the genes [189]. Multiple sequential steps mediate the biogenesis of miRNAs. Long primary miRNA transcripts (pri-miRNAs) are initially transcribed by RNA polymerase II [203]. These pri-miRNAs are characterized by having a length of several hundreds nucleotides with a 5' guanosine cap and a 3' polyadenylated tail [189]. Then, pri-miRNAs are processed into 70-120 nucleotides hairpin structured RNAs, known as precursor miRNAs (pre-miRNAs), by the Microprocessor complex in the nucleus. This complex is formed by the RNase III enzyme Drosha and DiGeorge syndrome critical region 8 (DGCR8), the dsRNA binding protein [204]. The enzyme Drosha is highly

INTRODUCTION

conserved in animals but not in plants [189]. DGCR8 recognizes motifs within the pri-miRNA, while Drosha makes the cleavage at the base of the characteristic hairpin structure [205].

Following Drosha processing, pre-miRNA is then exported into the cytoplasm by the complex exportin-5(XPO5)/RanGTP [206]. In the cytoplasm, pre-miRNAs are processed into mature 18-25 nucleotide-long duplexes involving the removal of the terminal loop. This process is mediated by the RNase III enzyme, Dicer, with several Dicer-associated proteins, including dsRNA-binding proteins, protein kinase RNA activator and transactivation response RNA binding protein [189,203].

Both strands are named according to directionality: 5p would correspond to the 5' end of the pre-miRNA hairpin and 3p to the 3' end. The two 5p and 3p strands are separated and one might be loaded into the catalytic Argonaute (AGO) family of proteins (AGO1-4) in an ATP-dependent manner. The selection of 5p or 3p strand is usually based on 5' instability or the presence of 5' uracil, and this loaded strand is termed the *guide* strand. The unloaded strand is called the *passenger* strand [205].

This *guide* strand associates with AGO proteins and other RNA binding proteins, forming a microribonuclear protein complex that is known as RNA-induced silencing complex (RISC) [189]. The formation of RISC stabilizes both AGO proteins and miRNAs [203]. The *passenger* strands of miRNA are usually degraded by cellular machinery [205] or, in some occasions, they might be associated with AGO proteins, which makes both strands to be functional miRNAs [189]. This whole process is known as the canonical pathway of miRNA biogenesis (Figure 4). However, multiple non-canonical miRNA biogenesis pathways have been also described. These non-canonical pathways might be grouped into Drosha/DGCR8-independent and Dicer-independent pathways and could use different combinations of the proteins involved in the canonical pathway [205].

In general miRNA abundance is correlated to the rates of primary-miRNA transcription that depends on different elements such as specific transcription factors and enhancers. In addition, post-transcriptional regulation of miRNA biogenesis is also achieved by controlling the machinery involved in biosynthesis [192]. It should be also highlighted that median half-life of the most abundant miRNAs might be 11.4 hours for the *guide* strand and 40 minutes for the *passenger* strand. However, the half-lives of some miRNA duplexes were similar for both strands what indicates a similar load into RISC and functionality [207].

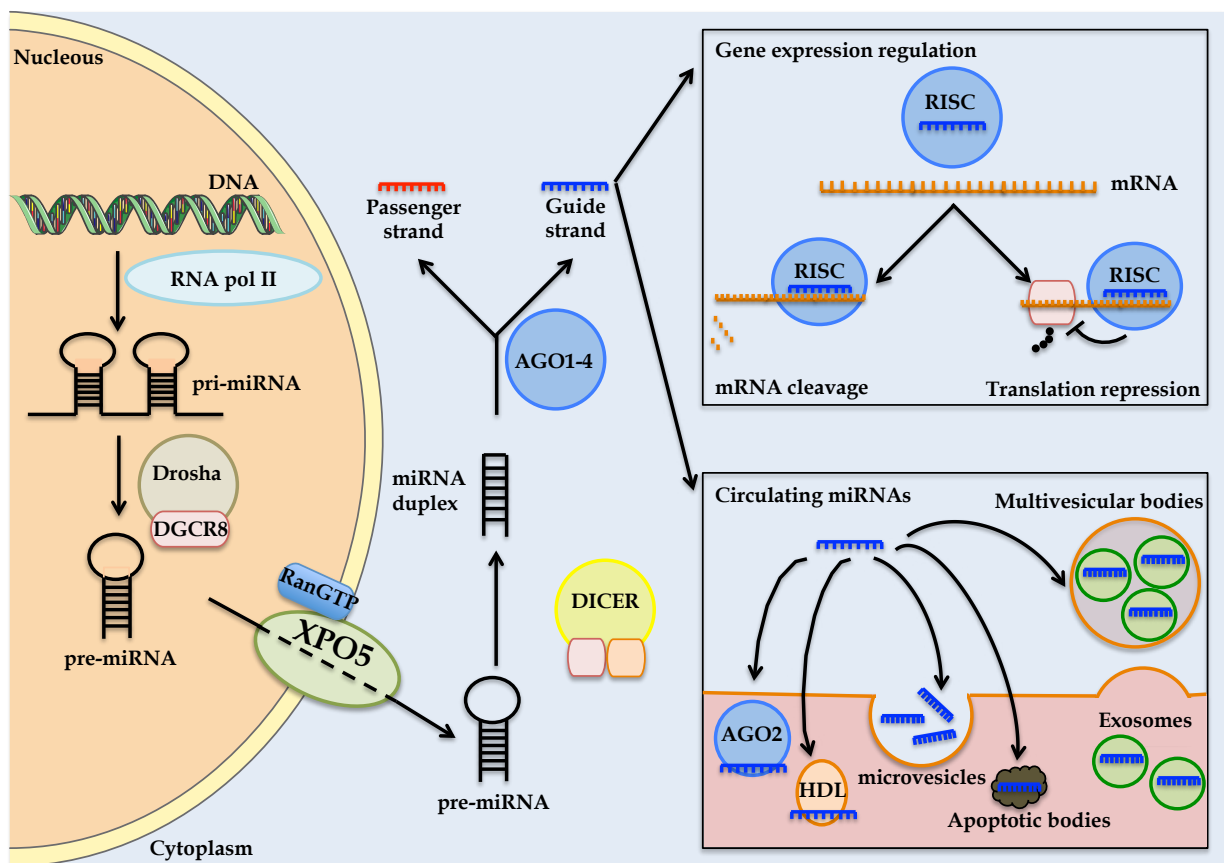


Figure 4. miRNA biogenesis and release of extracellular miRNAs. miRNAs are transcribed as pri-miRNAs in the nucleus, which is later cleaved into pre-miRNA. This precursor is exported to the cytoplasm, where it is processed by DICER to obtain mature miRNA. The guide strand is loaded into RISC to regulate gene expression or released to extracellular space. Muñoz-San Martín (2021).

INTRODUCTION

1.4.3 miRNA function

miRNAs guide RISC to specifically recognize mRNA and gene expression might be regulated by two mutually exclusive posttranscriptional mechanisms, translational repression or mRNA cleavage [208].

Target recognition depends on the miRNA 5' nucleotides 2-8, known as seed sequence [203]; although it has been proposed that the other part of miRNA, specially nucleotides 13-16, might contribute to target recognition [209]. The degree of miRNA-mRNA complementarity determines which regulatory mechanisms will be executed. A high degree of complementarity will lead to mRNA cleavage mechanisms, whereas a central mismatch will facilitate translational repression [208]. Specifically in animals, miRNA-mRNA complementarity is usually imperfect creating an internal bulge structure, so translational repression is the most observed mechanism [190]. There are several canonical site types for miRNA-mRNA interactions that are shown in Figure 5 [209,210]. In addition, there are marginal and atypical sites interaction [210]. miRNAs usually interact with mRNA targets in the 3'-untranslated region (UTR); although the 5'-UTR and protein-coding regions might also contain interaction sites [190]. Due to the shortness of seed sequence, one miRNA could regulate the expression of hundreds of target mRNAs [203].

INTRODUCTION

Recently, it has been proposed that miRNAs could also be present in the nucleus where they might activate gene transcription by targeting enhancers [212]. miR-122, highly abundant in human liver, is likely to facilitate replication of hepatitis C RNA [213].

1.4.4 Circulating miRNAs

Most miRNAs are located inside cells but, there are extracellular miRNAs that might be found in different biological fluids such as plasma, serum, urine or CSF: they are called circulating miRNAs [214]. In contrast to cellular miRNAs, circulating miRNAs are remarkably stable despite the existence of RNases in body fluids and unfavorable conditions due to their association with different molecules [215].

It has been suggested that they are delivered to the extracellular fluids by the passive leakage of apoptosis, necrosis or due to active secretion by cells (Figure 4) [216]. The majority of circulating miRNAs are transported associated with RNA binding proteins such as AGO2. They could also be secreted into circulation associated with lipoprotein complexes including high-density lipoprotein or low-density lipoprotein. Finally, active excretion also includes miRNA encapsulation in lipid or extracellular vesicles, but this method is only responsible for a small portion of circulating miRNAs [217].

Extracellular vesicles could be differentiated by physical and biochemical properties and/or sources [218]. Apoptotic bodies (500 nm–2 µm) are released by dying cells. Microvesicles (100-500 nm) are released by outward budding of plasma membrane and contains cytoplasmic material. Lastly, exosomes (30-100 nm) originate from endosomes and are released upon fusion of multivesicular bodies and the plasma membrane, releasing smaller vesicles [219]. Extracellular vesicles might contain a variety of cargo, including proteins, lipids, DNA, mRNA, and ncRNA as miRNAs [220,221].

In 2007, Valadi *et al.* proposed a novel paracrine mechanism for intercellular communication showing that extracellular miRNAs could be delivered into recipient cells, where they could alter gene expression [222]. Since then, growing evidences have supported the hypothesis of an active, controlled and specific secretion of circulating miRNAs [223]. Moreover, the content of these vesicles is not random and could be influenced by pathologic processes [215,220].

Circulating miRNAs present many properties to be considered as promising biomarkers for different pathological conditions as MS. However, there are fundamental gaps regarding their role in cell-to-cell communication that should be elucidated like excretion and uptake mechanisms or the required concentration to mediate any significant signaling [223,224].

1.4.5 Detection techniques

Conventional employed methods for the miRNA detection are Northern blot, quantitative real-time polymerase chain reaction (PCR) (qPCR), microarrays and Next Generation Sequencing (NGS) [225]. All these methods own unique advantages and shortcomings. Although mostly used methods in miRNA biomarker studies are qPCR and microarrays due to their cost-effectiveness and high reproducibility [226], NGS is also emerging as one of the preferred methods as it offers high sensitivity and allows the detection of new miRNA species [227].

However, considerable efforts have been made to develop new and emerging tools in order to improve miRNA detection. Among them, some methods, techniques and strategies should be mentioned such as nanomaterial-based methods, new nucleic acid amplification-based methods, lateral flow devices, electrochemical biosensors, colorimetric sensing strategies, microfluidic devices and mass spectrometry [225,228].

INTRODUCTION

1.4.6 Methodological challenges

miRNA profiling studies are placed as a great promise for MS biomarker field but it should be remarked that heterogeneous and conflicting results as well as lack of replication among studies are unsolved challenges. Some of the challenges are intrinsic to the complex biology of miRNAs, while others could be overcome with proper planning and funding [220].

Some of the pre-analytical factors that might have influence on miRNA studies are miRNA extraction, type of sample and inter-laboratory variability. First, miRNAs in biofluids could be associated with different proteins or be contained in exosomes or vesicles and the RNA extraction method for all of these components might yield different results. Sometimes, carriers are added during extraction to increase miRNA recovery [229]. In addition, circulating miRNA levels might suffer diurnal variation and be affected by hemolysis [229,230]. The second and a really important factor is the type of sample to be studied. It is widely known that different biofluids such as CSF, urine or serum might present different miRNA content and profiles but, even samples of serum and plasma showed different miRNA concentration affecting the spectrum of extracellular miRNA in blood [231]. Third, some protein studies have shown the existence of inter-laboratory variability that needs to be solved to achieve analytical accuracy [232]. A study carried out by Bargaje *et al.* analysing miRNA variability, showed the existence of variant and invariant miRNAs [233].

There are some analytical factors that might influence the lack of conclusive results. There are no standard endogenous controls for normalization [229], technical replicates for samples of very low miRNA concentration such as CSF should be a requisite [234] and, the choice of the specific methodology for detection should be based in the peculiarities of each study [230]. In addition, retrotranscription (RT) is a process that might produce variability in miRNA quantification [235]. Although preamplification is a step that really improves the

number of detected miRNAs, sometimes it might also increase variability [236,237].

1.4.7 Circulating miRNAs and MS

miRNA studies in MS have gained tremendous attention during the last years as they might provide new insights into disease pathology and therapeutic targets, as well as be promising candidates to be used as biomarkers. miRNA deregulation in MS individuals might be implicated in different processes such as immune cell activation and differentiation, neuronal development and function, formation of adhesion and gap junctions or the regulation of cell cycle and proliferation. Most of the studies have analyzed miRNA expression in blood cells in order to describe signatures in specific immune cells types [151]. Interestingly, five studies have addressed miRNA profiles from dissected WM and GM lesions of MS patients that could offer new clues about lesion development [238]. Most commonly deregulated miRNAs in these studies are miR-142-3p, miR-146a/b, miR-145, miR-155, miR-22, miR-223-3p, miR-326, miR-21 or miR-23a [151,239].

1.4.7.1 miRNAs in CSF

CSF is a really interesting fluid as it might better reflect the level of brain damage [239]. Since 2012, when Haghikia *et al.* published the first analysis of miRNA profiles in CSF [240], a total of 11 studies have been released in the MS field. The major findings of each study are shown in Table 4.

As it could be observed, miR-150 has been found up-regulated in RRMS in three studies [133,241,242], while miR-181c deregulation has been replicated in three other studies [240,243,244]. It should be mentioned that none of the studies have made a profound analysis of PPMS miRNA signatures.

INTRODUCTION

1.4.7.2 miRNAs in other biological fluids

Serum, plasma and urine have the advantage of being less invasive way than CSF to be collected. For this reason, the study of miRNAs in such biofluids has been wider in order to find new biomarkers that might be used for diagnosis, prognosis and assessment of therapy response [245]. The major finding of MS miRNA studies carried out in serum, plasma and urine are shown in tables 5-7.

Some miRNAs have been found deregulated in serum in several independent studies such as miR-23a [246,247], miR-155 [248,249], miR-320b [246,250,251] or miR-326 [248,249]. Specifically, miR-223 deregulation has been replicated in five studies [246,247,252-254]. In plasma studies, miR-22 [255,256], miR-92a [255,257] and, miR-648 [256,258] are the most replicated deregulated miRNAs.

Table 4. miRNA studies in CSF in MS.

CSF	Study	Year	RNA	Comparison	Study design	Major findings	Reference
1	Perdaens <i>et al.</i>	2020	Total RNA	MS (Rel-MS, Rem-MS) vs SC	Profiling and validation phases	MS vs SC: miR-150-5p, miR-155-5p / miR-15a-3p, miR-34c-5p, miR-297. Rel-MS vs Rem-MS or SC: miR-24-3p, miR-27a-3p, miR-27b-3p, miR-29c-3p, miR-125b-5p, miR-145-5p, miR-21-5p, miR-146a-5p. Rel-MS vs SC: miR-124-5p. Rem-MS vs Rel-MS and/or SC: miR-149-3p / miR-20a-5p, miR-33a-3p, miR-214-3p.	[242]
2	Kramer <i>et al.</i>	2019	Total RNA	MS (RRMS, SPMS, PPMS) vs OND	Specific miRNA analysis	MS vs OND: miR-181c, miR-633. SPMS vs PPMS: miR-181c, miR-633. SPMS vs RRMS: miR-181c.	[244]
3	Bruinsma <i>et al.</i>	2017	Total RNA	MS (RRMS, SPMS, PPMS) vs Controls	Specific miRNA analysis	MS vs Controls: Absence miR-219.	[259]
4	Liu <i>et al.</i>	2017	Total RNA	MS (Rel-MS, Rem-MS) vs HC	Specific miRNA analysis	Rel-MS vs Rem-MS and HC: miR-590.	[260]
5	Wu <i>et al.</i>	2017	Total RNA	MS (Rel-MS, Rem-MS) vs HC	Specific miRNA analysis	Rel-MS vs Rem-MS and HC: miR-448.	[261]
6	Mandolesi <i>et al.</i>	2017	Total RNA	RRMS (Gd+ RRMS, Gd- RRMS) vs OND	Specific miRNA analysis	Gd+ RRMS vs Gd- RRMS and OND: miR-142-3p.	[262]
7	Quintana <i>et al.</i>	2017	Total RNA	RRMS (LS_OCMB- RRMS, LS_OCMB+ RRMS) vs OND	Profiling and validation phases	MS vs OND: miR-30a-5p, miR-150, miR-328, miR-645 / miR-21, miR-106a, miR-146a, miR-191, miR-199a-3p, miR-365. LS_OCMB+ RRMS vs OND: miR-30a-5p, miR-150, miR-645 / miR-191.	[133]
8	Lecca <i>et al.</i>	2016	Total RNA	MS (Active MS, Inactive MS) vs OND	Specific miRNA analysis	Active MS vs Inactive MS and OND: miR-125a-3p.	[263]
9	Bergman <i>et al.</i>	2016	Total RNA	CIS (CIS-CIS, CIS-MS) vs RRMS vs NINDC vs INDC	Profiling and validation phases	RRMS vs NINDC and INDC: miR-150. CIS vs NINDC: miR-150. CIS-CIS vs CIS-MS: miR-150.	[241]
10	Ahlbrecht <i>et al.</i>	2016	Total RNA	CIS-CIS vs CIS-MS	Specific miRNA analysis	CIS-MS vs CIS-CIS: miR-181c, miR-922.	[243]
11	Haghikia <i>et al.</i>	2012	Total RNA	MS (RRMS, SPMS, PPMS) vs OND	Profiling and validation phases	MS vs OND: miR-181c, miR-633 / miR-922. RRMS vs SPMS: miR-181c, miR-633.	[240]

MS: multiple sclerosis; Rel-MS: relapsing MS; Rem-MS: remitting MS; SC: symptomatic controls; RRMS: relapsing-remitting MS; SPMS: secondary progressive MS; PPMS: primary progressive MS; OND: other neurological disease; HC: healthy controls; Gd+ RRMS: RRMS individuals with gadolinium-enhancing lesions; Gd- RRMS: RRMS individuals without gadolinium-enhancing lesions; LS_OCMB- RRMS: RRMS individuals with negative lipid-specific oligoclonal IgM bands; LS_OCMB+ RRMS: RRMS individuals with positive lipid-specific oligoclonal IgM bands; CIS: clinically isolated syndrome; CIS-CIS: CIS individuals who remained as CIS; CIS-MS: CIS individuals who converted to MS; NINDC: non-inflammatory neurologic disease controls; INDC: inflammatory neurological disease controls. Green color represents upregulated miRNAs; red color represents downregulated miRNAs. Muñoz-San Martín (2021).

Table 5. miRNA studies in serum in MS.

Serum	Study	Year	RNA	Comparison	Study design	Major findings	Reference
1	Perdaens <i>et al.</i>	2020	Total RNA	MS (Rel-MS, Rem-MS) vs SC	Profiling and validation phases	Rel-MS and Rem-MS vs HC: miR-15a-3p, miR-24-3p, miR-126-3p, miR-146a-5p, miR-181c-5p. Rel-MS vs HC: miR-214-3p.	[242]
2	Hemond <i>et al.</i>	2019	Total RNA	MS	Specific miRNA analysis	miR-22-3p, miR-361-5p, miR-345-5p: most valid differentiators of MRI phenotypes.	[264]
3	Vistbakka <i>et al.</i>	2018	Total RNA	MS (RRMS, PPMS) vs HC	Specific miRNA analysis	RRMS and PPMS vs HC: miR-24-3p, miR-191-5p. PPMS vs HC: miR-128-3p.	[265]
4	Regev <i>et al.</i>	2018	Total RNA	MS (RRMS, SPMS) vs HC	Specific miRNA analysis	RRMS vs HC: miR-484. SPMS vs HC: miR-320a, miR-320b, miR-320c, miR-484 / miR-140-5p, miR-142-5p.	[250]
5	Manna <i>et al.</i>	2018	Exosomes	IFN-b MS vs tnMS	Profiling and validation phases	IFN-b MS vs tnMS: miR-22-3p, miR-660-5p / let-7b-5p, miR-15b-3p, miR-19-3p, miR-23a-3p, miR-26a-5p, miR-122-5p, miR-142-3p, miR-146a-5p, miR-215-5p, miR-223-3p, miR-320b, miR-320d, miR-451a, miR-486-5p.	[246]
6	Wang <i>et al.</i>	2017	Total RNA	Rel-MS vs HC	Specific miRNA analysis	Rel-MS vs HC: ebv-miR-BHRF1-2-5p, ebv-miR-BHRF1-3.	[36]
7	Regev <i>et al.</i>	2017	Total RNA	MS	Profiling phase	miR-142-5p, miR-143-3p, miR-181c-3p, miR-181c-5p: protective correlations with T1:T2. miR-486-5p, miR-92a-3p: pathogenic correlations with T1:T2. miR-375, miR-629-5p: pathogenic correlation with brain atrophy.	[266]
8	Niwald <i>et al.</i>	2017	Exosomes	RRMS vs HC	Specific miRNA analysis	RRMS vs HC: miR-326 / miR-155, miR-301a.	[248]
9	Sharaf-Eldin <i>et al.</i>	2017	Total RNA	MS vs HC	Specific miRNA analysis	MS vs HC: miR-145, miR-223.	[254]
10	Ebrahimkhani <i>et al.</i>	2017	Exosomes	MS (RRMS, PMS) vs HC	Profiling phase	RRMS vs HC: miR-15b-5p, miR-30b-5p, miR-342-3p, miR451a. PMS vs HC: miR-3703p, miR-409-3p, miR-432-5p. RRMS vs PMS: miR-15b-5p, miR-23a-3p, miR-30b-5p, miR-223-3p, miR-342-3p, miR-374a-5p, miR-485-3p / miR-432-5p, miR-433-3p.	[247]
11	Selmaj <i>et al.</i>	2017	Exosomes	MS (Rel-MS, Rem-MS) vs HC	Profiling and validation phases	Rel-MS vs HC: miR-122-5p, miR-196b-5p, miR-301a-3p, miR-532-5p. Rel-MS vs Rem-MS: miR-122-5p, miR-196b-5p, miR-532-5p. Rem-MS vs HC: miR-122-5p.	[267]
12	Vistbakka <i>et al.</i>	2017	Total RNA	PMS (SPMS, PPMS) vs HC	Profiling and validation phases	PPMS vs HC: miR-26a-5p, miR-128-3p, miR-191-5p. SPMS vs HC: miR-26a-5p, miR-191-5p.	[268]
13	Regev <i>et al.</i>	2016	Total RNA	MS (RRMS, SPMS, PPMS) vs HC	Profiling and validation phases	MS vs HC: miR-25-3p, miR-140-3p, miR-320a, miR-320b, miR-486-5p / let-7c-5p, miR-365a-3p. RRMS vs PMS: miR-27a-3p. RRMS vs SPMS: miR-27a-3p, miR-376b-3p.	[251]
14	Ahlbrecht <i>et al.</i>	2016	Total RNA	CIS-CIS vs CIS-MS	Specific miRNA analysis	CIS-MS vs CIS-CIS: miR-922.	[243]
15	Mancuso <i>et al.</i>	2015	Total RNA	MS (Rel-MS, Rem-MS, SPMS, PPMS) vs HC	Specific miRNA analysis	MS vs HC: miR-572. PPMS vs HC: miR-572. Rem-MS vs HC: miR-572. SPMS vs PPMS: miR-572. Rel-MS vs Rem-MS: miR-572.	[269]
16	Zhang <i>et al.</i>	2014	Total RNA	MS (Rel-MS, Rem-MS) vs HC	Specific miRNA analysis	MS vs HC: miR-124, miR-146a, miR-150, miR-155, miR-326. Rel-MS vs Rem-MS: miR-155.	[249]

17	Ridolfi <i>et al.</i>	2013	Total RNA	MS (RRMS, PPMS) vs HC	Specific miRNA analysis	RRMS vs HC: miR-15b, miR-23a, miR-223. PPMS vs HC: miR-15b.	[253]
18	Fenoglio <i>et al.</i>	2013	Total RNA	MS (RRMS, PPMS) vs HC	Specific miRNA analysis	MS vs HC: miR-15b, miR-223. PPMS vs HC: miR-15b, miR-223.	[252]

MS: multiple sclerosis; Rel-MS: relapsing MS; Rem-MS: remitting MS; SC: symptomatic controls; RRMS: relapsing-remitting MS; PPMS: primary progressive MS; HC: healthy controls; SPMS: secondary progressive MS; tnMS: treatment-naive MS individuals; PMS: progressive MS; CIS-CIS: CIS individuals who remained as CIS; CIS-MS: CIS individuals who converted to MS. Green color represents upregulated miRNAs; red color represents downregulated miRNAs. Muñoz-San Martín (2021).

Table 6. miRNA studies in plasma in MS.

Plasma	Study	Year	RNA	Comparison	Study design	Major findings	Reference
1	Kimura <i>et al.</i>	2018	Exosomes	MS vs HC	Profiling and validation phases	MS vs HC: let-7c, miR-19b, miR-25, miR-92a.	[257]
2	Sáenz-Cuesta <i>et al.</i>	2018	Extracellular vesicles	MS (Before and after fingolimod treatment)	Profiling phase	Change of miRNA cargo after fingolimod treatment	[270]
3	Kacperska <i>et al.</i>	2015	Total RNA	MS (Rel-MS, Rem-MS) vs HC	Specific miRNA analysis	Rem-MS vs HC: let-7a, miR-648a.	[258]
4	Giovannelli <i>et al.</i>	2015	Exosomes	MS (RRMS, Ntz-RRMS) vs HC	Specific miRNA analysis	No differences in Polyomavirus JC miRNAs	[271]
5	Gandhi <i>et al.</i>	2013	Total RNA	MS (RRMS, SPMS) vs HC	Profiling and validation phases	RRMS vs HC: miR-22, miR-30e, miR-140-3p, miR-210, miR-500, miR-547-3p. SPMS vs HC: let-7a. RRMS vs SPMS: miR-92a1*, miR-135a, miR-454, miR-500, miR-574-3p.	[255]
6	Søndergaard <i>et al.</i>	2013	Total RNA	RRMS vs HC	Specific miRNA analysis	RRMS vs HC: miR-145 / miR-660, miR-939.	[272]
7	Siegel <i>et al.</i>	2012	Total RNA	MS vs HC	Profiling phase	MS vs HC: miR-22, miR-422a, miR-572, miR-614, miR-648, miR-1826 / miR-1979.	[256]

MS: multiple sclerosis; HC: healthy controls; Rel-MS: relapsing MS; Rem-MS: remitting MS; RRMS: relapsing-remitting MS; Ntz-RRMS: RRMS individuals treated with natalizumab; SPMS: secondary progressive MS. Green color represents upregulated miRNAs; red color represents downregulated miRNAs. Muñoz-San Martín (2021).

Table 7. miRNA studies in urine in MS.

Urine	Study	Year	RNA	Study design	Comparison	Major findings	Reference
1	Giovannelli <i>et al.</i>	2015	Exosomes	Specific miRNA analysis	MS (RRMS, Ntz-RRMS) vs HC	No differences in Polyomavirus JC miRNAs	[271]

MS: multiple sclerosis; RRMS: relapsing-remitting MS; Ntz-RRMS: RRMS individuals treated with natalizumab; HC: healthy controls. Green color represents upregulated miRNAs; red color represents downregulated miRNAs. Muñoz-San Martín (2021).

2. Hypothesis and Objectives

JUSTIFICATION:

MS is a complex disease and the interrelation between both genetic and environmental factors by means of epigenetic mechanisms still requires further investigations.

To study circulating miRNA signatures in CSF of individuals with different clinical forms of MS might be a first approach to know the epigenetic abnormalities and the pathogenic mechanisms of this neurological disease.

However, due to the invasiveness of the lumbar puncture, specific miRNA profiles in serum or plasma are interesting as they could become non-invasive biomarkers of diagnosis and prognosis.

HYPOTHESIS AND OBJECTIVES

HYPOTHESIS:

The main hypothesis of this doctoral thesis is that circulating miRNA profiles in MS individuals and controls might be different due to pathological events caused by the disease and those changes could be used as biomarkers in MS. Moreover, different clinical subtypes of MS or clinical characteristics could also be associated with specific miRNA profiles.

Specifically, the hypothesis gathered in this thesis are:

- 1. CSF miRNA studies should embrace specific proper analysis methods.**

CSF is a really valuable biofluid as it could mirror events of the CNS. However, it is known that the circulating miRNA content in CSF is much lower than the one found in other biofluids such as serum, plasma or even tears. As a consequence, miRNA profiling studies in CSF might require specific analysis procedures different from the ones established and proposed for other circulating miRNA studies in plasma or serum.

- 2. PPMS patients could present a specific circulating miRNA signature which could elucidate some of the mechanisms involved in neurodegeneration.**

Nowadays, PPMS patients are lacking treatment options unless they have inflammatory events. Most of the new therapeutic options that have emerged in the last years are focused in controlling the inflammation. Studying the circulating miRNA profile of PPMS compared to RRMS and controls, particularly in CSF, could contribute to understand the mechanisms involved in neurodegeneration that might be hidden in the more inflammatory clinical phenotypes of MS.

3. RIS patients might present differential circulating miRNA signatures depending on their conversion to CDMS.

It is known that around a third of RIS subjects could develop a symptomatic demyelinating event and convert to CDMS in the five-year follow-up. The choice of receiving treatment in RIS individuals to avoid or delay their conversion is still controversial. Those individuals who remain as RIS and those who finally convert to CDMS could present a differential circulating miRNA signature at the RIS diagnosis moment, which might be used as prognostic biomarker and help in the decision-making process.

4. Circulating miRNA profiles of RRMS patients could be different according to specific variables.

Some demographic, clinical radiological and environmental variables could be different among RRMS individuals. Similarly, their specific signature in CSF or plasma of cellular or viral miRNAs might vary depending on these variables and might be highly informative indicating which pathways are altered.

HYPOTHESIS AND OBJECTIVES

OBJECTIVES:

The following objectives have been set to test the previously indicated hypothesis:

General objectives:

1. To determine the suitable methodological approach to study CSF miRNAs
2. To study the circulating miRNA signatures in different MS phenotypes

Specific objectives:

1. To determine the suitable methodological approach to study CSF miRNAs
 - 1.1. To describe a specific panel to study CSF miRNAs.
 - 1.2. To propose a suitable flowchart to analyze CSF miRNA data.

2. To study the circulating miRNA signatures in different MS phenotypes
 - 2.1. To describe the circulating miRNA signature in CSF and serum of PPMS patients.
 - 2.2. To compare CSF miRNA deregulation in MS with the one observed during demyelination and remyelination in an organotypic culture model.
 - 2.3. To describe the miRNA signature in CSF and plasma samples of RIS individuals according to their conversion status.
 - 2.4. To study the expression of cellular and viral miRNAs in CSF or plasma of RRMS patients related to demographic, clinical, radiological and environmental variables.

3. Materials and Methods

3.1 STUDY POPULATION

The whole study population, composed by PPMS subjects, RIS subjects, RRMS subjects, subjects affected by other neurological disease controls (OND) and spinal anesthesia subjects (SAS), was divided in different subcohorts for each of the comparative studies made in this doctoral thesis. The inclusion and exclusion criteria for each study, the biological samples used in each case, as well as the characteristics of the specific cohort employed are explained and described in the corresponding Results Section.

Most individuals included were recruited at the Girona Neuroimmunology and Multiple Sclerosis Unit of Dr. Josep Trueta University Hospital (Girona, Spain). In order to increase the number of individuals, more samples were obtained from other units as the Immunology and Neurology departments of Ramón y Cajal University Hospital (Madrid, Spain), Neurology department of Arnau de Vilanova University Hospital (Lleida, Spain), Multiple Sclerosis Unit of Hospital Clínico San Carlos (Madrid, Spain) and Multiple Sclerosis Unit of Hospital Univeristari i Politècnic La Fe (Valencia, Spain).

3.1.1 Biological material

Different biological fluids (CSF, serum and plasma) for most of these subjects were obtained, processed and stored to their further use in the different studies.

CSF samples were obtained at the moment of the diagnosis by means of a lumbar puncture made by a neurologist. In case of SAS, this technique was performed by an anesthesiologist during surgery. After collecting CSF, it was centrifuged at 400 g, 19°C during 15 minutes in order to obtain cell-free CSF.

BD Vacutainer® tubes with separating gel were used to obtain **serum**. These tubes were left at room temperature for at least 30 minutes to let the clot be formed. Later on, tubes were centrifuged at 2000g, 19°C during 10 minutes and serum was extracted.

MATERIALS AND METHODS

BD Vacutainer® tubes with EDTA K2 were used to obtain **plasma and buffy coat** samples. After centrifugation at 2000 g, 19°C during 10 minutes, plasma was collected from the upper phase and the buffy coat gently pipetted.

Once aliquoted, all these biological materials were stored at -80°C until their use in further analyses.

3.1.2 Study variables

The analyzed variables in these studies could be grouped in three main sets: clinical, radiological and biochemical variables.

Clinical variables of individuals were collected by neurologists or nurses during medical visits: age at sampling (years), sex, ethnicity (European or North-African), basal EDSS (0-10) and smoking habits data (never/ever). For those with North-African origin, the age of migration to Europe was also requested.

Different **radiological variables** were analyzed and informed by a specialized neuroradiologist using brain and spinal images obtained by PD, T1, T2, FLAIR and post-Gd T1 sequences in MRI machines of 1.5 Tesla: number of T2 lesions, presence or absence and number of Gd+ lesions, number of spinal cord lesions, presence or absence of atrophy and presence or absence of black holes.

Different **biochemical variables** were determined. **Intrathecal synthesis of OCBG and LS_OCBM** was analyzed by IEF and immunoblotting as previously described [125]. IEF is a technique that separates proteins according to their isoelectric point (pH at which a protein carries no net electric charge). To determine **IgG Index**, quantification of IgG and albumin levels in both serum and CSF samples were required. The following formula was applied to know this index:

$$\text{IgG Index} = \frac{\text{CSF IgG} \times \text{serum albumin}}{\text{serum IgG} \times \text{CSF albumin}}$$

The levels of **CHI3L1 and NF-L in CSF** were studied by enzyme-linked immunosorbant assay (MicroVue YKL-40 EIA Kit, Quidel, Catalogue number: 8020 and; Uman Diagnostics, Catalogue number: 10-7001 CE, respectively) according to the manufacturers' instructions.

LIFECODES HLA-DRB1 SSO Typing Kit (Diagnóstica Longwood, Catalogue number: LC-628923) was used to determine **HLA-DRB1 alleles** in the studied individuals. These kits use specific sequences of oligonucleotides as probes to distinguish among the different alleles. For those individuals presenting at least one allele for HLA-DRB1*15, allelic discrimination for HLA-DRB1*15:01 or 15:03 was made by qPCR using TaqMan™ SNP genotyping assays.

Levels of **25-OH vitamin D** were assessed by electro-chemiluminescence (Elecsys Total Vitamin D, Catalogue number: 05894913190, 2015) and classified into two ranges: 0-20 ng/ml or >20 ng/ml.

Levels of **IgG anti-EBNA1** were quantitatively determined by chemiluminescence (Liaison EBNA IgG, Diasorin, Catalogue Number: 310520).

Semiquantitative determination of **IgG anti-cytomegalovirus (CMV)** was determined by chemiluminescent microparticle immunoassay (Architect CMV IgG, Abbott, Catalogue Number: 6C15-25).

3.2 BIOLOGICAL MATERIAL FROM MICE

Organoid cerebellar brain culture is one *ex vivo* model useful to specifically assess mechanisms of demyelination and remyelination without an inflammatory association [273]. This model presents several advantages as it contains all cells found in CNS in their native form and it is easy and reproducible. It can be used to measure demyelination and remyelination and to test different therapeutic compounds. Briefly, to establish murine organotypic brain slice culture, 300 µm thick slices of brain stem and cerebellum from new-born mice (postnatal day 1-postnatal day 2) were cultured and allowed to myelinate. To induce demyelination, lysolecithin (LPC) (Sigma-

MATERIALS AND METHODS

Aldrich, Missouri) in a concentration of 0.5 mg/ml was added to the culture medium at day 10-14. After 16 hours, LPC was removed and changed by fresh media. Remyelination could be assessed at day 7-14 after LPC treatment.

3.3 ETHICAL CONSIDERATIONS

The Ethics Committee and the Committee for Clinical Investigation from Dr. Josep Trueta University Hospital approved the protocol employed in this doctoral thesis. All participants signed a written informed consent.

The proposed research involving experiments with murine *ex vivo* organotypic brain culture was in accordance with the European Union (EU) legislation on Ethics and performed in the Royal College of Surgeons in Ireland (RCSI) licensed animal facilities. The RCSI Animal Research Ethics Committee granted ethical approval for the experiments verifying that all necessary steps to ensure animals' wellness and life quality were taken and protected. The experiments were performed in fully According to the three principles of "replacement, reduction and refinement" under EU Directive 2010/63/EU.

3.4 RNA EXTRACTION

3.4.1 RNA extraction from human samples

Circulating RNA from biofluids as serum, plasma or CSF can be purified from up to 625 μ l of starting material using the mirVana™ PARIS™ kit (Thermo Fisher Scientific, Massachusetts). The Ambion® PARIS (Protein And RNA Isolation System) technology was used to recover total RNA in the same sample. To optimize the recovery of small RNAs as miRNAs, this kit includes an organic extraction process followed by an immobilization of RNA on glass-fiber filter to ensure the purification of total RNA.

As biofluid samples used were free of cells, no lysis and homogenization steps were needed. The initial volume of sample (300 μ l in most cases) was mixed with the same volume of 2x Denaturing solution containing 375 μ l of 2-mercaptoethanol. At this point, two exogenous miRNAs (cel-miR-39 and cel-

miR-54) were added at 5 pM to assure the quality of the extraction process. Then, the same volume of acid-phenol:chloroform was added, vortexed for 30-60 seconds to mix properly, and centrifuged (17000g, 10 minutes, 19°C) to separate the solution into aqueous and organic phases. The upper, aqueous phase contains RNA, while DNA is contained in the interphase and the proteins are found in the lower, organic phase. The upper phase containing RNA is recovered and deposited in a new tube where is mixed with 1.25 volumes of 100% ethanol. This proportion was changed to 2 volumes of 100% ethanol in CSF samples from RIS study (section 4.5). The addition of ethanol is necessary to provide the appropriate binding conditions to the glass-fiber filter cartridges for all RNA molecules from 18 nucleotides. The mix was then added to the Filter Cartridge placed in the collection tube and after a quick centrifugation of 30 seconds at 8000g, the flow-through was discarded and different washing steps were made in order to remove phenol and other contaminants, while RNA is bound to the membrane. 700 µl of miRNA Wash Solution 1 (working solution mixed with ethanol) were applied to the Filter Cartridge and the collection tube was centrifuged for 15 seconds at 8000g. After discarding the flow-through, 500 µl miRNA Wash Solution 2/3 (mixed with ethanol) were applied to the Filter Cartridge and the collection tube was centrifuged for 15 seconds at 8000g. This step was repeated increasing centrifugation time to 2 minutes and after discarding the flow-through, the Filter Cartridge placed in the collection tube was subjected to a spin for 1 minute to remove residual fluid from the filter. Filter Cartridge was then transferred to a fresh collection tube and total RNA was finally eluted in 40 µl of preheated (95°C) Nuclease-free water (NF water) centrifuging 30 seconds at 8000g. Eluted RNA was stored at -80°C for posterior use.

3.4.2 RNA extraction from mice samples

To obtain RNA from cerebellar organotypic slices culture, a chemical extraction method was used. First, slices should be homogenized adding 500 µl of TRIzol™ (Invitrogen, California) using a syringe. This reagent is a monophasic solution of phenol, guanidine isothiocyanate and, other components that

MATERIALS AND METHODS

facilitates the isolation of a variety of RNA species of large and small molecular size, maintaining the integrity of RNA due to highly effective inhibition of RNase activity while disrupting cells and dissolving cell components during homogenization. The homogenate was centrifuged at 12000g for 10 minutes at 4°C and incubated for 5 minutes at room temperature (RoT). 100 µl of chloroform were added, the mixture was shaken vigorously for 15 seconds and then incubated at RoT for 3 minutes. The samples were centrifuged at 12000g for 15 seconds at 4°C. The resulting aqueous/upper phase was transferred to a fresh tube and 250 µl of isopropanol were added to let RNA to precipitate. After incubating at RoT during 10 minutes and centrifuging at 12000g for 10 minutes at 4°C, the supernatant was removed. RNA was washed with 500 µl of 75% ethanol and the sample was vortexed to completely mix. After centrifuging at 12000g for 5 minutes at 4°C, the supernatant was removed and the rest of ethanol were let to dry completely by opening the lid. RNA was then dissolved in 50 µl of NF water and incubated at 55-60°C during 10 minutes at 800rpm. It was stored at -80°C and, prior to its use in later analysis, its concentration and purity were measured by NanoDrop™ ND-Spectrophotometer (Thermo Fisher Scientific, Massachusetts).

3.5 miRNA DETECTION WITH TaqMan™ ADVANCED miRNA ASSAYS

To analyze miRNA expression in studied samples, the preparation of complementary DNA (cDNA) templates from miRNA was required to obtain more stable material to work with. Later on, these cDNA templates were subjected to qPCR amplification to detect specific miRNAs using TaqMan technology. After using the proper normalization method, the relative quantification (RQ) of miRNAs was calculated to be able to compare their expression between different biological groups.

3.5.1 miRNA cDNA synthesis

The Applied Biosystems™ TaqMan™ Advanced miRNA cDNA Synthesis kit (Applied Biosystems, California, USA) was used in most of the studies described in this doctoral thesis to obtain miRNA cDNA. This kit has been

specially designed to work with materials whose miRNA contents are limited such as serum or plasma. It employs a universal RT chemistry to obtain the cDNA template that will be used for mature miRNA detection and quantification with TaqMan™ Advanced miRNA Assays (see section 3.5.2).

This RT chemistry offers several really valuable features. First, prior to RT reaction, this kit uses 3' poly-A tailing and 5' ligation of an adaptor sequence to expand the mature miRNAs present in the sample on each end. Universal RT primers have been designed to recognize these sequences added at both 3' and 5' ends of mature miRNAs allowing all of them to be reverse transcribed to cDNA. Because of these three sequential steps in the workflow, higher specificity and flexibility are obtained. Later on, cDNA is amplified using the Universal miRNA-Amplification step (miR-Amp) primers that recognize these universal sequences on 3' and 5' ends, ensuring no amplification bias. This step has been designed to allow the quantification of low-expressing miRNA targets, what increases the sensitivity of this workflow. In Figure 6, a scheme of this protocol is shown.

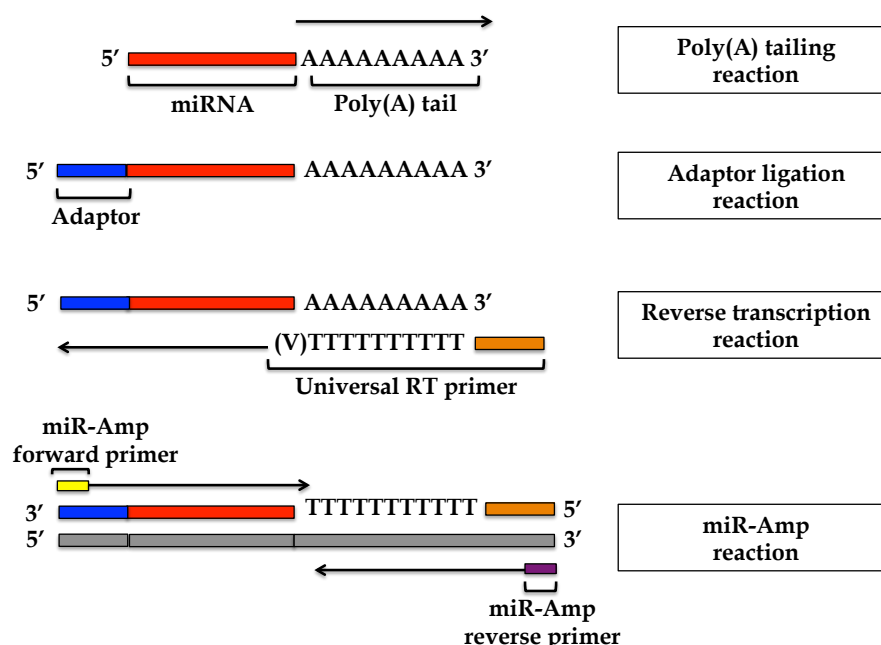


Figure 6. Scheme of Applied Biosystems™ TaqMan™ Advanced miRNA cDNA Synthesis kit workflow. Adapted from TaqMan™ Advanced miRNA Assay User Guide, Applied Biosystems. Publication number: 100027897, Revision: C [274].

MATERIALS AND METHODS

3.5.1.1 Poly(A) tailing reaction

To carry out Poly(A) tailing reaction, all the necessary components depicted in Figure 7a were mixed to prepare the required Reaction Mix. After placing 2 μ l of RNA samples in their corresponding spots in the reaction plate, 3 μ l of Poly(A) Tailing Reaction Mix were added to each sample and carefully centrifuged to obtain an homogenous mixture. The reaction plate was placed into a thermal cycler to be incubated (Figure 7b).

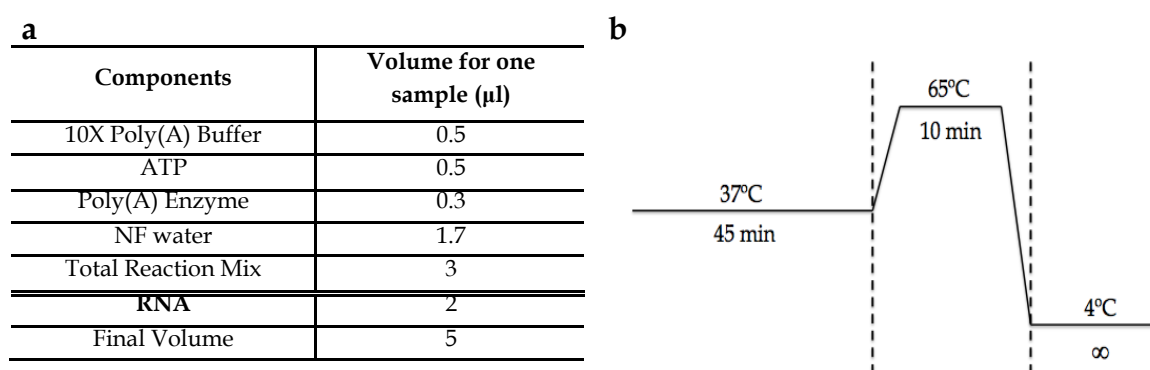


Figure 7. Reaction mix components and thermal cycling conditions for Poly(A) tailing reaction. (a) Components and (b) thermal cycling conditions.

3.5.1.2 Adaptor ligation reaction

To proceed with the Adaptor ligation reaction, the components depicted in Figure 8a were mixed to prepare Adaptor Ligation Reaction Mix. 10 μ l of this solution were added to each Poly(A) tailing reaction product reaching 15 μ l of final volume and carefully centrifuged to obtain an homogenous mixture. The reaction plate was placed into a thermal cycler to be incubated (Figure 8b).

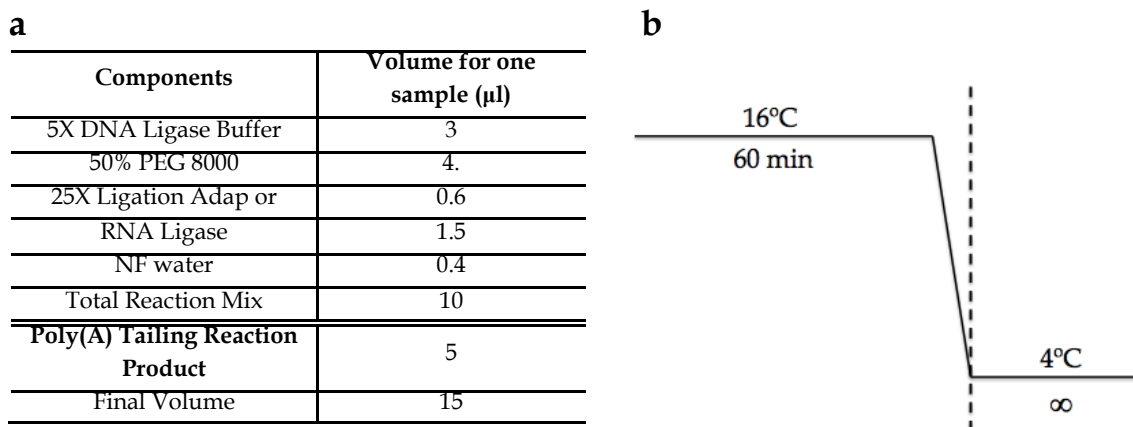


Figure 8. Reaction mix components and thermal cycling conditions for Adaptor ligation reaction. (a) Components and (b) thermal cycling conditions.

3.5.1.3 Reverse transcription reaction

Then, the universal RT reaction was carried out to obtain cDNA from all mature miRNA present in the sample. The preparation of the RT Reaction Mix followed the specifications of Figure 9a and 15 µl of this solution were mixed with each Adaptor ligation reaction product obtaining 30 µl of final volume. The reaction plate was placed into a thermal cycler to be incubated (Figure 9b).

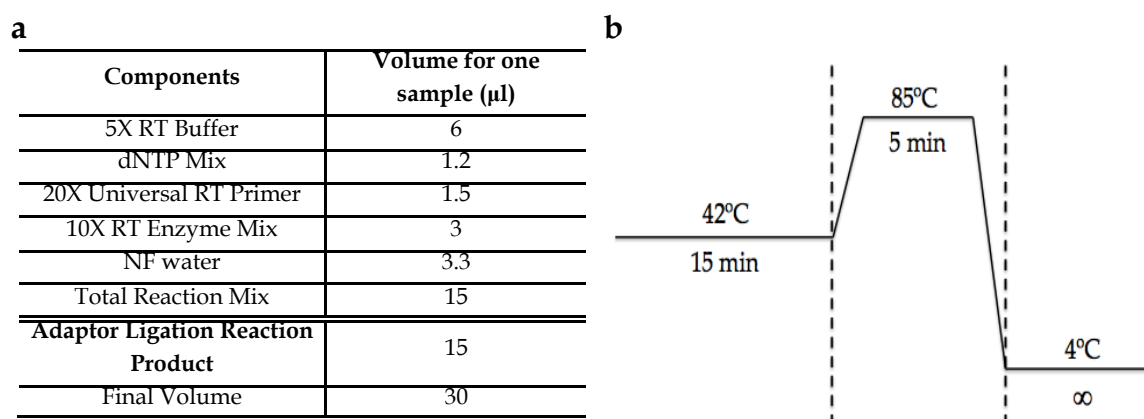


Figure 9. Reaction mix components and thermal cycling conditions for Reverse transcription reaction. (a) Components and (b) thermal cycling conditions.

MATERIALS AND METHODS

3.5.1.4 miR-Amp reaction

miR-Amp Reaction Mix was prepared according to indications depicted in Figure 10a. 45 μl of this mix were transferred to a new reaction plate. 5 μl of RT reaction product were added to reach a final volumen of 50 μl and the reaction plate was carefully centrifuged to obtain an homogenous mixture and placed into a thermal cycler to be incubated (Figure 10b). It should be noted that number of cycles were different depending on the posterior use and/or biological nature of the sample. 22 cycles were needed for preparing samples for profiling studies with OpenArray plates both for serum and CSF samples. For experiments aimed at detecting specific miRNAs by qPCR, 14 cycles were used in serum samples while 22 cycles were retained for CSF samples.

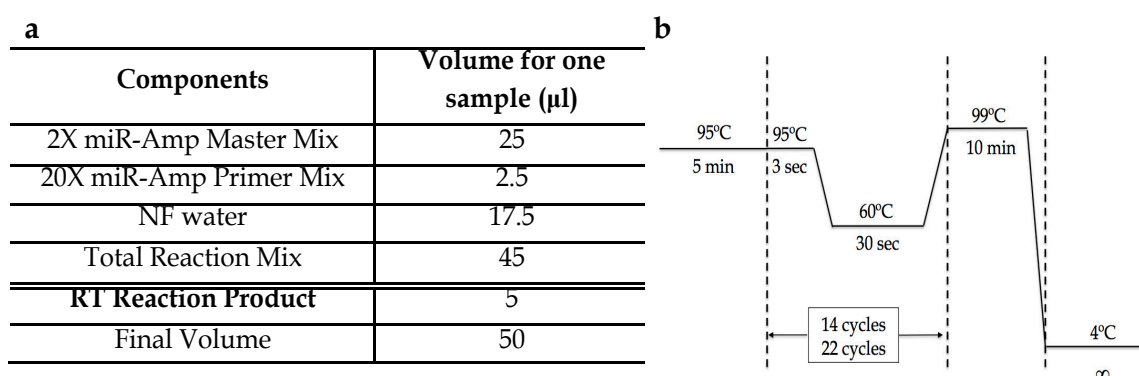


Figure 10. Reaction mix components and thermal cycling conditions for miR-Amp reaction. (a) Components and (b) thermal cycling conditions.

3.5.2 miRNA detection

To analyze miRNA expression in studied samples, cDNA templates were subjected to PCR amplification to detect specific miRNAs. miRNA expression levels were measured in most of the studies of this doctoral thesis using TaqMan Advanced miRNA assays technology. This chemistry is settled in the use of pre-formulated TaqMan hydrolysis probe and primer sets designed to allow the fluorophore-based detection of specific miRNAs during qPCR.

qPCR uses DNA polymerases to amplified miRNA target cDNA in this case, using sequence-specific primers. It is a method that allows the specific, sensitive and reproducible quantification of nucleic acids consisting of three major stages. Denaturation to bring double-stranded cDNA into single strands; annealing to let complementary sequences from primers and probes to hybridize and; extension to elongate new strands.

TaqMan probes are designed to anneal to a complementary sequence of a specific miRNA cDNA. The probes contain: a reporter dye at 5' end of the probe; a non-fluorescent quencher dye at 3' end of the probe and; a minor groove binder at 3' end to increase the melting temperature. When this probe is intact, the proximity between reporter dye and quencher dye suppresses the reporter fluorescence.

On the other hand, this technology also relies on the use of forward and reverse primers that anneals to complementary sequences along the miRNA cDNA templates. The binding sites depend on the target miRNA sequence.

Briefly, the forward and reverse primers anneals to their complementary sequences to allow the polymerization of the strand. Thus, only one specific miRNA will be subjected to the amplification in the reaction tube. TaqMan probe anneals to a sequence between the forward and reverse primers sites. During polymerization, the 5' nuclease assay process occurs to cleave probes that have annealed to miRNA target sequence. This split causes the separation of the reporter dye from the probe, distancing from quencher and increasing its fluorescence. This increase allows to quantify a specific miRNA product as fluorescence level detection is proportional to the number of PCR product molecules generated. Meanwhile, the polymerization of the strand continues and a new cycle of polymerization might be carried out. The cycle at which fluorescence of reporter dye reaches an established threshold (C_q) for each sample and each individual miRNA is measured. In Figure 11, a scheme of the workflow of qPCR with TaqMan Advanced miRNA assays is shown.

Two different approaches were used to quantify miRNA levels in the samples.

MATERIALS AND METHODS

First, an initial profiling stage analyzing a large number of miRNAs in a few samples was performed using OpenArray™ miRNA panels in most of cases. Instead, if analyzing few miRNAs in a larger number of samples was needed to validate specific results, qPCR with individual miRNA assays would be used. Both approaches are based in TaqMan Advanced miRNA assays technology.

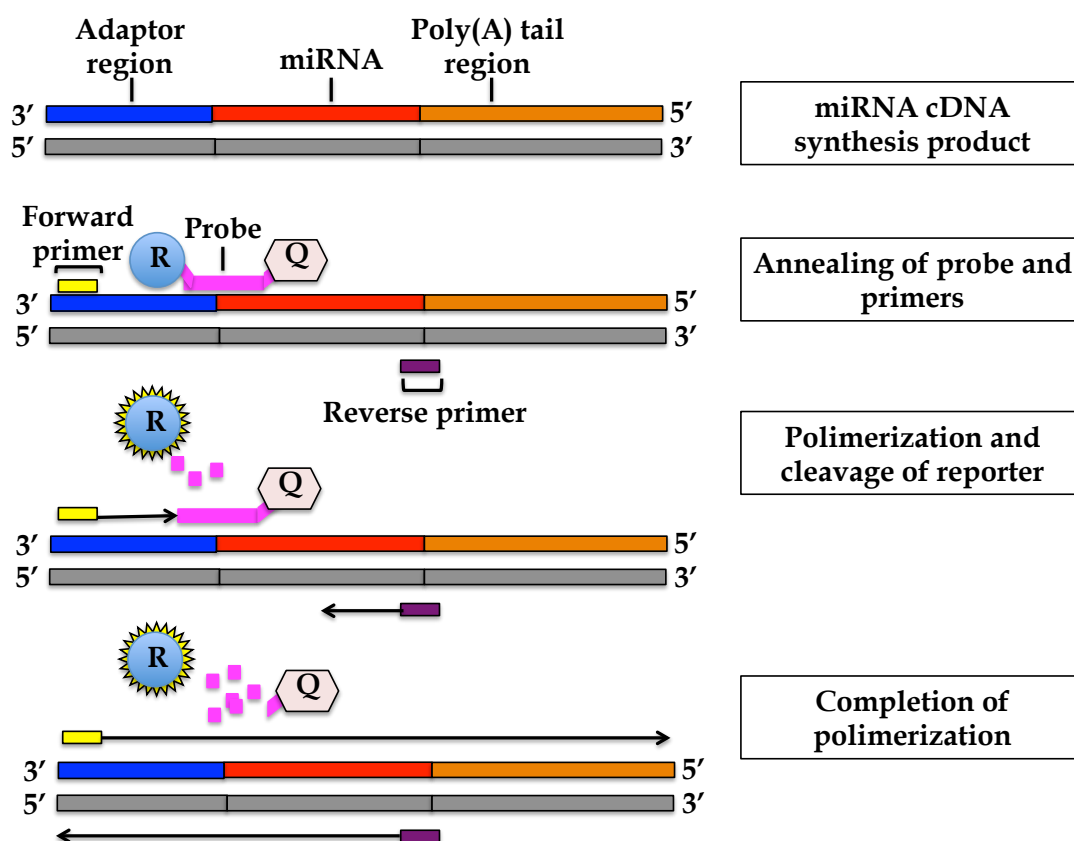


Figure 11. Scheme of TaqMan™ Advanced miRNA assays workflow. Adapted from TaqMan™ Advanced miRNA Assay User Guide, Applied Biosystems. Publication number: 100027897, Revision: C [274].

3.5.2.1 miRNA profiling by TaqMan™ OpenArray™ Human Advanced microRNA panel

TaqMan OpenArray Human Advanced microRNA plates were used to carry out a profiling step. They are high-throughput screening platforms that use small quantities of sample and reagents to analyze the expression of a wide variety of miRNAs. Each OpenArray plate contains 48 subarrays with 64

through-holes each, which is equivalent to eight 384-well qPCR plates. Each plate is the size of a microscope slide and each through-hole is 300 μm wide and 300 μm deep. TaqMan assays are pre-loaded into the through-holes during the manufacturing. The treatment of through-holes with hydrophilic coatings and the plate surface with hydrophobic coatings allows the retention of 33 nl of sample in each through-hole by surface tension. Figure 12 shows a schematic scheme of OpenArray disposition.

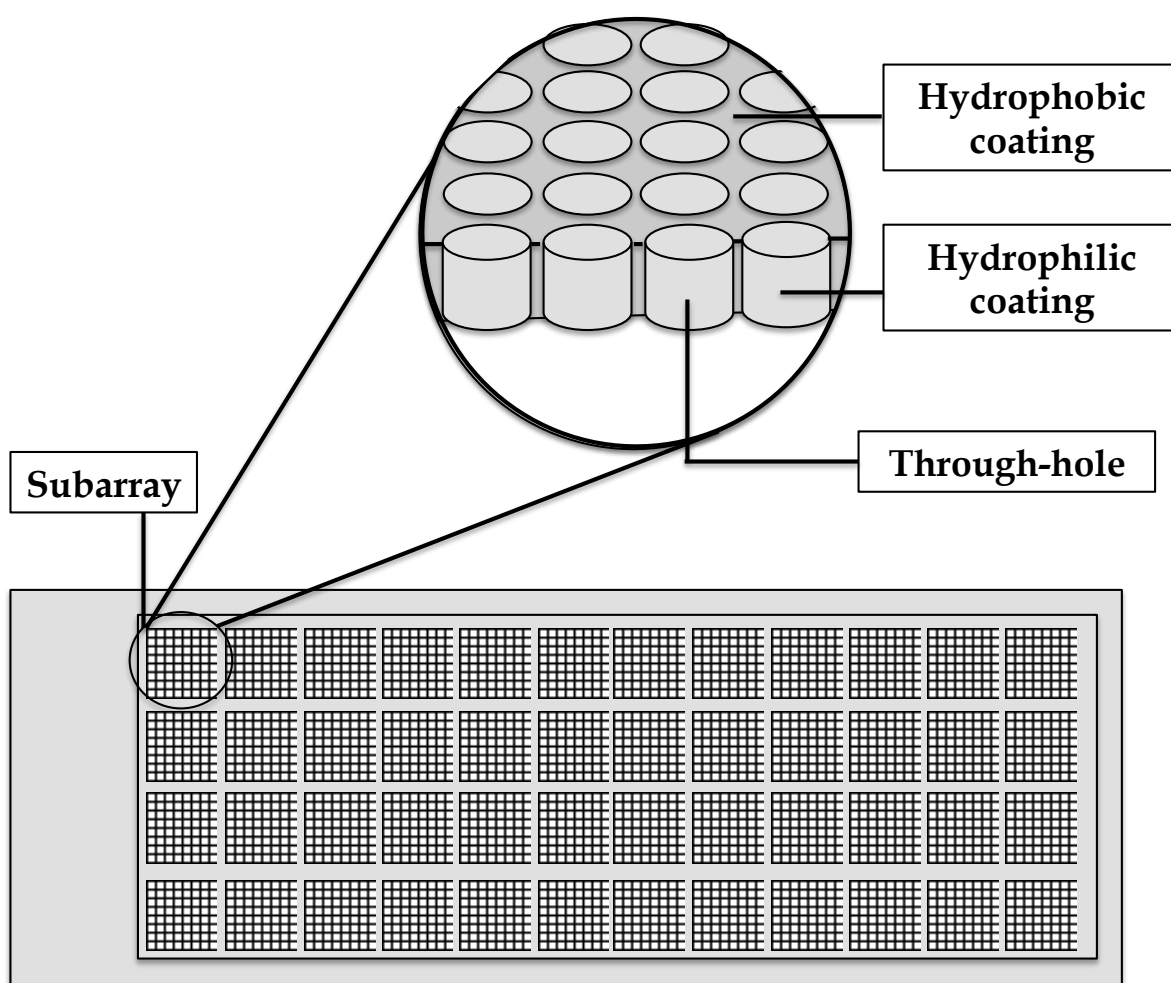


Figure 12. Schematic disposition of an OpenArray plate. Image adapted from TaqMan Advanced miRNA Assays, User Guide, Fixed-content, flexible-content, and custom-configured TaqMan OpenArray Plates, Publication Number: MAN0016124, Revision: B.0 [275].

Fixed-content TaqMan OpenArray Human Advanced microRNA (fc-OA) plates were used for serum samples. This format was pre-loaded with 754 human Advanced miRNA assays and allowed the analysis of three samples per plate.

MATERIALS AND METHODS

Custom-configured TaqMan OpenArray Human Advanced microRNA (cc-OA) plates were designed to analyze specifically 215 miRNAs (Annex I). This format was employed in CSF, murine samples, serum and plasma samples allowing the analysis of 12 samples per plate and samples were run in triplicate.

cDNA templates obtained with 22 miR-Amp cycles were diluted to 1:20 in 0.1X TE buffer to run a TaqMan OpenArray Plate. These diluted cDNA samples were combined with the same volume of TaqMan OpenArray Real-Time PCR Master Mix in tubes. Following the plate layout designated in the EDS experiment file created in the QuantStudio™ 12K Flex Software, 5 µL of the combined master mix and cDNA sample were added to determined wells in an OpenArray 384-well Sample Plate. The plate was centrifuged at 1000 rpm for 1 minute to allow a proper mixture and obtain an homogenous distribution of the solution through the well. The automated OpenArray AccuFill System was used to load the samples into the TaqMan OpenArray Plate through-holes from 384-well Sample Plate. Then, they were cycled and imaged with the QuantStudio 12K Flex Real-Time PCR System that offered C_q values for each sample and miRNA.

3.5.2.2 miRNA detection by quantitative real-time PCR with TaqMan™ Advanced microRNA assays

qPCR with Individual TaqMan Advanced hydrolysis probes (Applied Biosystems, California) were performed to determine expression levels of specific miRNAs. Preamplified cDNA templates were first diluted in NF water to obtain a final cDNA concentration of 1:10. This diluted cDNA (2.5 µl) were mixed with 7.5 µl of Reaction Mix as depicted in Figure 13a. Samples were run in triplicate. Individual miRNA expression was assessed with the Quant Studio™ 7 Flex System (Applied Biosystems, California) using the settings established in Figure 13b. This system measured and offered the C_q value for each sample and each individual miRNA.

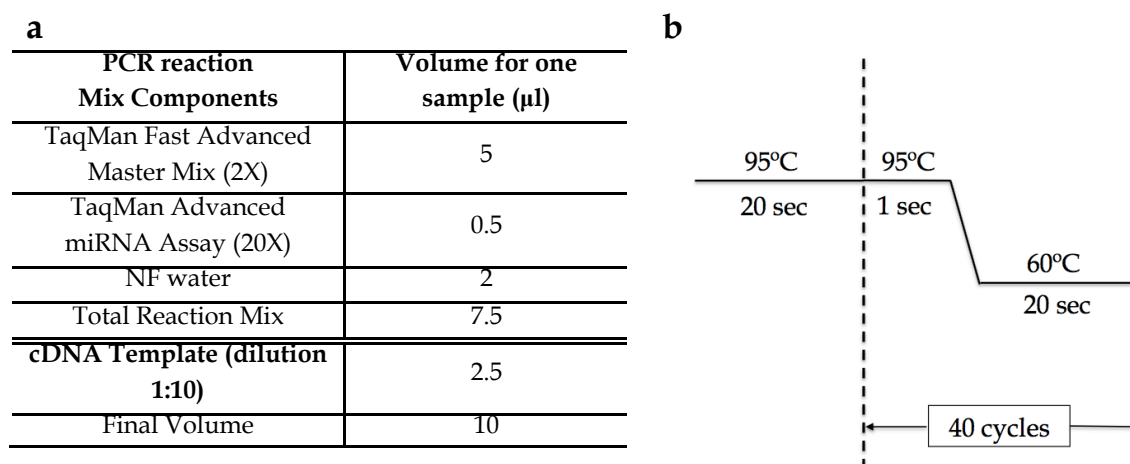


Figure 13. Reaction mix components and thermal cycling conditions for qPCR with Individual TaqMan Advanced hydrolysis probes. (a) Components and (b) thermal cycling conditions.

3.6 miRNA DETECTION WITH FIRST GENERATION TaqMan™ miRNA ASSAYS

Although most of the studies used the previously explained workflow to detect miRNA levels, two of the studies were carried out employing an older TaqMan technology version (first generation TaqMan microRNA assays). The basis of the process is quite similar to TaqMan Advanced protocol. First the preparation of cDNA templates from miRNA is required and these cDNA templates will be subjected to PCR amplification to detect specific miRNAs using TaqMan primer and probe sets. However, TaqMan Advanced miRNA reagents and first generation TaqMan miRNA technology are not compatible.

3.6.1 miRNA cDNA synthesis

miRNAs were reverse transcribed using TaqMan miRNA Reverse Transcription Kit, Multiplex RT Assays (Human pool Set A and B) and TaqMan microRNA assays (Applied Biosystems, California, USA). The absence of Poly(A) tailing and adaptor ligation steps leads to the loss of that universal character presented by the TaqMan Advanced technology. This technology presents two different approaches to obtain cDNA templates. On the one hand, the use of Megaplex Primers Pools allows the RT and

MATERIALS AND METHODS

preamplification up to 754 miRNAs (two different reactions covering 377 miRNAs each one). On the other hand, customised RT and preamplification primer pools allow obtaining specific miRNAs cDNA templates.

3.6.1.1 Reverse transcription reaction

RT reaction using Megaplex™ RT Primers pool was carried out preparing the Reaction Mix as indicated in Figure 14a. A quantity of 4.5 µl of this solution were mixed with 3 µl of RNA sample to obtain a final volume of 7.5 µl. After mixing properly, the reaction plate was placed into a thermal cycler to be incubated using the settings established in Figure 14b.

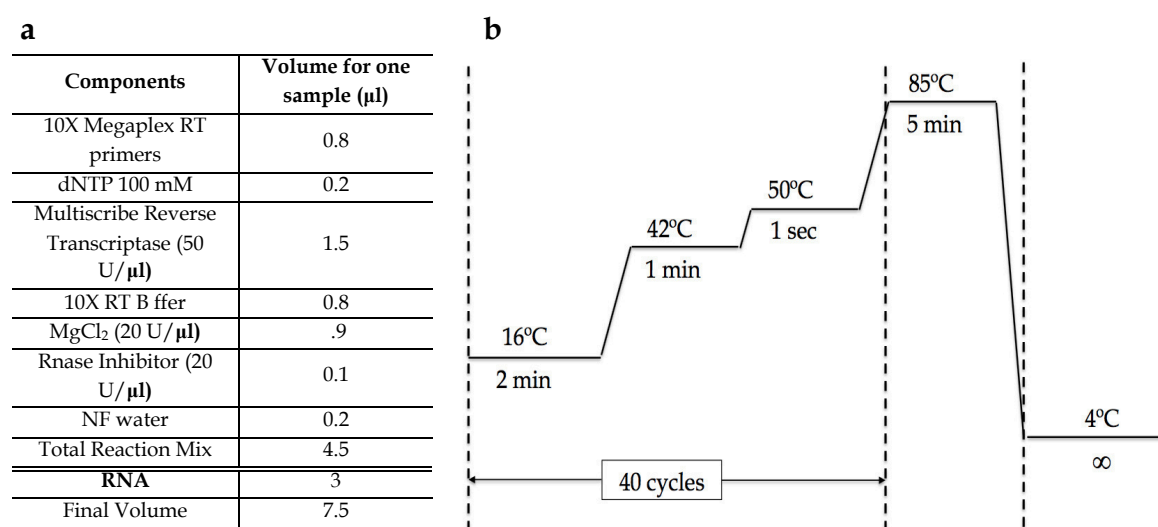


Figure 14. Reaction mix components and thermal cycling conditions for Reverse transcription reaction with Megaplex RT Primers pool. (a) Components and (b) thermal cycling conditions.

Specific miRNAs were retrotranscribed. Custom RT primer pools were prepared combining 10 µl of each individual 5X RT primer and adding NF water to a final volume of 1 ml. Once prepared, components indicated in Figure 15a were mixed and 12 µl of of this Reaction Mix were added to 3 µl of RNA sample. Then, the reaction plate was placed into a thermal cycler to be incubated (Figure 15b).

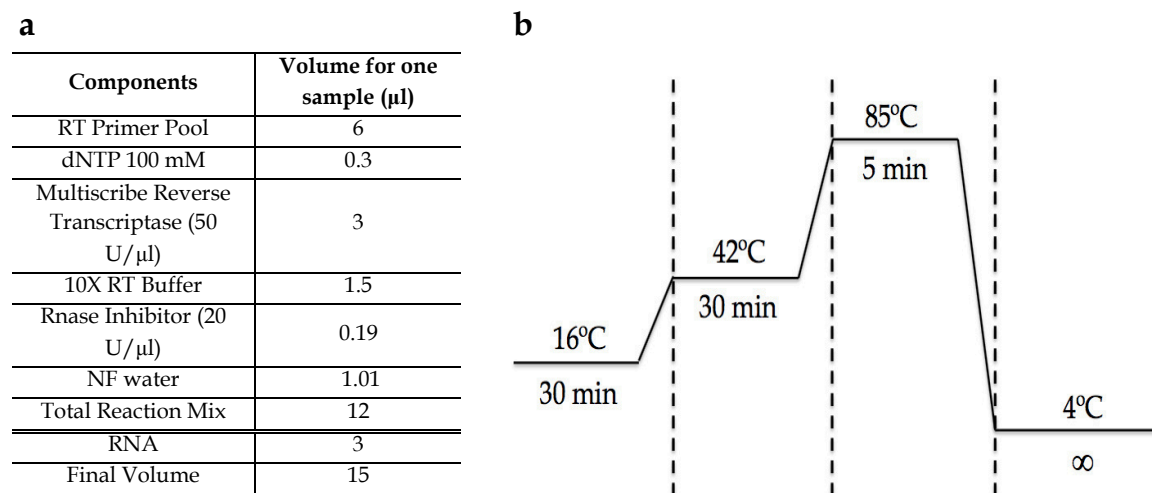


Figure 15. Reaction mix components and thermal cycling conditions for Reverse transcription reaction with custom RT Primers pool. (a) Components and (b) thermal cycling conditions.

3.6.1.2 Preamplification reaction

Preamplification (Preamp) step is mandatory before qPCR when analytical sensitivity is the utmost importance and the sample is limited [276]. RT products were preamplified by means of TaqMan PreAmp Master Mix and Megaplex™ PreAmp Primers (Human pool Set A and B) (Applied Biosystems), or by custom Preamp primer pool. Custom Preamp primer pools were prepared combining 10 μ l of each individual 20X TM primer and adding NF water to a final volume of 1 ml. Components indicated in Figure 16a were mixed and 8.75 μ l of this Reaction Mix were added to 3.75 μ l of RT product. Then, the reaction plate was placed into a thermal cycler to be incubated (Figure 16b).

MATERIALS AND METHODS

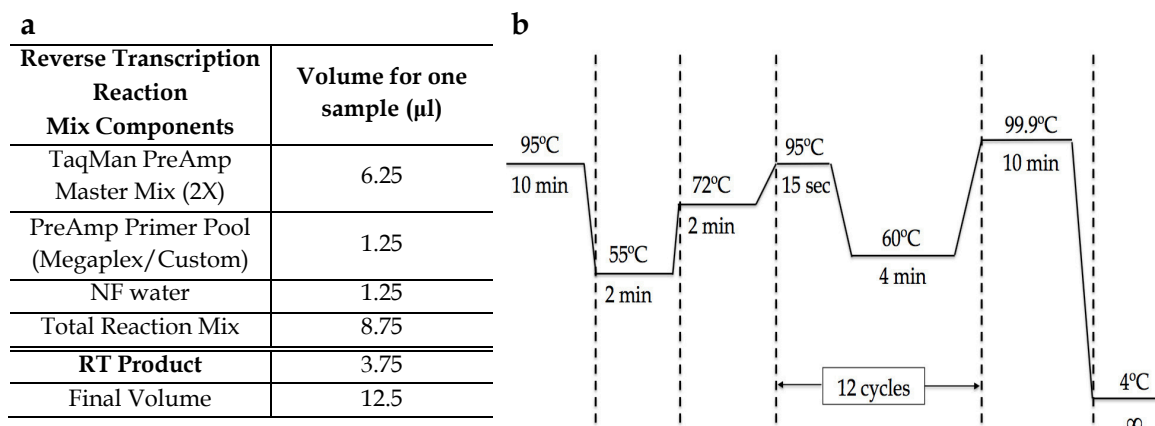


Figure 16. Reaction mix components and thermal cycling conditions for preamplification reaction. (a) Components and (b) thermal cycling conditions.

3.6.2 miRNA detection

3.6.2.1 miRNA detection by real-time PCR with TaqMan™ microRNA assays

miRNA detection was studied by qPCR with Individual TaqMan hydrolysis probes (Applied Biosystems, California). These TaqMan probes technology has been previously explained (section 3.5.2). However, as this cDNA synthesis process lacks of Poly(A) tailing and adaptor ligation, the specificity with these first generation TaqMan microRNA assays is lower than the one presented with TaqMan Advanced technology. Preamplified cDNA templates were diluted in NF water to obtain a final cDNA concentration of 1:50 and 1:200 for CSF or plasma samples, respectively. A quantity of 5 μl of Reaction Mix was mixed with 5 μl of diluted cDNA in each well of a 384-wells plate (Figure 17a). Samples were run in triplicate. Individual miRNA expression was assessed with the Quant Studio 7 Flex System (Applied Biosystems) (Figure 17b). This system measured and offered the Cq value for each sample and each individual miRNA.

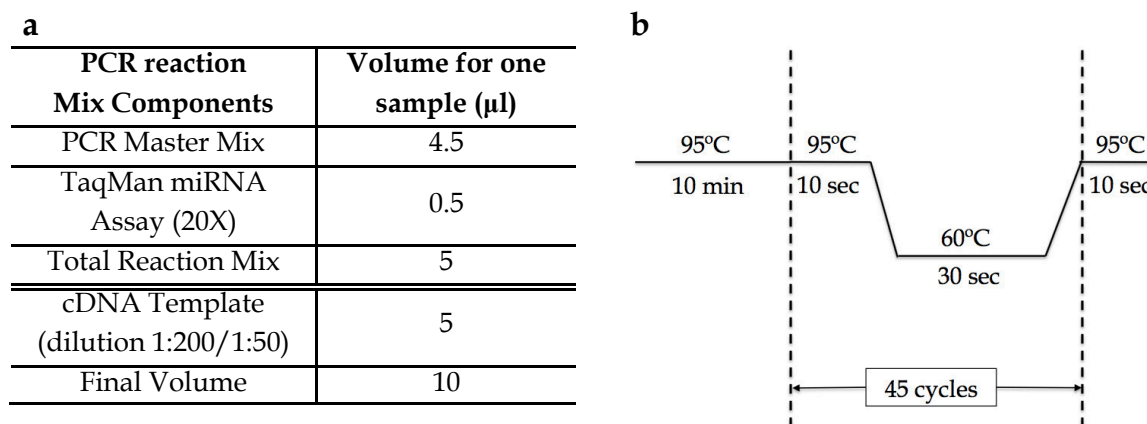


Figure 17. Reaction mix components and thermal cycling conditions for qPCR with Individual First Generation TaqMan hydrolysis probes. (a) Components and (b) thermal cycling conditions.

3.7 miRNA EXPRESSION NORMALIZATION

Normalization is an essential procedure in qPCR experiments to control variations in RNA extraction and RT reaction yield and efficiency of amplification [277]. Applying a proper normalization method bring out the true biological changes and reduce the variability induced during the whole process [278]. Two different approaches to detect miRNA expression levels have been described in this thesis. Profiling studies employing OpenArray plates offer data from a large number of miRNA in few samples. On the other hand, individual qPCR experiments result in C_q values of few specific miRNAs in wider cohorts of samples. Therefore, it is understandable that both approaches are usually treated differently in terms of normalization strategies.

3.7.1 Normalization of TaqMan™ OpenArray™ miRNA plates

Three different normalization methods for high-throughput experiments with OpenArray plates were evaluated in this doctoral thesis (see section 4.2.5). The global normalization (GN) method has been previously proposed and validated for array-based experiments. It uses the mean expression value of all miRNAs. Other methods for profiling experiments, as the quantile normalization (QN) or the rank-invariant set normalization (RIN), were also evaluated [278]. QN method assumes that data for each sample have the same overall rank-order

MATERIALS AND METHODS

quantile distribution. The overall expression levels are then adjusted to obtain an equal distribution for all samples [279]. RIN method assume that some miRNA are expressed at near constant levels across all samples and conditions. The method identifies invariant miRNAs using the large available dataset [279].

3.7.2 Normalization of individual qPCR experiments

When a limited list of miRNAs in wider cohorts is evaluated, the search of candidate reference miRNAs that show a relatively constant and abundant expression between samples and biological group becomes a necessary step. There is no a universal endogenous miRNA for all experimental situations and tissue or biofluid, this is the reason why the utility of endogenous miRNAs as normalizers must be experimentally validated for particular tissues, cell types or biofluids and specific experimental designs [278]. We used three diferent algorithms to identify stable miRNAs (see section 4.1.6): Normfinder [280], geNorm [281] and, the coefficient of variation (CV) score. The summarized stability score (SSS) for each miRNA was calculated to summarize the results from geNorm, Normfinder and CV score algorithms [278].

3.8 miRNA RELATIVE QUANTIFICATION

Once Cq values for specific miRNAs and samples were obtained and the proper normalization strategy was decided, analysis of qPCR data was done to determine changes in miRNA expression. This quantification was made by two different methods. The ΔC_t method measures the difference in Cq value between the target miRNA and reference miRNA normalizers using the following formula [282]:

$$2^{-(Cq A - Cq B)}$$

Cq A: Cq value target miRNA
Cq B: Mean Cq value global/endogenous miRNA

This formula corrects the data for differences in the amount of RNA added for each sample and reduced the variation caused by RT and PCR processes.

Statistical analyses explained in Section 3.10 were used to determine the existence of any statistical significant difference in miRNA expression between the studied groups.

Another employed method was the $\Delta\Delta C_t$ method to determine RQ respect to a reference group [282].

$$2^{-[(Cq A - Cq B)t - (Cq C - Cq D)]}$$

Cq A: Cq value target miRNA, target sample

Cq B: Mean Cq value global/endogenous miRNA, target sample

Cq C: Cq value target miRNA, reference sample

Cq D: Mean Cq value global/endogenous miRNA, reference sample

3.9 *IN SILICO* TOOLS

Experimentally validated targets for differentially expressed miRNAs were retrieved from miRTarBase [283]. Those validated genes by western blot, reporter assay and/or qPCR were introduced in Enrichr to explore the gene ontology (GO) biological processes [284]. Associated GO terms were clustered according to their relatedness using REVIGO after removing redundant terms [285]. Cytoscape software was used to create miRNA-target interaction networks [286].

Different repositories containing expression profiles of miRNAs in tissue [287], primary cells [288] and biofluids [289] were used to study potential tissue and cellular sources of miRNAs.

3.10 STATISTICAL ANALYSES

Demographic, clinical, genetic and radiological data are shown as absolute and relative frequencies in case of categorical variables while continuous variables are represented by median and quartiles. The homogeneity of basal characteristics of study groups was determined by Fisher's exact test for categorical variables and non-parametric Mann-Whitney U test (two-groups comparisons) or Kruskal Wallis test (multiple comparisons) as corresponding

MATERIALS AND METHODS

for continuous variables. All variables were measured by researchers blind to clinical data.

The choice of a suitable flowchart to analyze OpenArray data from CSF samples is described in section 4.2. The Kappa Index obtained through Cohen's κ test was used to determine agreement between methods. Mann-Whitney U test or Kruskal Wallis test were used to analyze differential distribution for continuous variables. The χ^2 goodness-of-fit test was used to determine whether the data distribution followed the observed distribution. Linear relationship between quantitative variables was measured with the Spearman's Rho coefficient (r_s) obtained with Spearman's test. The intraclass correlation coefficient (ICC) was calculated based on a mean-rating ($k=3$), consistency, two-way random-effects model.

Statistical differences on miRNA expression between studied groups were determined by Mann-Whitney U test or Kruskal Wallis test as appropriate. All analyses were two-tailed and the significance level was set to 0.05. *Post hoc* analyses were performed using the Bonferroni correction. r_s was calculated to establish the linear relationship between miRNA expression variables and quantitative variables. Receiver-operating characteristics (ROC) curves were generated and the area under the curve (AUC) and its corresponding confidence interval were estimated to evaluate the ability of specific miRNAs to distinguish between different conditions.

Statistical analyses were performed in Statistical Package for the Social Sciences (SPSS) version 25.0 (IBM SPSS Statistics for Windows, NY;USA). Figures were built using GraphPad PRISM v.5 (GraphPad Software, La Jolla California USA).

Before proceeding with Results section, Table 8 summarizes the methodology used in each miRNA study that has been carried out during this doctoral thesis.

Table 8. Summary of the methodology employed in each study.

Study	Biological material	RNA Extraction Method	cDNA synthesis	Phase	miRNA detection	Normalization method	miRNA Quantification	
<i>PPMS</i>	CSF	miRVANA	Advanced	Profiling	Custom OA	GN	2- Δ Ct	
	Serum	miRVANA	Advanced		Fixed OA	GN	2- Δ Ct	
	CSF	miRVANA	Advanced	Validation	qPCR	EN	2- Δ Ct	
	Serum	miRVANA	Advanced		qPCR	EN	2- Δ Ct	
<i>Tissue vs Human samples</i>	Murine culture	Chemical	Advanced	Profiling	Custom OA	GN	2- $\Delta\Delta$ Ct	
	CSF	miRVANA	Advanced		Custom OA	GN	2- $\Delta\Delta$ Ct	
<i>RIS</i>	CSF	miRVANA	Advanced	Profiling	Custom OA	GN	2- Δ Ct	
	Plasma	miRVANA	Advanced		Custom OA	GN	2- Δ Ct	
<i>RRMS</i>	<i>Ethnicity</i>	CSF	miRVANA	Advanced	Profiling	Custom OA	GN	2- Δ Ct
	<i>Age at onset</i>	CSF	miRVANA	Advanced	Profiling	Custom OA	GN	2- Δ Ct
	<i>Active lesions</i>	CSF	miRVANA	FG	Validation	qPCR	EN	2- Δ Ct
		Plasma	miRVANA	FG		qPCR	EN	2- Δ Ct
	<i>EBV</i>	Plasma	miRVANA	FG	Validation	qPCR	EN	2- Δ Ct

PPMS: primary progressive multiple sclerosis; RIS: radiologically isolated syndrome; RRMS: relapsing-remitting multiple sclerosis; CSF: cerebrospinal fluid; EBV: Epstein-Barr virus; FG: First Generation TaqMan miRNA assay technology; OA: OpenArray; GN: global normalization; EN: endogenous normalization.

4. Results

4.1 DESCRIPTION OF A PANEL OF CSF-ENRICHED miRNA USEFUL TO STUDY DIFFERENT NEUROLOGICAL DISEASES

The main aim of this part was to customize a panel of miRNA assays to be used in CSF studies using TaqMan™ Advanced miRNA technology from Applied Biosystems™.

As miRNA detection following this protocol has not been previously described in CSF samples, different volumes of initial sample and an increase in the number of cycles of miR-Amp reaction proposed by the manufacturer were tested in order to improve the detection range and define optimal conditions to be used with CSF samples for individual qPCR reactions. Once the protocol was adjusted to ensure detection of miRNA in CSF, a set of 216 miRNAs were selected to be included in the customized panels and their expression and abundance in CSF were analyzed in two different subsets of samples. In addition, some miRNAs were proposed as suitable endogenous controls for CSF. We characterized CSF-enriched miRNAs and described a suitable tool to study different neurological diseases as MS.

4.1.1 Optimization of TaqMan Advanced miRNA technology protocol for CSF samples

TaqMan Advanced miRNA cDNA synthesis Kit is required for preparing cDNA template that will be used with individual TaqMan® Advanced miRNA assays for qPCR. It was necessary to prove the feasibility of employing this technology with CSF samples and determine the optimal conditions to ensure miRNA detection, as it has been described to be used with serum or plasma samples.

Two different initial CSF volumes (300 µl or 500 µl) from which RNA was extracted were tested and combined with different number of cycles in the miR-Amp reaction for individual qPCR (14 cycles or 22 cycles).

RESULTS

For that reason, two individual TaqMan® Advanced miRNA assays (miR-16 and miR-24) were used to test three different combinations to guarantee an optimal detection in CSF samples.

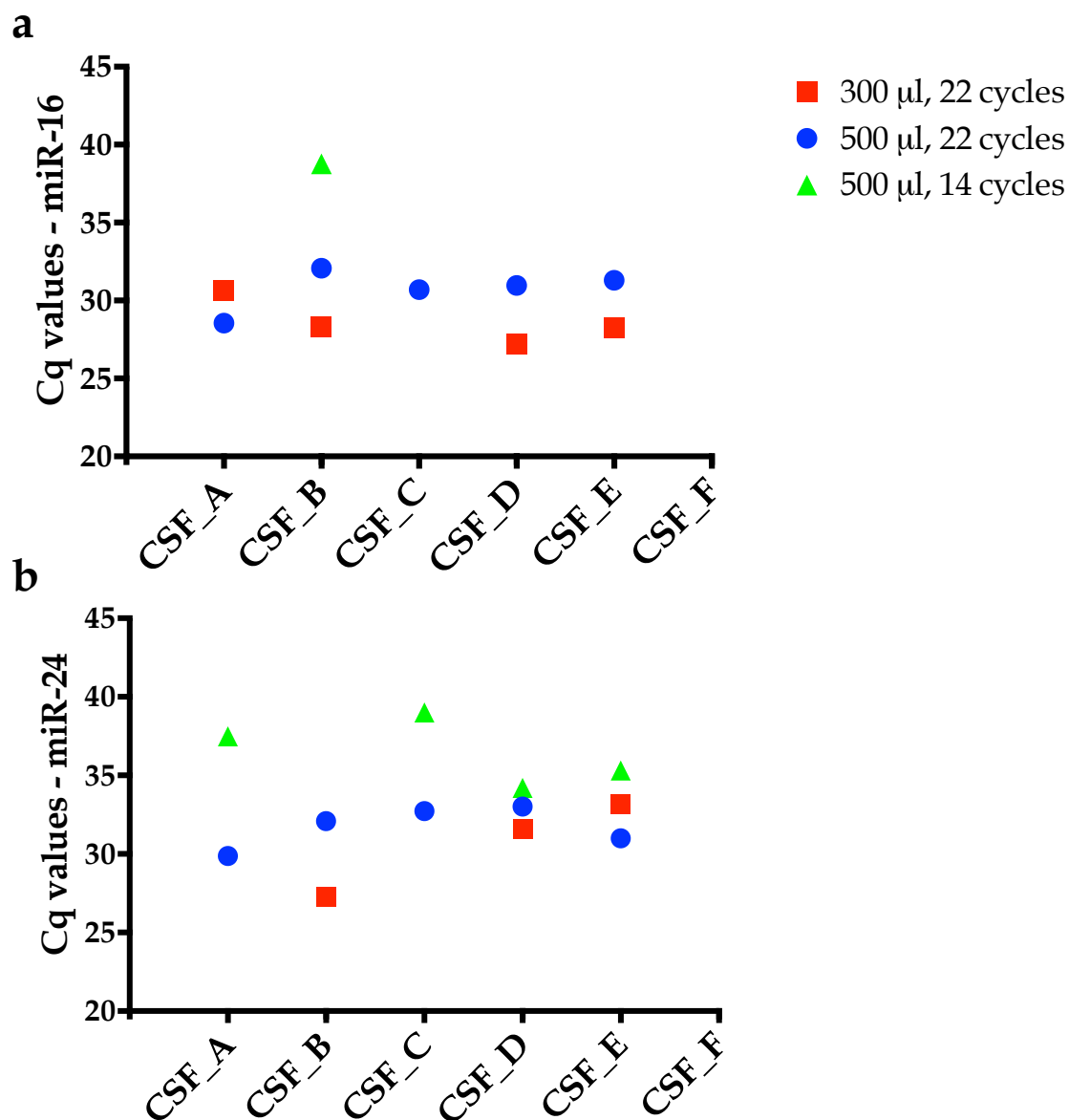


Figure 18. Impact of initial CSF volume and number of cycles of miR-Amp reaction in Cq values distribution. Individual TaqMan® Advanced miRNA assays for miR-16 (a) and miR-24 (b) were used to test combinations of initial CSF volume and number of cycles of miR-Amp reaction: 300 µl and 22 cycles (red squares), 500 µl and 22 cycles (blue circles) and 500 µl and 14 cycles (green triangles).

As observed in Figure 18, an initial volume of CSF of 300 μl whose extracted RNA was put through a miR-Amp reaction of 22 cycles (red squares) was enough to ensure an optimal detection of CSF miRNAs as it presented Cq values in the range considered quantitative. An initial volume of 500 μl combined with 22 cycles of miR-Amp reaction (blue circles) also offered an optimal detection. However, when RNA extracted from 500 μl of CSF was only submitted to 14 cycles of miR-Amp reaction (green triangles) the obtained Cq values could not be considered quantitative.

4.1.2 Platform format selection for the study of CSF miRNAs in OpenArray Human Advanced miRNA panels

Once confirmed that CSF miRNAs were detected using individual assays by qPCR, four fc-OA panels containing 754 TaqMan Advanced miRNA assays were used to establish the average miRNA detection in serum and CSF samples and propose the proper format to make a screening miRNA study in both biofluids.

As mentioned previously, TaqMan OpenArray Advanced miRNA panels have not been used in CSF samples and due to the considerable reduction in reaction volume when compared to qPCR (from 10 μl in qPCR to 33 nl in OpenArray), to compare the performance of 500 μl and 300 μl of initial CSF volume as we did with individual qPCR was considered necessary.

Three samples of RNA extracted from 500 μl of CSF, three samples of RNA extracted from 300 μl of CSF and six samples of RNA extracted from 300 μl of serum were used to test the performance of fc-OA panels.

As observed in Figure 19, 500 μl of CSF samples (blue columns) presented an average number of detected miRNAs of 89 whereas 300 μl of CSF samples (red columns) showed a mean detection of 79 miRNAs what indicated a percentage of detection of 11.8% and 10.5% respectively, from the total miRNA set. Serum samples (orange columns) presented a mean number of detected miRNAs of 221, which was equivalent to 29.3%.

RESULTS

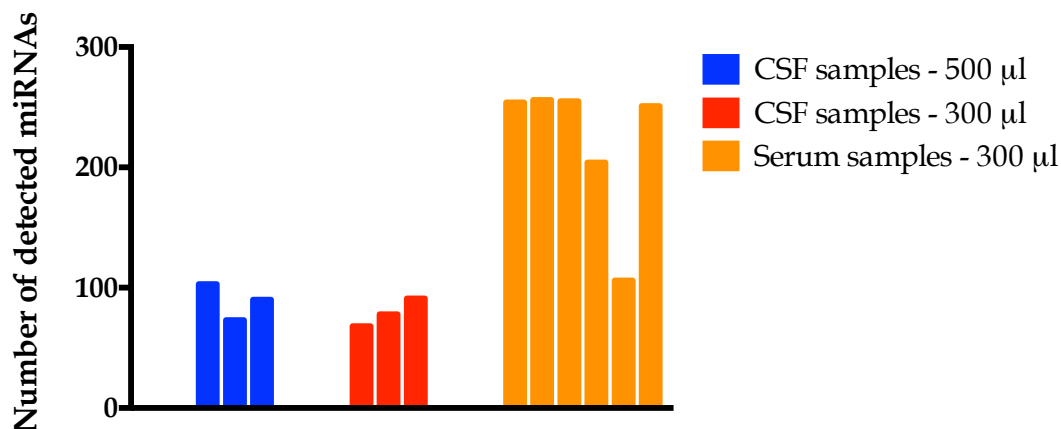


Figure 19. miRNA detection in CSF and serum samples in TaqMan® OpenArray® Human Advanced microRNA panels. The number of miRNAs with valid Cq values detected in each tested sample was represented in each column. Blue columns represents CSF samples whose initial volume was 500 µl, red columns represents CSF samples whose initial volume was 300 µl and orange columns represents serum samples.

As starting from an initial volume of 300 µl of CSF showed a detection comparable to the one presented by 500 µl of CSF, henceforth, total RNA from CSF would be extracted from 300 µl of sample and 22 cycles in miR-Amp reaction would be used in order to ensure an appropriate detection by TaqMan® Advanced miRNA assays both in individual qPCR reactions and OpenArray® plates.

Due to the low detection presented by CSF samples, to customize TaqMan OpenArray Human Advanced microRNA panels for studying CSF miRNA profiles was chosen. The selected 224 format allows simultaneously to analyze 12 samples covering a total of 216 miRNAs plus one mandatory control (miR-16). miRNAs should meet at least one of the following criteria to be included in the panel:

1. previously associated with MS in tissue, serum/plasma or CSF.
2. particularly brain-enriched.
3. detectable in CSF based on existing literature and/or our previous experience.
4. potential endogenous normalizer.
5. negative control.

The list of 216 miRNA assays included in these customized TaqMan OpenArray Human Advanced microRNA panels is included in Annex I.

4.1.3 Customized OpenArray plates performance

Once assured that miRNAs from CSF were detected by fc-OA panels, different aspects concerning the performance of the cc-OA panels were analyzed using two sets of samples from two different RT reactions. 174 samples were retrotranscribed in cohort 1 (C1) belonging to different PPMS, RRMS and OND individuals, while RT reaction comprising samples in cohort 2 (C2) included 114 samples from PPMS, RRMS, OND and SAS subjects (Table 9).

Table 9. Distribution of samples in C1 and C2 cohorts used to test OpenArray plates performance.

Groups	C1 samples	C2 samples
PPMS	45 (25.9)	9 (7.9)
RRMS	102 (58.6)	66 (57.9)
OND	27 (15.5)	6 (5.3)
SAS	-	33 (29.0)
Total	174	114

C1: cohort 1; C2: cohort 2; PPMS: primary progressive multiple sclerosis; RRMS: relapsing-remitting multiple sclerosis; OND: other neurological diseases; SAS: spinal anesthesia subjects. Categorical variables were shown as absolute and relative frequencies.

The mean Cq value, the count of valid Cq value in the Cq range 15-35, invalid Cq (Cq value < 15) or undetectable Cq (Cq > 35) were used to exclude samples whose miRNA detection was not good enough [290] (Figure 20). The average count of valid Cq value among all samples was 84 and 85 miRNAs for C1 and C2 respectively. All the samples with less than 84/85 detected valid Cq values (n=83 and n=56 for C1 and C2) were rejected for further analyses. As observed in Figure 20, that subset of samples also presented a more non-uniform tendency in Cq value mean (yellow line). For that reason, the remaining samples (n=91 and n=58) with an average count of valid Cq values over the total mean and a more stable Cq mean tendency were used for the next analyses concerning miRNA assays performance in CSF.

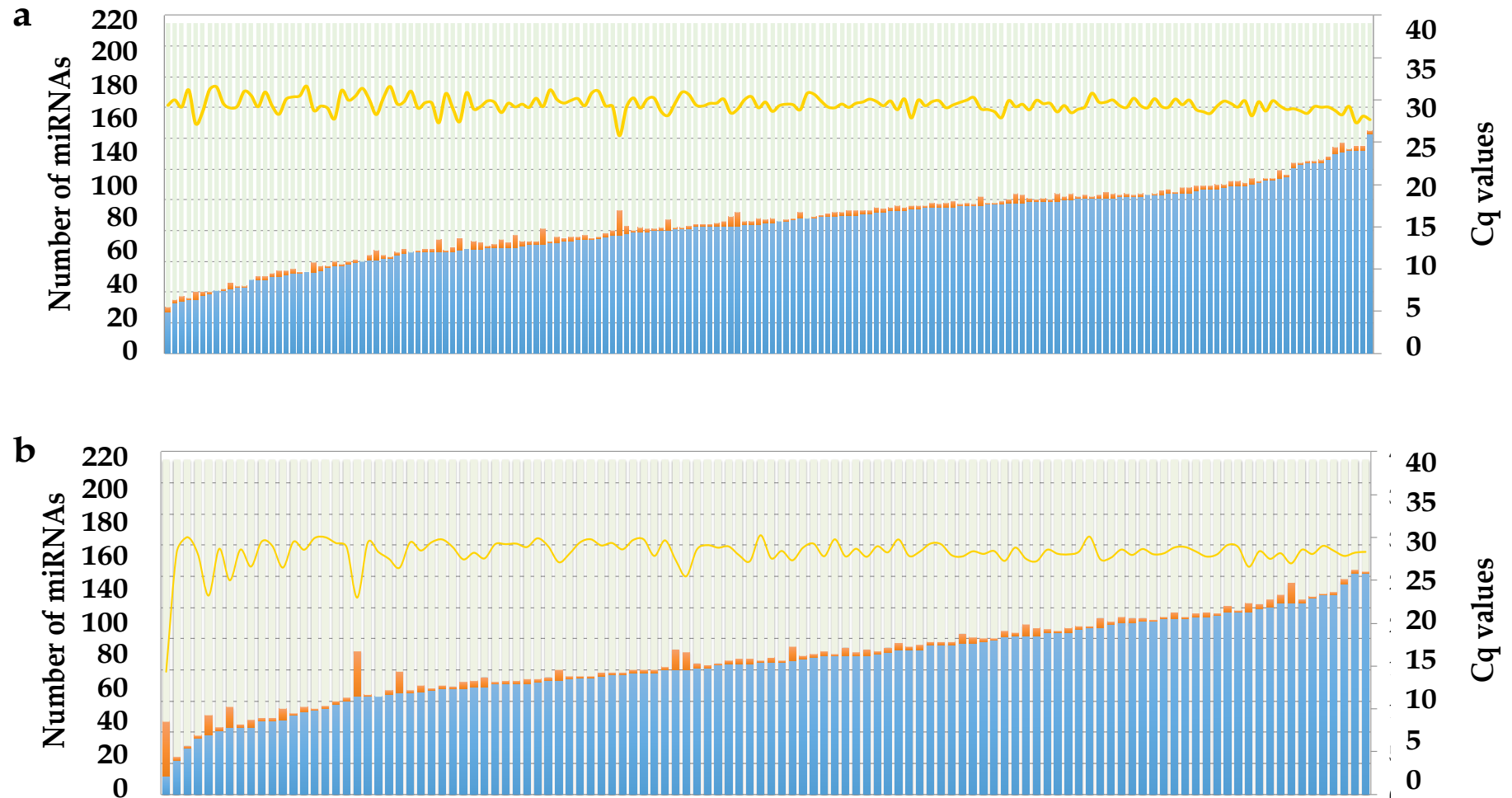


Figure 20. Cq values mean and count of valid Cq values for each sample in C1 (a) and C2 (b). Yellow line (right Y axis) corresponds to the mean Cq value for each sample. Left Y axis represents number of miRNAs (from a total of 216) with Valid (blue), invalid (orange) and undetectable (green) Cq values for each sample.

Once the suitable samples were selected, different aspects related to OpenArray performance should be taken into account.

First, when analyzing miRNA differential expression, only those miRNAs present in at least 70% of samples will be employed in the analysis. In tables 10 and 11, miRNA classification according to the percentage of samples in which they are detectable is shown for each cohort. As it could be observed, C1 and C2 presented reproducible results, showing similar detection patterns.

Table 10. miRNA classification according to the detectability in C1.

Detection (% samples)	Number of miRNAs (%)	miRNAs
100%	4 (1.9)	miR-101-3p, miR-143-3p, miR-23a-3p, miR-30d-5p
99%-70%	79 (36.7)	let-7a-5p, let-7b-5p, let-7c-5p, let-7f-5p, let-7g-5p, let-7i-5p, miR-100-3p, miR-100-5p, miR-107, miR-10b-5p, miR-124-3p, miR-125a-5p, miR-125b-5p, miR-1260a, miR-128-3p, miR-1298-5p, miR-130a-3p, miR-137, miR-142-3p, miR-144-3p, miR-145-5p, miR-146a-5p, miR-148a-3p, miR-148b-3p, miR-150-5p, miR-151a-3p, miR-15a-5p, miR-181a-5p, miR-185-5p, miR-186-5p, miR-195-5p, miR-199a-3p, miR-199a-5p, miR-19a-3p, miR-204-5p, miR-20a-5p, miR-21-5p, miR-219a-5p, miR-22-3p, miR-221-3p, miR-223-3p, miR-23b-3p, miR-24-3p, miR-25-3p, miR-26b-5p, miR-27a-3p, miR-27b-3p, miR-29a-3p, miR-30c-5p, miR-320a, miR-320b, miR-335-5p, miR-338-3p, miR-342-3p, miR-34a-5p, miR-34b-5p, miR-34c-5p, miR-361-5p, miR-374b-5p, miR-376a-3p, miR-423-5p, miR-424-5p, miR-448, miR-449b-5p, miR-450b-3p, miR-451a, miR-452-3p, miR-497-5p, miR-645, miR-652-3p, miR-653-3p, miR-660-5p, miR-664a-3p, miR-770-5p, miR-885-5p, miR-9-3p, miR-9-5p, miR-92b-3p, miR-939-5p
69%-50%	25 (11.6)	let-7b-3p, miR-1-3p, miR-103a-3p, miR-133a-3p, miR-135a-5p, miR-151a-5p, miR-15b-5p, miR-181c-5p, miR-1911-5p, miR-196a-5p, miR-26a-5p, miR-28-5p, miR-29c-5p, miR-302d-3p, miR-30c-2-3p, miR-34b-3p, miR-376c-3p, miR-378a-3p, miR-378a-5p, miR-516b-5p, miR-525-3p, miR-633, miR-93-5p, miR-99a-3p, miR-99b-5p
49%-30%	34 (15.8)	let-7e-5p, let-7f-2-3p, miR-106b-3p, miR-106b-5p, miR-1264, miR-129-2-3p, miR-132-3p, miR-133b, miR-145-3p, miR-17-5p, miR-181b-5p, miR-190a-5p, miR-193a-5p, miR-203a-3p, miR-205-5p, miR-210-3p, miR-222-3p, miR-302b-3p, miR-32-5p, miR-339-5p, miR-34c-3p, miR-361-3p, miR-411-5p, miR-412-3p, miR-425-5p, miR-483-3p, miR-484, miR-501-3p, miR-502-3p, miR-505-3p, miR-524-3p, miR-576-3p, miR-583, miR-937-3p
30%-1%	68 (31.6)	miR-103a-2-5p, miR-10a-5p, miR-122-5p, miR-1247-5p, miR-1249-3p, miR-125a-3p, miR-126-5p, miR-127-3p, miR-1292-5p, miR-142-5p, miR-146b-5p, miR-153-3p, miR-155-5p, miR-181d-5p, miR-183-3p, miR-191-3p, miR-191-5p, miR-194-5p, miR-19b-3p, miR-200c-3p, miR-206, miR-216a-5p, miR-218-5p, miR-27b-5p, miR-30a-3p, miR-30c-1-3p, miR-30e-3p, miR-31-5p, miR-323a-3p, miR-325, miR-326, miR-328-3p, miR-34a-3p, miR-363-3p, miR-369-3p, miR-369-5p, miR-373-3p, miR-375, miR-410-3p, miR-449a, miR-450b-5p, miR-452-5p, miR-454-3p, miR-455-3p, miR-483-5p, miR-486-5p, miR-487a-3p, miR-489-3p, miR-490-3p, miR-513a-5p, miR-515-3p, miR-518d-3p, miR-518e-3p, miR-518f-3p, miR-520h, miR-532-3p, miR-532-5p, miR-548d-5p, miR-548e-3p, miR-548k, miR-548n, miR-570-3p, miR-615-3p, miR-628-3p, miR-642a-5p, miR-656-3p, miR-876-3p, miR-92a-3p
0%	5 (2.3)	miR-211-5p, miR-383-5p, miR-523-3p, miR-551a, miR-593-5p

RESULTS

Table 11. miRNA classification according to the detectability in C2.

Detection (% samples)	Number of miRNAs (%)	miRNAs
100%	13 (6.1)	let-7b-5p, miR-125a-5p, miR-125b-5p, miR-1260a, miR-137, miR-143-3p, miR-150-5p, miR-186-5p, miR-199a-3p, miR-204-5p, miR-23a-3p, miR-23b-3p, miR-451a
99%-70%	62 (28.8)	let-7a-5p, let-7c-5p, let-7f-5p, let-7g-5p, let-7i-5p, miR-100-3p, miR-100-5p, miR-101-3p, miR-10b-5p, miR-124-3p, miR-1298-5p, miR-133b, miR-142-3p, miR-144-3p, miR-145-5p, miR-146a-5p, miR-148a-3p, miR-151a-3p, miR-15a-5p, miR-17-5p, miR-181a-5p, miR-181c-5p, miR-193a-5p, miR-195-5p, miR-20a-5p, miR-21-5p, miR-22-3p, miR-221-3p, miR-223-3p, miR-24-3p, miR-25-3p, miR-26a-5p, miR-26b-5p, miR-27a-3p, miR-27b-3p, miR-29a-3p, miR-29c-5p, miR-30d-5p, miR-320a, miR-320b, miR-335-5p, miR-342-3p, miR-34a-5p, miR-34c-5p, miR-361-5p, miR-374b-5p, miR-378a-3p, miR-423-5p, miR-448, miR-449b-5p, miR-450b-3p, miR-452-3p, miR-645, miR-652-3p, miR-653-3p, miR-660-5p, miR-664a-3p, miR-770-5p, miR-9-5p, miR-92b-3p, miR-939-5p, miR-99b-5p
69%-50%	35 (16.3)	let-7e-5p, miR-103a-3p, miR-107, miR-130a-3p, miR-135a-5p, miR-148b-3p, miR-151a-5p, miR-15b-5p, miR-185-5p, miR-190a-5p, miR-1911-5p, miR-196a-5p, miR-199a-5p, miR-19a-3p, miR-219a-5p, miR-222-3p, miR-28-5p, miR-30c-2-3p, miR-30c-5p, miR-338-3p, miR-34b-3p, miR-34b-5p, miR-34c-3p, miR-376a-3p, miR-378a-5p, miR-424-5p, miR-483-3p, miR-497-5p, miR-501-3p, miR-516b-5p, miR-525-3p, miR-633, miR-885-5p, miR-93-5p, miR-99a-3p
49%-30%	34 (15.8)	let-7b-3p, let-7f-2-3p, miR-1-3p, miR-106b-5p, miR-126-5p, miR-127-3p, miR-128-3p, miR-132-3p, miR-133a-3p, miR-155-5p, miR-181b-5p, miR-205-5p, miR-302b-3p, miR-302d-3p, miR-30c-1-3p, miR-30e-3p, miR-31-5p, miR-32-5p, miR-339-5p, miR-361-3p, miR-376c-3p, miR-411-5p, miR-412-3p, miR-425-5p, miR-483-5p, miR-484, miR-502-3p, miR-518f-3p, miR-524-3p, miR-576-3p, miR-583, miR-9-3p, miR-92a-3p, miR-937-3p
30%-1%	67 (31.2)	miR-106b-3p, miR-10a-5p, miR-122-5p, miR-1247-5p, miR-1249-3p, miR-125a-3p, miR-1264, miR-129-2-3p, miR-1292-5p, miR-142-5p, miR-145-3p, miR-146b-5p, miR-153-3p, miR-181d-5p, miR-191-3p, miR-191-5p, miR-194-5p, miR-19b-3p, miR-200c-3p, miR-203a-3p, miR-206, miR-210-3p, miR-216a-5p, miR-218-5p, miR-27b-5p, miR-30a-3p, miR-323a-3p, miR-325, miR-326, miR-328-3p, miR-34a-3p, miR-363-3p, miR-369-3p, miR-369-5p, miR-373-3p, miR-383-5p, miR-410-3p, miR-449a, miR-450b-5p, miR-452-5p, miR-454-3p, miR-455-3p, miR-486-5p, miR-487a-3p, miR-489-3p, miR-490-3p, miR-505-3p, miR-513a-5p, miR-515-3p, miR-518d-3p, miR-518e-3p, miR-520h, miR-523-3p, miR-532-3p, miR-532-5p, miR-548d-5p, miR-548e-3p, miR-548k, miR-548n, miR-551a, miR-570-3p, miR-593-5p, miR-615-3p, miR-628-3p, miR-642a-5p, miR-656-3p, miR-876-3p
0%	4 (1.9)	miR-103a-2-5p, miR-183-3p, miR-211-5p, miR-375

Second, among those miRNAs detectable in at least 70% of samples, 20 most abundant miRNAs (lower Cq values) in CSF in C1 and C2 were identified by ranking average Cq values of all samples, as shown in Figure 21. 17 miRNAs coincided as the most abundant in both cohorts, miR-770-5p being the one presenting the lowest mean Cq value (21.61 and 21.21 for C1 and C2, respectively).

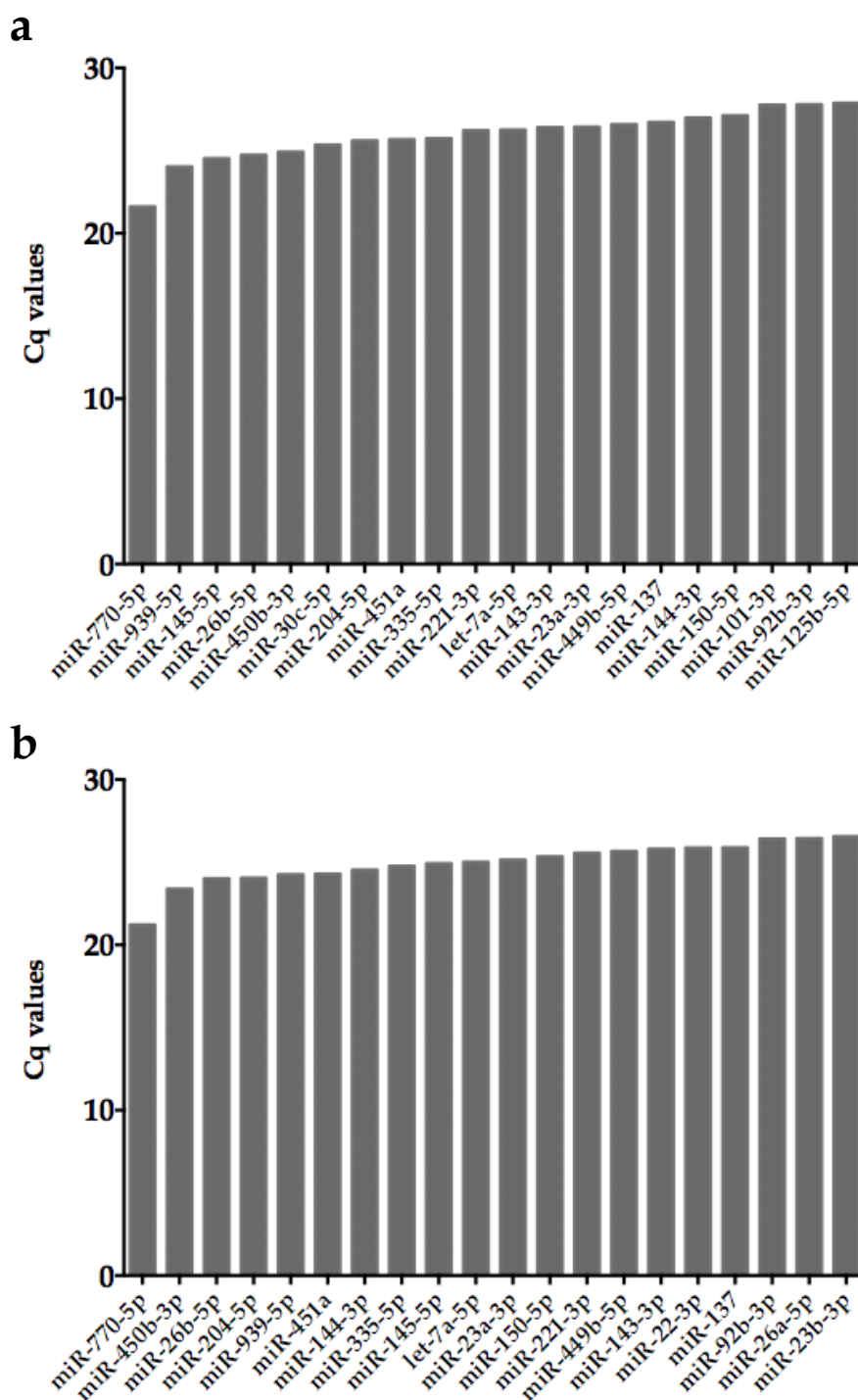


Figure 21. miRNA abundance in C1 and C2. Mean Cq value for each miRNA detected in at least 70% samples was calculated in C1 (a) and C2 (b).

Third, some important available information generated by QuantStudio™ 12K Flex software is the Amp Score, which is a metric of the quality of the reaction, and the Cq confidence value, a measure of Cq reliability. These two parameters are associated to

RESULTS

each amplification curve and to be acceptable and be included in further analysis, these values should be equal or above 1.24/1.1 and 0.8/0.6 respectively, according to manufacturer. The relation of these parameters with the detectability of miRNA (percentage of samples) was further analyzed and represented in Figure 22.

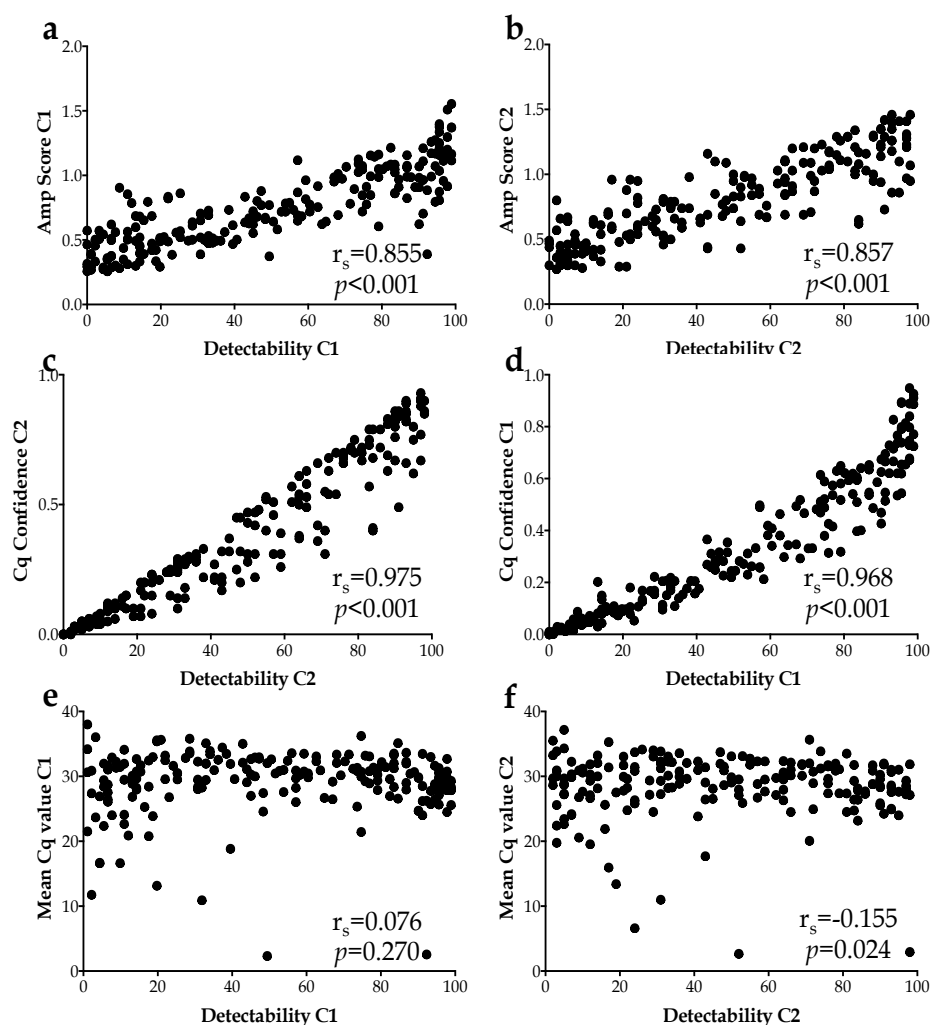


Figure 22. Scatter plot of correlation between Amp Score/Cq Confidence/Mean Cq value and detectability for each miRNA in C1 and C2. Scatter plots showing the relationship between Amp Score and detectability for C1 (a) and for C2 (b), Cq Confidence and detectability for C1 (c) and for C2 (d) and, Mean Cq value and detectability for C1 (e) and for C2 (F). Each dot corresponds to one miRNA. r_s : Spearman's Rho; p : p value.

Both Amp Score and Cq Confidence strongly positively correlated with detectability ($r_s = 0.855$; $p < 0.001$ for C1; $r_s = 0.857$; $p < 0.001$ for C2 and $r_s = 0.975$; $p < 0.001$ for C1; $r_s = 0.968$; $p < 0.001$ for C2, respectively). Selecting those miRNAs that are detected in at least 70% of samples to further analysis of differential expression involves ensuring

good quality of the data. However, the mean Cq value did not correlate with detectability for C1 ($r_s=0.076$; $p=0.270$) and only showed a mild negative relation for C2 ($r_s=-0.155$; $p=0.024$). This finding reinforces the idea of not using Cq value in CSF samples either for sample rejection or for assuring optimal amplification curves.

4.1.4 Variability of replicates measurements

To study the variability and reproducibility of replicates measurements, six samples were run in triplicates in the customized OpenArray® plates. The Cq values of four miRNAs of each detectability category (except 0% samples) were taken and the CV between replicates, a measure of precision, was calculated for each one (Figure 23). Except for miRNAs detected in at least 30% of samples (orange columns) whose CV between replicates were elevated, all categories presented a comparable replicate variability.

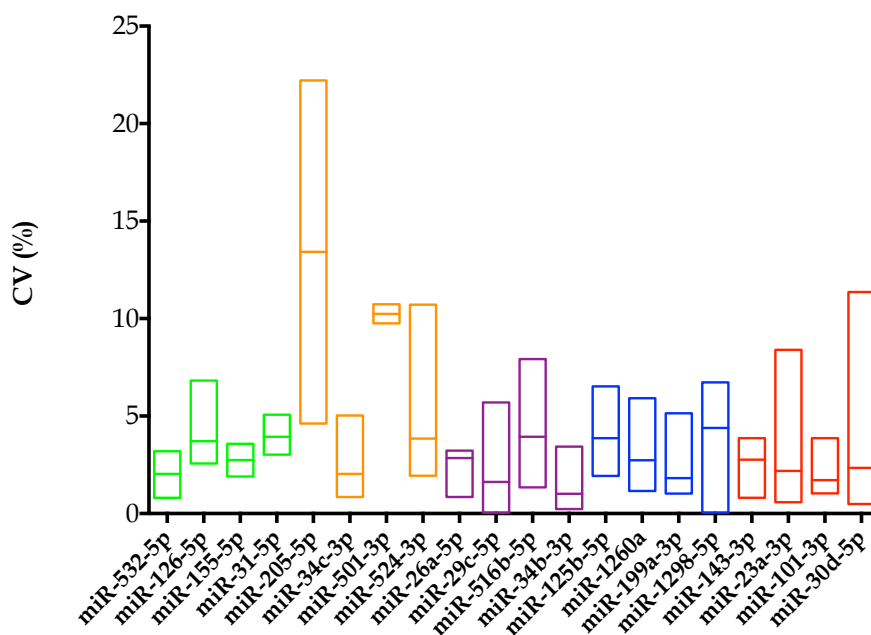


Figure 23. CV of replicates measurements for different miRNAs. Six samples were measured in triplicates and four miRNAs for each category of detectability were selected. Each miRNA corresponds to one floating bar (minimum to maximum CV value) and the line represents the median. The color of each floating bar represents one of these categories: red: 100% samples; blue: 99%-70% samples; purple: 69%-50% samples; orange: 49%-30% samples and; green: 29%-1% samples.

RESULTS

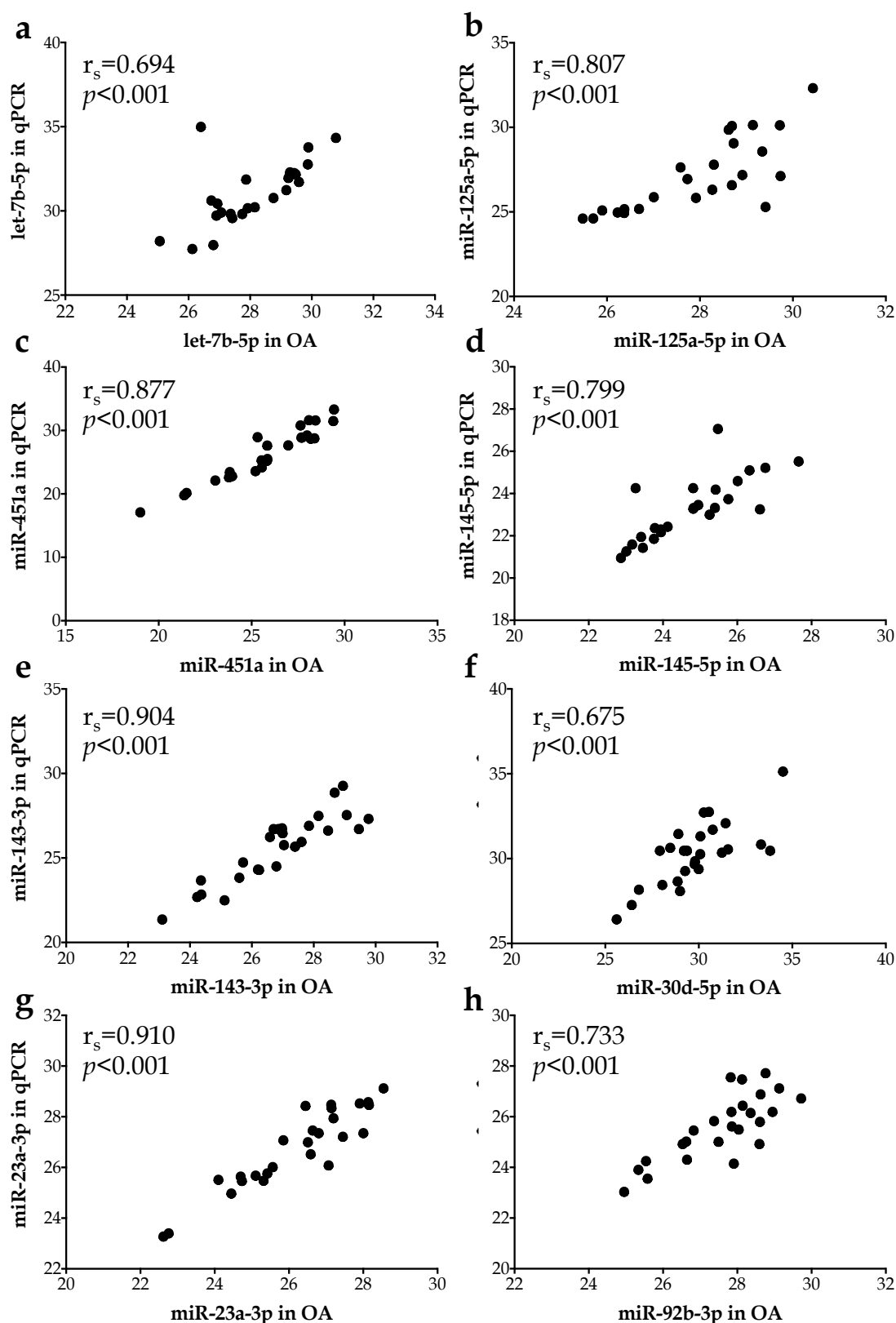


Figure 24. Correlation of Cq raw data values in OpenArray and Cq raw data values in individual qPCR. Scatter plots showing the relationship between Cq values for (a) let-7b-5p, (b) miR-125a-5p, (c) miR-143-3p, (d) miR-145-5p, (e) miR-23a-3p, (f) miR-30d-5p, (g) miR-451a and, (h) miR-92b-3p. r_s : Spearman's Rho; p : p value.

4.1.5 Correlation between individual qPCR (22 cycles) and OpenArray performance

The majority of studies involving a screening miRNA profile with high throughput platforms as OpenArray are usually followed by a validation phase in which more samples are used and an individual miRNA expression is assessed by qPCR in order to validate the deregulation observed at screening. The change from OpenArray panels to qPCR entails an important increase of volume reaction (from 33 nl to 10 µl) what requires a certain correlability in Cq values results between platforms in order to be able to validate the findings. For this reason, the correlation between Cq raw data values coming from OpenArray panels and qPCR for nine individual miRNAs in 26 samples were studied. Spearman's test established that all miRNAs presented a positive strong correlation between Cq values obtained by OpenArray panels and qPCR (Figure 24).

4.1.6 Search of suitable endogenous controls

Normalization is an essential procedure in qPCR experiments to control variations in extraction yield, RT yield and efficiency of amplification, thus enabling comparisons of miRNA concentrations between different samples [277]. Although a normalization method based on the mean expression value of all miRNAs has been proposed and validated for array-based approaches qPCR data (screening phase), the search of a candidate reference endogenous miRNAs is necessary for posterior studies, which will evaluate a limited panel of miRNAs in a wider cohort (validation phase) [278]. The utility of these miRNAs as endogenous normalizers (EN) must be experimentally validated for particular tissues, cell types or biofluids and specific experimental designs. Until now, there is no study proposing reliable endogenous controls for CSF using TaqMan Advanced miRNA assays technology. For this reason, a search of endogenous controls to use in qPCR experiments with CSF samples was made using the OpenArray data obtained from C1 and C2.

RESULTS

First, we selected those overlapped miRNAs detected in at least 70% of samples in C1 and C2 (66 matching miRNAs) and used three different algorithms to identify stable miRNAs in each cohort separately: Normfinder [280], geNorm [281] and, the CV score. These algorithms generate a score that represents the stability in such a way that the smaller the score is, the higher expression stability the miRNA has.

As observed in Figure 25, these three algorithms positively correlated between them in C1 and C2 ($p < 0.001$ in both cases), indicating that the stability score proposed for each miRNA by each algorithm is equivalent and similarly positioned in the whole set of studied miRNAs.

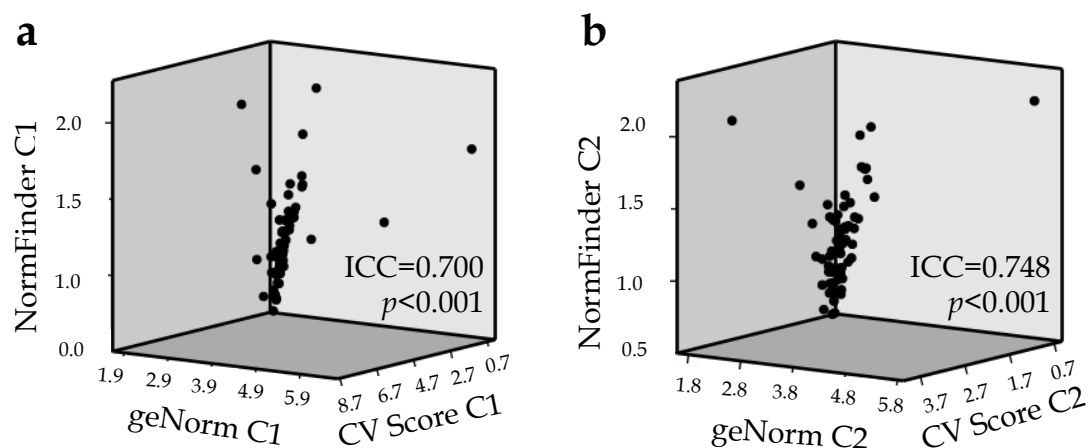


Figure 25. Correlation of stability scores obtained by three different algorithms for C1 and C2. geNorm stability score is represented in X axis, Normfinder stability score is represented in Y axis and, the CV score is represented in Z axis for C1 (a) and for C2 (b). Two-Way Random Consistency Intraclass Correlation Coefficient was used to measure the correlation levels between the three methods. ICC: intraclass correlation; p : p value.

At the same time, the correlation in the stability scores obtained by each algorithm between the two different cohorts was analyzed to study the intra-platform reproducibility of the results (Figure 26). geNorm, Normfinder and CV stability scores positively correlated for C1 and C2 ($p < 0.001$; $p < 0.001$ and $p = 0.001$, respectively) indicating a strong reproducibility of miRNA stability between OpenArray plates.

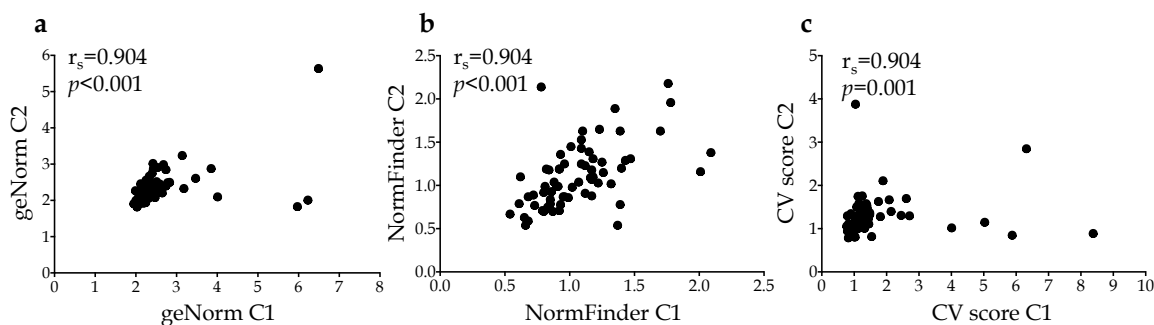


Figure 26. Correlation of stability values for each employed algorithm between C1 and C2 data. (a) geNorm stability value is represented in Y axis for C1 and X axis for C2; (b) Normfinder stability value is represented in Y axis for C1 and X axis for C2; (c) CV Score is represented in Y axis for C1 and X axis for C2. Spearman's correlation test was used to measure the correlation levels between pairs. r_s : Spearman's Rho; p : p value.

Once assured that the stability values of each miRNA candidate has been reproducible by three different algorithms and in two different cohorts, the next step was selecting candidates miRNAs as EN. From the total set of candidates, 17 miRNAs, whose stability scores were the lowest (highest stability) and comparable between algorithms and cohorts, were selected. To outline the results from geNorm, Normfinder and CV score algorithms, the SSS for each miRNA was calculated [278]. In table 12, stability scores obtained for each miRNA and final SSS score are represented, showing that miR-23a-3p, miR-26b-5p, miR-125a-5p, miR-335-5p or miR-92b-3p might be suitable EN for CSF studies.

RESULTS

Table 12. miRNA stability scores for geNorm, Normfinder and CV algorithms and SSS score for CSF samples.

miRNA	geNorm	NormFinder	CV Score	SSS Score
miR-101-3p	1,63 (12)	0,83 (12)	0,98 (17)	2,07 (14)
miR-125a-5p	1,46 (4)	0,63 (3)	0,59 (3)	1,69 (3)
miR-143-3p	1,59 (8)	0,79 (8)	0,73 (9)	1,92 (9)
miR-151a-3p	1,71 (15)	0,90 (15)	0,85 (12)	2,11 (15)
miR-15a-5p	1,71 (16)	0,91 (16)	0,93 (16)	2,15 (17)
miR-181a-5p	1,67 (16)	0,87 (14)	0,80 (11)	2,05 (13)
miR-186-5p	1,72 (17)	0,92 (17)	0,88 (13)	2,14 (16)
miR-21-5p	1,66 (6)	0,74 (6)	0,62 (5)	1,82 (6)
miR-221-3p	1,61 (11)	0,81 (11)	0,61 (4)	1,90 (8)
miR-23a-3p	1,43 (1)	0,61 (1)	0,65 (6)	1,68 (2)
miR-26b-5p	1,46 (3)	0,64 (4)	0,46 (1)	1,66 (1)
miR-27a-3p	1,58 (7)	0,77 (7)	0,71 (8)	1,89 (7)
miR-335-5p	1,52 (5)	0,72 (5)	0,56 (2)	1,77 (5)
miR-652-3p	1,60 (10)	0,79 (9)	0,91 (15)	2,00 (12)
miR-653-3p	1,60 (9)	0,80 (10)	0,89 (14)	1,99 (11)
miR-9-5p	1,64 (13)	0,83 (13)	0,76 (10)	1,99 (10)
miR-92b-3p	1,44 (2)	0,62 (2)	0,66 (7)	1,70 (4)

miRNA stability scores are represented for each algorithm and its ranked position from the total set of 17 miRNAs is in brackets. CV: coefficient of variation; SSS: summarized stability score.

Despite selecting the best EN for CSF samples, establishing the optimum number of reference miRNAs must be experimentally determined. geNorm also generates a pairwise stability measure to determine if adding more reference miRNA for the normalization process is beneficial. As shown in Figure 27, the recommended cut off value of 0.15 indicates that the use of eight EN in CSF samples would offer an acceptable stability of the reference miRNA combination [291].

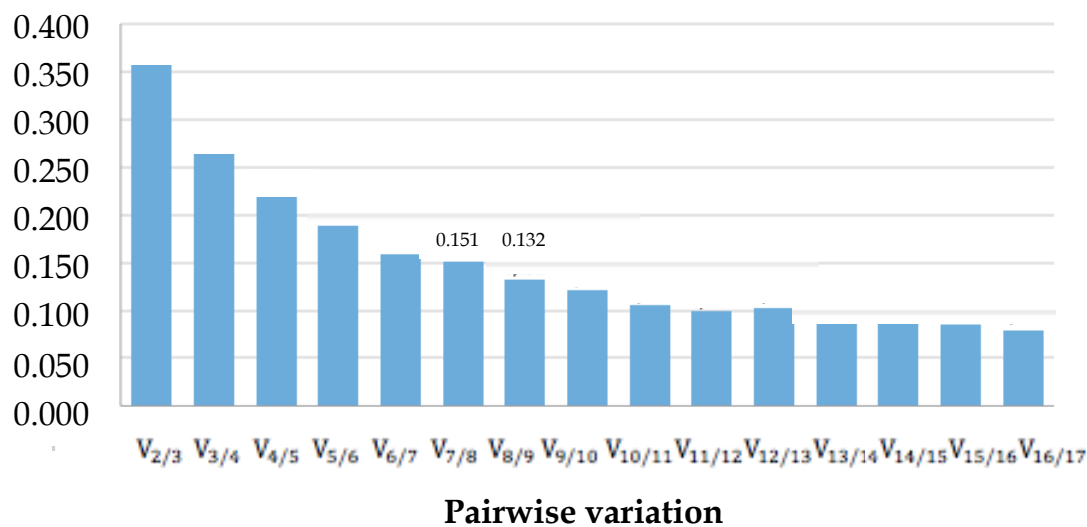


Figure 27. Evaluation of the optimum number of reference miRNAs according to the geNorm software. Pairwise variation between samples is reduced by the inclusion of additional reference miRNAs. The magnitude of the change in the normalization factor after the inclusion of an ninth additional reference gene implies a value under the recommended cut off of 0.15 shows that the use of eight endogenous controls is optimum for CSF samples.

4.1.7 Summary

TaqMan Advanced miRNA technology from Applied Biosystems™ is suitable for studying samples of at least 300 µl of CSF as long as 22 cycles of preamplification step are carried out.

The cc-OA plates with 216 loaded miRNA assays allow the detection of approximately 35% of these miRNAs in at least 70% of studied samples, being miR-770-5p the one with the lowest Cq values. These platforms present a good correlation with individual qPCR data.

Although the use of eight endogenous controls in CSF samples is highly recommended, miR-23a-3p, miR-26b-5p, miR-125a-5p, miR-335-5p and miR-92b-3p are the most stable miRNAs in CSF.

These OpenArray plates might be used to carry out miRNA screening studies not only in MS, but also in other neurological diseases as they can detect a wide range of CSF-enriched miRNAs.

RESULTS

4.2 CHOICE OF A SUITABLE FLOWCHART TO ANALYZE OpenArray miRNA DATA IN CSF SAMPLES

The objective of this part was to describe the most suitable way to analyze data from TaqMan OpenArray Human Advanced microRNA panels in CSF samples. Different strategies were used for the analyses in some of the steps of the process: handling technical replicates, selecting curve quality control conditions, handling missing data and selecting normalization method. A similar procedure was used in serum samples to prove that CSF analyses should be CSF-specific due to the different nature and characteristics of these biofluids. Each analysis step involves different challenges and the results of each strategy were compared in order to establish the best option (Figure 28).

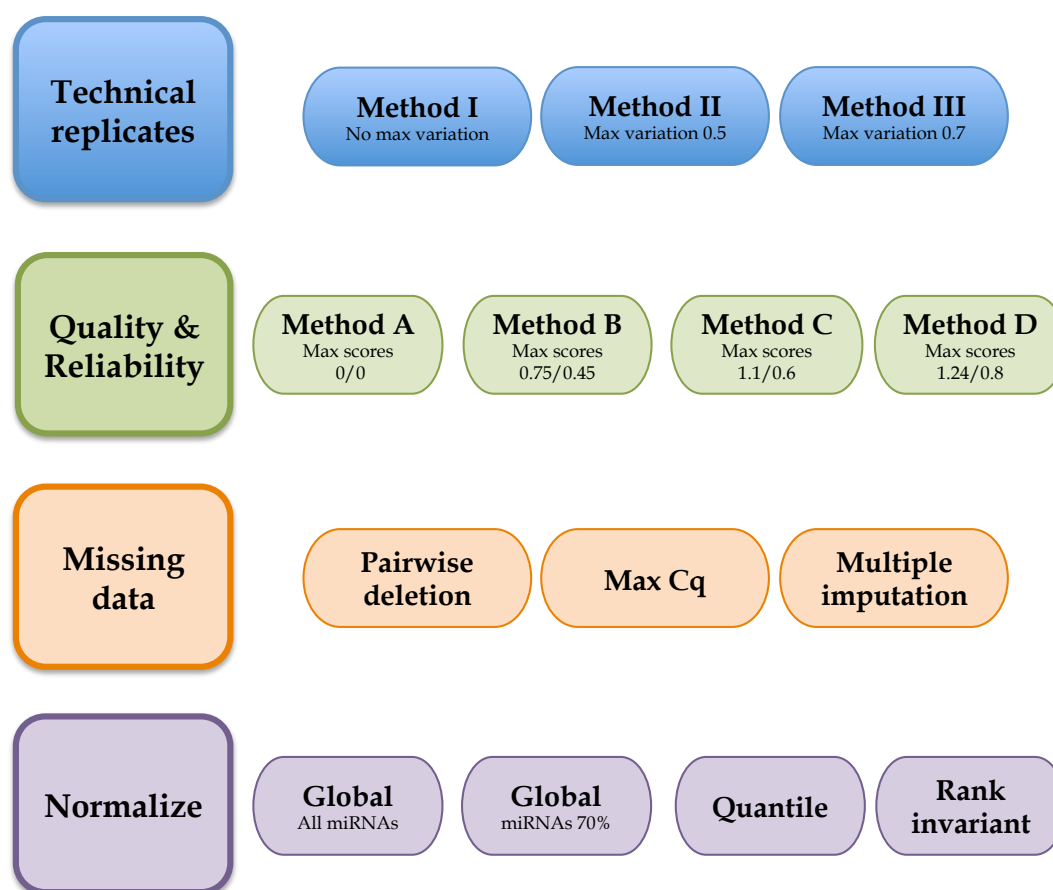


Figure 28. Scheme of the four steps of the OpenArray analysis flowchart under comparison. Each step presents different employed strategies. Max: maximum.

4.2.1 Samples

To develop this whole section, 28 CSF samples and 20 serum samples were used to analyze their miRNA content by TaqMan OpenArray Human Advanced microRNA panels. Those samples belonged to RRMS patients and OND individuals. Each CSF sample was run in triplicate in the cc-OA panels described in previous section, whereas serum sample was run just once in fc-OA panels (756 miRNA assays). However, to compare the analysis method between serum and CSF, only information of the 215 miRNAs included in the CSF panels was used for serum.

Henceforth, three datasets (Cq values) were used:

- CSF samples without replicates (NoRep_CSF)
- CSF samples with triplicates (Trip_CSF)
- Serum samples without replicates (Serum)

As it was shown in previous Results section, to exclude any sample (due to low miRNA detection), the total count of valid Cq values detected should be taken into account more than the mean Cq value for each sample. Cq values in this study were considered as valid if they were situated in the Cq interval 15-35 for CSF samples and 15-28 for serum samples.

As shown in Figures 29a and 29b, CSF_3 and CSF_5 were the samples with lower number of valid Cq values for both NoRep_CSF and Trip_CSF datasets and were excluded for posterior analyses. Similarly, Serum_7 was highlighted by presenting the lowest number of valid Cq values and was discarded (Figure 29c).

RESULTS

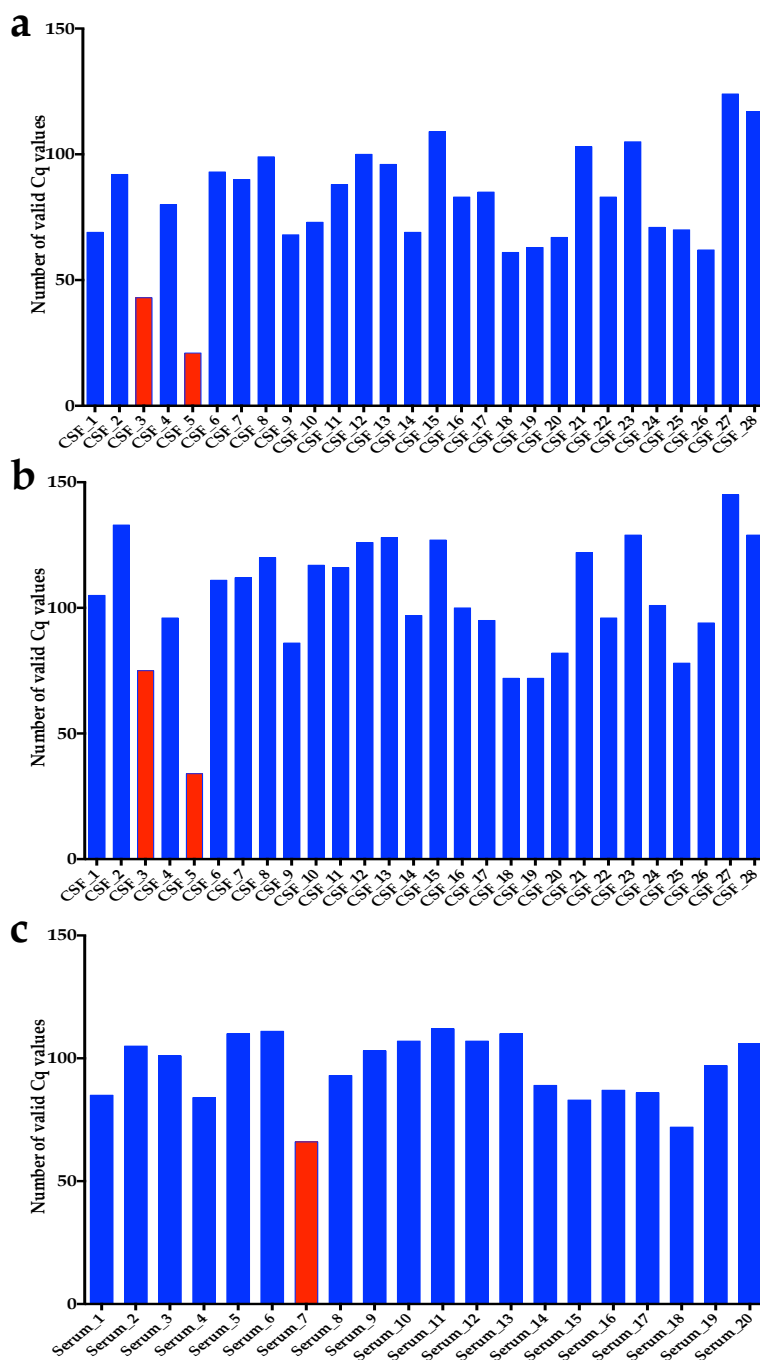


Figure 29. Column graphs showing the valid number of Cq values detected in each sample. Valid number of Cq values for (a) NoRep_CSF, (b) Trip_CSF and (c) Serum datasets. Cq values were considered valid if they belonged to Cq values interval 15-35 for CSF and 15-28 for serum samples. Red columns corresponds to discarded samples.

4.2.2 Technical replicates

One of the first choices that should be faced when working with technical replicates is how to handle those values. Usually, the variation between technical measurements must be at most 0.5 cycles but, in order to avoid unnecessary loss of data points when working with circulating miRNAs De Ronde *et al* suggested an acceptable range in replicates depending on the mean Cq value (from 0.5 when mean Cq value is 25 to 1.9 for mean Cq value of 35) [290]. However, as their study was based on blood samples and CSF miRNA content is lower than serum or plasma (higher Cq values), the use of this interval with CSF might suppose more loss of analyzable data points. For this reason, another method with a more permissive allowed variation of 0.7 for Cq values ranging from 15 to 28 was proposed in order to increase analyzable miRNAs and a more strict variation of 0.9 for Cq values from 28 to 35 in order to avoid important quantification differences (Table 13).

Table 13. Description of used methods to handle technical replicates in Trip_CSF dataset.

	Method I	Method II	Method III
Maximum variation Cq 15-28	-	0.5	0.7
Maximum variation Cq 28-35	-	1.9	0.9
Minimum number of valid replicates	1	2	2

Three different methods were used to handle technical replicates and compared. Method I represents a non-strict method where mean value of replicates was calculated regardless of Cq variation and number of valid replicates. Method II is the one described by De Ronde *et al* [290] for blood samples where allowed Cq replicates variations depends on the mean Cq value. Method III is a new suggested method for CSF samples where a maximum variation of 0.7 between replicates is allowed for mean Cq values ranging 15-28 whereas a maximum variation of 0.9 is accepted when mean Cq values rises to 28-35.

The chosen method to handle technical replicates should offer a number of miRNAs to be analyzed as high as possible showing low variability between replicates. After handling replicates properly and, as a first approach, the percentage of samples in

RESULTS

which each miRNA was detected was calculated and classified each miRNA according to this percentage in Trip_CSF dataset (Figure 30).

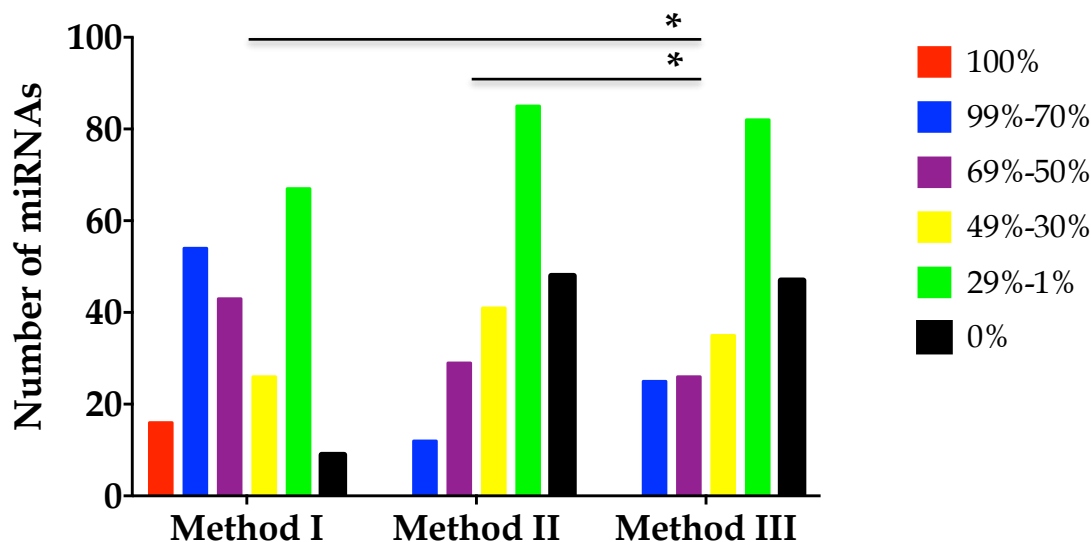


Figure 30. Column graphs showing the number of miRNAs detected in different percentages of samples for each handling replicates method. Each color represents miRNAs that were detected in different percentages of CSF samples: red=100% samples; blue=99%-70% samples; purple=69%-50% samples; yellow=49%-30% samples; green=29%-1% samples; black=0% samples. * indicates p values below 0.050 in Cohen's Kappa test, which means agreement among methods.

The Kappa Index, obtained through Cohen's Kappa (κ) test, was run to determine if there was agreement between the studied methods on measuring the category of sample percentage detection of each miRNA. There was agreement between Methods I-III and II-III ($\kappa=0.109$, $p<0.001$; $\kappa=0.763$, $p<0.001$, respectively) but disagreement between Methods I-II ($\kappa=0.051$, $p=0.092$). This means that non-strict Method I and Method II differ in classifying miRNA output according to the samples where they are detected but, Method III represents a halfway between them. In addition, another data is shown in Figure 29 as Method I offered 70 miRNAs to be further analyzed (those detected in at least 70% of total samples) compared to 12 by Method II and 25 by Method III.

However, as low variability between replicates is also a requirement for choosing the method, CV between replicates, a measure of precision, was measured and

compared for those potential analyzable miRNAs (detected in 70% of samples) for each method.

There were statistically significant differences in CV among the three methods ($p < 0.001$). *Post hoc* analyses revealed that these differences were due to Method I as distribution of CV for Method II and Method III could be considered equal ($p = 0.556$) (Figure 31).

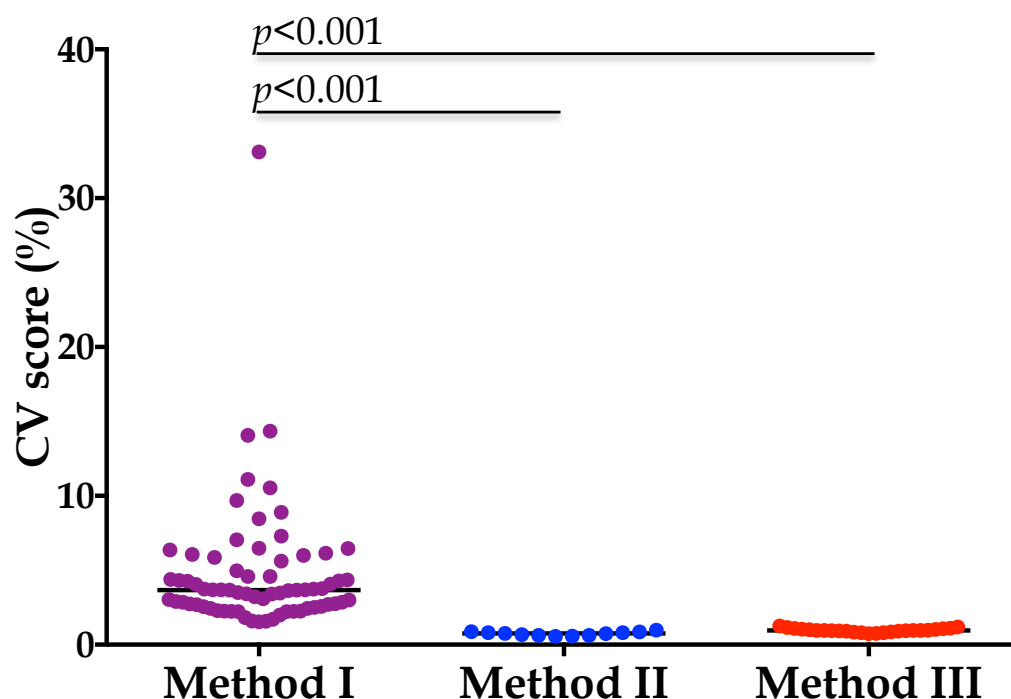


Figure 31. CV of technical replicates of analyzable miRNA for each method. Each dot represents one analyzable miRNA (detected in at least 70% of CSF samples) and the line represents the median. Kruskal Wallis test was used to measure distribution differences between methods.

To sum up, although Method I offers the largest number of potential analyzable miRNAs, the variability of technical replicates is extremely high due to lack of strictness. Therefore, as Method III offers a greater number of analyzable miRNAs than Method II in agreement with the classification of how detectable a miRNA is and the CV of replicates is not different from Method II, the use of a variation of 0.7 for Cq values ranging from 15 to 28 and 0.9 for Cq values from 28 to 35 is suggested from now on to analyze technical replicates in CSF samples in OpenArray data.

RESULTS

4.2.3 Evaluation of quality and reliability of Cq values

Once we have established how to handle technical replicates with Trip_CSF dataset, the three previously described datasets were used to move forward with next sections. QuantStudio™ 12K Flex software generates Cq values and provides exportable experimental data that can be further analyzed. Some important information available is the Amp Score, which is a metric of the quality of the reaction, and the Cq confidence value, a measure of Cq reliability [292]. As a default setting, these values should be equal or above 1.24 and 0.8 respectively, although another cut off of 1.1 and 0.6 is also acceptable. This means that those amplification curves whose Amp Score and Cq confidence values don't reach the cut off will be discarded for the posterior miRNA analysis. However, as proposed in this section, CSF should not be treated as serum or plasma. For that reason, another approaches for Trip_CSF, NoRep_CSF and Serum datasets (Table 14) were used and their performances compared to find the most suitable method for CSF.

Table 14. Description of methods to evaluate quality and reliability of Cq values in studied datasets.

	Method A	Method B	Method C	Method D
Amp Score	-	0.75	1.1	1.24
Cq Confidence	-	0.45	0.6	0.8
Cq values interval	15-35	15-35#/15-28*	15-35#/15-28*	15-28

Four different methods were used to measure quality and reliability of Cq values. Different allowed Amp Score, Cq Confidence values and Cq intervals combinations were proposed. # indicates Cq values intervals used for CSF datasets.* indicates Cq values intervals used for Serum dataset.

Although the recommended combination is Method C or Method D, the application or the use of these strict analyses in CSF samples might suppose an important loss of potential analyzable data. The chosen combination of quality and reliability parameters for CSF should offer a number of miRNAs to be analyzed as high as possible showing acceptable quality.

First, after rejecting Cq data not fulfilling the established AmpScore, Cq Confidence and Cq interval established by each method, the percentage of samples in which each miRNA was detected was calculated for NoRep_CSF, Trip_CSF and Serum datasets and each miRNA was classified according to this percentage (Figure 32).

Cohen's κ test was run to determine if there was agreement between the studied methods (A, B, C or D) for each dataset on measuring the category of sample percentage detection of each miRNA. On one hand, in NoRep_CSF dataset, there was agreement between Methods A-B, A-C and B-C ($\kappa=0.837$, $p<0.001$; $\kappa=0.555$, $p=0.041$; $\kappa=0.619$, $p<0.001$, respectively) but disagreement between A-D, B-D and C-D ($\kappa=-0.042$, $p=0.055$; $\kappa=-0.031$, $p=0.193$; $\kappa=0.001$, $p=0.975$; respectively). In Trip_CSF dataset, there was also agreement between Methods A-B, A-C and B-C ($\kappa=0.901$, $p<0.001$; $\kappa=0.668$, $p<0.001$; $\kappa=0.739$, $p<0.001$, respectively) but disagreement between A-D and B-D ($\kappa=-0.001$, $p=0.962$; $\kappa=0.020$, $p=0.497$; respectively). It should be noted that Methods C-D presented agreement ($\kappa=0.080$, $p=0.021$), unlike NoRep_CSF dataset, probably due to the different dynamics in miRNA detectability observed after applying Method C in the two CSF datasets. Despite this difference, it might be supposed that A, B and C method would be comparable for CSF samples on account of miRNA detectability. On the other hand, the presence of agreement between all Methods ($p<0.001$) in Serum dataset begins to highlight the existing differences between both biofluids.

RESULTS

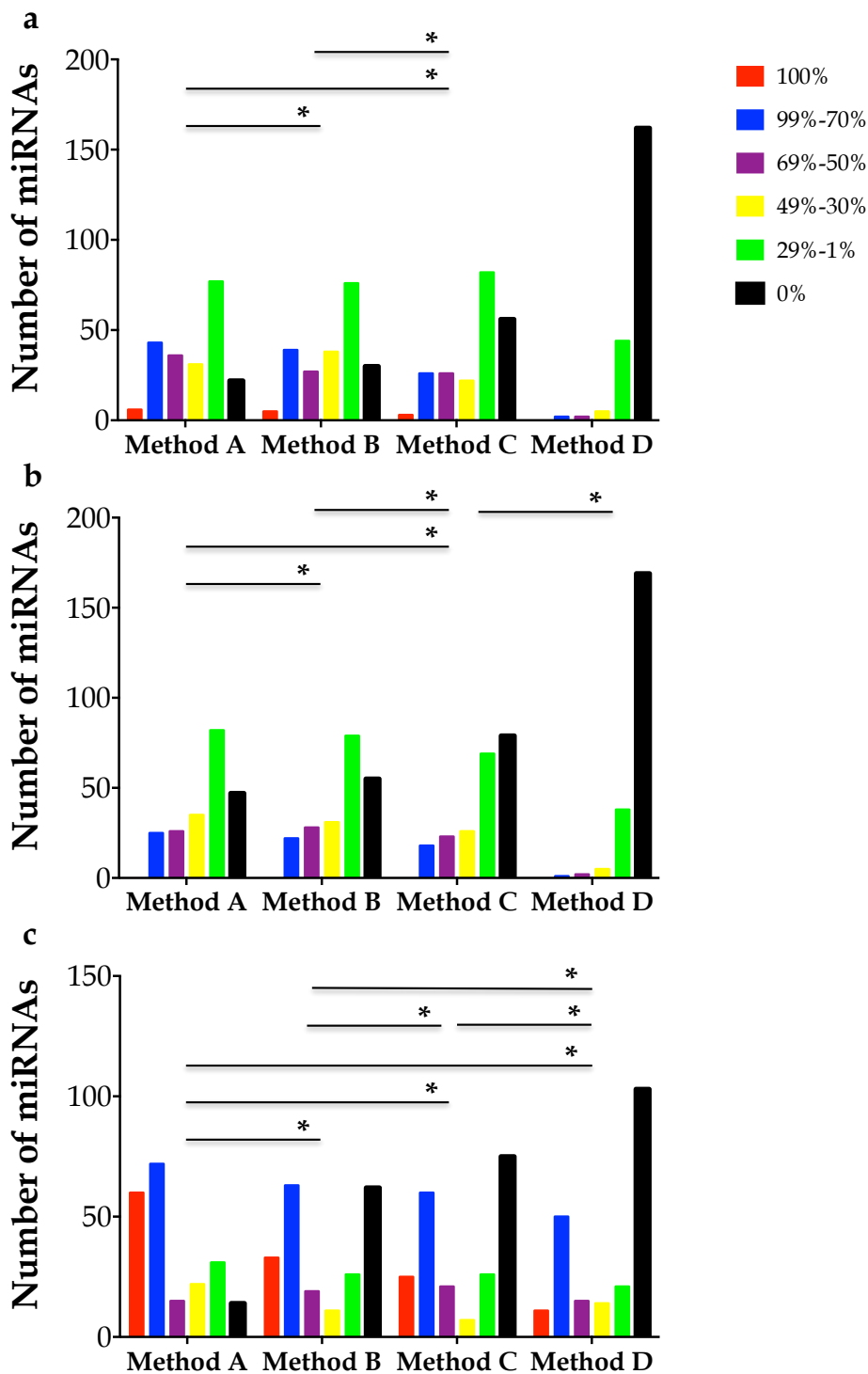


Figure 32. Column graphs showing the number of miRNAs detected in different percentages of samples according to each quality parameters combination. Each color represents miRNAs that were detected in different percentages of CSF or serum samples for (a) NoRep_CSF, (b) Trip_CSF and, (c) Serum datasets: red=100% samples; blue=99%-70% samples; purple=69%-50% samples; yellow=49%-30% samples; green=29%-1% samples; black=0% samples. * indicates p values below 0.050 in Cohen's Kappa test, which means agreement among methods.

Second, Method A offers the highest number of analyzable miRNAs compared to B and C but might suppose the use of amplification curves data of bad quality. For this reason, Amp Score and Cq Confidence values for miRNAs included in each method (A, B, C) in CSF datasets were compared and none statistical differences between methods were observed (Figure 33). This means that Method A offers more analyzable miRNAs with comparable quality parameters than B and C.

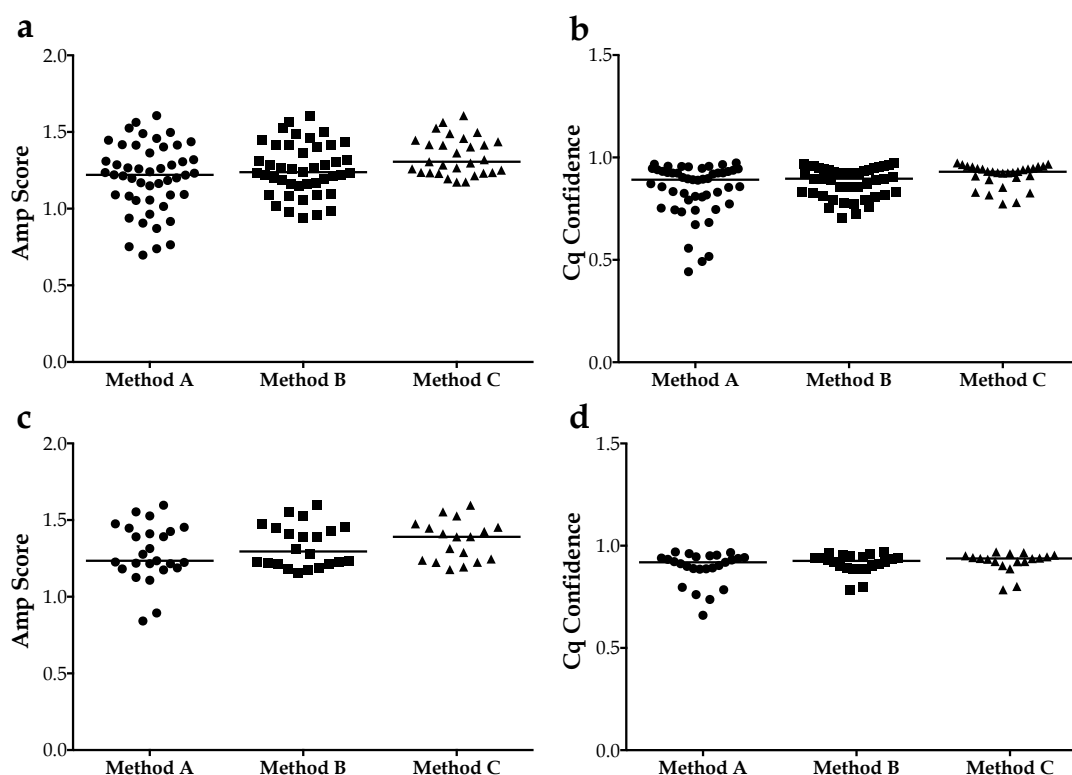


Figure 33. Amp Score and Cq Confidence values for NoRep_CSF and Trip_CSF datasets. (a) Amp Score values and (b) Cq Confidence values for NoRep_CSF; (c) Amp Score values and (d) Cq Confidence values for Trip_CSF. Each dot represents a specific miRNA, line represents median. Kruskal Wallis test was used to measure statistical differences.

Third, as one of the aim of this section was to prove that CSF analyses should be not the same than the one employed with serum samples due to the different nature of the biofluids, the distribution of detectability categories for miRNAs for each method (A, B, C and D) was compared between NoRep_CSF/Trip_CSF and Serum datasets. The X^2 goodness-of-fit test was used to determine whether the distribution of miRNAs in the categorical variable (% of samples) follows the distribution observed

RESULTS

in Serum dataset. All p values were less than 0.001 what indicates that CSF data did not fit the observed distribution in Serum dataset, remarking the difference of these biofluids.

Therefore, the recommended Amp Score and Cq Confidence values of 1.1 and 0.6 respectively, would be the employed for Serum datasets from now on. However, these parameters won't be taking into account with CSF samples as this choice offered the highest number of potential analyzable miRNAs without assuming a perceived change in amplification curve quality.

4.2.4 Handling missing data

Another challenge that should be faced is handling missing data in the dataset. A large number of missing data might be expected when working with low concentrations of miRNAs. Usually, these missing data are ignored and the subsequent miRNA analysis is made without this information, what is known as pairwise deletion method (PW). However, the exclusion of missing data might lead to loss of statistical power and loss of data points. The most common way to solve this is replacing all missing values with a Cq value corresponding to the maximum number of cycles run in the qPCR equipment (MaxCq). A new approach was proposed by de Ronde *et al* [290] (dR) where missing data were distinguished between "undetectable" (missing data due to target concentration is zero or too low to be measured quantitatively) and "invalid" (missing data due to technical errors). Once categorized, "undetectable" values were substituted by the highest Cq+1 for each miRNA and "invalid" missing data were replaced by multiple imputation. The main aim of this section was to compare the performance of PW, MaxCq and dR methods in handling missing data. With this objective, a real dataset (RD) was obtained from Serum (28 miRNAs and 19 samples with complete miRNA information) that would suppose the basis for next work.

The proportion and distribution of "Undetectable" and "Invalid" values was studied from the final group of analyzable miRNAs (detected in 70% samples) in

NoRep_CSF, Trip_CSF and Serum datasets. To recreate these behaviours in RD, random values were generated by RStudio to establish miRNA detectability and specific “Undetectable”/“Invalid” missing values. Figure 34 shows colored schemes of the behaviors of NoRep_CSF, Trip_CSF and Serum datasets and the subsequent recreation in RD (28 miRNAsx19 samples) for each one.

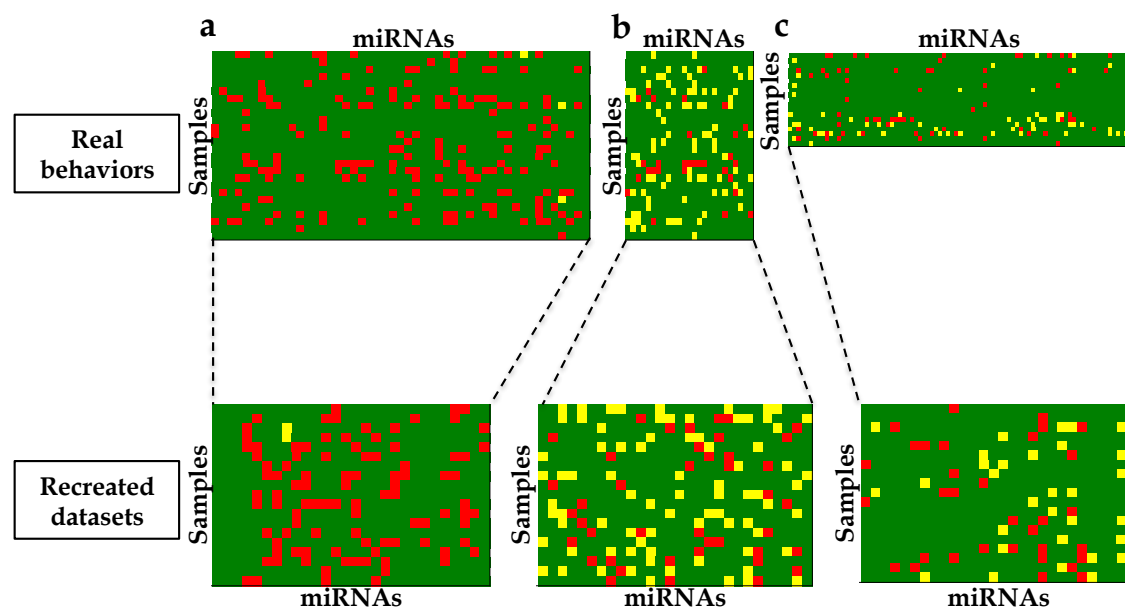


Figure 34. Colored schemes showing datasets behaviours and simulated recreations. Green: valid values; red: undetectable values and; yellow: invalid values. Each square represents a specific value for one miRNA and one sample. (a) Behaviour of NoRep_CSF dataset and its corresponding recreated dataset from real dataset, (b) Behaviour of Trip_CSF dataset and its corresponding recreated dataset from real dataset and, (c) Behaviour of Serum dataset and its corresponding recreated dataset from real dataset.

Once simulated, the substitution of “Undetectable” and “Invalid” values as appropriate according to PW, MaxCq or dR method was made. Two different approaches were used to compare the performance of each method with the complete RD.

First, CV for each miRNA was calculated and compared as observed in Figure 35. MaxCq method produced CV distribution that significantly differed from the RD, PW and dR methods. There were statistically significant differences in CV between

RESULTS

the methods ($p < 0.001$). *Post hoc* analyses revealed that these differences were due to MaxCq as distribution of CV for RD, PW and dR could be considered equal.

Second, as the miRNA mean value might be used as a possible way of normalizing data, correlation of miRNA mean value between RD and recreated datasets were made to confirm which method resembled more to the real information. As observed in Figure 36, all methods strongly correlated with the real mean miRNA value but PW obtained the highest Spearman's Rho coefficients.

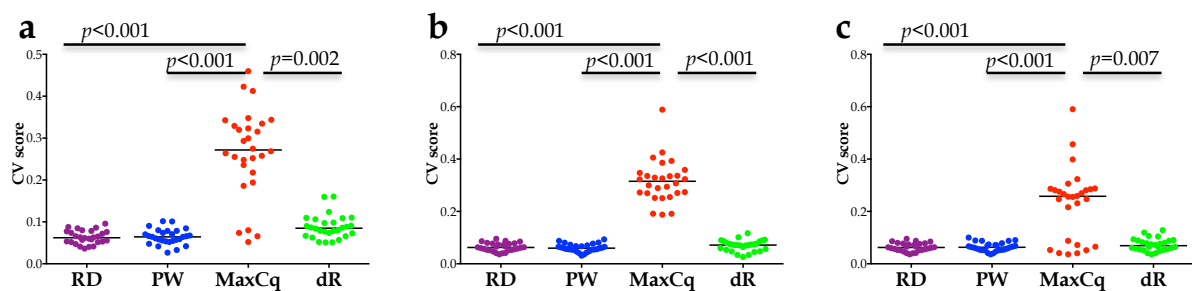


Figure 35. CV distribution for RD, PW, MaxCq and dR methods in each dataset. CV scores for (a) No_Rep_CSF, (b) Trip_CSF and (c) Serum datasets. CV: coefficient of variation; RD: real dataset; PW: pairwise deletion method; MaxCq: maximum Cq from qPCR machine; dR: method described by de Ronde et al [290]. Each dot represents one miRNA and the line represents the median. Kruskal Wallis test was used to measure statistical differences.

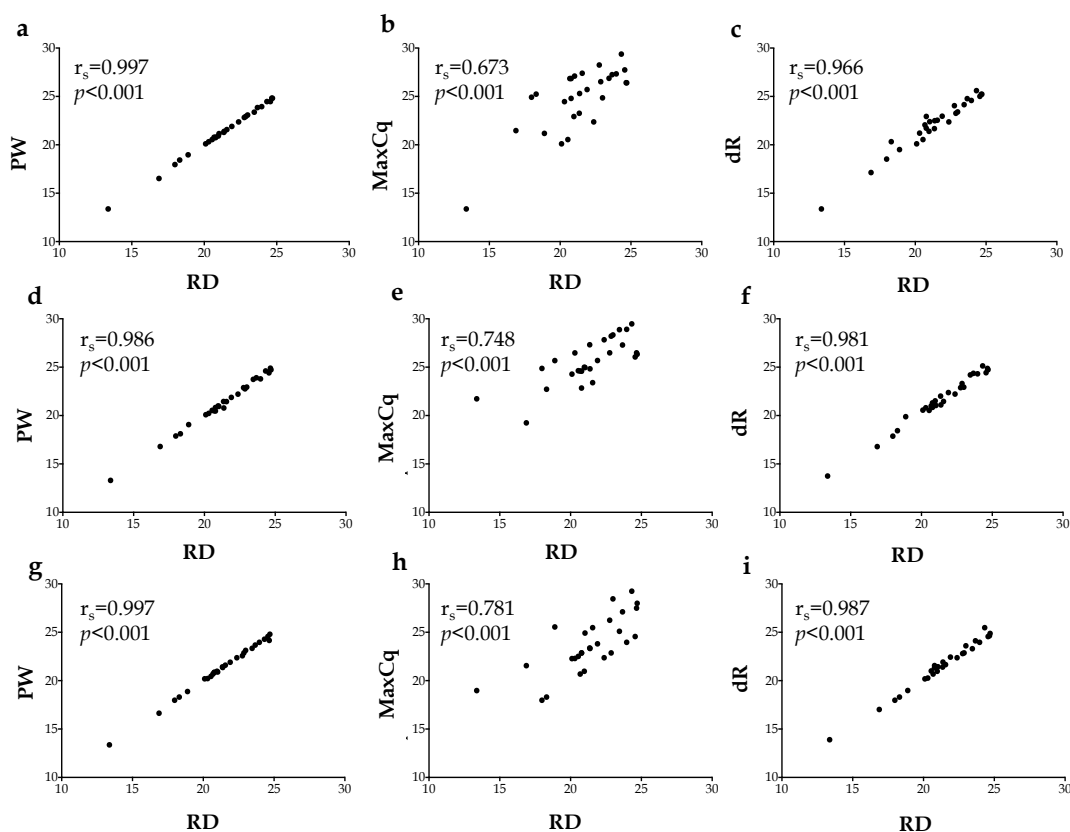


Figure 36. Scatter plot showing association between the real mean miRNA value and recreated values. Correlation between real miRNA mean value and miRNA mean value for NoRep_CSF in PW (a), MaxCq (b) and dR (c). Correlation between real miRNA mean value and miRNA mean value for Trip_CSF in PW (d), MaxCq (e) and dR (f). Correlation between real miRNA mean value and miRNA mean value for Serum in PW (g), MaxCq (h) and dR (i). Spearman's correlation test was used to measure the correlation levels between pairs. r_s : Spearman's Rho; p : p value.

To sum up, from now PW method will be used to handle missing data and these "empty" values will remain without numerical value.

4.2.5 Normalization methods for OpenArray plates in CSF samples

As explained in previous chapter, normalization is an essential procedure in qPCR experiments to control variations in extraction yield, RT yield and efficiency of amplification. Suitable EN for CSF were previously identified and the optimum number of candidates to be used in experiments involving individual qPCR was established in eight miRNAs. However, for array-based qPCR data like this one, GN, a normalization method based on the mean expression value of all miRNAs has been

RESULTS

proposed and validated. Another methods have been also evaluated before for profiling experiments as QN or RIN. In this section, GN using all available miRNA data (GN_All), GN using analyzable miRNA data (GN_70%), QN and RIN methods were compared to establish the optimal approach to be used in our cohort (Figure 37).

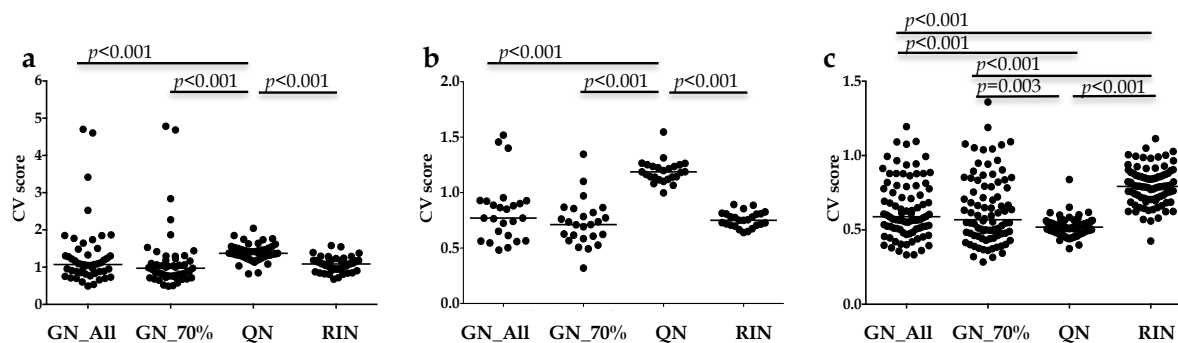


Figure 37. CV distribution for GN_All, GN_70%, QN and RIN normalization methods in each dataset. CV scores for (a) No_Rep_CSF, (b) Trip_CSF and (c) Serum datasets. CV: coefficient of variation; GN: global normalization; GN_All: GN using all available miRNA data; GN_70%: GN using analyzable miRNA data; QN: quantile normalization; RIN: rank-invariant normalization method. Each dot represents one miRNA and the line represents the median. Kruskal Wallis test was used to measure statistical differences.

The CV was calculated for each normalization method. The lower CV was, the more reproducible and reliable the normalization method was. There were statistically significant differences in CV between the methods ($p < 0.001$) in the three datasets. *Post hoc* analyses revealed that these differences were due to QN method in NoRep_CSF and Trip_CSF datasets (adjusted p values under 0.001 respect the other methods) (Figure 36), being GN_70% the method with the lowest CV median value for CSF. However, in serum samples, except for GN_All and GN_70% whose adjusted p value was 1.000, CV distributions differed between methods, being QN the one with lowest median value.

4.2.6 Replicates vs individual measurements in OpenArray

To be able to detect any significant differential expression between biological groups, miRNA RQ should be calculated using $\Delta\Delta C_t$ method. RQ using OND as reference

group was obtained for each miRNA not only in Trip_CSF and NoRep_CSF datasets, but also in the other two remaining CSF datasets that were used to obtain the triplicates measurements. These data were used to compare reproducibility of results between plates and to propose an appropriate approach when designing miRNA screening studies.

As observed in Figure 38, positive correlations were observed in RQ values between datasets. The strongest associations were obtained between triplicates measurements and individual datasets, as Trip_CSF is formed by three individual measurements.

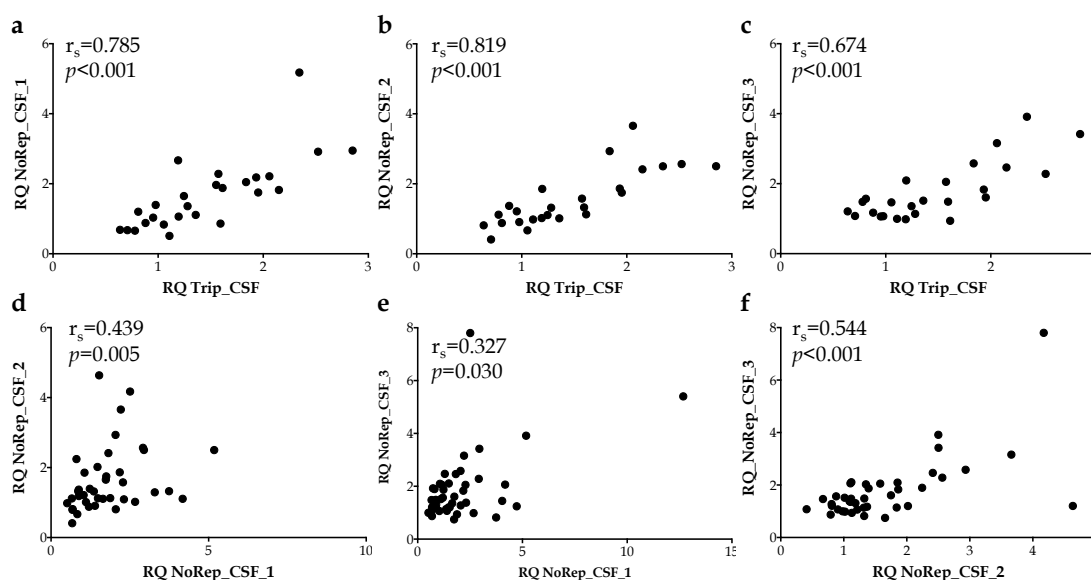


Figure 38. Scatter plot showing association between miRNA relative quantifications in Trip_CSF and NoRep_CSF datasets. Correlation between RQ in (a) Trip_CSF and NoRep_CSF_1, (b) Trip_CSF and NoRep_CSF_2, (c) Trip_CSF and NoRep_CSF_3, (d) NoRep_CSF_1 and NoRep_CSF_2, (e) NoRep_CSF_1 and NoRep_CSF_3 and, (f) NoRep_CSF_1 and NoRep_CSF_3.

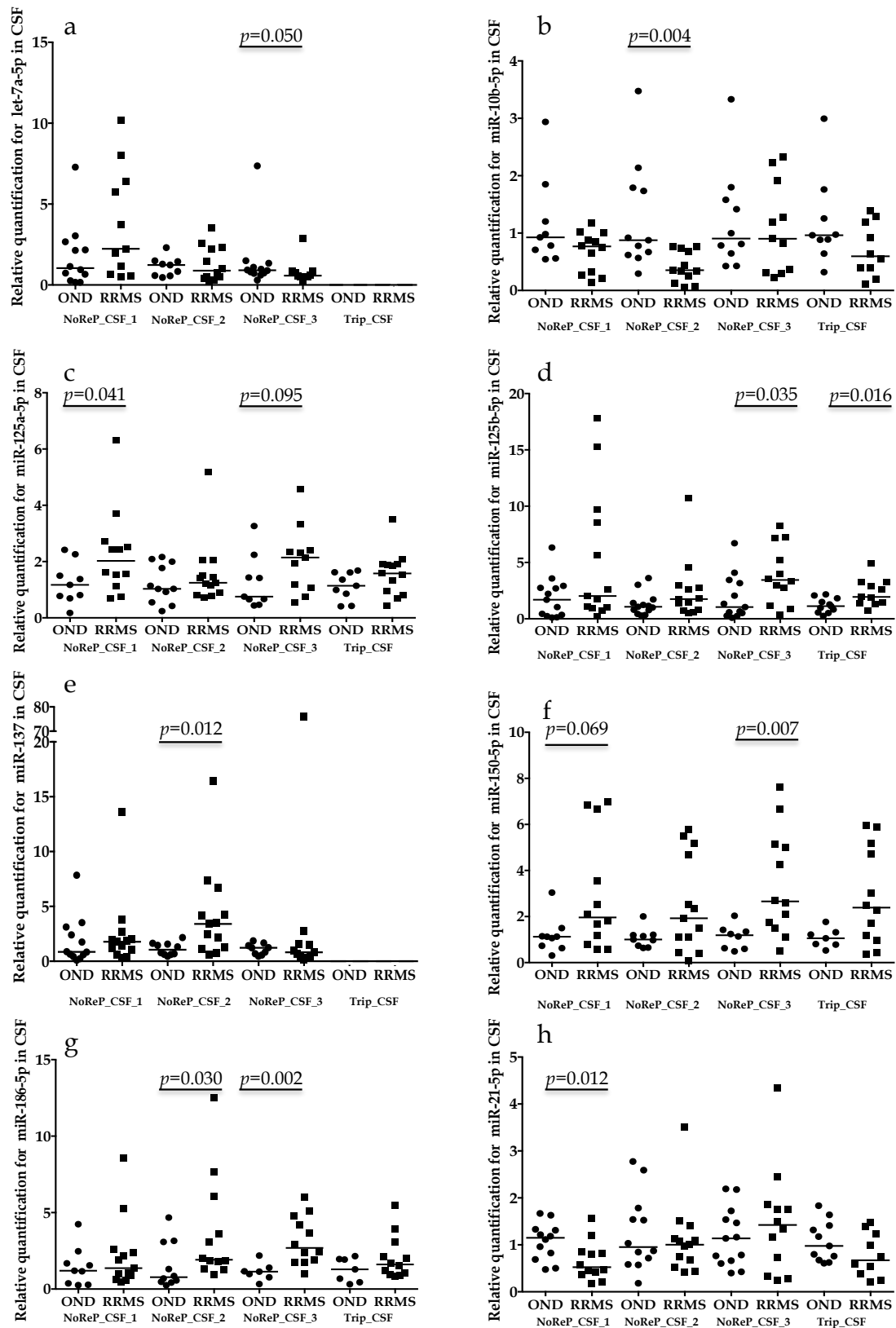
However, when using RQ values to establish the existence of differential expression between OND and RRMS groups, the statistical significances didn't match between all datasets (Table 15). Eight of 13 miRNAs showed statistical significance in only one of the datasets. Other two presented differential expression in two datasets, while miR-9-5p was significantly down-regulated in two of the datasets and had a tendency to be deregulated in another one.

RESULTS

Table 15. Relative quantification of miRNA expression in RRMS *vs* OND in CSF samples in individual measurements or triplicate measurements analysis.

	NoRep_CSF_1		NoRep_CSF_2		NoRep_CSF_3		Trip_CSF	
	RQ	<i>p</i> value	RQ	<i>p</i> value	RQ	<i>p</i> value	RQ	<i>p</i> value
let-7a-5p	3.744	0.169	1.324	0.862	0.820	0.050		
miR-10b-5p	0.673	0.169	0.410	0.004	1.077	0.705	0.708	0.182
miR-125a-5p	2.283	0.041	1.578	0.531	2.052	0.095	1.574	0.164
miR-125b-5p	5.177	0.204	2.501	0.153	3.913	0.035	2.344	0.016
miR-137	2.508	0.470	4.173	0.012	7.802	0.603		
miR-150-5p	2.947	0.069	2.503	0.164	3.418	0.007	2.850	0.100
miR-186-5p	2.214	0.471	3.659	0.030	3.158	0.002	2.059	0.261
miR-21-5p	0.660	0.012	1.116	0.650	1.481	0.650	0.780	0.132
miR-221-3p	1.738	0.272	1.655	0.492	0.746	0.035		
miR-25-3p	1.298	0.882			2.470	0.089		
miR-497-5p	0.681	0.196	0.793	0.023	0.874	0.251		
miR-9-5p	0.685	0.032	0.812	0.059	1.209	0.776	0.638	0.014
miR-92b-3p	0.834	0.088	0.670	0.101	1.467	0.118	1.054	0.972

RQ: relative quantification. Statistical differences were determined by Mann-Whitney U test.



RESULTS

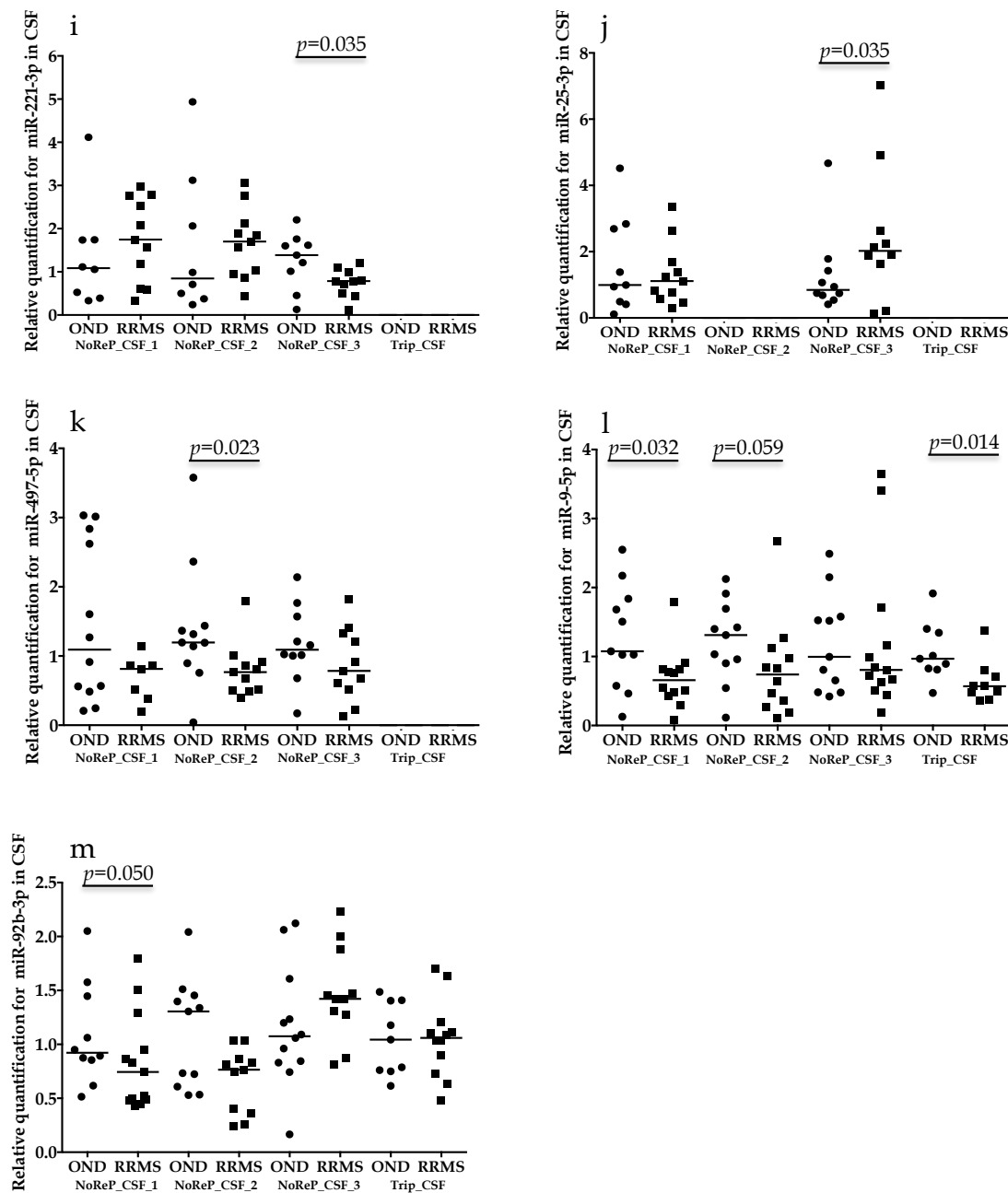


Figure 39. Relative quantification of miRNA levels in CSF of RRMS and OND in individual and triplicates measurements in OpenArray analysis. Dot plots for normalized values of (a) let-7a-5p, (b) miR-10b-5p, (c) miR-125a-5p, (d) miR-125b-5p, (e) miR-137, (f) miR-150-5p, (g) miR-186-5p, (h) miR-21-5p, (i) miR-221-3p, (j) miR-25-3p, (k) miR-497-5p, (l) miR-9-5p and (m) miR-92b-3p in CSF samples according to the group in individual measurement datasets and triplicates dataset. The dot indicates one sample and the line indicates the median. U-Mann Whitney test was used to determine statistical differences between groups.

On the other hand, Figure 39 showed the distribution of RQ values of OND and RRMS for each dataset. Five of 13 miRNA RQ distributions (let-7a-5p, miR-137, miR-

21-5p, miR-221-3p and miR-92b-3p) differed between datasets according to the median values, while the other presented a more similar appearance.

These observations might suggest two aspects to consider. First, the need to validate these profiling studies in larger cohorts should be a mandatory requirement. Second, despite the discrepancy in significant differences, RQ distributions remained mostly homogenous between dataset, which might support the idea of avoiding strictness in screening phases. Therefore, although it is unusual running each CSF sample per triplicate in OpenArray plates during profiling phases, we highly recommend this approach if possible in order to have a wider and more robust range of data.

4.2.7 Summary

miRNA content in CSF and serum samples was not the same, which makes miRNA detection different in terms of quantity and quality in both biofluids. For this reason, the subsequent OpenArray data analysis should be CSF-specific. The parallel comparison with Serum dataset evidenced the differences between biofluids.

We proposed to run each CSF sample per triplicate allowing a maximum variation of 0.7 between Cq replicates (0.9 in Cq interval 28-35). The fact of carrying on with the analysis with those miRNAs detected in at least 70% of samples allowed the inclusion of amplification curves with good quality, so using Amp Score and Cq Confidence values was not necessary.

Regarding handling missing data, it was not required to use a replacement method since PW showed the least CV and the strongest correlation with the real data.

GN was the chosen method to normalize CSF and calculate RQ values. Figure 40 shows the scheme of the different analyzed steps with the choice for each dataset.

RESULTS

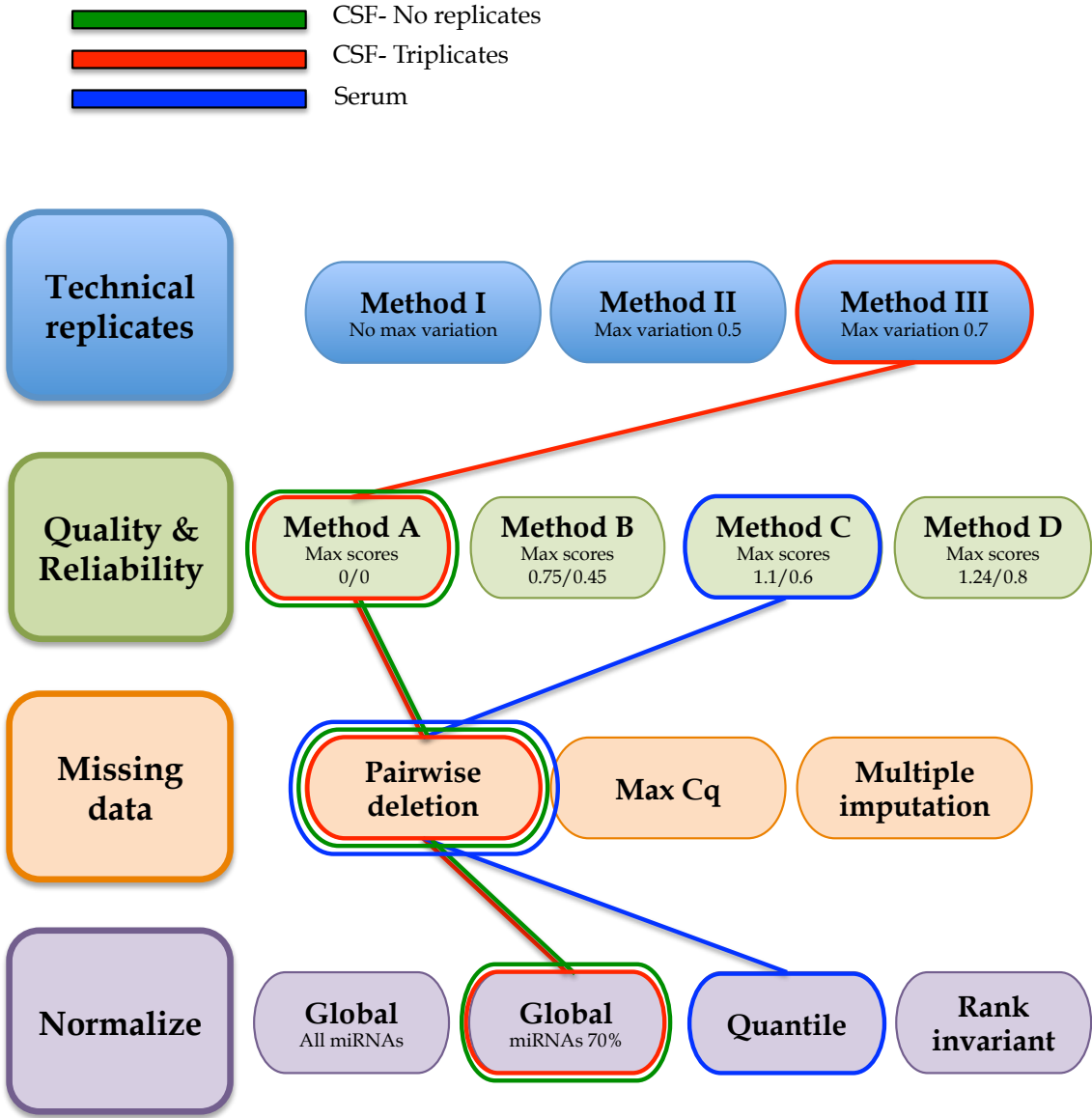


Figure 40. Scheme of the four steps of the OpenArray analysis flowchart under comparison with the selected method for each dataset. Green line represents NoRep_CSF dataset, red line represents Trip_CSF dataset and, blue line represents Serum dataset.

4.3 STUDY OF THE CIRCULATING miRNA PROFILES IN PPMS PATIENTS

The main objective of this section was to describe a specific miRNA signature of PPMS patients in both CSF and serum compared to OND and RRMS samples. The cc-OA panels previously described and fc-OA panels were used to screen miRNA expression in CSF and serum samples, respectively. Next, those miRNAs whose expression was found deregulated in PPMS samples were explored in a larger cohort by means of individual qPCR in order to validate the results from screening phase and correlate them with other variables.

4.3.1 Samples: inclusion and exclusion criteria

Patients included in this study were recruited at the Girona Neuroimmunology and Multiple Sclerosis Unit of Dr. Josep Trueta University Hospital (Girona, Spain), in the Immunology and Neurology Departments of Ramón y Cajal University Hospital (Madrid, Spain) and in the Multiple Sclerosis Unit of Hospital Universitari i Politècnic La Fe (Valencia, Spain). All participants signed a written informed consent. To be included in the study, participants over 18 years old should have been diagnosed with RRMS or PPMS according to McDonald 2010 criteria or with OND. Those individuals diagnosed with SPMS or receiving disease-modifying treatment at the moment of sample extraction were excluded.

4.3.2 Clinical characteristics of the studied cohort

This study comprised 111 individuals (60.4% women) with a median age of 51.5 years old. 49 subjects belonged to PPMS group (55.1% women), 35 to RRMS (68.6% women) and, 27 were OND individuals (59.3% women). Clinical, radiological and genetic data are shown in Table 16. No significant differences were observed in sex between groups. Age at sampling showed statistically significant differences between groups ($p < 0.001$) as RRMS individuals were younger than PPMS and OND. As our main focus was to describe a characteristic miRNA profile for PPMS and it has been established that this clinical subtype is associated with an older onset age compared to RRMS [293], we assured that OND group did not show differences with PPMS

RESULTS

regarding age. In addition, EDSS scores for PPMS were higher compared to RRMS (PPMS median=3.0 vs RRMS median=1.5; $p=0.030$) and the presence of Gd+ lesions in MRI was lower in PPMS group ($p=0.033$). The intrathecal synthesis of OCGB and OCMB_LS was not present in any of OND subjects ($p<0.001$ and $p=0.003$, respectively).

Table 16. Demographic, clinical, radiological and genetic data of the studied cohorts in PPMS study.

	Whole group	OND	RRMS	PPMS	<i>p</i> value
n	111	27	35	49	
Sex					0.457
Male	44 (39.6)	11 (40.7)	11 (31.4)	22 (44.9)	
Female	67 (60.4)	16 (59.3)	24 (68.6)	27 (55.1)	
Age at sampling (years)	51.5 (45.0-59.0)	56.0 (48.0-65.5)	47.5 (40.0-51.0)	56.0 (48.0-61.0)	<0.001
EDSS at sampling	3.0 (2.5-4.0)	-	1.5 (1.0-2.0)	3.0 (3.0-4.0)	0.030
OCGB					<0.001
Absence	33 (34.0)	23 (100.0)	5 (15.6)	5 (11.9)	
Presence	64 (66.0)	0 (0.0)	27 (84.4)	37 (88.1)	
LS_OCMB					0.003
Absence	69 (79.3)	23 (100.0)	20 (62.5)	26 (81.3)	
Presence	18 (20.7)	0 (0.0)	12 (37.5)	6 (18.8)	
IgG Index	0.823 (0.630-0.992)	0.572 (0.481-0.712)	0.891 (0.777-1.056)	0.846 (0.630-1.015)	0.128
T2 lesions					0.272
<9 lesions	7 (25.0)	-	1 (16.7)	6 (27.3)	
10-20 lesions	10 (35.7)	-	3 (50.0)	7 (31.8)	
21-50 lesions	9 (32.1)	-	1 (16.7)	8 (36.4)	
51-100 lesions	1 (3.6)	-	1 (16.7)	0 (0.0)	
>100 lesions	1 (3.6)	-	0 (0.0)	1 (4.6)	
Gd+ lesions					0.033
Absence	34 (73.9)	-	2 (33.3)	32 (80.0)	
Presence	12 (26.1)	-	4 (66.7)	8 (20.0)	
HLA-DRB1*15:01					0.484
Absence	29 (78.4)	10 (90.9)	8 (72.7)	11 (73.3)	
Presence	8 (21.6)	1 (9.1)	3 (27.3)	4 (26.7)	

OND: other neurological diseases individuals; RRMS: relapsing-remitting multiple sclerosis individuals; PPMS: primary progressive multiple sclerosis individuals. Categorical variables were shown as absolute and relative frequencies. Continuous variables were presented by median and Q1-Q3: First quartile-Third quartile. n: number of samples; EDSS: Expanded Disability Status Scale; OCGB: oligoclonal IgG bands; OCMG_LS: lipid-specific oligoclonal IgM bands; Gd+: gadolinium enhancing lesions.

4.3.3 To establish a characteristic miRNA signature in CSF of PPMS patients

To define a characteristic miRNA profile in CSF of PPMS patients, first of all, a screening phase was designed using cc-OA panels. 41 samples (13 OND, 12 RRMS and 16 PPMS) were used in this phase per triplicate. 27 miRNAs were detected in 70% of total samples (at least 50% of samples in each group). Five miRNAs showed significant differences or tendency to be deregulated in some of the groups (Table 17, Figure 41).

Table 17. Differential miRNA expression among groups in CSF samples in the screening phase of PPMS study.

miRNA	Comparison	OND (n=13) Median (Q1-Q3)	RRMS (n=12) Median (Q1-Q3)	PPMS (n=16) Median (Q1-Q3)	<i>p</i> value
miR-125a-5p		0.981 (0.752-1.307)	1.487 (1.090-1.712)	1.549 (0.924-1.666)	0.070
	OND vs RRMS				0.139
	OND vs PPMS				0.110
	RRMS vs PPMS				1.000
miR-125b-5p		0.746 (0.408-1.000)	1.196 (1.054- 1.883)	0.947 (0.595-1.818)	0.052
	OND vs RRMS				0.045
	OND vs PPMS				0.540
	RRMS vs PPMS				0.788
miR-143-3p		2.400 (1.340-5.419)	3.075 (2.536-4.669)	1.043 (0.923-2.934)	0.035
	OND vs RRMS				1.000
	OND vs PPMS				0.309
	RRMS vs PPMS				0.043
miR-29a-3p		0.693 (0.521-0.880)	0.575 (0.382-0.822)	1.219 (0.781-1.567)	0.077
	OND vs RRMS				0.936
	OND vs PPMS				0.829
	RRMS vs PPMS				0.071
miR-451a		2.798 (1.355-5.473)	2.954 (2.345-6.053)	6.237 (3.586-20.244)	0.078
	OND vs RRMS				1.000
	OND vs PPMS				0.090
	RRMS vs PPMS				0.385

OND: other neurological diseases individuals; RRMS: relapsing-remitting multiple sclerosis individuals; PPMS: primary progressive multiple sclerosis individuals. Q1-Q3: First quartile-Third quartile. Statistical differences were determined by Kruskal-Wallis test.

RESULTS

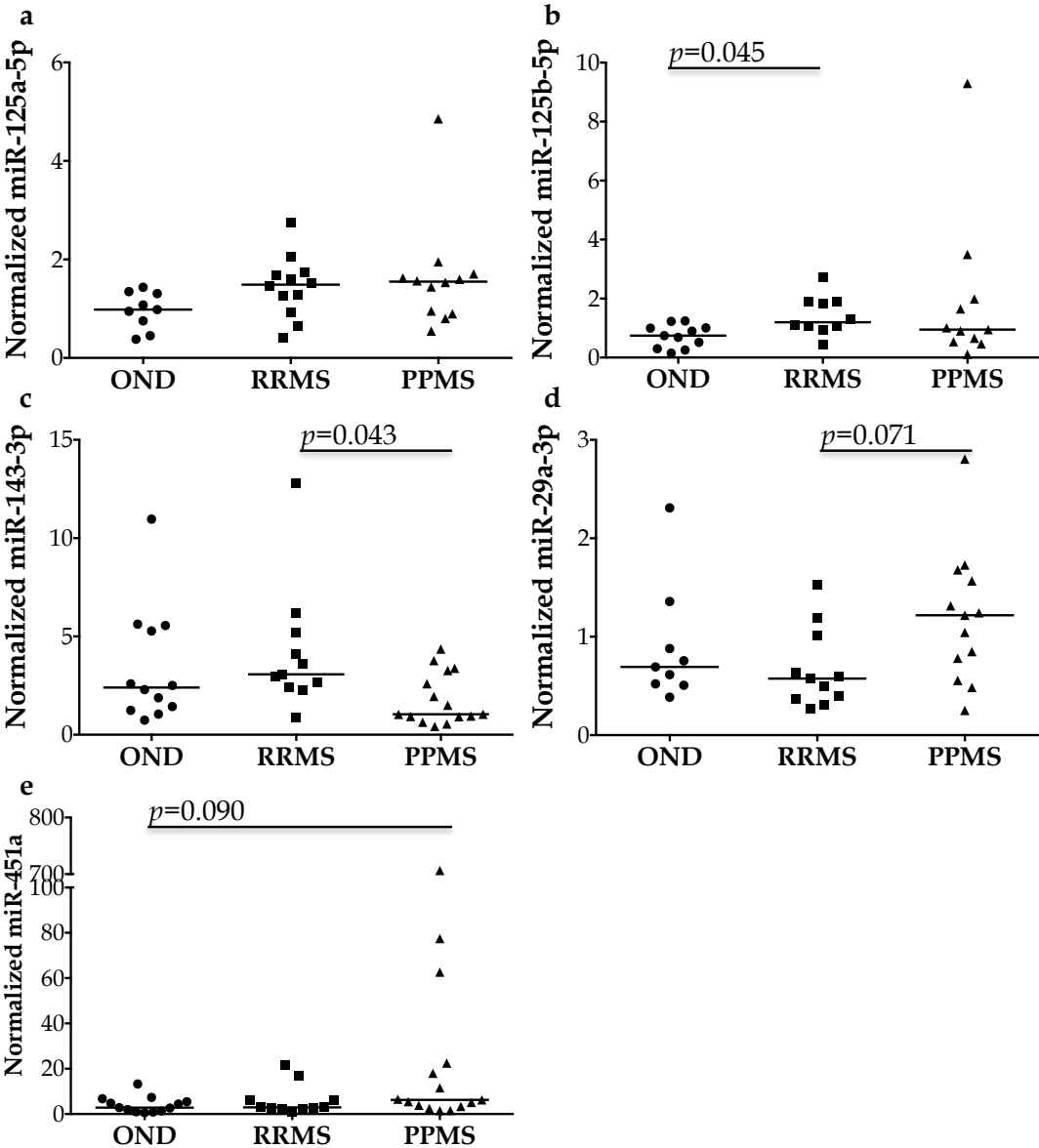


Figure 41. Differentially expressed miRNAs in CSF in the screening phase of PPMS study. Dot plots for normalized values of (a) miR-125a-5p, (b) miR-125b-5p, (c) miR-143-3p, (d) miR-29a-3p and, (e) miR-451a in CSF samples according to the group. The dot indicates one sample and the line indicates the median. Kruskal wallis test was used to determine statistical differences among groups.

Four miRNAs, let-7b-5p, miR-125a-5p, miR-143-3p and miR-451a, were further analyzed in a bigger cohort of 100 samples (27 OND, 31 RRMS and 42 PPMS) by individual qPCR. These miRNAs were selected according to the screening phase results or interesting results from previous publications. let-7b-5p and miR-143-3p were downregulated in PPMS samples compared to OND after normalizing using

the mean value of eight EN miRNAs (miR-16+miR-24+miR-125a+miR-30d+miR-26b+miR-145+miR-92b+miR-23a) (Table 18 and Figure 42).

Table 18. Differential miRNA expression among groups in CSF samples in the validation phase of PPMS study.

miRNA	Comparison	OND (n=25) Median (Q1-Q3)	RRMS (n=28) Median (Q1-Q3)	PPMS (n=35) Median (Q1-Q3)	<i>p</i> value
let-7b-5p		0.126 (0.061-0.605)	0.083 (0.036-0.297)	0.068 (0.023-0.091)	0.033
	OND vs RRMS				0.782
	OND vs PPMS				0.029
	RRMS vs PPMS				0.370
miR-125a-5p		0.895 (0.492-2.907)	0.723 (0.437-1.780)	0.892 (0.671-2.078)	0.825
	OND vs RRMS				1.000
	OND vs PPMS				1.000
	RRMS vs PPMS				1.000
miR-143-3p		5.111 (2.068-7.909)	3.241 (1.933-5.517)	2.409 (1.333-4.573)	0.045
	OND vs RRMS				0.833
	OND vs PPMS				0.039
	RRMS vs PPMS				0.612
miR-451a		2.274 (1.003-9.797)	1.657 (0.358-5.752)	2.506 (0.235-17.464)	0.584
	OND vs RRMS				1.000
	OND vs PPMS				1.000
	RRMS vs PPMS				1.000

OND: other neurological diseases individuals; RRMS: relapsing-remitting multiple sclerosis individuals; PPMS: primary progressive multiple sclerosis individuals. Q1-Q3: First quartile-Third quartile. Statistical differences were determined by Kruskal-Wallis.

RESULTS

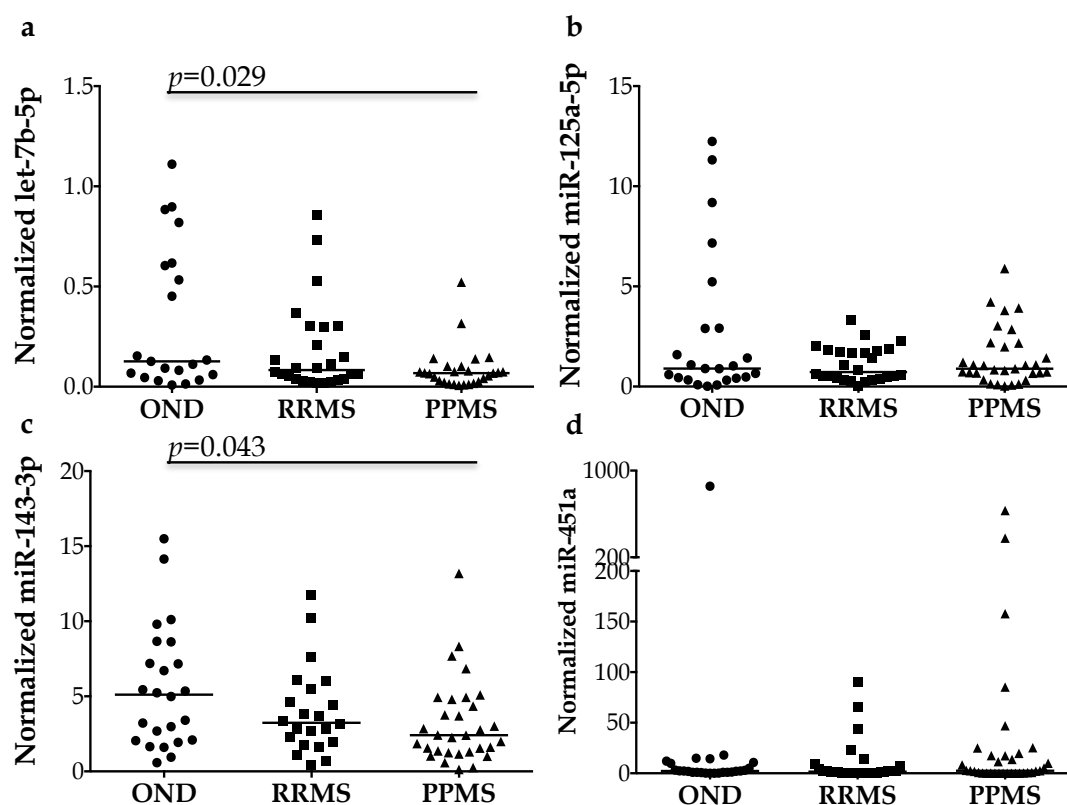


Figure 42. Differentially expressed miRNAs in CSF in the validation phase of PPMS study. Dot plots for normalized values of (a) let-7b-5p, (b) miR-125a-5p, (c) miR-143-3p and (d) miR-451a in CSF samples according to the group. The dot indicates one sample and the line indicates the median. Kruskal wallis test and Mann-Whitney U test for the post hoc analysis were used to determine statistical differences among groups.

4.3.4 To establish a characteristic miRNA signature in serum of PPMS patients

As made with CSF samples, a screening phase with fc-OA panels was designed and 34 serum samples (9 OND, 10 RRMS and 15 PPMS) were used in this phase. 127 miRNAs were detected in 70% of samples in each group. After normalizing using the global mean value of all miRNAs, 10 miRNAs showed significant differences or tendency to be deregulated in some of the groups (Table 19, Figure 43).

Table 19. Differential miRNA expression among groups in serum samples in the screening phase.

miRNA	Comparison	OND (n=9) Median (Q1-Q3)	RRMS (n=10) Median (Q1-Q3)	PPMS (n=15) Median (Q1-Q3)	p value
miR-142-5p		4.992 (2.788-7.162)	8.192 (5.364-13.513)	8.532 (6.582-10.454)	0.051
	OND vs RRMS				0.123
	OND vs PPMS				0.073
	RRMS vs PPMS				1.000
miR-148a-3p		1.723 (1.363-2.431)	1.716 (1.281-2.131)	2.592 (1.763-3.166)	0.043
	OND vs RRMS				1.000
	OND vs PPMS				0.155
	RRMS vs PPMS				0.085
miR-186-5p		1.136 (1.020-1.361)	1.217 (0.844-1.538)	0.636 (0.472-0.937)	0.044
	OND vs RRMS				1.000
	OND vs PPMS				0.079
	RRMS vs PPMS				0.179
miR-20a-5p		5.264 (4.059-9.843)	6.102 (4.796-7.026)	9.584 (6.379-12.256)	0.075
	OND vs RRMS				1.000
	OND vs PPMS				0.218
	RRMS vs PPMS				0.142
miR-26a-5p		1.409 (0.875-4.312)	6.310 (3.299-10.798)	5.941 (2.092-9.896)	0.059
	OND vs RRMS				0.056
	OND vs PPMS				0.316
	RRMS vs PPMS				0.988
miR-320b		7.049 (4.384-9.896)	8.164 (5.918-8.915)	2.660 (2.088-3.367)	0.005
	OND vs RRMS				1.000
	OND vs PPMS				0.038
	RRMS vs PPMS				0.013
miR-326		0.427 (0.230-0.907)	0.697 (0.573-0.880)	0.259 (0.125-0.304)	0.007
	OND vs RRMS				1.000
	OND vs PPMS				0.113
	RRMS vs PPMS				0.008
miR-421		0.117 (0.091-0.136)	0.103 (0.089-0.151)	0.185 (0.144-0.227)	0.005
	OND vs RRMS				1.000
	OND vs PPMS				0.026
	RRMS vs PPMS				0.017

RESULTS

miR-502-3p	0.298 (0.248-0.455)	0.413 (0.341-0.455)	0.570 (0.436-0.637)	0.024
OND vs RRMS				1.000
OND vs PPMS				0.050
RRMS vs PPMS				0.095
miR-652-3p	5.899 (5.703-6.333)	6.984 (6.523-7.798)	3.686 (5.519-5.680)	0.033
OND vs RRMS				1.000
OND vs PPMS				0.365
RRMS vs PPMS				0.034

OND: other neurological diseases individuals; RRMS: relapsing-remitting multiple sclerosis individuals; PPMS: primary progressive multiple sclerosis individuals. Q1-Q3: First quartile-Third quartile. Statistical differences were determined by Kruskal-Wallis.

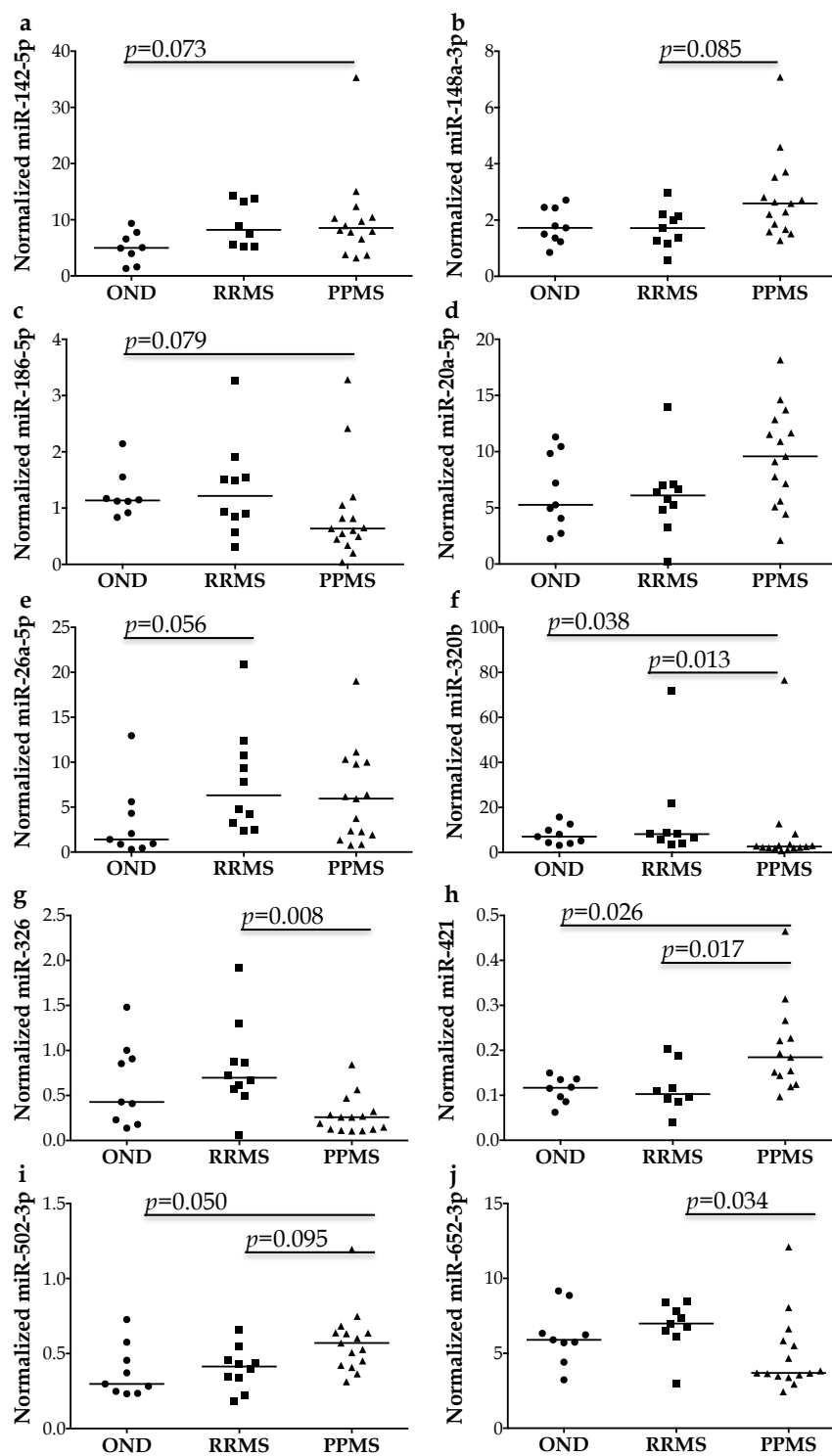


Figure 43. Differentially expressed miRNAs in serum in the screening phase of PPMS study. Dot plots for normalized values of (a) miR-142-5p, (b) miR-148a-3p, (c) miR-186-5p, (d) miR-20a-5p, (e) miR-26a-5p, (f) miR-320b, (g) miR-326, (h) miR-421, (i) miR-502-3p and (j) miR-652-3p in serum samples according to the group. The dot indicates one sample and the line indicates the median. Kruskal wallis test was used to determine statistical differences among groups.

RESULTS

Deregulation of these 10 miRNAs was further analyzed in a bigger cohort of 107 samples (26 OND, 32 RRMS and 49 PPMS) by individual qPCR. miR-20a-5p and miR-320b seemed to be deregulated in PPMS against RRMS and OND, after normalizing using the mean value of two EN miRNAs (miR-23a-3p and miR-15a-5p). miR-26a-5p was downregulated in PPMS versus RRMS and miR-142-5p was upregulated in RRMS against OND (Table 20 and Figure 44).

Table 20. Differential miRNA expression among groups in serum samples in the validation phase.

miRNA	Comparison	OND (n=23) Median (Q1-Q3)	RRMS (n=32) Median (Q1-Q3)	PPMS (n=46) Median (Q1-Q3)	p value
miR-142-5p		0.379 (0.267-0.491)	0.618 (0.379-0.909)	0.501 (0.299-0.774)	0.042
	OND vs RRMS				0.036
	OND vs PPMS				0.392
	RRMS vs PPMS				0.565
miR-20a-5p		0.261 (0.174-0.361)	0.341 (0.260-0.455)	0.453 (0.317-0.603)	0.002
	OND vs RRMS				0.439
	OND vs PPMS				0.002
	RRMS vs PPMS				0.134
miR-26a-5p		0.388 (0.295-0.546)	0.471 (0.317-0.693)	0.343 (0.261-0.506)	0.042
	OND vs RRMS				0.572
	OND vs PPMS				1.000
	RRMS vs PPMS				0.036
miR-320b		0.045 (0.016-0.073)	0.032 (0.017-0.052)	0.018 (0.010-0.048)	0.094
	OND vs RRMS				1.000
	OND vs PPMS				0.170
	RRMS vs PPMS				0.281

OND: other neurological diseases individuals; RRMS: relapsing-remitting multiple sclerosis individuals; PPMS: primary progressive multiple sclerosis individuals. Q1-Q3: First quartile-Third quartile. Statistical differences were determined by Kruskal-Wallis.

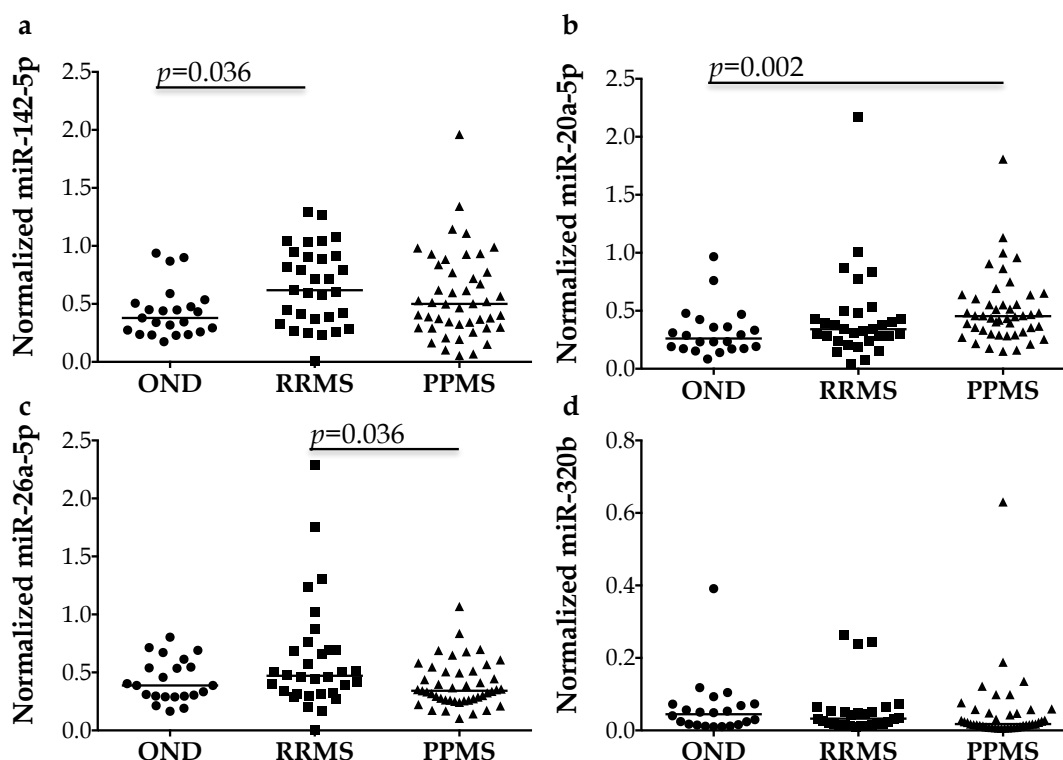


Figure 44. Differentially expressed miRNAs in serum in the validation phase. Dot plots for normalized values of (a) miR-142-5p, (b) miR-20a-5p, (c) miR-26a-5p and (d) miR-320b in serum samples according to the group. The dot indicates one sample and the line indicates the median. Kruskal wallis test was used to determine statistical differences between groups.

4.3.5 Correlation of deregulated miRNA expression with radiological and clinical variables

The correlation between deregulated miRNA levels in the validation stage and the number of T2 and Gd+ lesions in MRI and EDSS at sampling was studied. The expression of miR-148a-3p, miR-320b and miR-421 in serum correlated with the number of T2 lesions. miR-142-5p and miR-148a-3p levels were negatively correlated with the number of Gd+ lesions. However, there was no observed correlation between miRNA levels and EDSS (Table 21).

RESULTS

Table 21. Association of serum miRNA levels with radiological and clinical variables at sampling.

	T2 lesions		Gd+ lesions		EDSS	
	r_s	p value	r_s	p value	r_s	p value
miR-142-5p	-0.291	0.200	0.474	0.002	0.048	0.864
miR-148a-3p	-0.535	0.012	0.357	0.020	-0.219	0.432
miR-320b	0.479	0.044	0.027	0.872	0.236	0.438
miR-421	-0.486	0.026	-0.018	0.910	-0.266	0.379

Spearman's correlation test was used to measure the correlation levels between serum miRNA levels and number of T2 or Gd+ lesions or EDSS at sampling. r_s : Rho of Spearman; p : p value.

4.3.6 miRNA signature in PPMS according to the inflammatory activity

PPMS cohort could be divided in two sub-groups according to the inflammatory activity (presence of Gd+ lesions in MRI, increased number of T2 lesions in follow-up MRI and/or presence of intrathecal synthesis of LS_OCMB). Screening cohort was formed by 20 CSF samples (13 Non-inflammatory PPMS and seven Inflammatory PPMS) and 15 serum samples (seven Non-inflammatory PPMS and eight inflammatory PPMS).

Table 22 and Table 23 show median miRNA expression values that might be deregulated in PPMS patients according to their inflammatory status in CSF and serum samples, respectively.

Table 22. Differential miRNA expression between PPMS patients according to inflammatory activity in CSF samples at the screening phase.

miRNA	Non-inflammatory PPMS (n=13)	Inflammatory PPMS (n=7)	<i>p</i> value
	Median (Q1-Q3)	Median (Q1-Q3)	
miR-125b-5p	0.816 (0.446-2.282)	0.289 (0.252-0.293)	0.093
miR-1260a	0.167 (0.135-0.443)	0.723 (0.382-1.063)	0.044
miR-145-5p	8.206 (3.512-12.024)	1.826 (1.770-3.038)	0.082
miR-199a-3p	0.752 (0.246-0.847)	0.183 (0.084-0.326)	0.029
miR-204-5p	1.173 (0.862-4.425)	5.275 (3.295-5.514)	0.098
miR-23a-3p	3.186 (2.420-3.945)	1.546 (0.917-1.695)	0.001
miR-23b-3p	0.611 (0.552-0.816)	0.238 (0.162-0.499)	0.029
miR-451a	7.352 (3.615-26.845)	1.710 (1.303-2.559)	0.018
miR-92b-3p	1.019 (0.396-1.183)	1.565 (1.419-2.460)	0.059

PPMS: primary progressive multiple sclerosis individuals. Q1-Q3: First quartile-Third quartile. Statistical differences were determined by Mann-Whitney U test.

Table 23. Differential miRNA expression between PPMS patients according to inflammatory activity in serum samples at the screening phase.

miRNA	Non-inflammatory PPMS (n=7)	Inflammatory PPMS (n=8)	<i>p</i> value
	Median (Q1-Q3)	Median (Q1-Q3)	
miR-103a-2-5p	1.128 (1.100-1.328)	1.035 (0.654-1.194)	0.094
miR-106b-3p	0.193 (0.133-0.227)	0.070 (0.040-0.076)	0.009
miR-106b-5p	2.028 (1.349-2.455)	4.052 (2.351-4.942)	0.054
miR-140-3p	1.128 (1.043-1.279)	1.638 (1.288-2.019)	0.073
miR-148a-3p	2.155 (1.722-2.836)	3.272 (2.450-4.399)	0.094
miR-193b-3p	0.143 (0.110-0.195)	0.055 (0.051-0.082)	0.073
miR-22-3p	12.534 (7.374-18.424)	6.548 (3.116-11.053)	0.094
miR-99b-5p	0.156 (0.142-0.191)	0.063 (0.046-0.106)	0.030

PPMS: primary progressive multiple sclerosis individuals. Q1-Q3: First quartile-Third quartile. Statistical differences were determined by Mann-Whitney U test.

Among all these miRNAs, potential deregulation of miR-145-5p, miR-199a-3p, miR-23a-3p, miR-451 and miR-92b-3p in CSF was further analyzed in a bigger cohort of 38 individuals (19 non-inflammatory PPMS and 19 inflammatory PPMS). miR-103a-2-

RESULTS

5p, miR-106b-5p, miR-148a-3p, miR-193b-3p and miR-99b-5p levels were studied in serum samples of a 45 individuals cohort (23 non-inflammatory PPMS and 22 inflammatory PPMS). Median expression values, first-third quartiles (Q1-Q3) and *p* values for each miRNA are shown in Table 24 and Table 25. miR-92b-3p presented a tendency to be upregulated in CSF of PPMS individuals with inflammatory activity, while miR-103a-2-5p was statistically significant downregulated in serum samples of inflammatory PPMS (*p*=0.057 and *p*=0.008, respectively) (Figure 45).

Table 24. Differential miRNA expression between PPMS patients according to inflammatory activity in CSF samples at the validation phase.

miRNA	Non-inflammatory PPMS (n=19)	Inflammatory PPMS (n=19)	<i>p</i> value
	Median (Q1-Q3)	Median (Q1-Q3)	
miR-145-5p	25.306 (17.505-40.224)	22.824 (6.446-41.731)	0.339
miR-199a-3p	3.488 (1.763-4.271)	3.015 (1.667-7.669)	0.544
miR-23a-3p	2.769 (1.792-3.552)	2.444 (1.553-6.104)	0.885
miR-451a	11.028 (0.817-24.936)	4.833 (0.407-34.543)	0.885
miR-92b-3p	3.426 (1.889-5.743)	5.321 (3.786-22.821)	0.057

PPMS: primary progressive multiple sclerosis individuals. Q1-Q3: First quartile-Third quartile. Statistical differences were determined by Mann-Whitney U test.

Table 25. Differential miRNA expression between PPMS patients according to inflammatory activity in serum samples at the validation phase.

miRNA	Non-inflammatory PPMS (n=23)	Inflammatory PPMS (n=22)	<i>p</i> value
	Median (Q1-Q3)	Median (Q1-Q3)	
miR-103a-2-5p	0.055 (0.039-0.078)	0.037 (0.028-0.047)	0.008
miR-106b-5p	0.128 (0.088-0.179)	0.128 (0.108-0.209)	0.892
miR-148a-3p	0.193 (0.127-0.277)	0.207 (0.159-0.320)	0.617
miR-193b-3p	0.015 (0.010-0.025)	0.010 (0.005-0.019)	0.247
miR-99b-5p	0.006 (0.004-0.011)	0.006 (0.004-0.008)	0.661

PPMS: primary progressive multiple sclerosis individuals. Q1-Q3: First quartile-Third quartile. Statistical differences were determined by Mann-Whitney U test.

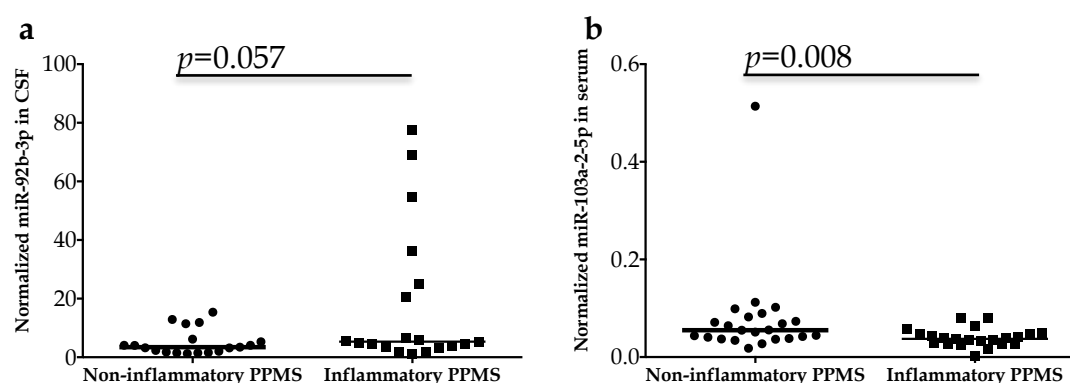


Figure 45. Differentially expressed miRNAs in the validation phase in PPMS individuals according to the inflammatory activity. Dot plots for normalized values of (a) miR-92b-3p in CSF and (b) miR-103a-2-5p in serum according to the inflammatory status. The dot indicates one sample and the line indicates the median. Kruskal wallis test was used to determine statistical differences between groups.

4.3.7 Summary

This study focused on describing miRNA profiles in CSF and serum samples from PPMS patients compared to RRMS and OND individuals has highlighted specific miRNA signatures in PPMS.

let-7b-5p and miR-143-3p were downregulated in PPMS CSF samples compared to OND. Deregulation of miR-20a-5p in PPMS serum samples against OND was found. miR-26a-5p was also downregulated in PPMS versus RRMS and miR-142-5p was upregulated in RRMS against OND.

When analyzing miRNA profiles in PPMS cohort depending on their inflammatory activity, miR-92b-3p presented a tendency to be upregulated in CSF of PPMS individuals with inflammatory activity, while miR-103a-2-5p was statistically significant downregulated in serum samples of inflammatory PPMS individuals.

RESULTS

4.4 RELATION OF THE CSF miRNA PROFILE OF MS INDIVIDUALS WITH THE miRNA SIGNATURE DURING DEMYELINATION AND REMYELINATION IN CEREBELLAR ORGANOTYPIC CULTURE MODEL

As murine *ex vivo* cerebellar culture is a model used to study demyelination and remyelination processes, the main objective of this part was to compare CSF miRNA profiles from PPMS and RRMS patients with the miRNA signature of this model during demyelination and remyelination in a preliminary study in order to move along in the knowledge of these processes. With this purpose, miRNA expression pattern in *ex vivo* cerebellar organotypic culture was studied during demyelination and remyelination compared to normal condition (myelination) using cc-OA plates. miRNA profile of CSF PPMS and RRMS individuals and cultures were compared in order to propose potential miRNAs involved in demyelination and neurorepair.

4.4.1 To establish a characteristic miRNA signature in murine *ex vivo* cultures by OpenArray

A preliminary experiment (n=1) of demyelination/remyelination in *ex vivo* cerebellar culture was established. miRNA profiles were analyzed in myelinated, demyelinated and remyelinated conditions and the expression profiles compared (Figure 46). Several miRNAs showed differential expression between conditions.

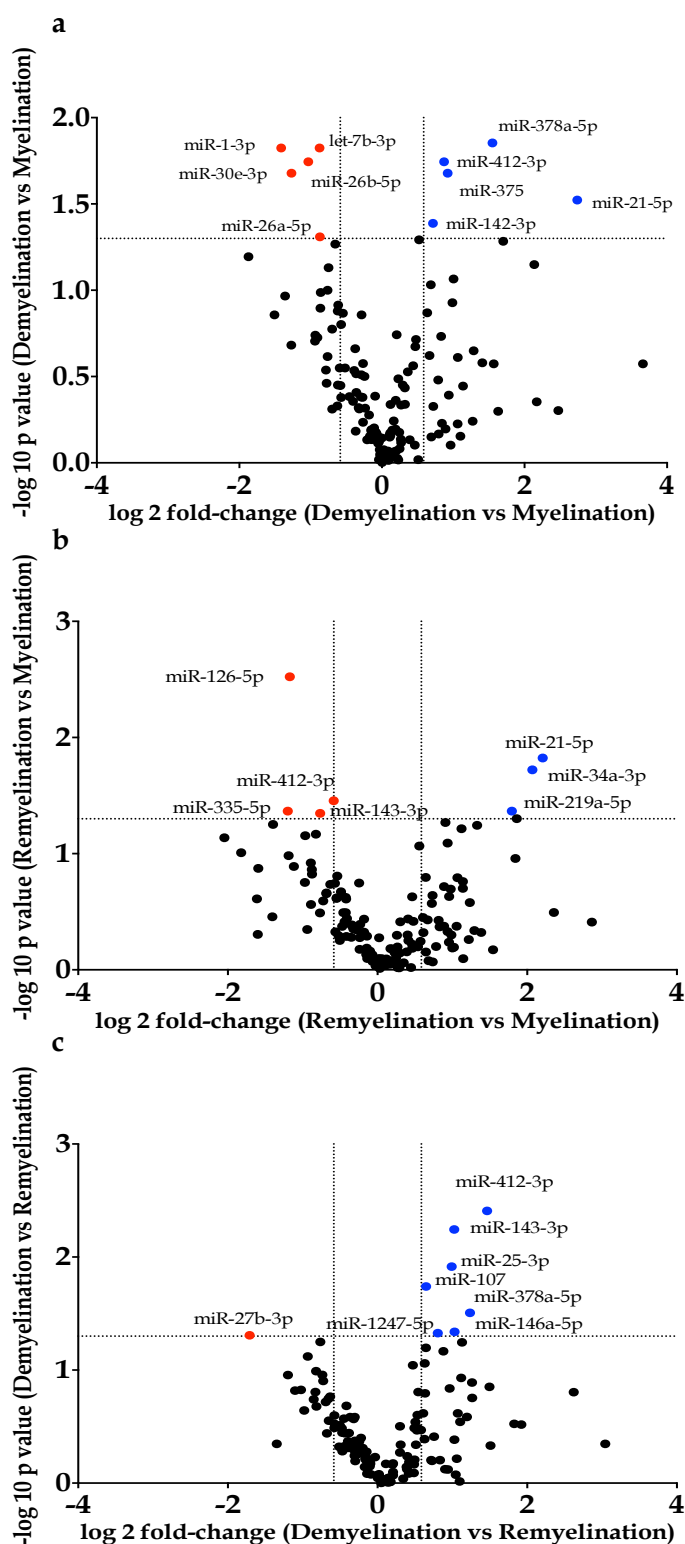


Figure 46. Volcano plots representing changes in miRNA expression in *ex vivo* cerebellar tissue culture during different conditions. (a) miRNA changes between demyelinated and myelinated cultures; (b) miRNA changes between remyelinated and myelinated cultures and; (c) miRNA changes between demyelinated and remyelinated cultures. Red circles represent down-regulated miRNAs ($p < 0.050$); blue circles represent up-regulated miRNAs ($p < 0.050$).

RESULTS

Four miRNAs should be highlighted as they appeared deregulated in at least two of the three comparisons. miR-378a-5p appeared as upregulated during demyelination when compared with myelination and remyelination. miR-412-3p expression changed during culture conditions as it increased during demyelination to later decreased in remyelination phase. miR-21-5p was found upregulated in both demyelination and remyelination. Conversely miR-143-3p levels were downregulated in remyelination. Figure 47 shows RQ distribution for these four miRNAs during the three studied conditions.

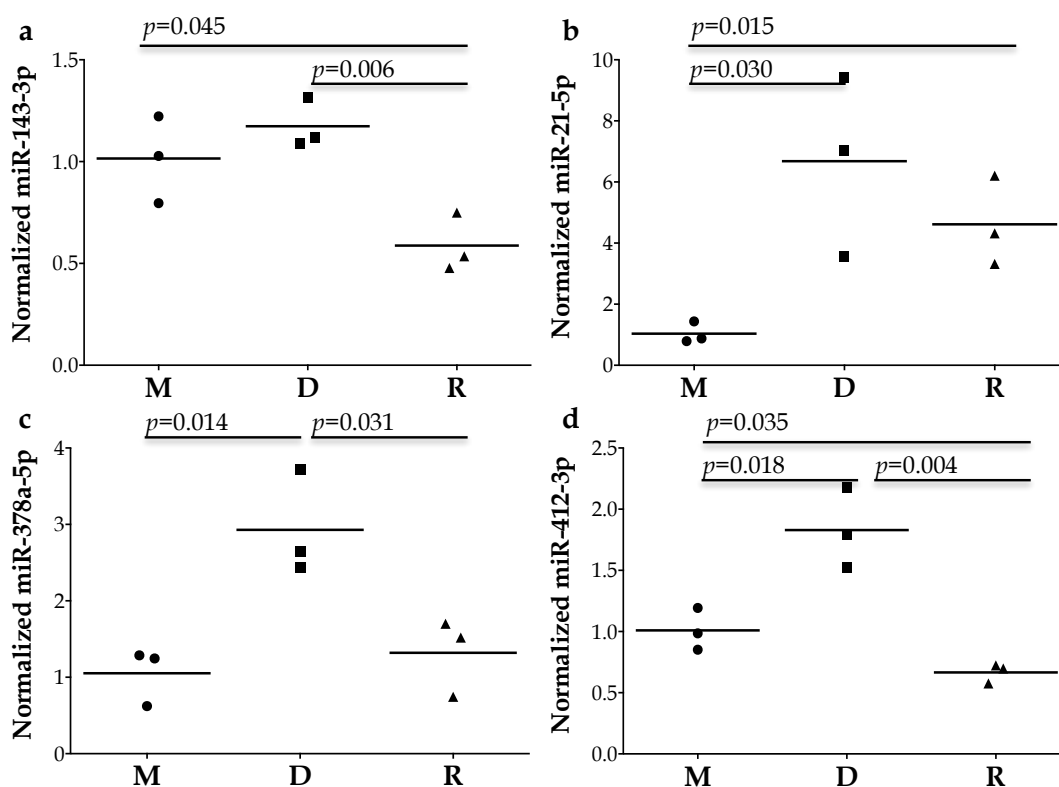


Figure 47. Differentially expressed miRNAs during normal myelination, demyelination and remyelination. Dot plots for normalized values of (a) miR-143-3p; (b) miR-21-5p; (c) miR-378a-5p and; (d) miR-412-3p in *ex vivo* cerebellar tissue culture. The dot indicates one sample and the line indicates the mean. Student's T test was used to determine statistical differences between pairs. M: myelination; D: demyelination; R: remyelination.

4.4.2 Comparison of non-inflammatory PPMS and RRMS vs SAS

This exploratory study comprised 34 individuals (58.8% women) with a median age of 51.0 years. 13 subjects belonged to non-inflammatory PPMS group (61.5% women), 12 to RRMS (58.3% women), while 9 were SAS individuals (55.6% women). Clinical data as sex and age are shown in Table 26. No significant differences were observed in either sex or age at sampling among groups.

Table 26. Demographic data of the studied cohort.

Baseline characteristics	Whole group	SAS	RRMS	Non-inflammatory PPMS	<i>p</i> value
n	34	9	12	13	
Sex					1.000
Male	14 (41.2)	4 (44.4)	5 (41.7)	5 (38.5)	
Female	20 (58.8)	5 (55.6)	7 (58.3)	8 (61.5)	
Age	51.0 (48.0-56.0)	51.0 (48.0-54.0)	49.0 (48.0-53.5)	55.0 (49.0-57.0)	0.400

SAS: spinal anesthesia subjects; RRMS: relapsing-remitting multiple sclerosis individuals; Non-inflammatory PPMS: non-inflammatory primary progressive multiple sclerosis individuals. Categorical variable (sex) was shown as absolute and relative frequencies and their statistical differences were determined by Fisher's exact test. Continuous variable (age) was presented by median and Q1-Q3: First quartile-Third quartile and their statistical differences were determined by Kruskal-Wallis test.

miRNA profiles in CSF were analyzed comparing PPMS and RRMS against SAS samples separately and the changes in miRNA expression are shown in Figure 48. Several miRNAs showed differential expression between biological groups.

RESULTS

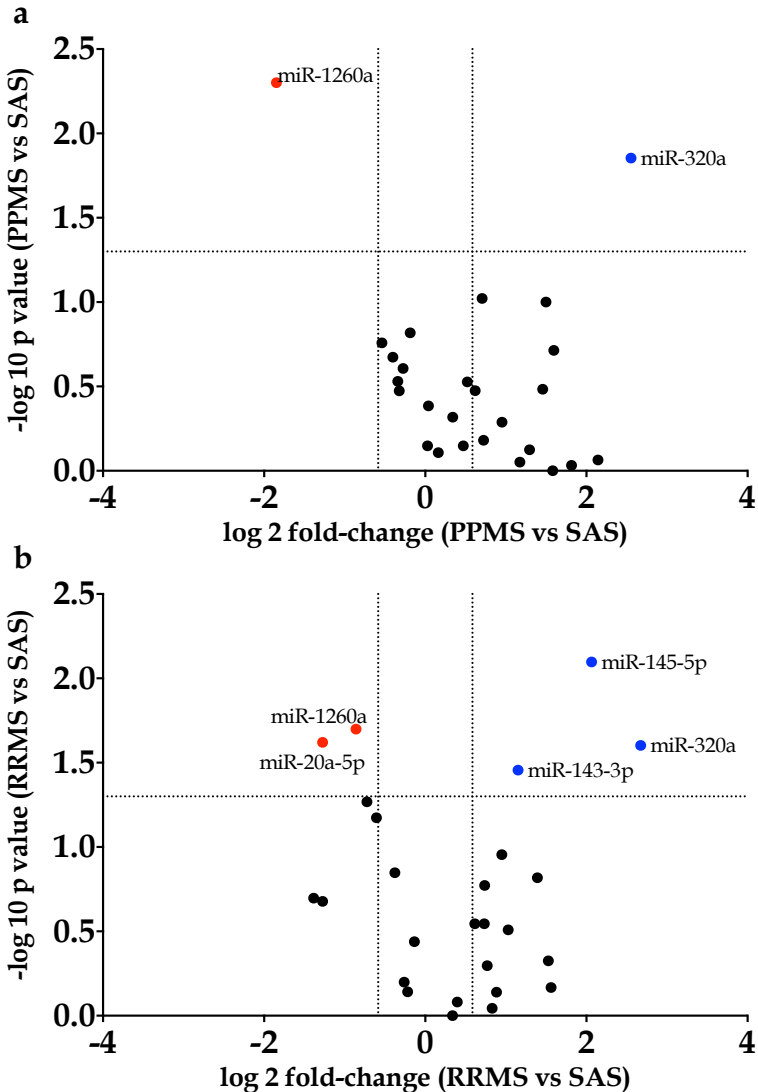


Figure 48. Volcano plots representing changes in miRNA expression in CSF samples for different clinical MS subtypes. (a) miRNA changes between PPMS and SAS; (b) miRNA changes between RRMS and SAS. Red circles represent down-regulated miRNAs ($p < 0.050$); blue circles represent up-regulated miRNAs ($p < 0.050$).

As observed in Figure 49, miR-320a presented overexpression in both non-inflammatory PPMS and RRMS when compared to SAS and miR-1260a was downregulated in both groups. In addition, RRMS also presented increased levels of miR-143-3p and miR-145-5p, whereas miR-20a-5p levels were diminished.

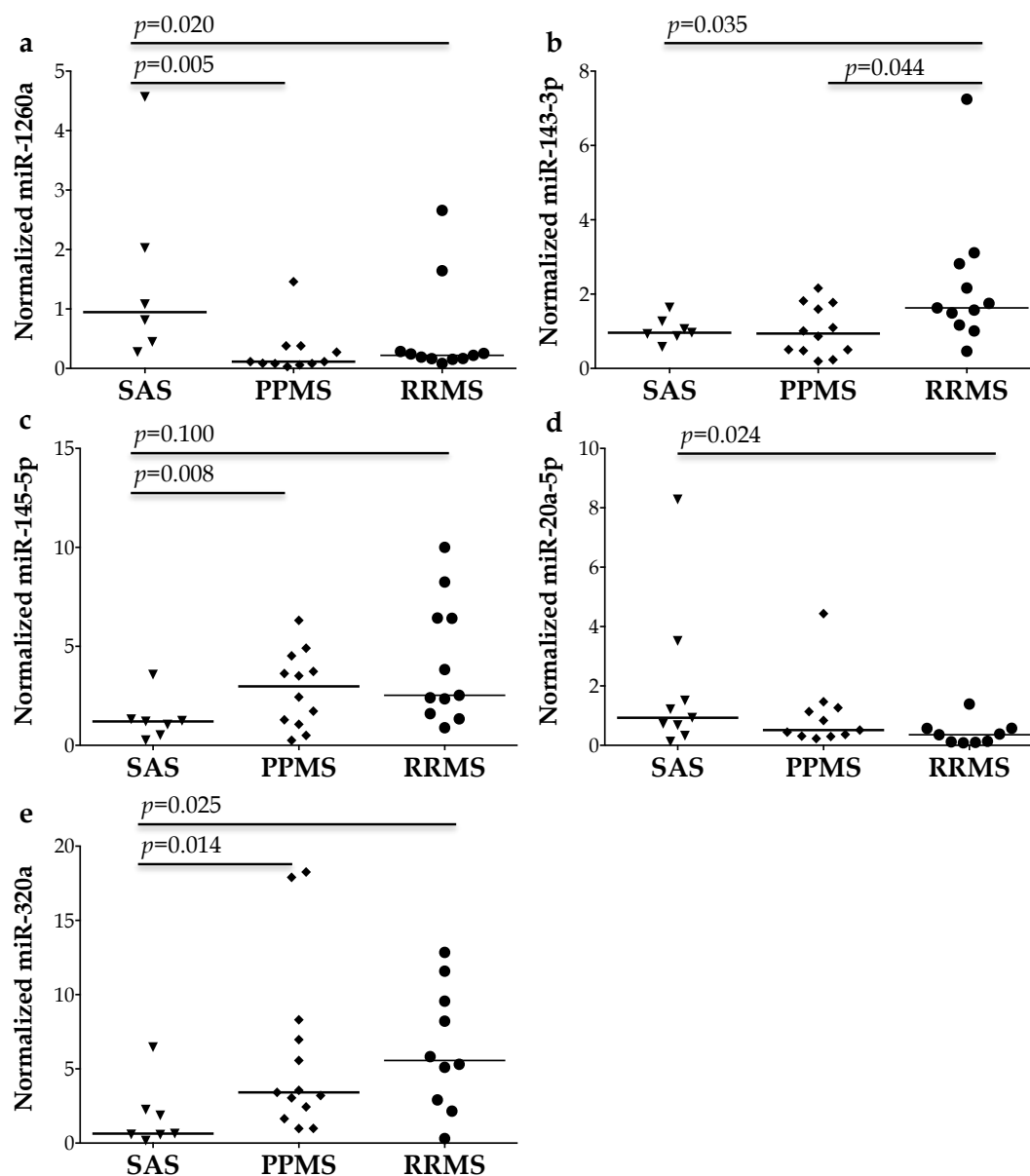


Figure 49. Differentially expressed miRNAs in CSF samples of SAS, PPMS and RRMS individuals. Dot plots for normalized values of (a) miR-1260a, (b) miR-143-3p, (c) miR-145-5p, (d) miR-20a-5p and, (e) miR-320a in CSF samples. The dot indicates one sample and the line indicates the median. Mann-Whitney U test was used to determine statistical differences between pairs. SAS: spinal anesthesia subjects; PPMS: primary progressive multiple sclerosis; RRMS: relapsing-remitting multiple sclerosis.

RESULTS

4.4.3 Cross-analysis of miRNA expression between murine *ex vivo* cultures and human CSF samples

A preliminary cross reference analysis was made between human miRNAs in non-inflammatory PPMS and RRMS CSF samples (*vs* SAS individuals) and those detected in *ex vivo* cerebellar culture during demyelination and remyelination (*vs* normal myelination). Venn diagrams showed the overlapping up-/downregulated miRNAs between demyelinated and remyelinated brain tissue, and PPMS and RRMS samples (Figure 50).

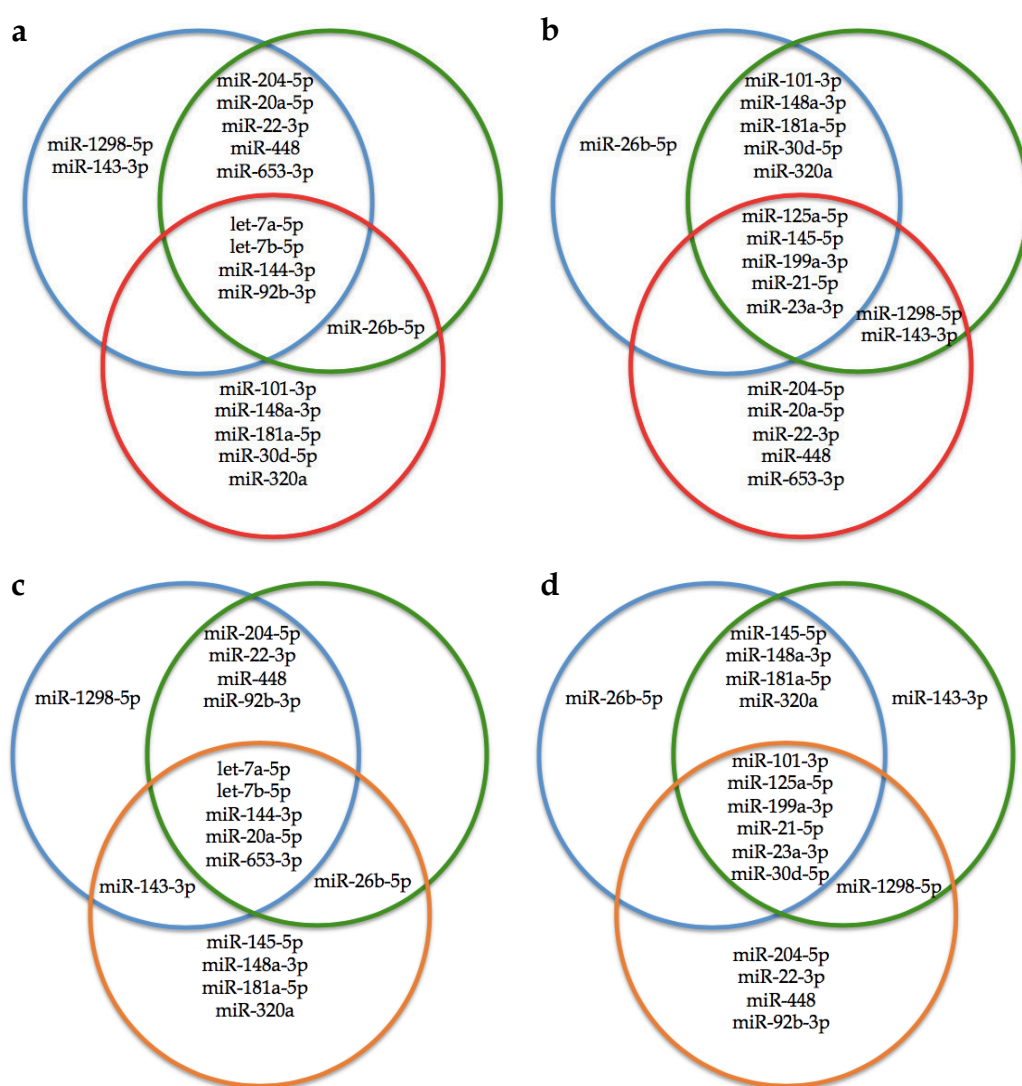


Figure 50. Venn diagrams plot the number of decreased/increased miRNAs in different conditions. Blue circles corresponds to PPMS group; green circle corresponds to RRMS group; red circle correspond to demyelination and; orange circle corresponds to remyelination. A and C show downregulated miRNAs; B and D show upregulated miRNAs.

It is interesting to highlight those miRNAs whose decreased or increased levels were overlapped among human samples and tissue. let-7a-5p, let-7b-5p and miR-144-3p presented decreased levels in human samples and tissue in both demyelination and remyelination conditions (Figures 51a, 51b and 51c). miR-92b-3p showed overlapping decreased levels only during demyelination as its expression increased in remyelination (Figure 51d). On the other hand, miR-20a-5p and miR-653-3p presented the opposite trend; as their levels increased after demyelination, their expression decreased during remyelination showing overlap with human samples (Figures 51e and 51f).

Regarding miRNAs with increased levels, miR-125a-5p, miR-199a-5p, miR-21-5p and miR-23a-3p presented increased levels in human samples and tissue in both demyelination and remyelination conditions (Figures 52a, 52b, 52c and 52d). miR-145-5p showed overlapping enhanced levels only during demyelination as its expression decreased in remyelination (Figure 52e). On the contrary, miR-101-3p and miR-30d-5p presented the opposite trend; as their levels increased in remyelination, after their expression had become diminished during demyelination (Figures 52f and 52g).

Regarding miR-143-3p (Figure 53), when it overlapped with demyelination condition, its expression is only decreased in PPMS as RRMS shared increased levels with demyelination. However, during remyelination its levels significantly decreased.

RESULTS

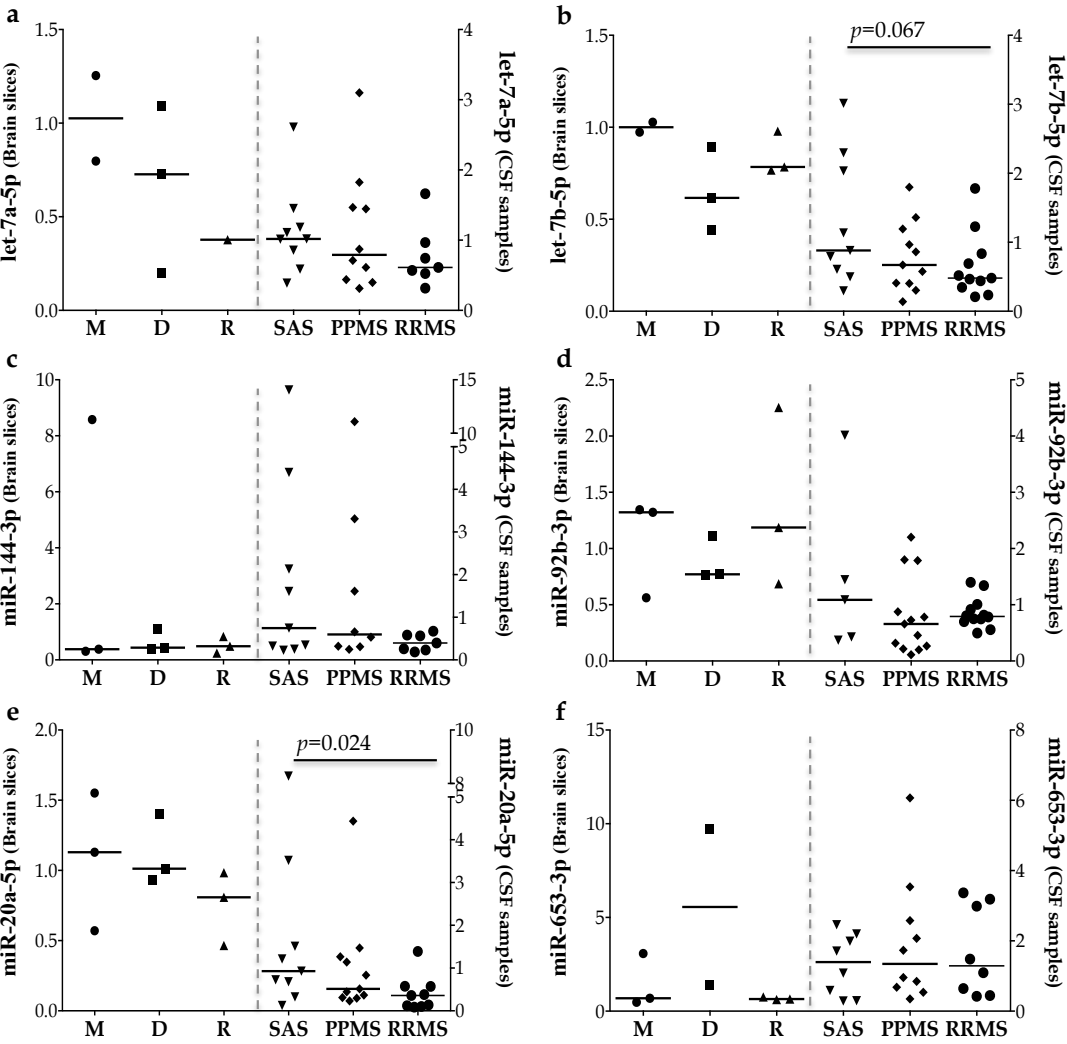


Figure 51. Dot plots of overlapped miRNAs with reduced levels among *ex vivo* cultures and human MS samples. Dot plots for normalized values of (a) let-7a-5p, (b) let-7b-5p, (c) miR-144-3p, (d) miR-92b-3p, (e) miR-20a-5p and, (f) miR-653-3p in *ex vivo* cultures during normal myelination (M), demyelination (D) and remyelination (R) in left Y axis and in human CSF samples of spinal anesthesia subjects (SAS), primary progressive multiple sclerosis (PPMS) and relapsing-remitting multiple sclerosis (RRMS) in right Y axis. The dot indicates one sample and the line indicates the median.

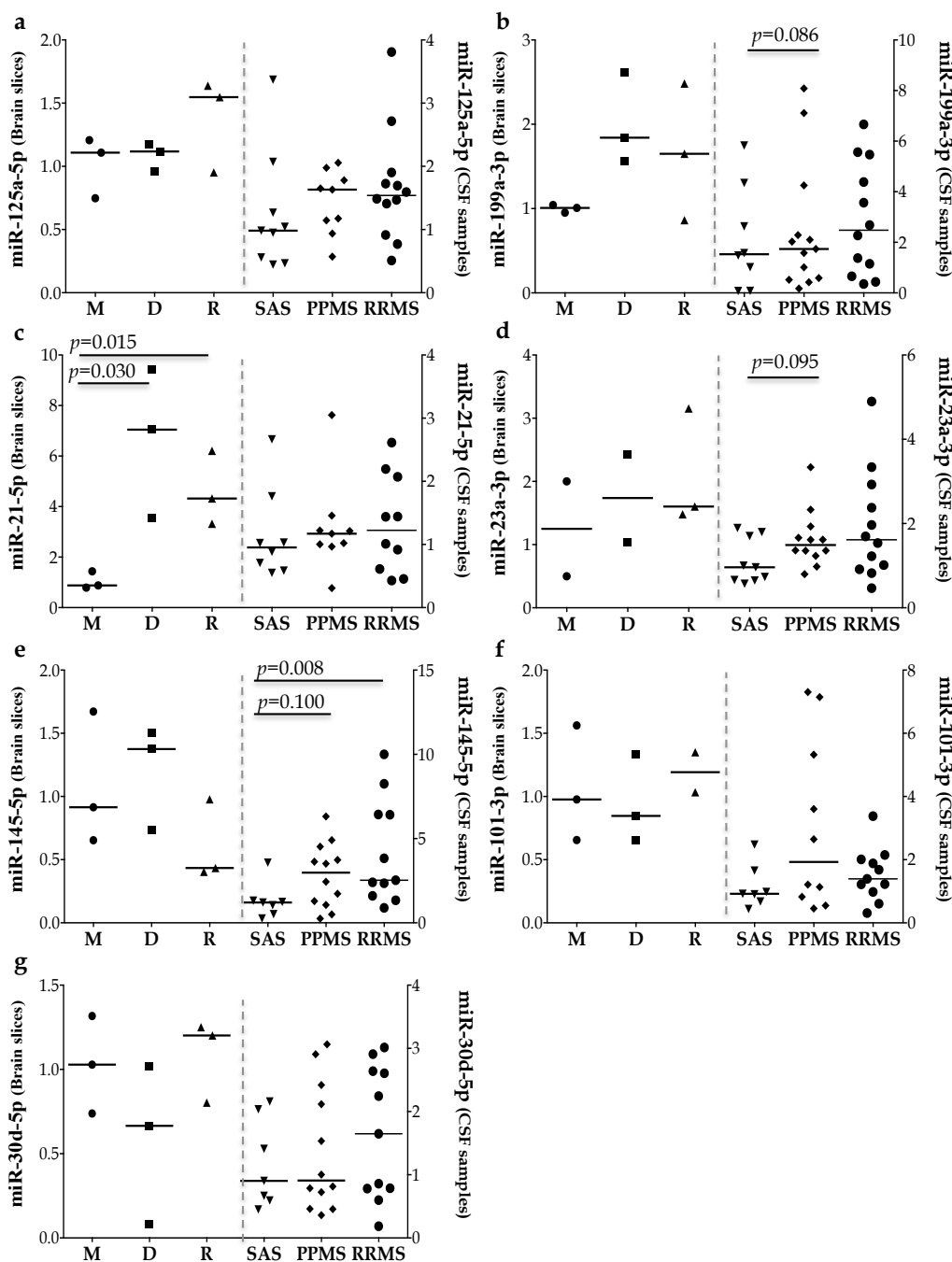


Figure 52. Dot plots of overlapped miRNAs with increased levels among *ex vivo* cultures and human MS samples. Dot plots for normalized values of (a) miR-125a-5p, (b) miR-199a-5p, (c) miR-21-5p, (d) miR-23a-3p, (e) miR-145-5p, (f) miR-101-3p and, (g) miR-30d-5p in *ex vivo* cultures during normal myelination (M), demyelination (D) and remyelination (R) in left Y axis and in human CSF samples of spinal anesthesia subjects (SAS), primary progressive multiple sclerosis (PPMS) and relapsing-remitting multiple sclerosis (RRMS) in right Y axis. The dot indicates one sample and the line indicates the median. Student's T test and Mann-Whitney U test were used to determine statistical differences between pairs in *ex vivo* cultures and human samples, respectively.

RESULTS

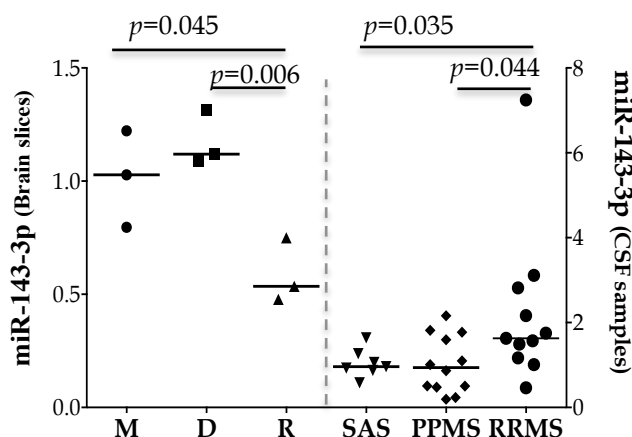


Figure 53. Dot plots of normalized miR-143-3p levels in *ex vivo* cultures and human MS samples. Dot plot for normalized values of miR-143-3p in *ex vivo* cultures during normal myelination (M), demyelination (D) and remyelination (R) in left Y axis and in human CSF samples of spinal anesthesia subjects (SAS), primary progressive multiple sclerosis (PPMS) and relapsing-remitting multiple sclerosis (RRMS) in right Y axis. The dot indicates one sample and the line indicates the median. Student's T test and Mann-Whitney U test were used to determine statistical differences between pairs in *ex vivo* cultures and human samples, respectively.

4.4.4. Summary

The comparative analysis between *ex vivo* models and human CSF samples might be a valuable approach to propose new miRNAs involved in demyelination, remyelination and neurorepair. Some interesting miRNAs need to be highlighted such as miR-143-3p, miR-21-5p or miR-145-5p as their expression was found deregulated in some of the studied conditions and/or their expression pattern could be similar between *ex vivo* and *in vivo* demyelinating processes (murine cultures *vs* CSF samples).

4.5 STUDY OF THE CIRCULATING miRNA SIGNATURE IN RIS INDIVIDUALS

The main aim of this part was to describe a specific profile of miRNAs in CSF and plasma in RIS patients according to their conversion to CDMS status after 5 years of follow-up in order to study their potential role as prognostic factors. The cc-OA panels previously described were used to screen miRNA expression in CSF and plasma samples. Additionally, other variables previously described as predictive biomarkers of clinical conversion in RIS patients were analyzed in this cohort.

4.5.1 Clinical characteristics of the RIS patients

This was a longitudinal exploratory study comprising 15 patients with RIS (73.3% women) with a median age of 38 years. Conversion was observed in seven patients (RIS-Conversion) (100.0% women), while eight patients remained as RIS (RIS-RIS) (50.0% women) after five-year follow-up. No significant differences were observed in sex or age between RIS-RIS and RIS-Conversion individuals. Clinical, radiological and genetic data collected close to the sample extraction date, as well as levels of vitamin D, one of the environmental risk factors in MS, did not reveal any differences between both groups either, except for an increased number of T2 lesions in the RIS-Conversion group (RIS-RIS median=9.5 lesions *vs* RIS-Conversion median=27.0 lesions; $p=0.043$). Although the presence of black holes in MRI did not reach statistical significance ($p=0.055$), it was observed in 50.0% of RIS-Conversion patients versus 0.0% of RIS-RIS patients (Table 27).

RESULTS

Table 27. Demographic, clinical, radiological and genetic data of the studied RIS cohort.

Baseline characteristics	Whole group	RIS-RIS	RIS-Conversion	<i>p</i> value
n	15	8	7	
Sex				0.077
Male	4 (26.7)	4 (50.0)	0 (0.0)	
Female	11 (73.3)	4 (50.0)	7 (100.0)	
Age (years)	38.0 (32.0-48.5)	38.5 (33.0-52.0)	37.0 (29.0-43.0)	0.336
Time of follow-up (years)	6.5 (5.8-6.5)	6.5 (5.3-7.0)	6.5 (6.0-6.5)	1.000
EDSS	1.50 (1.00-2.00)	1.25 (0.50-1.75)	1.50 (1.25-2.25)	0.232
Vitamin D				0.592
<20 ng/ml	8 (57.1)	5 (71.4)	3 (42.9)	
>20 ng/ml	6 (42.9)	2 (28.6)	4 (57.1)	
OCGB				0.200
Absence	3 (20.0)	3 (37.5)	0 (0.0)	
Presence	12 (80.0)	5 (62.5)	7 (100.0)	
Index IgG	9.749 (0.583-1.736)	0.634 (0.567-0.986)	1.779 (1.502-1.811)	0.127
T2 lesions	13.5 (9.0-28.0)	9.5 (4.5-19.5)	27.0 (12.0-31.0)	0.043
Gd+ lesions				1.000
Absence	12 (85.7)	7 (87.5)	5 (83.3)	
Presence	2 (14.3)	1 (12.5)	1 (16.7)	
Spinal cord lesions	0.0 (0.0-2.0)	0.0 (0.0-0.5)	2.0 (1.0-2.0)	0.230
Black holes				0.055
Absence	11 (78.6)	8 (100.0)	3 (50.0)	
Presence	3 (21.4)	0 (0.0)	3 (50.0)	
Atrophy				1.000
Absence	13 (92.9)	7 (87.5)	6 (100.0)	
Presence	1 (7.1)	1 (12.5)	0 (0.0)	
HLA-DRB1*15:01 or *03				0.315
Absence	7 (46.7)	5 (62.5)	2 (28.6)	
Presence	8 (53.3)	3 (37.5)	5 (71.4)	
CHI3L1 (ng/ml)	183.256 (122.485-219.874)	158.873 (113.094-210.824)	215.218 (175.367-252.844)	0.435
NF-L (pg/ml)	258.177 (177.907-615-137)	204.572 (103.626-480.788)	615.137 (258.177-857.226)	0.171

RIS-RIS: individuals who remained as RIS after five years of monitoring; RIS-Conversion: individuals who converted to CIS or MS within five years of monitoring; Categorical variables were shown as absolute and relative frequencies. Continuous variables were presented by median and Q1-Q3: First quartile-Third. n: number of samples; OCGB: oligoclonal IgG bands; Gd+: gadolinium enhancing lesions; CHI3L1: Chitinase 3 like-1; NF-L: neurofilament light chain.

4.5.2 CHI3L1 and NF-L levels in CSF

CHI3L1 and NF-L levels in CSF were tested to compare RIS-RIS and RIS-Conversion subjects. No changes in CHI3L1 and NF-L levels were observed (RIS-RIS median=158.873 ng/ml *vs* RIS-Conversion median=215.218 ng/ml; $p=0.435$; RIS-RIS median=204.572 pg/ml *vs* RIS-Conversion median=615.137 pg/ml; $p=0.171$; respectively) (Table 27).

A strong correlation was observed between CSF levels of CHI3L1 and NF-L ($r_s=0.852$, $p<0.001$). Further association analyses between CHI3L1, NF-L and radiological variables revealed a correlation only between NF-L and number of T2 lesions, and a tendency between NF-L and Gd+ lesions ($r_s=0.600$ and $p=0.030$; $r_s=0.498$ and $p=0.083$; respectively).

4.5.3 miRNA profile in CSF

Twelve patients with available CSF were analyzed for the screening of circulating miRNAs in cell-free CSF. These samples detection was unexpectedly lower compared with other studies and the quality of many curves was not good. For that reason, it was decided to establish a criteria to analyze these OpenArray plates different than the established in section 4.2. First, Amp Score and CqConfidence value were set to 0.75 and 0.45 respectively and, those curves with such values below the established threshold were discarded. Second, those miRNAs detected in at least 50% of CSF samples were further chosen to analyze their differential expression between studied groups. Based on this, 124 of 216 analyzed miRNAs were detected fulfilling the established criteria of detection quality but only 15 miRNAs were present in at least 50% of CSF samples.

Three of the selected miRNAs presented differential expression in RIS-RIS and RIS-Conversion patients: miR-144-3p, miR-448 and miR-653-3p were upregulated in the RIS-Conversion group (Table 28, Figure 54).

RESULTS

Table 28. Differential miRNA expression between groups in CSF samples in RIS study.

	RIS-RIS (n=7)		RIS-Conversion (n=5)		<i>p</i> value
	Median	Q1-Q3	Median	Q1-Q3	
miR-144-3p	0.405	0.308-0.409	1.082	0.827-1.036	0.016
miR-448	0.086	0.071-0.109	0.307	0.252-0.536	0.005
miR-653-3p	0.271	0.233-0.299	0.421	0.403-0.609	0.030

RIS-RIS: individuals who remained as RIS after five years of monitoring; RIS-Conversion: individuals who converted to CIS or MS after five years of monitoring; n: number of samples; Q1-Q3: First quartile-Third quartile. Statistical differences were determined by Mann-Whitney U test.

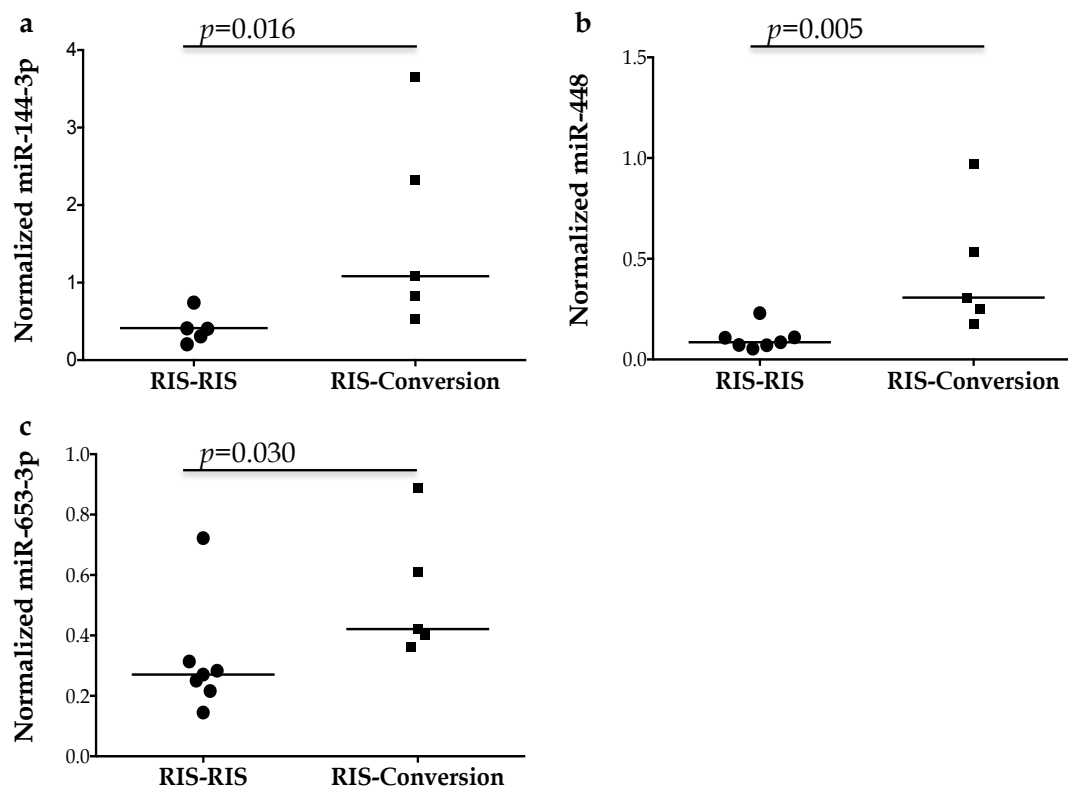


Figure 54. Differentially expressed miRNAs in CSF in RIS study. Dot plots for normalized value of (a) miR-144-3p, (b) miR-448 and, (c) miR-653-3p in CSF samples according to the conversion status. The dot indicates one sample and the line indicates the median. Mann-Whitney U test was used to determine statistical differences between groups.

4.5.4 miRNA profile in plasma

Samples of all RIS-RIS and RIS-Conversion patients were used for the screening of circulating miRNAs in plasma. We found that 130 miRNAs were detected in at least 50% of plasma samples.

Two different normalization strategies were used and the differential expression between groups was studied in both cases (Table 29). On one hand, GN that uses the mean value of all detectable miRNAs as normalizer value was used. On the other hand, the mean value of miR-20a, miR-103a and miR-191 was used, as they were the most stable miRNAs provided by the Relative Quantification module in the Thermo Fisher Cloud. Six miRNAs were significantly deregulated ($p < 0.050$) with both normalization strategies. miR-142-3p, miR-338-3p, miR-363-3p, miR-374b-5p and miR-424-5p were downregulated while miR-483-3p was upregulated (Table 29, Figure 55) in RIS-Conversion patients.

Table 29. Differential miRNA expression between groups in plasma samples in RIS study.

	Global Normalization			Endogenous Normalization		
	RIS-RIS Median (Q1-Q3)	RIS-Conversion Median (Q1-Q3)	<i>p</i> value	RIS-RIS Median (Q1-Q3)	RIS-Conversion Median (Q1-Q3)	<i>p</i> value
n	8	7		8	7	
miR-142-3p	8.783 (7.695-9.991)	4.893 (3.760-6.882)	0.029	1.504 (1.357-1.955)	0.872 (0.765-1.152)	0.004
miR-338-3p	0.120 (0.083-0.134)	0.051 (0.035-0.069)	0.014	0.020 (0.013-0.024)	0.009 (0.007-0.011)	0.021
miR-363-3p	0.392 (0.261-0.505)	0.139 (0.098-0.247)	0.030	0.060 (0.056-0.074)	0.027 (0.017-0.050)	0.045
miR-374b-5p	0.473 (0.310-0.601)	0.176 (0.138-0.316)	0.029	0.083 (0.065-0.094)	0.033 (0.026-0.056)	0.029
miR-424-5p	0.189 (0.179-0.249)	0.076 (0.050-0.110)	0.002	0.040 (0.028-0.048)	0.014 (0.010-0.020)	0.006
miR-483-3p	0.053 (0.045-0.061)	0.089 (0.079-0.220)	0.009	0.011 (0.006-0.013)	0.018 (0.015-0.044)	0.030

RIS-RIS: patients who remained as RIS after five years of monitoring; RIS-Conversion: patients who converted to CIS or MS after five years of monitoring; n: number of samples; Q1-Q3: First quartile-Third quartile. Statistical differences were determined by Mann-Whitney U test.

RESULTS

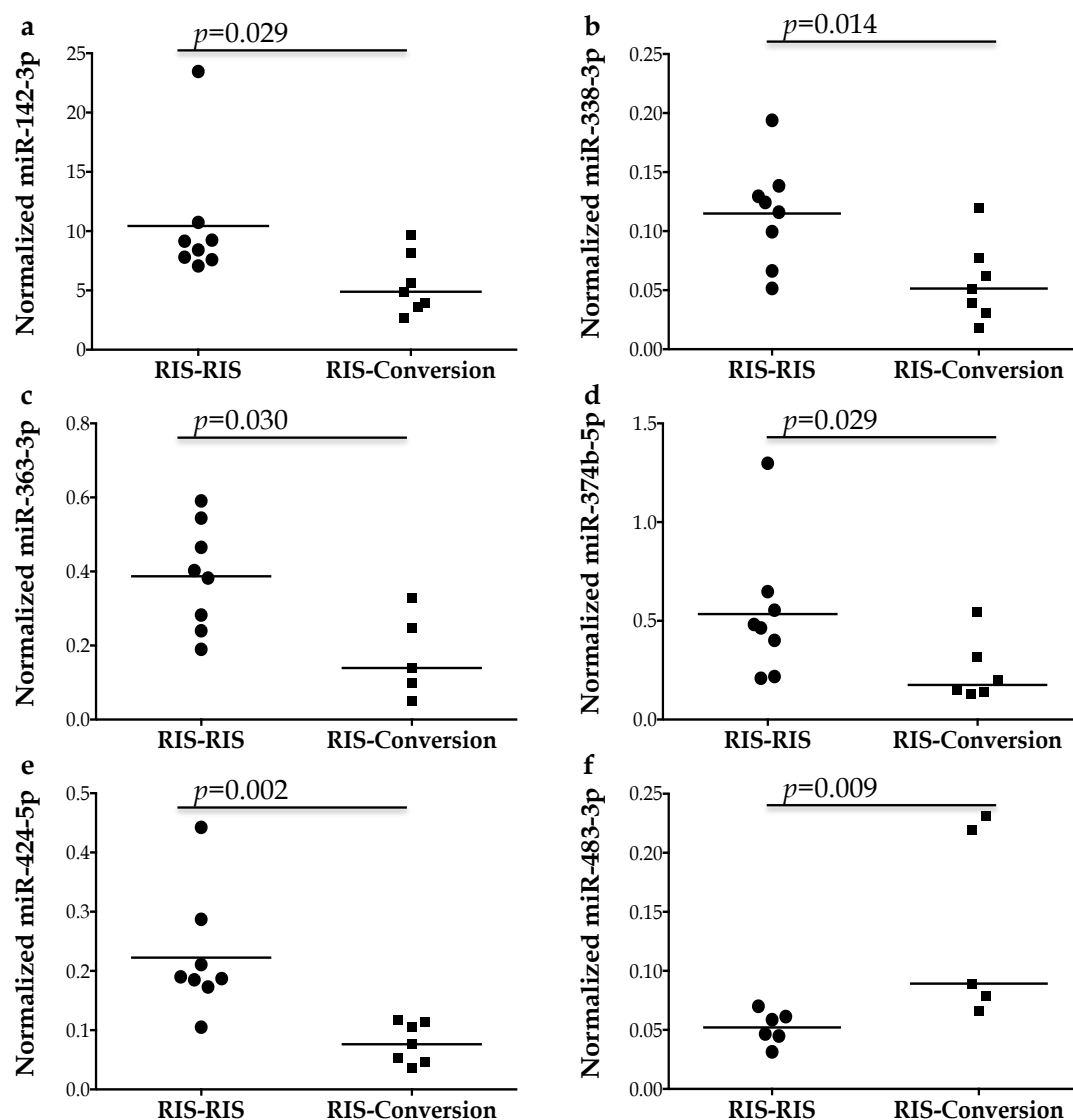


Figure 55. Differentially expressed miRNAs in plasma in RIS study. Dot plots for normalized value of (a) miR-142-3p, (b) miR-338-3p, (c) miR-363-3p, (d) miR-374b-5p, (e) miR-424-5p and, (f) miR-483-3p in plasma samples according to the conversion status. Global normalization data were used in the Figure. The dot indicates one sample and the line indicates the median. Mann-Whitney U test was used to determine statistical differences between groups.

4.5.5 Targets, pathways and cellular/tissue enriched sources analysis of selected miRNAs

Experimentally validated human targets for all deregulated miRNAs were retrieved from miRTarBase. Those targets with strong evidence for CSF or for plasma were

uploaded separately to Enrichr to explore the GO biological processes (Table 30, Table 31).

Table 30. List of strongly validated targets for CSF deregulated miRNAs in RIS study.

miR-144-3p	miR-448	miR-653-3p
ADAMTS1	ADAM10	n/a
APP	BCL2	
CFTR	CXCL12	
ETS1	IGF1R	
EZH2	ITPR1	
FGA	KDM2B	
FGB	MAP2K1	
FGG	MPPED2	
IRS1	SATB1	
MAP3K8		
MET		
MTOR		
NFE2L2		
NOTCH1		
PBX3		
PLAG1		
PTEN		
PTGS2		
SMAD4		
TGFB1		
TTN		
TUG1		
XIST		
ZEB1		
ZEB2		
ZFX		

RESULTS

Table 31. List of strongly validated targets for plasma deregulated miRNAs in RIS study.

miR-142-3p	miR-338-3p	miR-363-3p	miR-374b-5p	miR-424-5p	miR-483-3p
ABCG2	ADAM17	BCL2L11	AKT	ANLN	BBC3
APC	CCND1	CASP3	RECK1	ATF6	CDK4
ARNTL	CDH2	CDKN1A	VEGFA	CCND1	CTGF
BOD1	DAB2IP	CREB1	WNT16	CCND3	DLC1
CCNT2	HIF1A	FBXW7		CCNE1	EI24
DOCK6	IRS2	GAP43		CCNF	IGF1
EGR2	ITGB3	HIVEP1		CDC14A	PARD3
HMGA1	MACC1	NOTCH1		CDC25A	RASGRF1
HMGB1	MAP1A	PDPN		CDK6	SMAD4
HOXA10	MMP2	REG4		CDX2	SRF
HOXA7	MMP9	S1PR1		CHEK1	
HOXA9	NOVA1	SOX4		CUL2	
HSPA1B	NRP1			FASN	
IL1A	PKLR			FGF2	
LGR5	PKM			FGFR1	
LPP	PLA2G4B			HIF1A	
LRRC32	PREX2			ITPR1	
PRKCA	SMO			KDM5B	
PROM1	SOX4			KIF23	
PTPN23	SSX2IP			MAP2K1	
RAC1	TAZ			MYB	
ROCK2	UBE2Q1			NFIA	
TAB2	ZBTB18			PIAS1	
TGFBR1	ZEB2			PLAG1	
THBS4				PTCH1	
				SIAH1	
				SMAD3	
				SMAD7	
				SOCS2	
				SOCS6	
				SPI1	
				TGFBR3	
				WEE1	

Clustered GO terms revealed that target genes for CSF-deregulated miRNAs were involved in distinct biological processes related to cell adhesion and migration or cytokine-mediated signalling pathways (Figure 56).

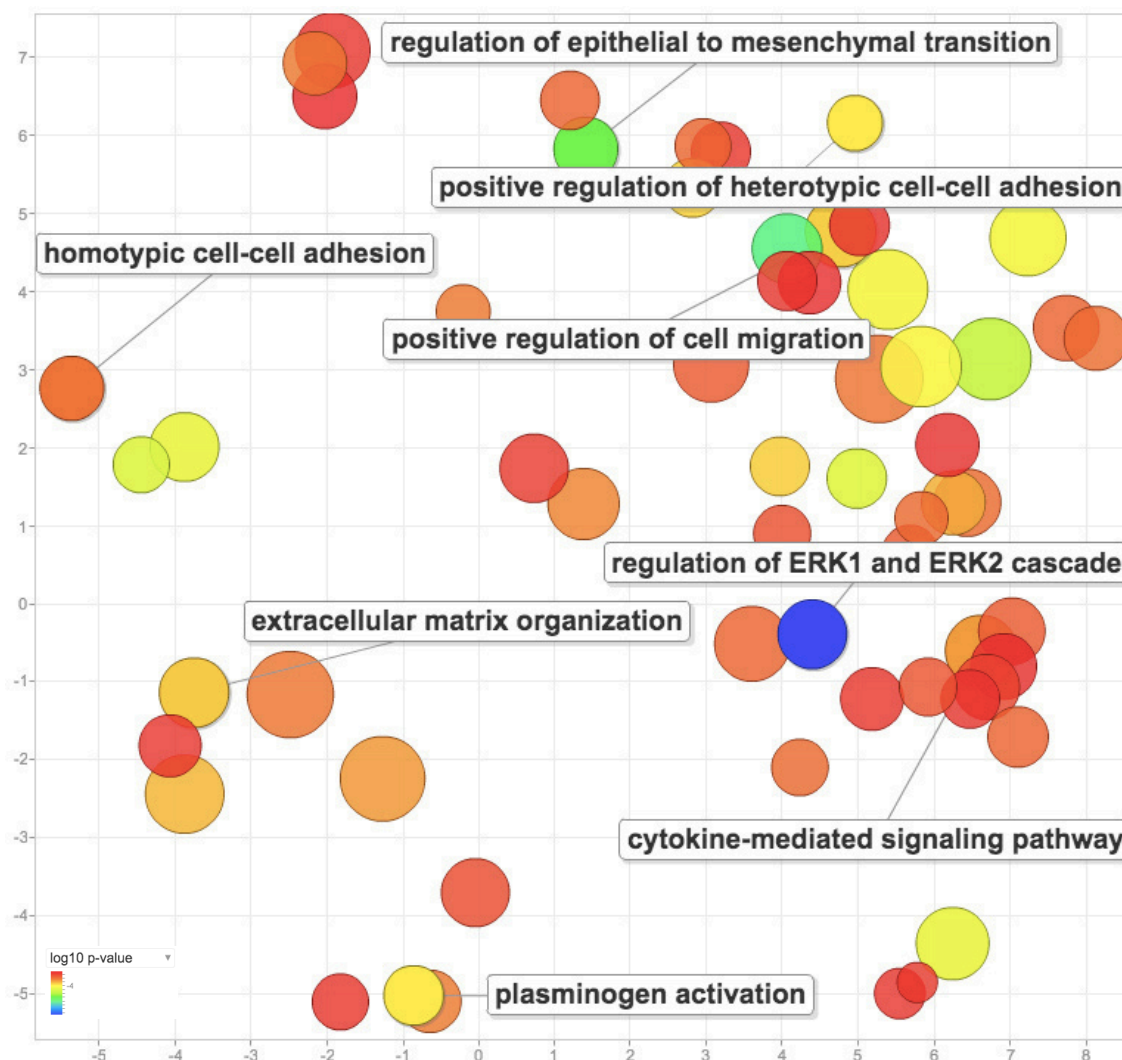


Figure 56. Visualization of the significantly associated GO biological processes in CSF using REVIGO. Visualization of the significantly associated GO biological processes in CSF using REVIGO. The semantic similarity-scatterplot shows the cluster representatives after the redundancy reduction. The bubble size indicates the frequency of the GO term and the color indicates the log₁₀ (adjusted p-value). Color legend is shown in the right corner of the Figure. GO: gene ontology.

RESULTS

Regarding plasma-deregulated miRNAs targets, cellular processes involving cytokine stimulus and adherens junction organization were highlighted, among others (Figure 57).



Figure 57. Visualization of the significantly associated GO biological processes using REVIGO in plasma. Visualization of the significantly associated GO biological processes in plasma using REVIGO. The semantic similarity-scatterplot shows the cluster representatives after the redundancy reduction. The bubble size indicates the frequency of the GO term and the color indicates the \log_{10} (adjusted p-value). Color legend is shown in the right corner of the Figure. GO: gene ontology.

Potential miRNA's source studies using public repositories as human miRNA tissue Atlas [287] and FANTOM5 [288] showed high expression of most deregulated miRNAs in natural killer cells, T cells or B cells, as well as in brain.

4.5.6 Association of miRNA levels with radiological and CSF biochemical variables

The correlation between all deregulated miRNA levels and number of T2 lesions in MRI as a radiological variable, and CHI3L1 and NF-L levels in CSF was studied. The expression of miR-448 in CSF positively correlated with the number of T2 lesions. In plasma, whereas miR-363-3p only had a negative correlation with T2 lesions, miR-483-3p levels were positively associated with number of T2 lesions, CHI3L1 and NF-L levels (Table 32).

Table 32. Association of miRNA levels with number of T2 lesions, CHI3L1 and NF-L levels in RIS study.

	T2 lesions		CHI3L1		NF-L	
	r_s	p value	r_s	p value	r_s	p value
miR-448	0.620	0.032	0.112	0.729	0.287	0.366
miR-363-3p	-0.596	0.041	-0.318	0.340	-0.591	0.056
miR-483-3p	0.685	0.029	0.685	0.029	0.685	0.029

r_s : Spearman's Rho coefficient. miRNA expression values used for association study obtained from CSF for miR-448 and from plasma (global normalization) miR-363-3p and miR-483-3p.

4.5.7 Summary

This exploratory study reports a signature pattern of circulating miRNAs in RIS individuals, differentiating those who finally converted to CDMS from those that remained as RIS. Specifically, miR-144-3p, miR-448 and miR-653-3p were deregulated in CSF and, miR-142-3p, miR-338-3p, miR-363-3p, miR-374b-5p and miR-424-5p were deregulated in plasma samples. *In silico* analyses concerning the biological processes in which these miRNAs are involved and their cellular or tissular origin might suggest a potential interest in studying miRNA functionality in immune cells in further studies.

These results were published in *Epigenomics*, reference: Muñoz-San Martín M, Torras S, Robles-Cedeño R, Buxó M, Gómez I, Matute-Blanch C, Comabella M, Villar LM, Perkal H, Quintana E, Ramió-Torrentà L. Radiologically isolated syndrome: targeting microRNAs as prognostic biomarkers. *Epigenomics* 2020; 12(23):2065. doi: 10.2271/epi-2020-0172 (Annex II).

RESULTS

4.6 STUDY OF CIRCULATING miRNA PROFILES IN CSF OF RRMS PATIENTS

This part is divided in three sections as CSF miRNA profiles in RRMS individuals were compared according to different variables as ethnicity, age at onset or absence/presence of Gd+ lesions in MRI.

4.6.1 Comparison of CSF miRNA profiles in MS patients according to their ethnic origin

The aim of this preliminary study was to identify the existence of a differential profile of circulating CSF miRNAs between individuals with RRMS based on their ethnic origin, as a lot of studies have shown a more aggressive clinical course in MS patients of North African origin residing in Europe [294]. In addition, a sub-analysis was made in which North African individuals were divided according to the age of migration to Europe.

4.6.1.1 Clinical characteristics of the studied patients

Patients included in this study were recruited at the Girona Neuroimmunology and Multiple Sclerosis Unit of Dr. Josep Trueta Univeristy Hospital (Girona, Spain) and all participants signed a written informed consent. They were diagnosed with RRMS according to McDonald 2010 criteria and were not receiving disease-modifying treatment at the moment of sample. A cohort of 20 individuals was studied: 10 European origin (MS-E) and 10 North-African (MS-NA).

No significant differences were observed in sex or age between MS-E and MS-NA individuals. Clinical, radiological and genetic data collected close to the sample extraction date are shown in Table 33. MS-NA presented statistically significant lower levels of vitamin D (MS-NA median=5.80 ng/ml *vs* MS-E median=25.45 ng/ml; $p<0.001$) and a tendency to have higher number of T2 lesions in MRI than MS-E (MS-NA median=38 lesions *vs* MS-E median=10.5 lesions; $p=0.066$), as well as increased levels of IgG anti-CMV (MS-NA median=184.6 AU/ml *vs* MS-E median=100.3 AU/ml; $p=0.079$).

Table 33. Demographic, clinical, radiological and genetic data of the studied RRMS cohort with different ethnic origin.

	Whole group	MS-E	MS-NA	<i>p</i> value
Sex				1.000
Male	4 (20.0)	2 (20.0)	2 (20.0)	
Female	16 (80.0)	8 (80.0)	8 (80.0)	
Age (years)	30.5 (25.0-33.0)	32.0 (27.0-32.0)	25.0 (17.0-37.0)	0.436
EDSS	2.0 (1.5-2.0)	2.0 (1.0-2.0)	2.0 (1.5-2.0)	0.730
Number T2 lesions	22.0 (12.0-40.5)	10.5 (7.0-28.0)	38.0 (13.0-47.0)	0.066
Gd+ lesions				0.308
Absence	5 (31.3)	1 (14.3)	4 (44.4)	
Presence	11 (68.8)	6 (85.7)	5 (55.6)	
Vitamin D levels (ng/ml)	11.80 (5.80-25.45)	25.45 (17.00-27.75)	5.80 (5.10-6.80)	<0.001
HLA-DRB1*15:01				0.301
Absence	9 (64.3)	4 (50.0)	5 (83.3)	
Presence	5 (35.7)	4 (50.0)	1 (16.7)	
OCGB				1.000
Negative	1 (5.6)	0 (0.0)	1 (11.1)	
Positive	17 (94.4)	9 (100.0)	8 (88.9)	
LS_OCMB				0.576
Negative	14 (77.8)	6 (66.7)	8 (88.9)	
Positive	4 (22.2)	3 (33.3)	1 (11.1)	
IgG_CMV				1.000
Negative	3 (15.8)	2 (20.0)	1 (11.1)	
Positive	16 (84.2)	8 (80.0)	8 (88.9)	
IgG_CMV levels (AU/ml)	123.0 (84.2-175.4)	100.3 (73.3-134.7)	184.6 (87.1-522.2)	0.079

MS-E: MS individuals of European origin; MS-NA: MS individuals of North-African origin. Categorical variables were shown as absolute and relative frequencies and their statistical differences were determined by Fisher's exact test. Continuous variables were presented by median and Q1-Q3: First quartile-Third quartile and their statistical differences were determined by Mann-Whitney U test. EDSS: Expanded Disability Status Scale; Gd+: gadolinium enhanced; OCGB: oligoclonal IgG bands; LS_OCMB: lipid-specific oligoclonal IgM bands; IgG_CMV: immunoglobulin G anti-citomegalovirus.

RESULTS

4.6.1.2 miRNA profile in CSF

To study the existence of a characteristic miRNA profile in CSF of MS individuals according to their ethnic origin, cc-OA panels were used per triplicate. 38 miRNAs were detected in 70% samples (at least 50% of samples in each group). When comparing the expression of miRNAs in CSF between MS-E and MS-NA, overexpression of miR-335-5p and miR-653-3p was observed in MS-NA ($p=0.008$ and $p=0.027$, respectively). Furthermore, two other miRNAs (miR-143-3p and miR-20a-5p) showed a tendency to be deregulated. Table 34 shows median expression values and p values for these miRNAs and Figure 58 shows dot plots.

Table 34. Differential miRNA expression between MS individuals of different ethnic origin in CSF samples.

miRNA	MS-E (n=10)		MS-NA (n=10)		p value
	Median	Q1-Q3	Median	Q1-Q3	
miR-143-3p	5.103	4.037-6.460	3.246	2.594-3.414	0.079
miR-20a-5p	0.364	0.260-0.481	0.566	0.397-0.965	0.094
miR-335-5p	5.776	4.440-6.834	9.355	7.892-9.806	0.008
miR-653-3p	0.367	0.355-0.595	1.092	0.567-2.064	0.027

MS-E: MS individuals of European origin; MS-NA: MS individuals of North-African origin. Q1-Q3: First quartile-Third quartile. Statistical differences were determined by Mann-Whitney U test.

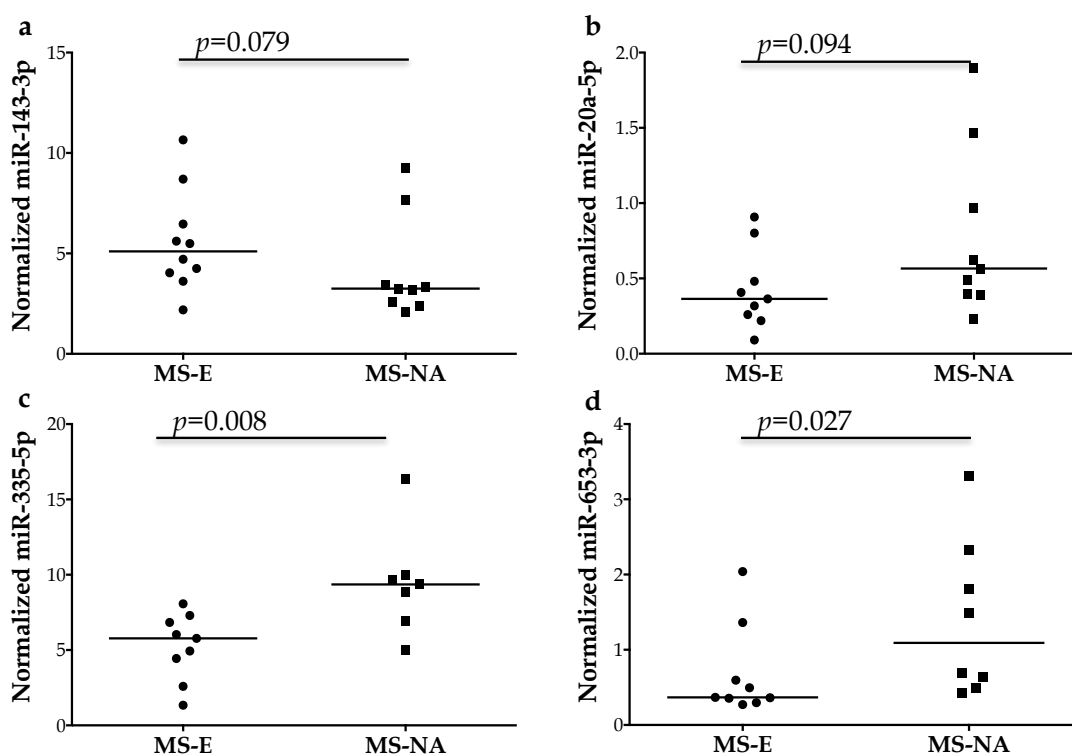


Figure 58. Differentially expressed miRNAs in CSF from MS individuals with different ethnic origin. Dot plots for normalized value of (a) miR-143-3p, (b) miR-20a-5p, (c) miR-335-5p and (d) miR-653-3p in CSF samples according to the ethnic origin. The dot indicates one sample and the line indicates the median. Mann-Whitney U test was used to determine statistical differences between groups.

4.6.1.3 Association of miRNA levels with other variables

We studied the correlation between CSF miRNA levels and number of T2 lesions in MRI, levels of vitamin D and EDSS. The expression of miR-142-3p and miR-451a in CSF correlated with the number of T2 lesions negatively and positively, respectively. miR-143-3p and miR-335-5p had a positive and negative correlation with levels of vitamin D. Last, miR-21-5p levels were positively associated with EDSS (Table 35, Figure 59).

RESULTS

Table 35. Association of CSF miRNA levels with number of T2 lesions, levels of vitamin D and EDSS.

	T2 lesions		Vitamin D levels		EDSS	
	r_s	p value	r_s	p value	r_s	p value
miR-142-3p	-0.537	0.048	-0.068	0.810	-0.216	0.405
miR-143-3p	-0.040	0.893	0.539	0.038	-0.011	0.965
miR-21-5p	0.297	0.302	-0.374	0.209	0.652	0.008
miR-26b-5p	0.173	0.612	-0.172	0.594	0.560	0.046
miR-335-5p	0.273	0.417	-0.636	0.026	-0.171	0.558
miR-451a	0.588	0.027	-0.352	0.198	-0.160	0.540

r_s : Spearman's Rho coefficient. miRNA expression values used for association study obtained from CSF.

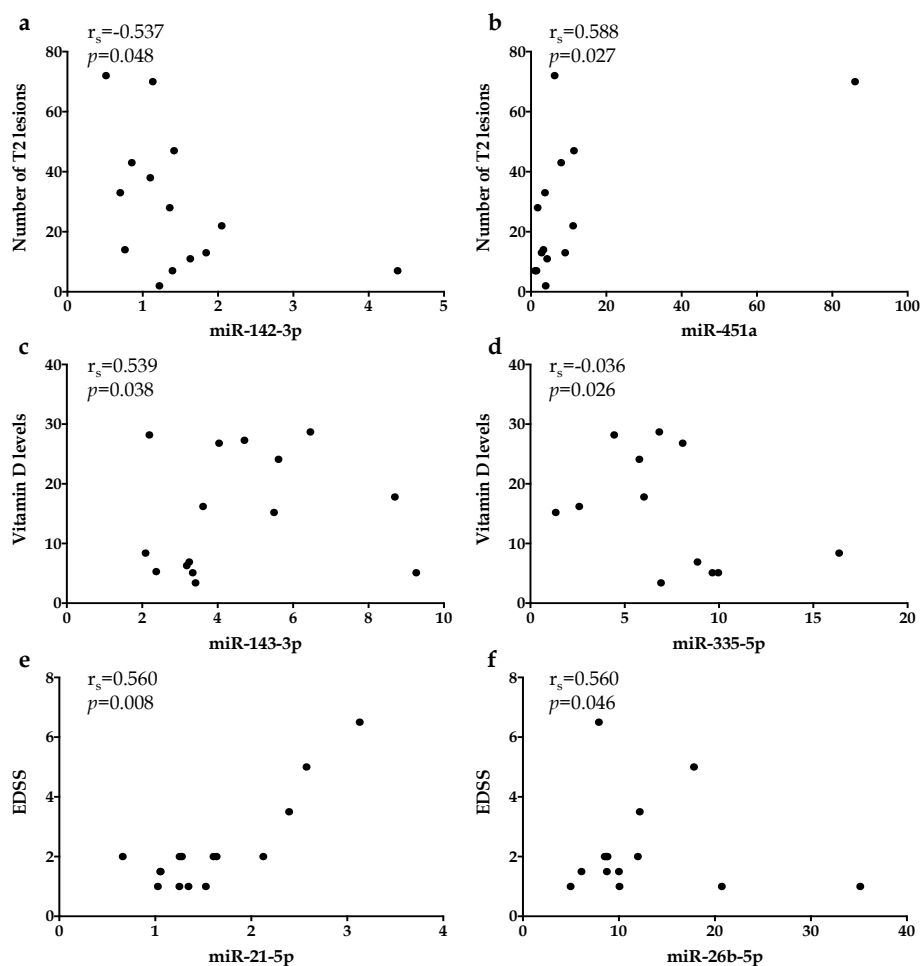


Figure 59. Correlation of normalized Ct values in CSF samples with radiological and clinical variables. Scatter plots showing the relationship between (a) miR-142-5p and number of T2 lesions, (b) miR-451a and number of T2 lesions, (c) miR-143-3p and vitamin D levels, (d) miR-335-5p and vitamin D levels, (e) miR-21-5p and EDSS and, (f) miR-26b-5p and EDSS. r_s : Spearman's Rho; p : p value.

4.6.1.4 Analysis depending on age of migration to Europe

MS-NA subjects were subclassified according to their migration age to Europe: before 15 years or born in Europe (n=3) (MS-NA (<15)) *vs* after 15 years old (n=6) (MS-NA (>15)). No significant differences were observed in sex between MS-E (80.0% women), MS-NA (<15) (100.0% women) and MS-NA (>15) (66.7% women) individuals. However, MS-NA (<15) were younger than other groups when were diagnosed (median=17 years). Clinical, radiological and genetic data collected close to the sample extraction date are shown in Table 36.

MS-NA (>15) presented statistically significant lower levels of vitamin D (MS-NA (<15) median=6.9 ng/ml *vs* MS-NA (>15) median=5.1 ng/ml *vs* MS-E median=25.45 ng/ml; $p=0.004$). MS-NA (<15) presented a tendency to have higher number of Gd+ lesions in MRI than MS-NA (>15) ($p=0.056$).

miR-145-5p, miR-150-5p, miR-335-5p and miR-653-3p showed significant differences between some of the 3 groups (Figure 60). Specifically, miR-150-5p, previously related to inflammation in CSF from MS individuals, showed very low levels in MS-NA that migrated older than 15 years of age.

Table 36. Clinical, radiological and miRNA data of the studied RRMS cohort.

Comparison	MS-E (n=10)	MS-NA (<15) (n=3)	MS-NA (>15) (n=6)	<i>p</i> value
	Median (Q1-Q3)	Median (Q1-Q3)	Median (Q1-Q3)	
Age at diagnosis (years)	32.0 (27.0-32.0)	17.0 (16.6-17.0)	35.0 (26.0-42.0)	0.018
MS-E <i>vs</i> MS-NA (<15)				0.060
MS-E <i>vs</i> MS-NA (>15)				0.015
MS-NA (>15) <i>vs</i> MS-NA (<15)				1.000
Vitamin D levels (ng/ml)	25.45 (17.00-27.75)	6.9 (6.60-7.65)	5.1 (4.25-5.90)	0.004
MS-E <i>vs</i> MS-NA (<15)				0.161
MS-E <i>vs</i> MS-NA (>15)				0.004
MS-NA (>15) <i>vs</i> MS-NA (<15)				1.000
Number T2 lesions	10.5 (7.0-28.0)	38 (25.5-40.5)	22 (13.0-47.0)	0.238
MS-E <i>vs</i> MS-NA (<15)				0.474
MS-E <i>vs</i> MS-NA (>15)				0.475
MS-NA (>15) <i>vs</i> MS-NA (<15)				1.000
IgG_CMV levels (AU/ml)	100.3 (73.3-134.7)	87.1 (84.2-136.1)	184.6 (159.3-522.2)	0.179
MS-E <i>vs</i> MS-NA (<15)				1.000
MS-E <i>vs</i> MS-NA (>15)				0.194
MS-NA (>15) <i>vs</i> MS-NA (<15)				0.844
miR-145-5p	11.819 (8.088-15.412)	1.381 (1.290-4.543)	20.017 (14.076-39.154)	0.034
MS-E <i>vs</i> MS-NA (<15)				0.224
MS-E <i>vs</i> MS-NA (>15)				0.604
MS-NA (>15) <i>vs</i> MS-NA (<15)				0.028
miR-150-5p	6.180 (3.372-6.773)	7.992 (7.105-11.433)	2.339 (0.515-4.683)	0.020
MS-E <i>vs</i> MS-NA (<15)				1.000
MS-E <i>vs</i> MS-NA (>15)				0.076
MS-NA (>15) <i>vs</i> MS-NA (<15)				0.036

miR-335-5p		5.776 (4.440-6.834)	7.487 (5.012-9.962)	9.502 (8.140-13.009)	0.048
	MS-E <i>vs</i> MS-NA (<15)				0.861
	MS-E <i>vs</i> MS-NA (>15)				0.048
	MS-NA (>15) <i>vs</i> MS-NA (<15)				1.000
miR-653-3p		0.367 (0.355-0.595)	2.400 (1.494-3.307)	0.691 (0.635-1.805)	0.042
	MS-E <i>vs</i> MS-NA (<15)				0.095
	MS-E <i>vs</i> MS-NA (>15)				0.212
	MS-NA (>15) <i>vs</i> MS-NA (<15)				1.000

MS-E: MS individuals of European origin; MS-NA (<15): MS individuals of North-African origin who were born in Europe or moved to Europe before 15 years old; MS-NA (>15): MS individuals of North-African origin who moved to Europe after 15 years old.

RESULTS

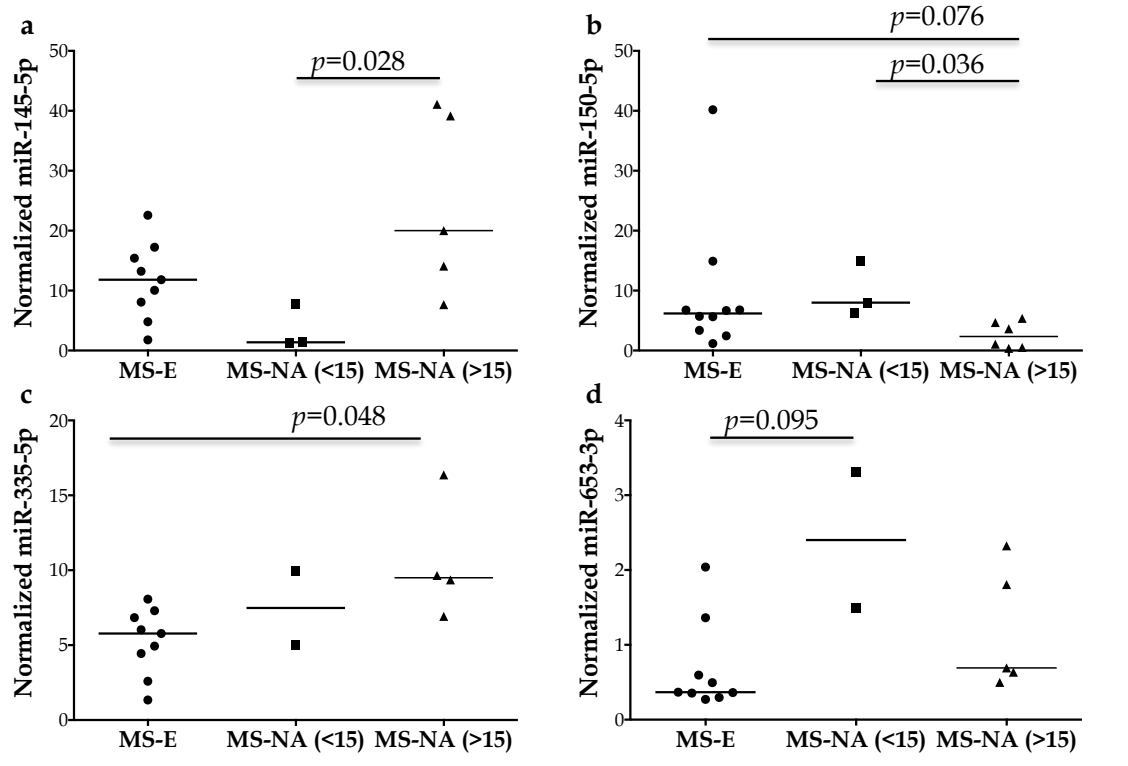


Figure 60. Differentially expressed miRNAs in CSF from RRMS individuals with different ethnic origin and age of migration. Dot plots for normalized value of (a) miR-143-3p, (b) miR-150-5p, (c) miR-335-5p and, (d) miR-653-3p in CSF samples according to the ethnic origin. The dot indicates one sample and the line indicates the median. Kruskal Wallis test was used to determine statistical differences between groups.

4.6.1.5 Summary

These results showed the presence of a differential expression in miRNAs between RRMS patients depending on their ethnic origin. miR-335-5p and miR-653-3p were overexpressed in MS-NA individuals, while miR-143-3p and miR-20a-5p showed a tendency to be deregulated. Interestingly, when subclassifying NA-MS patients, we could observe different expression patterns depending on migration to Europe age that might suggest the need for further studies to establish the role of these miRNAs in the development and aggressiveness of MS according to the ethnic origin.

4.6.2 Comparison of CSF miRNA profiles in RRMS patients depending on age at disease onset

The mean age of onset for MS is between 25 and 35 years old but, there are individuals with earlier and later MS onset. The aim of this preliminary study was to identify the existence of a differential profile of circulating CSF miRNAs between individuals with RRMS based on the age of disease onset, as these individuals might present distinct features and characteristics.

4.6.2.1 Clinical characteristics of the studied patients

Patients included in this study were recruited at the Girona Neuroimmunology and Multiple Sclerosis Unit of Dr. Josep Trueta University Hospital (Girona, Spain) and all participants signed a written informed consent. Samples were extracted at the moment of RRMS diagnosis according to McDonald 2010 criteria and were not receiving disease-modifying treatment at the moment of sampling. A cohort of 34 individuals was studied: 11 RRMS individuals whose age at onset was below 25 years old (RRMS<25), 11 RRMS subjects whose age at onset was between 25 and 35 years old (25<RRMS<35) and 12 RRMS individuals with an onset after 45 years old (RRMS>45).

Clinical, radiological and genetic data collected close to the sample extraction date are shown in Table 37. No significant differences were observed in any variable between groups, except for age at sampling as expected.

RESULTS

Table 37. Demographic, clinical, radiological and genetic data of the studied RRMS cohort with different age at onset.

Variable	Whole group	RRMS<25	25<RRMS<35	RRMS>45	<i>p</i> value
n	34	11	11	12	
Sex					0.577
Male	10 (29.4)	3 (27.3)	2 (18.2)	5 (41.7)	
Female	24 (70.6)	8 (72.7)	9 (81.8)	7 (58.3)	
Age (years)	32.0 (25.0-48.0)	22.0 (19.0-25.0)	32.0 (28.0-32.0)	49.0 (48.0-53.5)	<0.001
EDSS	2.00 (1.25-2.75)	2.00 (1.00-2.00)	2.00 (1.00-2.50)	2.00 (1.50-3.25)	0.532
T2 lesions					0.629
0-9	8 (30.8)	4 (40.0)	3 (37.5)	1 (12.5)	
10-20	11 (42.3)	4 (40.0)	2 (25.0)	5 (62.5)	
20-50	6 (23.1)	2 (20.0)	2 (25.0)	2 (25.0)	
50-100	1 (3.9)	0 (0.0)	1 (12.5)	0 (0.0)	
Gd+ lesions					0.430
Absence	8 (32.0)	4 (44.4)	1 (12.5)	3 (37.5)	
Presence	17 (68.0)	5 (55.6)	7 (87.5)	5 (62.5)	
OCGB					0.758
Negative	3 (9.4)	1 (10.0)	0 (0.0)	2 (16.7)	
Positive	29 (90.6)	9 (90.0)	10 (100.0)	10 (83.3)	
LS_OCMB					0.660
Negative	17 (54.8)	4 (40.0)	6 (60.0)	7 (63.6)	
Positive	14 (45.2)	6 (60.0)	4 (40.0)	4 (36.4)	
HLA-DRB1*15:01					0.210
Negative	17 (63.0)	5 (55.6)	4 (44.4)	8 (88.9)	
Positive	10 (37.0)	4 (44.4)	5 (55.6)	1 (11.1)	

RRMS<25: RRMS individuals whose age at onset was below 25 years; 25<RRMS<35: RRMS individuals whose age at onset was between 25 and 35 years old; RRMS>45: RRMS individuals whose age at onset was above 45 years old. Categorical variables were shown as absolute and relative frequencies and their statistical differences were determined by Fisher's exact test. Continuous variables were presented by median and Q1-Q3: First quartile-Third quartile and their statistical differences were determined by Kruskal Wallis test. EDSS: Expanded Disability Status Scale at extraction; Gd+: gadolinium enhanced; OCGB: oligoclonal IgG bands; LS_OCMB: lipid-specific oligoclonal IgM bands.

4.6.2.2 miRNA profile in CSF

To study the characteristic miRNA profile in CSF of MS individuals according to the age of disease onset, cc-OA panels were used per triplicate. 36 miRNAs were detected in 70% samples (at least 50% of samples in each group). When comparing the expression of miRNAs in CSF between the three groups, only let-7c-5p showed a tendency to be deregulated in some of the groups as shown in Table 38 and Figure 61.

Table 38. Median expression values of normalized let-7c-5p for each group.

miRNA	RRMS<25 (n=11)	25<RRMS<35 (n=11)	RRMS>45 (n=12)	<i>p</i> value
	Median (Q1-Q3)	Median (Q1-Q3)	Median (Q1-Q3)	
let-7b-5p	0.305 (0.233-0.339)	1.028 (0.347-1.442)	0.425 (0.368-1.242)	0.071
RRMS<25 vs 25<RRMS<35				0.109
RRMS<25 vs RRMS>45				0.174
25<RRMS<35 vs RRMS>45				1.000

RRMS<25: RRMS individuals whose age at onset was below 25 years; 25<RRMS<35: RRMS individuals whose age at onset was between 25 and 35 years old; RRMS>45: RRMS individuals whose age at onset was above 45 years old. Q1-Q3: First quartile-Third quartile. Statistical differences were determined by Kruskal Wallis test.

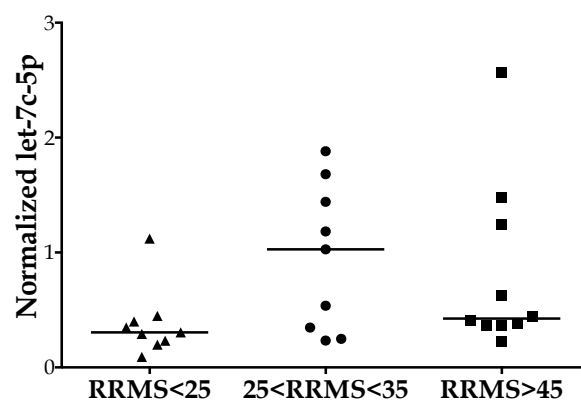


Figure 61. Dot plot for normalized levels of let-7c-5p in CSF of RRMS individuals depending on age at onset. The dot indicates one sample and the line indicates the median.

RESULTS

4.6.2.3 miRNA CSF profile comparison between individuals of early and late onset

A comparison between individuals belonging to early and late onset, RRMS<25 and RRMS>45, was made. From a total of 36 expressed miRNAs, only three miRNAs showed a tendency to be deregulated, as observed in Table 39 and Figure 62. While let-7c-5p and miR-448 might be downregulated in the younger group, miR-204-5p presented a higher expression in RRMS<25 than in RR>45.

Table 39. Median expression values of miRNAs for RRMS<25 and RRMS>45.

miRNA	RRMS<25 (n=11)		RRMS>45 (n=12)		<i>p</i> value
	Median	Q1-Q3	Median	Q1-Q3	
let-7c-5p	0.305	0.233-0.399	0.425	0.368-1.242	0.053
miR-204-5p	8.769	7.113-15.747	5.297	2.432-9.027	0.043
miR-448	0.377	0.224-0.597	0.103	0.086-0.294	0.067

RRMS<25: RRMS individuals whose age at onset was below 25 years; RRMS>45: RRMS individuals whose age at onset was above 45 years old. Q1-Q3: First quartile-Third quartile. Statistical differences were determined by U-Mann Whitney test.

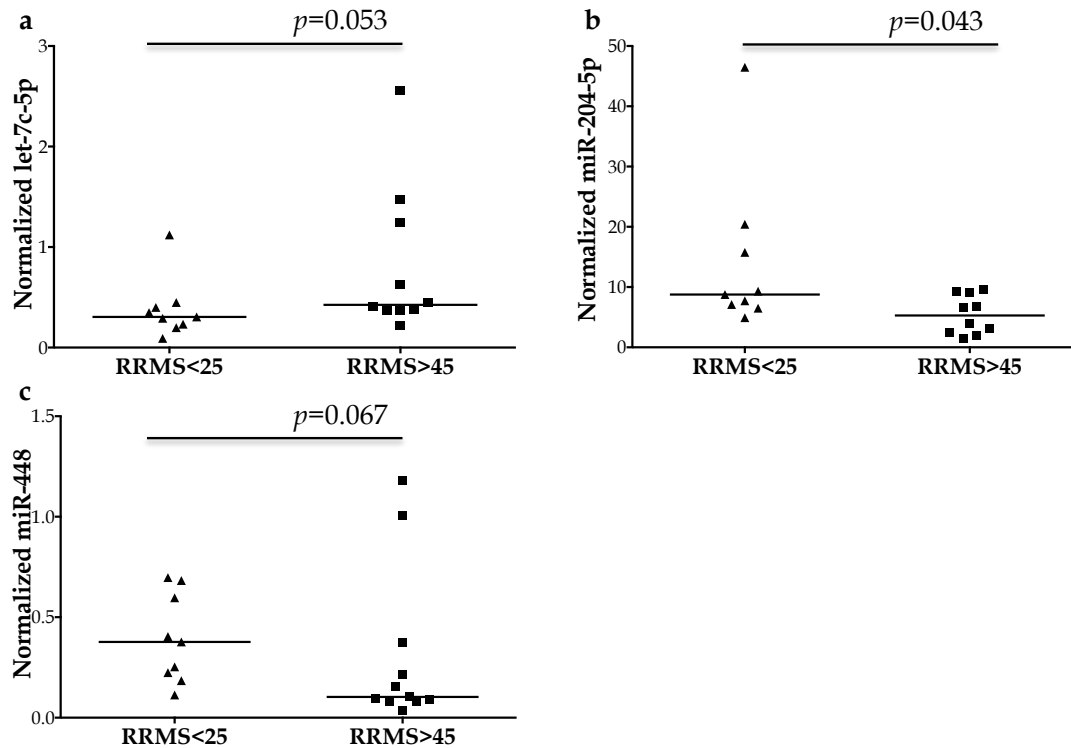


Figure 62. Differentially expressed miRNAs in CSF from RRMS individuals with early and late MS onset. Dot plots for normalized values of (a) let-7c-5p, (b) miR-204-5p and, (c) miR-448 in CSF samples according to age of onset. The dot indicates one sample and the line indicates the median. U-Mann Whitney test was used to determine statistical differences between groups.

4.6.2.6 Summary

This preliminary study did not show the existence of a differential profile of CSF miRNAs in RRMS individuals depending on the age of disease onset. Some potential deregulations in let-7c-5p, miR-204-5p and miR-448 between early and late onsets might require further validation in bigger cohorts. Therefore, the role of circulating miRNAs in the involved pathological processes might be the same regardless age of MS onset.

RESULTS

4.6.3 Comparison of active lesions-enriched miRNAs in CSF according to the presence of Gd+ lesions in MRI

The aim of this part was to test the presence of a set of deregulated miRNAs, previously reported by Junker *et al* in active MS lesions from brain biopsies [295], in CSF of MS patients, and to study their association with the presence of Gd+ lesions to assess their value as biomarkers of MS activity. miRNA expression was assessed by individual qPCR with first generation Individual TaqMan hydrolysis probes. Target and pathway analysis was made and deregulated miRNA and candidate targets expression were correlated *in silico*.

4.6.3.1 Clinical characteristics of patients

Forty-six MS patients (71.7% women) with a mean age and standard deviation of 33.98±9.66 were studied. Gd+ lesions were present in 56.5% of the subjects. No differences were observed for either sex distribution or age between patients with absence (Gd-) and presence of Gd+. Gd+ group presented a statistically increased number of T2 lesions (Table 40).

Table 40. Demographic data of the study MS cohort according to the absence or presence of Gd+ lesions.

	Gd- (n=20)	Gd+ (n=26)	p value
Age (mean ± SD)	31.15 ± 10.373	36.15 ± 8.652	0.081
Sex (male/female)			0.818
Male	6 (30.00%)	7 (26.92%)	
Female	14 (70.00%)	19 (73.08%)	
EDSS at sampling (median, Q1-Q3)	2.0 (1.0-2.5)	2.0 (1.5-2.13)	0.819
OCGB			0.432
Negative	1 (5.26%)	0 (0.00%)	
Positive	18 (94.74%)	25 (100.00%)	
LS_OCMB			0.393
Negative	14 (73.68%)	16 (61.54%)	
Positive	5 (26.32%)	10 (38.46%)	
T2 lesions			0.004
<9 lesions	12 (66.67%)	4 (16.67%)	
10-20 lesions	5 (27.78%)	10 (41.67%)	
21-50 lesions	1 (5.56%)	8 (33.33%)	
51-100 lesions	0 (0.00%)	2 (8.33%)	

Gd-: patients without gadolinium enhanced lesions; Gd+: patients with gadolinium enhanced lesions; SD: standard deviation; OCGB: oligoclonal IgG bands; N/P: negative/positive; LS_OCMB: lipid-specific oligoclonal IgM bands.

4.6.3.2 Detection of miRNAs in CSF

Seven of 28 miRNAs reported as deregulated in active MS lesions [295] were detected in at least 75% of CSF samples, assessed in triplicate by Cq values lower than 37 (miR-155, miR-223, miR-21, miR-320, miR-328, miR-146a and miR-146b). A group of five miRNAs was present in a range between 75% and 40% of samples (miR-34a, miR-130a, miR-214, miR-27a and miR-656) while the others showed very low expression measures or were undetected (Table 41).

RESULTS

Table 41. List of 28 analyzed miRNAs and percentage of detection for each miRNAs in CSF.

	Gd- (<i>n</i> =20)		Gd+ (<i>n</i> =26)		Total percentage of detection
	<i>n</i>	%	<i>n</i>	%	
miR-155	20	100.00	26	100.00	100.00
miR-223	19	95.00	26	100.00	97.83
miR-21	18	90.00	25	96.15	93.48
miR-320	19	95.00	24	92.31	93.48
miR-328	16	80.00	23	88.46	84.78
miR-146a	17	85.00	21	80.77	82.61
miR-146b	15	75.00	22	84.62	80.44
miR-34a	13	65.00	14	53.85	58.70
miR-130a	10	50.00	17	65.39	58.70
miR-214	10	50.00	14	53.85	52.17
miR-27a	10	50.00	12	46.15	47.83
miR-656	7	35.00	13	50.00	43.48
miR-487b	8	40.00	4	15.39	26.09
miR-200c	6	30.00	6	23.08	26.09
miR-184	4	20.00	5	19.23	19.57
miR-23a	3	15.00	4	15.39	15.22
miR-139	2	10.00	4	15.39	13.04
miR-340	3	15.00	2	7.69	10.87
miR-142-5p	2	10.00	2	7.69	8.70
miR-23b	2	10.00	1	3.85	6.52
miR-650	1	5.00	1	3.85	4.35
miR-193a	1	5.00	0	0.00	2.17
miR-181c	0	0.00	1	3.85	2.17
miR-326	0	0.00	0	0.00	0.00
miR-142-3p	0	0.00	0	0.00	0.00
miR-199a	0	0.00	0	0.00	0.00
miR-22	0	0.00	0	0.00	0.00
miR-15a	0	0.00	0	0.00	0.00

4.6.3.3 Differential miRNA values in CSF of MS patients with Gd+ lesions

After normalizing using miR-17, differential expression of the seven miRNAs detected in at least 75% of the CSF samples was tested to compare Gd- and Gd+ patients. Increased expression of miR-21, miR-146a and miR-146b was found in Gd+ patients (Table 42, Figure 63).

Table 42. Differential miRNA expression between groups in CSF of MS patients depending on the absence or presence of Gd+ lesions.

	Gd- (<i>n</i> =20)		Gd+ (<i>n</i> =26)		<i>p</i> value
	Median	Q1-Q3	Median	Q1-Q3	
miR-21	0.014	0.010-0.022	0.029	0.013-0.052	0.024
miR-146a	0.065	0.031-0.136	0.135	0.082-0.239	0.016
miR-146b	0.008	0.002-0.020	0.021	0.012-0.052	0.030
miR-155	0.007	0.002-0.016	0.011	0.006-0.019	0.163
miR-223	0.066	0.043-0.328	0.124	0.088-0.226	0.232
miR-320	0.038	0.010-0.048	0.042	0.026-0.087	0.271
miR-328	0.007	0.003-0.012	0.011	0.005-0.026	0.143

Gd-: patients without gadolinium enhanced lesions; Gd+: patients with gadolinium enhanced lesions; Q1-Q3: First quartile-Third quartile.

ROC curves were performed to determine the potential discriminatory capacity provided by each single miRNA present in cell-free CSF for detecting brain acute inflammatory activity. miR-21, miR-146a and miR-146b presented AUC values of 0.703, 0.728 and 0.712 respectively, which support a valuable discriminatory indicator to differentiate Gd- from Gd+ patients. Logistic regression analysis was performed to evaluate the discriminatory ability of selected miRNAs combination. Variables were dichotomized according to cut-off values deduced from ROC analysis (AUC=0.867) (Table 43, Figure 64).

RESULTS

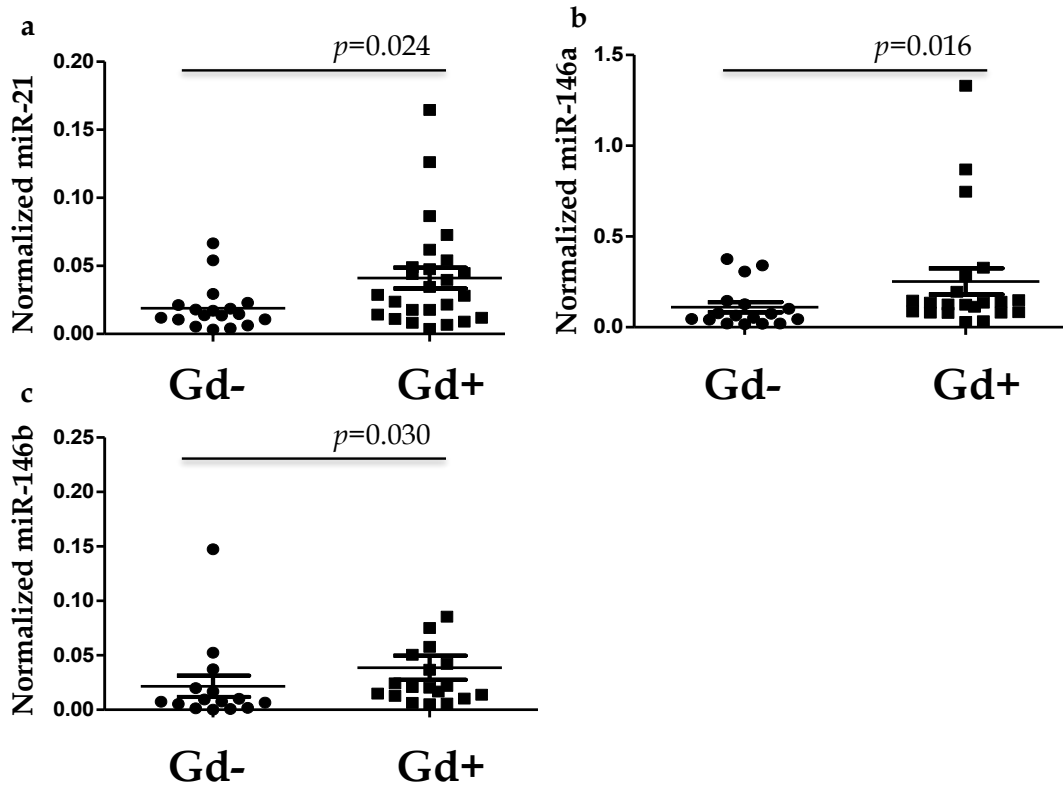


Figure 63. Differentially expressed miRNAs in CSF samples according to the absence or presence of Gd+ lesions. Dot plots for normalized value of (a) miR-21, (b) miR-146a and (c) miR-146b in patients according to the absence or presence of Gd+ lesions in MRI. The line indicates the median and Mann-Whitney U test was used to determine statistical differences between groups.

Table 43. Capacity of selected miRNAs to detect inflammatory activity in CNS.

	AUC	95% CI	Cut-off values	Sensitivity (%)	Specificity (%)	LR+	LR-
miR-21	0.703	0.543-0.863	0.028	60.00	77.78	2.70	0.51
miR-146a	0.728	0.553-0.904	0.010	90.48	64.71	2.56	0.15
miR-146b	0.712	0.531-0.894	0.078	81.82	66.67	2.45	0.27
miR-21+miR-146a+miR-146b	0.867	0.736-0.997		94.12	69.23	3.06	0.08

AUC: area under curve; CI: confidence interval; LR+: positive likelihood ratio; LR-: negative likelihood ratio.

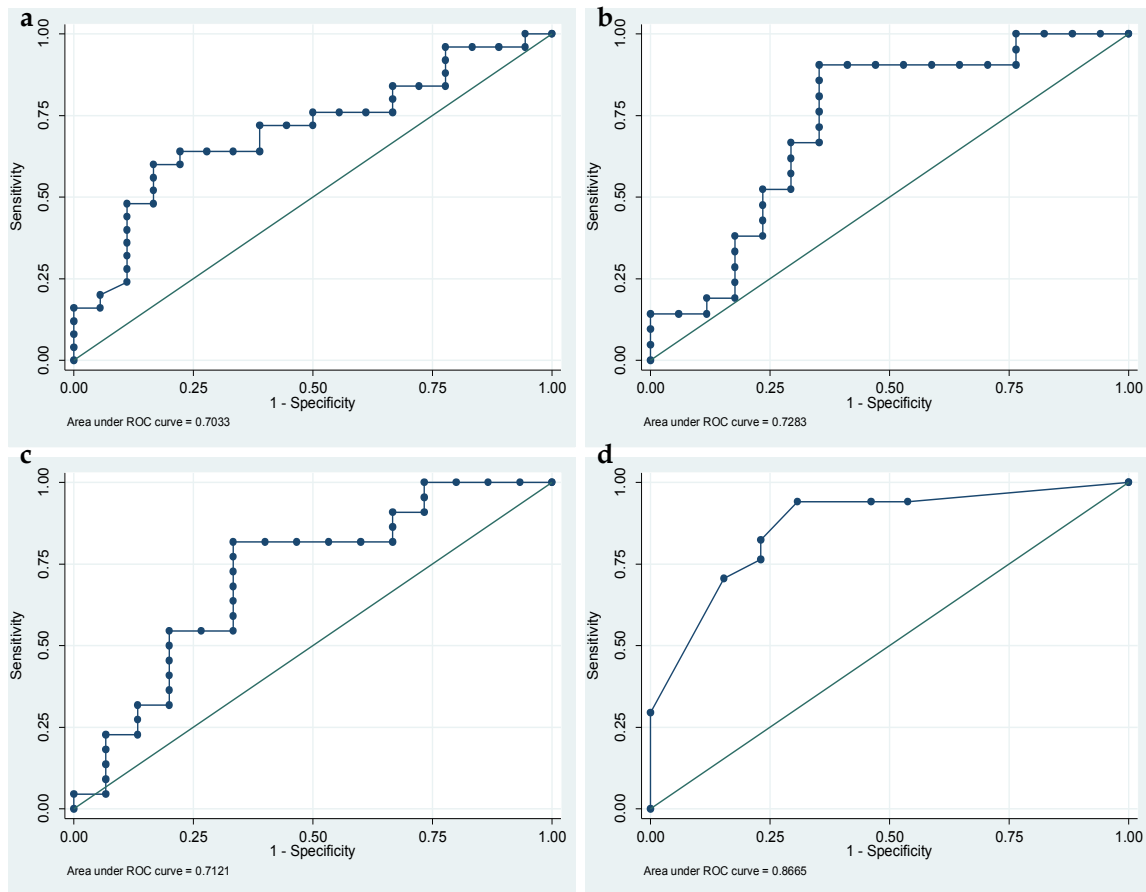


Figure 64. ROC analysis of individual and combined miRNAs to discriminate inflammatory activity. Receiver Operating Characteristics analysis of (a) miR-21-5p, (b) miR-146a, (c) miR-146b and (d) combined miR-21, miR-146a and miR-146b in CSF to discriminate inflammatory activity.

4.6.3.4 Correlation between deregulated miRNAs and CSF NF-L levels

Differential expression of NF-L levels was tested to compare Gd- and Gd+ subjects (Figure 65). Increased expression of NF-L was found in CSF of Gd+ patients (median Gd-=462.5 ng/l *vs* median Gd+=1116.0 ng/l; $p=0.010$).

The correlation between CSF deregulated miRNA levels and NF-L levels was also studied. The expression of miR-146b presented a strong positive correlation with NF-L ($r_s=0.682$ and $p=0.001$), while miR-21 and miR-146a showed a moderate relationship ($r_s=0.374$ and $p=0.086$, $r_s=0.400$ and $p=0.090$, respectively). NF-L levels

RESULTS

also presented a strong correlation with the number of Gd+ lesions ($r_s=0.620$ and $p=0.001$) (Figure 66).

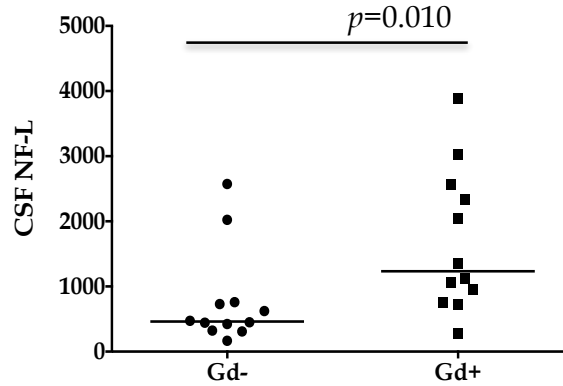


Figure 65. Differential expression of NF-L in CSF according to the absence or presence of Gd+ lesions. Dot plots for levels of NF-L in CSF according to the absence or presence of Gd+ lesions. The line indicates the median and Mann-Whitney U test was used to determine statistical differences between groups.

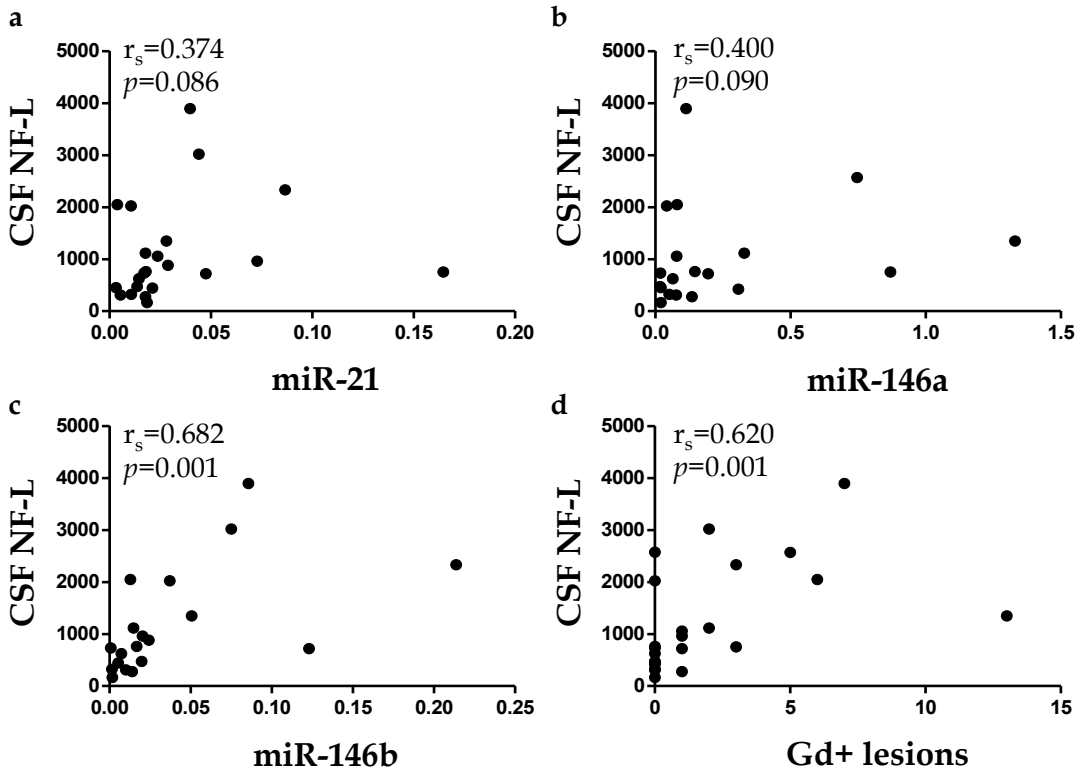


Figure 66. Scatter plot of correlation between NF-L in CSF and miRNA levels. Scatter plots showing the relationship between NF-L levels in CSF and expression levels of (a) miR-21, (b) miR-146a, (c) miR-146b and, (d) number of Gd+ lesions. Significant positive correlations were observed in all cases, illustrating a link between axonal damage and candidate miRNAs expression. r_s : Spearman’s Rho; p : p value.

4.6.3.5 Association of CSF miRNA expression with radiological and clinical variables

Levels of miR-21, miR-146a and miR-146b in CSF positively correlated with the number of Gd+ lesions. In addition, the expression of miR-21 and miR-155 mirrored the number of T2 lesions. Finally, miR-21 was also associated with the basal EDSS score (Table 44).

Table 44. Correlations between radiological and clinical data with miRNA expression levels in CSF.

	No. of Gd+ lesions		No. of T2 lesions		Basal EDSS	
	r_s	p value	r_s	p value	r_s	p value
miR-21	0.379	0.015	0.377	0.017	0.440	0.003
miR-146a	0.463	0.004	0.125	0.474	0.030	0.856
miR-146b	0.349	0.040	0.004	0.984	-0.299	0.072
miR-155	0.270	0.077	0.308	0.047	-0.010	0.949
miR-223	0.159	0.309	0.113	0.481	0.249	0.099
miR-320	0.187	0.243	0.035	0.831	0.035	0.825
miR-328	0.298	0.073	0.213	0.211	-0.089	0.592

r_s : Spearman's Rho coefficient. miRNA expression values used for association study obtained from CSF.

4.6.3.6 Target and pathway analysis of miR-21, miR-146a and miR-146b

Experimentally validated human molecules with strong evidence for being targets for miR-21, miR-146a and miR-146b were retrieved from miRTarBase (Table 45) and then, uploaded to Enrichr to explore the GO biological processes [283,284].

RESULTS

Table 45. Validated targets for miR-21-5p, miR-146a-5p and miR-146b-5p from miRTarBase.

miR-21-5p	miR-21-5p	miR-146a-5p	miR-146a-5p	miR-146b-5p
AKT2	NTF3	BCLAF1	RARB	CARD10
ANKRD46	PCBP1	BGLAP	RHO	CCDC6
ANP32A	PDCD4	BRCA1	RHOA	CDKN1A
APAF1	PELI1	BRCA2	RNF11	EGFR
BASP1	PIAS3	CARD10	ROBO1	ERBB4
BCL2	PIK3R1	CASP7	ROCK1	HNRNPD
BCL6	PLAT	CCDC6	S100A12	IL1RAP
BMPR2	PLOD3	CCL5	SIKE1	IL1RL2
BTG2	PPARA	CCNA2	SLPI	IL6
CBX4	PPIF	CCND1	SMAD2	IRAK1
CCL20	PTEN	CCND2	SMAD4	KIT
CCR1	PTPN14	CD40LG	SMN1	MALAT1
CDC25A	PTX3	CD80	SOS1	MMP16
CDK2AP1	RASA1	CDKN1A	SOX2	MYO6
CLU	RASGRP1	CDKN3	SPP1	NFKB1
COL4A1	RECK	CFH	STAT1	NOVA1
CXCL10	REST	CNOT6L	TGFB1	PAX8
DAXX	RFFL	COP58	TLR2	PDGFRA
DDAH1	RHO	COX2	TLR4	RARB
DERL1	RHOB	CPM	TRAF6	S100A12
DOCK4	RMND5A	CXCL12	UHRF1	SCUBE2
DOCK5	RPS7	CXCL8	WASF2	SLC5A5
DOCK7	RTN4	CXCR4	ZNF117	TLR4
DUSP10	SASH1	DUSP1		TRAF6
E2F1	SATB1	EGFR		UHRF1
E2F2	SECISBP2L	ELAVL1		ZNF117
EGFR	SERPINB5	ERBB4		ZNRF3
EIF4A2	SERPINI1	FADD		
ELAVL4	SETD2	FAF1		
ERBB2	SIRT2	FANCM		
FASLG	SMAD7	FAS		
FBXO11	SMARCA4	HOXD10		
FMOD	SMN1	ICAM1		
GAS5	SOD3	IL1RAP		
GDF5	SOX2	IL1RL2		
HIPK3	SOX5	IL6		
HNRNPK	SP1	IRAK1		
HPGD	SPRY2	IRAK2		
ICAM1	STAT3	IS2		
IGF1R	TCF21	KDM2B		
IL12A	TGFB1	KIF22		
IL1B	TGFB2	L1CAM		

IRAK1	TGFBI	LAMC2
ISCU	TGFBR2	LFNG
JAG1	TGFBR3	LIN52
JMY	TGIF1	LRP2
LRRFIP1	TIAM1	MIF
MAP2K3	TIMP3	MTA2
MARCKS	TM9SF3	MYO6
MEF2C	TNFAIP3	NFAT5
MMP2	TNFRSF10B	NFKB1
MMP9	TOPORS	NOS1
MSH2	TOR1AIP2	NOTCH1
MSH6	TP53BP2	NOTCH2
MTAP	TP63	NUMB
MYC	TPM1	PA2G4
MYD88	VEGFA	PLAUR
NCAPG	VHL	PRKCE
NCOA3	WWP1	PTGES2
NFIA	YOD1	PTGS2
NFIB		RAC1

Clustered GO terms revealed that miRNAs target genes were involved in distinct biological processes such as apoptosis, cell migration and proliferation and cytokine-mediated signaling pathways (Figure 67).

The miRNA-target interaction network showed interleukin receptor-associated kinase 1 (*IRAK1*) and epidermal growth factor receptor (*EGFR*) as shared targets for the three deregulated miRNAs (Figure 68).

RESULTS



Figure 67. Pathway and target analysis of miR-21, miR-146a and miR-146b. Visualization of the significantly associated GO biological processes using REVIGO. The semantic similarity-scatterplot shows the cluster representatives after the redundancy reduction. The bubble size indicates the frequency of the GO term and the color indicates the \log_{10} (adjusted p -value). Color legend is shown in the left corner of the Figure.

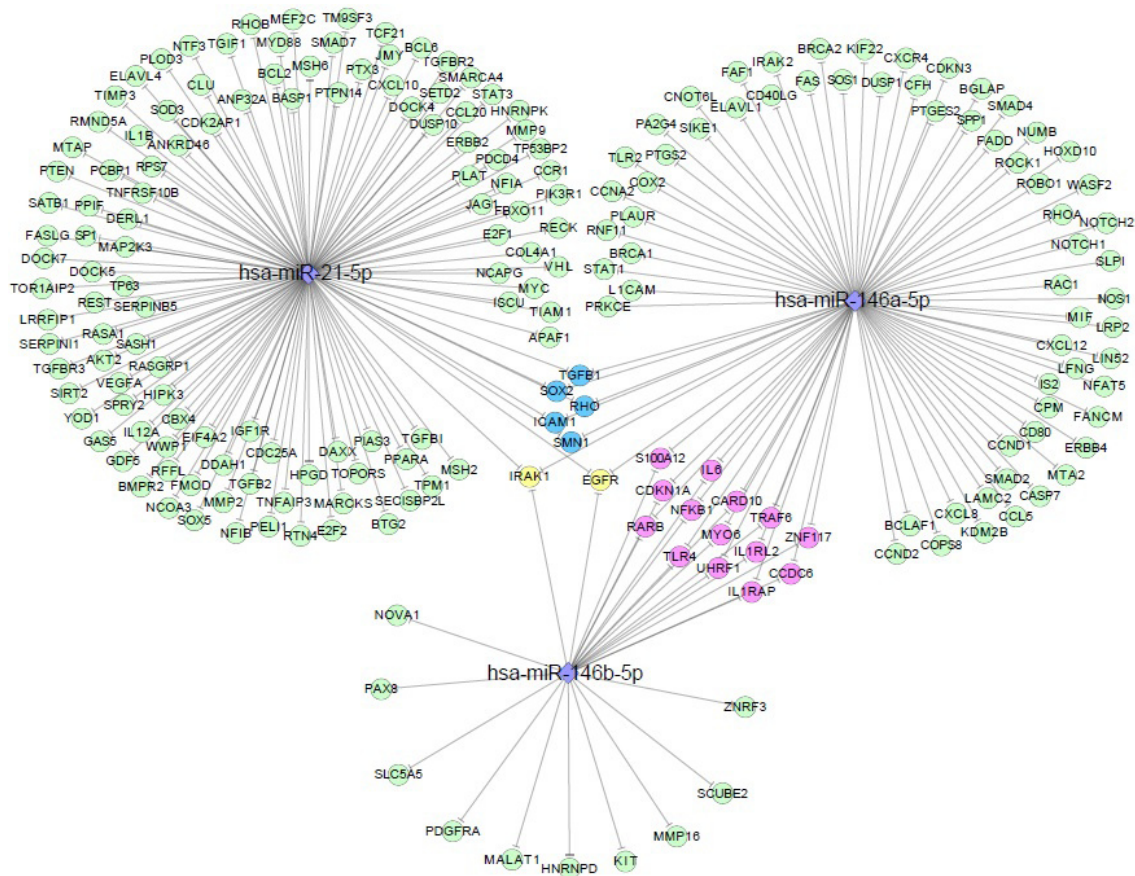


Figure 68. Target analysis of miR-21, miR-146a and miR-146b. microRNA-target interaction network generated by Cytoscape software. Targets with strong experimental evidence for miR-21, miR-146a and miR-146b were retrieved from miRTarBase. Blue-colored targets correspond to those targets shared by miR-21 and miR-146a; pink-colored targets corresponds to those targets shared by miR-146a and miR-146b; yellow-colored targets corresponds to those targets shared by the three deregulated miRNAs.

4.6.3.7 Correlation analysis of miRNAs and mRNA expression in *in silico* datasets

In order to evaluate the possible interaction between miR-21, miR-146a and miR-146b and their shared targets *IRAK1* and *EGFR*, the publicly available datasets GSE28487 (miRNA expression) and GSE28490 (mRNA expression) belonging to the SuperSeries GSE28492 from GEO [296] were used. As different immune cells are involved in the CNS inflammatory processes observed in MS [297], these microarray datasets, containing normalized data for gene and miRNA expression levels from human immune cells subsets, were chosen. We found that *IRAK1* was

RESULTS

strongly negatively correlated to miR-146a and miR-146b expression ($r_s = -0.670$ and $r_s = -0.635$, respectively), while the relation with miR-21 did not reach statistical significance. However, the expression of *EGFR* was not correlated with the expression of these miRNAs (Figure 69).

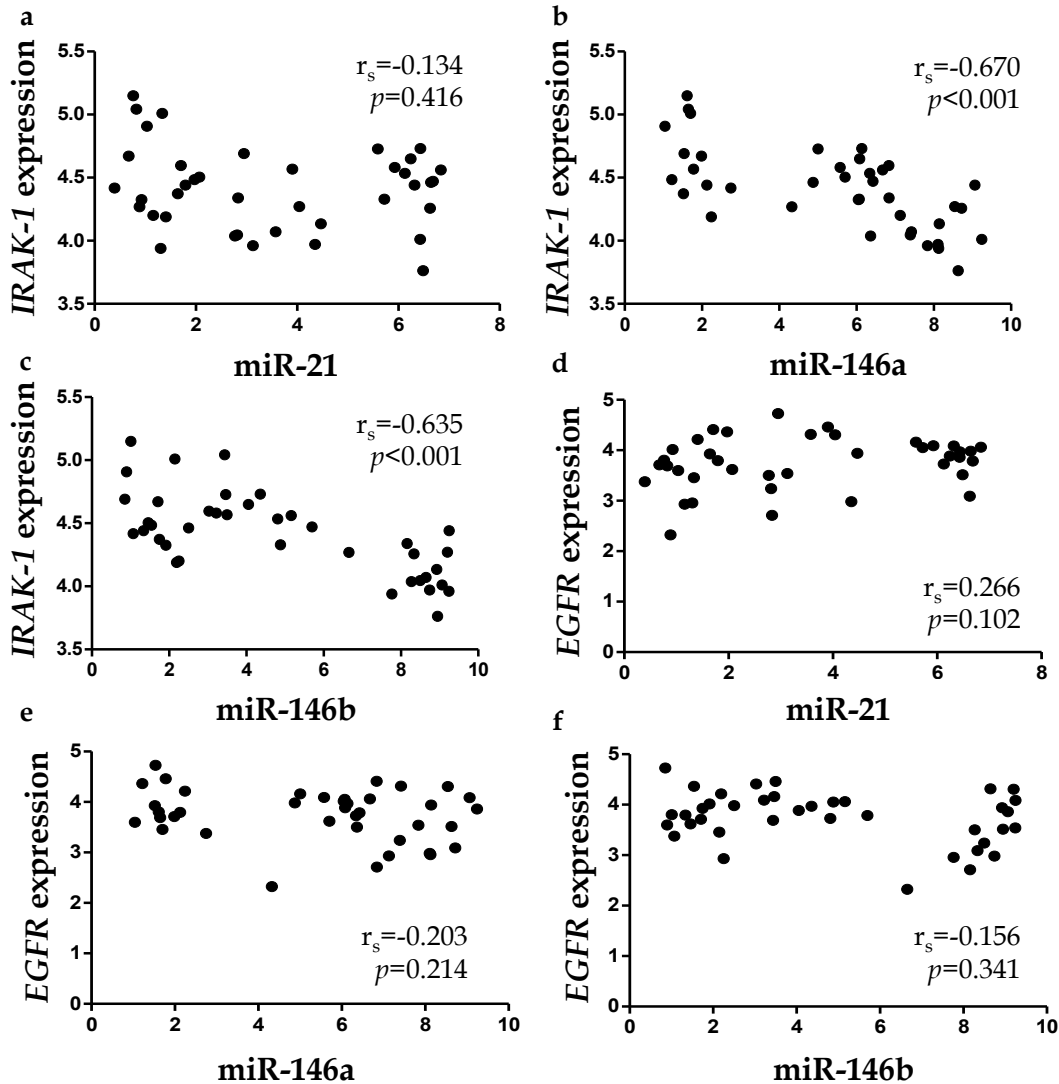


Figure 69. Correlation analysis of deregulated miRNAs and candidate targets mRNA expression in publicly available datasets. miRNA and mRNA expression profile of GSE28487 and GSE28490, respectively from Gene Expression Omnibus (GEO) DataSets (<https://www.ncbi.nlm.nih.gov/gds/>) was obtained. Scatter plots of correlations between (a) miR-21, (b) miR-146a and (c) miR-146 and *IRAK-1* and (d) miR-21, (e) miR-146a and (f) miR-146 and *EGFR* were presented. r_s : Spearman's Rho; p : p value.

4.6.3.8 Plasma expression of miR-21, miR-146a and miR-146b

Circulating miRNAs from plasma samples of 30 patients included in the CSF study (13 Gd- and 17 Gd+ patients) were extracted and quantified by qPCR. Differential expression analysis of miRNAs in plasma based on Gd- or Gd+ status revealed no significant differences for the three deregulated miRNAs in CSF (Table 46).

Table 46. Differential miRNA expression between groups in plasma samples.

	Gd- (<i>n</i> =13)		Gd+ (<i>n</i> =17)		<i>p</i> value
	Median	Q1-Q3	Median	Q1-Q3	
miR-21	0.801	0.587-0.869	0.595	0.528-0.778	0.157
miR-146a	2.612	2.089-2.831	2.108	1.894-2.555	0.086
miR-146b	1.098	0.928-1.359	1.080	0.960-1.180	0.621

Gd-: patients without gadolinium enhanced lesions; Gd+: patients with gadolinium enhanced lesions; Q1-Q3: First quartile-Third quartile.

Furthermore, no significant correlation between CSF and plasma miRNA levels was found, with the exception of miR-146b ($r_s = -0.398$ and $p = 0.049$) (Figure 70). Moreover, no association was observed between plasma miRNA levels and number of Gd+ lesions. Only plasma level of miR-146a showed a positive correlation with EDSS ($r_s = 0.383$ and $p = 0.037$).

RESULTS

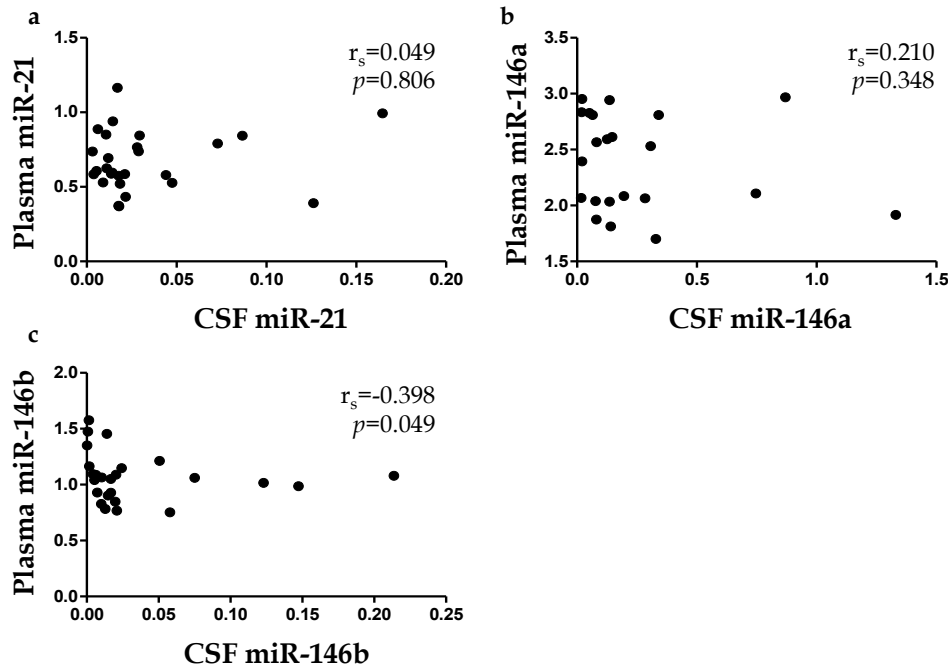


Figure 70. Correlation of normalized Cq values between CSF and plasma samples. Scatter plot for normalized values of CSF and plasma levels of (a) miR-21, (b) miR-146a and (c) miR-146b. r_s : Rho of Spearman; p : p value.

4.6.3.9 Summary

Overexpression of miR-21, miR-146a and miR-146b in cell-free CSF were able to discriminate MS patients with Gd+ lesions in the MRI. All data point to the hypothesis that an overexpression of these miRNAs in CSF is induced to counteract the pro-inflammatory milieu in MS and they might be released into the CSF in an attempt to reduce the harmful damage into the brain. However, additional functional studies and analyses of larger cohorts are needed to validate these results and to elucidate the real role of these miRNAs in the context of MS.

These results were published in *Journal of Neuroinflammation*, reference: Muñoz-San Martín M, Reverter G, Robles-Cedeño R, Buxó M, Ortega FJ, Gómez I, Tomàs-Roig J, Celarain N, Villar LM, Perkal H, Fernández-Real JM, Quintana E, Ramió-Torrentà L. Analysis of miRNA signatures in CSF identifies upregulation of miR-21 and miR-146a/b in patients with multiple sclerosis and active lesions. *J Neuroinflammation* 2019; 16(1):220. doi: 10.1186/s12974-019-1590-5 (Annex II).

4.7 STUDY OF CIRCULATING VIRUS-ENCODED miRNAs IN MS PATIENTS AND HEALTHY CONTROLS

The aim of this section was to compare virus-encoded miRNA expression in plasma samples from MS patients and healthy individuals, as EBV is one of the environmental factors involved in the development of MS and the viral genome encodes 44 miRNAs that might regulate human gene expression. Seven ebv-miRNAs were selected and their detection in plasma samples was assured by qPCR and compared between groups.

4.7.1 Selection of EBV-encoded miRNA assays and detection in plasma samples

First, seven first generation TaqMan miRNA assays targeting individual EBV-encoded miRNAs were chosen for assuring their presence in plasma by qPCR. The selected miRNAs were: ebv-miR-BART22 whose expression was detected in a previous unpublished study of this group; ebv-miR-BHRF1-2-5p, ebv-miR-BHRF1-3 and ebv-miR-BART6-5p because the first couple was deregulated and the last one detected in plasma samples of MS patients in the study of Wang YF *et al* [36]; ebv-miR-BART7-3p, ebv-miR-BART11-5p, ebv-miR-BART19-5p that were deregulated in B lymphocytes of MS patients in the study of Sievers C *et al* [35].

As described in section 3.6.2.1, cDNA from plasma samples is usually diluted to 1:200 prior its analysis by qPCR with Individual TaqMan hydrolysis probes. As human miRNA content in plasma is reduced compared with cellular or tissular sources and viral miRNA expression is expected to be even lower, the normal preamplified cDNA dilution to be charged in qPCR plates was modified using 1:50 cDNA:water dilution. ebv-miR-BART7-3p was the only ebv-encoded miRNA, from all seven, that was detected in plasma samples.

RESULTS

4.7.2 Demographic data of Girona cohort

Once established the optimal conditions to detect ebv-BART7-3p in plasma samples, MS patients and OND individuals recruited at the Girona Neuroimmunology and Multiple Sclerosis Unit of Dr. Josep Trueta Univeristy Hospital (Girona, Spain) whose serological tests assured that they had been previously infected by EBV were selected. Plasma samples were extracted at the moment of diagnosis and none of MS patients were receiving DMTs at the moment of sampling. A cohort of 82 individuals was studied: 48 MS individuals and 34 OND subjects. Demographic, clinical and, genetic data are shown in Table 47. Analyzed variables did not show any difference between groups, except for EBNA-1 levels that were increased in MS group and higher percentage of HLA-DRB1*15:01 positive individuals that observed in MS subjects.

4.7.3 Comparison of viral miRNA expression between MS patients and OND controls in Girona cohort

ebv-miR-BART7-3p expression was normalized by the mean value of miR-186 and miR-106a and its differential expression in plasma between OND and MS individuals did not show any statistically significant difference (Table 48 and Figure 71).

Table 47. Demographic, clinical and, genetic data of the studied cohort in EBV study.

	Whole group	OND	MS	<i>p</i> value
n	82	34	48	
Sex				0.465
Male	23 (28.05)	11 (32.35)	12 (25.00)	
Female	59 (71.95)	23 (67.65)	36 (75.00)	
Age (years)	37.0 (31.0-46.0)	39.5 (32.0-49.0)	36.5 (28.0-45.0)	0.222
EBNA-1 levels	405.0 (236.0-580.0)	294.5 (85.3-490.0)	535.5 (340.0-600.0)	0.025
HLA-DRB1*15:01				0.007
Absence	52 (73.2)	27 (90.0)	25 (61.0)	
Presence	19 (26.8)	3 (10.0)	16 (39.0)	
Smoking				0.218
Never	28 (34.57)	14 (42.42)	14 (29.17)	
Ever	53 (65.43)	19 (57.58)	34 (70.83)	
Vitamin D				0.130
<20 ng/ml	13 (44.83)	2 (22.22)	11 (55.00)	
>20 ng/ml	16 (55.17)	7 (77.78)	9 (45.00)	

OND: other neurological disease individuals; MS: multiple sclerosis individuals. Categorical variables were shown as absolute and relative frequencies and their statistical differences were determined by Fisher's exact test. Continuous variables were presented by median and Q1-Q3: First quartile-Third quartile and their statistical differences were determined by Mann-Whitney U test.

Table 48. ebv-miR-BART7-3p expression in plasma samples of OND and MS individuals.

miRNA	Whole group (n=82)		OND (n=34)		MS (n=48)		<i>p</i> value
	Median	Q1-Q3	Median	Q1-Q3	Median	Q1-Q3	
ebv-BART7-3p	0.0001	0.0001-0.001	0.0003	0.00004-0.002	0.0001	0.0001-0.001	0.462

OND: other neurological disease, MS: multiple sclerosis, Q1-Q3: First quartile-Third quartile.

RESULTS

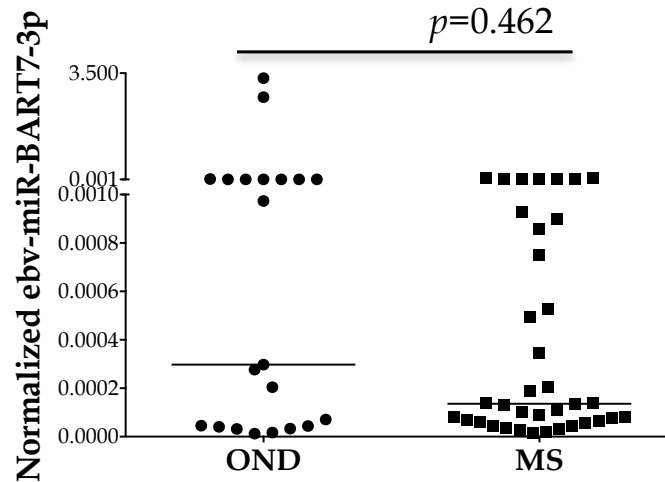


Figure 71. Normalized expression of ebv-miR-BART7-3p in plasma samples of OND and MS individuals. The line indicates the median and Mann-Whitney U test was used to determine statistical differences between groups.

MS group could be divided in two sub-groups: CIS or RRMS individuals. Surprisingly, when ebv-miR-BART7-3p normalized expression was compared between these two groups, almost a statistical significant overexpression in RRMS patients was observed (Median CIS=0.0001; Median RRMS=0.003; p value=0.053) (Figure 72).

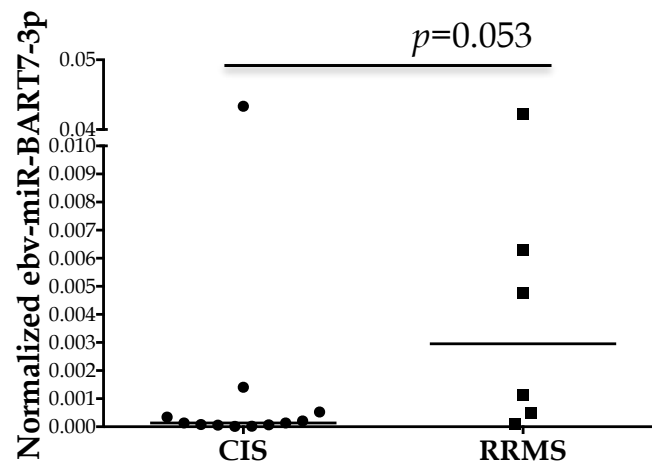


Figure 72. Normalized expression of ebv-miR-BART7-3p in plasma samples of CIS and RRMS individuals. The line indicates the median and Mann-Whitney U test was used to determine statistical differences between groups.

Although no differences were found in relapse occurrence after two years of receiving immunomodulator treatment between CIS and RRMS individuals ($p=0.643$), ebv-miR-BART7-3p expression was also upregulated in those MS individuals who suffered any relapse in two-year time frame since sampling ($p=0.002$) (Figure 73).

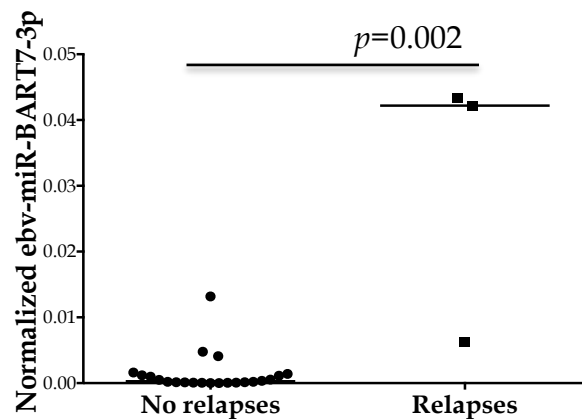


Figure 73. Normalized expression of ebv-miR-BART7-3p in plasma samples of MS individuals according to the absence or presence of relapses in the next two years. The line indicates the median and Mann-Whitney U test was used to determine statistical differences between groups.

Although sample size for either RRMS and presence of relapses are quite small, it would be worthy to analyze ebv-miR-BART7-3p expression in a bigger cohort with data concerning disease activity and progression.

4.7.4 Comparison of viral miRNA expression between MS patients and OND controls in a bigger cohort

In order to increase the number of individuals, more MS and OND samples were obtained from other units as Neurology department of Arnau de Vilanova University Hospital (Lleida, Spain) and Multiple Sclerosis Unit of Hospital Clínico San Carlos (Madrid, Spain) until reaching a total cohort of 130 individuals. As

RESULTS

previously observed, ebv-BART7-3p did not show any statistically significant difference between MS and OND individuals (Table 49).

Table 49. Differential expression of ebv-miR-BART7-3p in plasma samples of the validation cohort.

miRNA	Whole group (n=130)		OND (n=58)		MS (n=72)		p value
	Median	Q1-Q3	Median	Q1-Q3	Median	Q1-Q3	
ebv-miR-BART7-3p	0.001	0.0001-0.005	0.001	0.0001-0.004	0.0002	0.0001-0.005	0.412

OND: other neurological disease, MS: multiple sclerosis, Q1-Q3: First quartile-Third quartile.

Interestingly, when we analyzed ebv-BART7-3p expression in samples from Lleida and Madrid units separately, despite not reaching statistical significance, the expression is higher in MS group (Table 50 and Table 51).

Table 50. Differential expression of ebv-miR-BART7-3p in plasma samples of the cohort from Lleida.

miRNA	Whole group (n=24)		OND (n=12)		MS (n=12)		p value
	Median	Q1-Q3	Median	Q1-Q3	Median	Q1-Q3	
ebv-miR-BART7-3p	0.004	0.0002-0.012	0.002	0.0003-0.006	0.012	0.0002-0.015	0.240

OND: other neurological disease, MS: multiple sclerosis, Q1-Q3: First quartile-Third quartile.

Table 51. Differential expression of ebv-miR-BART7-3p in plasma samples of the cohort from Madrid.

miRNA	Whole group (n=24)		OND (n=12)		MS (n=12)		p value
	Median	Q1-Q3	Median	Q1-Q3	Median	Q1-Q3	
ebv-miR-BART7-3p	0.004	0.001-0.065	0.001	0.001-0.055	0.006	0.002-0.116	0.282

OND: other neurological disease, MS: multiple sclerosis, Q1-Q3: First quartile-Third quartile.

4.7.5 Summary

Only ebv-miR-BART7-3p could be detected in plasma samples from MS and OND individuals. There were no differential expression between MS and OND individuals in any of the studied cohorts. However, within MS group, ebv-miR-BART7-3p in plasma samples was upregulated in RRMS compared to CIS individuals and in those individuals who had suffered any relapse in two-year time frame since sampling.

5. Discussion

MS is a chronic complex neurological disease of the CNS characterized by the infiltration of inflammatory cells in the parenchyma, appearance of demyelination with various degrees of remyelination, gliosis and, axonal damage [2]. Whereas the most common phenotype, RRMS, is associated with an important inflammatory burden, 15% of individuals present PPMS, characterized by sterile-associated damage, demyelination and disability from the onset [11]. All current DMTs are focused on modulating the immune response and are only suitable for RRMS, showing little efficacy in PPMS, SPMS and later stages of RRMS [298]. Epigenetics is involved in the complex interaction between some genetic and environmental factors producing the pathology and the symptoms in MS [299]. miRNAs, small ncRNA molecules that participate in the regulation of gene expression, are one of these epigenetic mechanisms and due to their roles in processes such as inflammatory responses and myelination, several studies have been designed to analyze their capacity as disease biomarkers in biological fluids as serum or CSF [220].

In this doctoral thesis, specific miRNA signatures in different clinical and pre-clinical phenotypes of MS are described. Most of these studies have been performed profiling a high number of miRNAs in different biological fluids using OpenArray plates. Due to the lack of consensus in the way of analyze these data in CSF, the most appropriate strategy for this analysis has been first defined.

Regarding miRNA profiles, on one hand, we have focused on PPMS individuals. The observed miRNA deregulation in CSF and serum samples from patients and the association of MS clinical manifestations with *ex vivo* demyelinating models might be an interesting tool to further define the mechanisms involved in neurodegeneration that might be hidden in the more inflammatory clinical MS phenotypes.

On the other hand, circulating miRNA profiles in RIS individuals differentiating those who were finally converted to CDMS have been described. In addition,

DISCUSSION

despite the fact that most miRNA studies in MS have been carried out in RRMS, miRNA deregulation in this MS phenotype depending on different clinical variables has been analyzed to describe their potential role as informative factor or biomarker in the aggressiveness and/or activity of RRMS individuals.

Finally, the expression of virus-encoded miRNAs in plasma samples of RRMS and control subjects has been explored in order to clarify the epigenetic impact of EBV on the development of the disease.

5.1 DESCRIPTION OF A PANEL OF CSF-ENRICHED miRNA USEFUL TO STUDY NEUROLOGICAL DISEASES

CSF is a clear liquid located around and within the organs of the CNS and might be clinically examined through lumbar puncture to create a differential diagnosis as occurred in MS [117]. One of its essential functions is the maintenance of an appropriate chemical environment for neural tissue. As the interstitial fluid of CNS and CSF are in anatomic continuity, this valuable biofluid might mirror events of CNS [118]. In addition, CSF composition, mainly composed of water (99%) with 1% formed by proteins, ions, neurotransmitters or glucose [122], is controlled by the interfaces BBB, BCSFB and, CSF brain barrier that provide a relatively stable environment unlike blood [118]. Even though it is a sample that is obtained through a more invasive technique, it might be very useful for studying the pathogenic mechanisms of neurological diseases as it is a relatively cell- and microorganism-free fluid [300].

miRNAs have been detected in different biological fluids as plasma, serum or CSF, where they remain highly stable unlike what happens with cellular miRNAs [205]. For this reason, circulating miRNA profiles have been widely studied in different conditions to exploit their potential as biomarkers. However, since 2012 when the first study describing CSF miRNAs in MS was published [240], only 11 works have been focused on this topic, which shows the research deficiencies existing in this

scope. Only four studies have described CSF miRNA profiles in MS [133,240–242], whereas the other have analyzed specific miRNA expression levels. However, all these profiling studies have used pre-configured miRNA detection platforms, frequently used in studies involving other biological material. miRNAs might present different levels of expression and their composition can vary between tissues and biofluids [287] and CSF contains lower levels of miRNA than serum or plasma [301]. For this reason, firstly it is necessary to analyze and study CSF miRNA profiles to design specific platforms that allow us to extract all the informative potential that CSF could offer.

CSF miRNA levels using TaqMan Advanced miRNA technology from Applied Biosystems was analyzed for the first time in order to design CSF-enriched miRNA panels. On the one hand, the protocol established by the manufacturer should be modified to increase the yield of miRNA quantification in CSF samples. On this occasion, preamplification cycles were increased to 22 cycles, which is not surprising since preamp step is usually mandatory before qPCR reaction when analytical sensitivity is the utmost importance and/or the sample is limiting, as happens with CSF [276]. On the other hand, it was verified that detectable miRNA in CSF samples was lower than the content found in other biofluids as serum [301].

Wang *et al.* defined a specific CSF-miRNA panel to be used in the study of Alzheimer's disease in 2017 [302]. They customized TaqMan Low-Density Array (TLDA) panels containing 47 miRNAs. TLDA's function as an array of reaction wells for a PCR step, where each well is pre-loaded with a TaqMan expression assay that detects the amplification of the specific target [303]. However, as it was explained in Results Section, up to 79 miRNAs were detected in our studied cohort. Therefore, to customize OpenArray plates targeting 216 miRNAs using the new TaqMan Advanced miRNA technology was chosen. Firstly, the utilization of OpenArray instead of TLDA's brings the efficient advantage of analyzing a bigger number of samples in a shorter period of time [304]. Secondly, this new TaqMan Advanced miRNA technology allows a more universal and specific detection of

DISCUSSION

miRNA [305], which encourages to use the new available and developed methodologies.

The performance of these cc-OA plates was tested in order to determine their suitability to be used in reliable measurement of CSF miRNAs. There are few studies focused in analyzing reproducibility and performance in miRNA detection by high-throughput platforms. Farr *et al.* compared the detection of cellular and circulating miRNAs (human islets and serum samples, respectively) in different qPCR platforms [304]. They observed positive correlation between individual qPCR and OpenArray Cq values, as we did observe, supporting the idea that OpenArray system produced reproducible results. They also showed the increase of replicate measurements variability as miRNA abundance decreased (higher Cq values) in OpenArray. Whereas it is known that cellular and serum miRNA contents are quite abundant compared to the one in CSF [301], it was not possible to make this analysis as all obtained Cq values were comprised within a narrow Cq interval. Instead, quality of amplification curves, defined by Amp Score and Cq confidence values, were related to the detectability category of each miRNA and the fact of proceeding to further analyses with those miRNAs detected in at least 70% of studied samples would imply the use of qPCR data with good quality curves.

From the eight most abundant miRNAs found in the studied CSF cohorts, only two of them (miR-204-5p and miR-451a) were included in the panel described by Wang *et al* [302], while other six (miR-145-5p, miR-26b-5p, miR-335-5p, miR-450b-3p, miR-770-5p and miR-939-5p) were not analyzed. All of them were included in the cc-OA panels because they were detected in a pilot study made to establish CSF miRNA detection with fc-OA plates. In addition, except for miR-450b-3p, miR-770-5p and miR-939-5p, the other five miRNAs were detected in other miRNAs studies carried out with human CSF MS samples performed in TLDA [133,241]. Regarding differential miRNA expression related to MS, miR-145 has been found deregulated in MS several studies differentiating patients from healthy individuals

and monitoring response to IFN therapy [255,306]. Søndergaard *et al.* described miR-145 upregulation and miR-939 downregulation among others in plasma of MS patients [272]. Another study made by Magner *et al.* found increased levels of miR-145-5p and diminished expression of miR-451a in leukocytes of untreated RRMS patients compared to healthy controls [307]. Differential expression of exosomal miR-451a in relation to controls was found in serum of RRMS in another study [247]. Although miR-204-5p, miR-26b-5p, miR-770-5p and miR-939-5p could be found in brain and spinal cord tissue as established in the Human miRNA tissue atlas [287], only miR-335-3p has been titled as a brain-enriched miRNA involved in aging and age-related neurological diseases [308,309].

An essential step in qPCR experiments is the normalization procedure, which enables to control variations in extraction and RT yield, efficiency of amplification. It is required before any comparison in miRNA concentrations between different samples and biological groups is performed [277]. The search of candidate EN miRNAs is necessary for later studies [278]. In this doctoral thesis, three different methods have been used in CSF samples. The NormFinder approach calculates the stability based on the intergroup and intragroup variation; the GeNorm algorithm ranks genes based on pairwise correlation and CV analysis calculates the variance of a miRNA across all samples taken together [310]. Positive correlation among these three methods in both studied cohorts was observed, as previously found by Chan *et al.* [311]. For that reason, SSS as proposed by Marabita *et al.* was calculated in order to summarize all this information [278].

miR-23a-3p, miR-26b-5p, miR-125a-5p, miR-335-5p and miR-92b-3p were proposed as the most stable miRNAs in CSF samples. Although miR-23a-3p might have been proposed as an optimal reference miRNA in cervical tissue [312], it has also been found involved in some aspects related to melanoma growth and progression [313]. This reinforces the necessity of experimental validation of any endogenous miRNAs as normalizers for particular tissues, cell types or biofluids and specific experimental designs [314]. Some miRNAs previously used as EN in CSF are miR-

DISCUSSION

24 [315], miR-17 [133] or, miR-320a [316]. In addition, although the preferred method for normalization of individual qPCR data is the utilization of a minimum of two endogenous reference miRNAs [317], the analysis determined that eight EN miRNAs are the optimum number for CSF samples.

As the interest in high-throughput platforms is highly manifest in the field of miRNA biomarkers [304], a panel of CSF-enriched miRNAs was presented and a set of endogenous controls to be used in neurological diseases as MS was proposed. However, redefining the format by reducing the number of assays as not all the miRNAs available in the cc-OA plates were detected might be a future prospect.

5.2 CHOICE OF A SUITABLE FLOWCHART TO ANALYZE OpenArray miRNA DATA IN CSF SAMPLES

The results obtained in different miRNA studies performed in MS might be disparate and even contradictory. These discrepancies might be due to the diverse employed methods but also to the heterogeneity and variability of clinical forms [151]. For this reason, it is always vitally important to clarify the study design, the methodology used and the type of samples and cohorts. Although guidelines to better use and present qPCR experimental data have been published in order to unify methodologies and increase agreements between studies [277] and new pipelines to improve performance of qPCR experiments detecting circulating miRNAs have been proposed [290], a special attention should be given to CSF studies. As already commented, CSF is a really valuable biofluid for research in neurological disorders and its miRNA content is much lower than the one found in other biofluids [318].

Until now, there are only three published studies that have used OpenArray plates to profile CSF miRNA signatures in different conditions and, none of them were carried out in MS or used the new Taqman Advanced technology, as done in this

doctoral thesis. It is striking that being such a low number of studies, there are some analytical discrepancies among them. OpenArray platforms show remarkable sensitivity to analysis considerations [319]. The first study was carried out by Denk *et al.* in 2015 to study Alzheimer's disease and they established the Cq cut-off in 34 and used the "measure of relevance" method to study differential expression of miRNAs in CSF [320]. The other two existing studies employed quite similar strategies although some subtle differences could be observed. The first one, whose aim was finding CSF biomarkers for glioblastoma, established the cut-off for Cq in 35 and employed GN using the arithmetic mean of miRNA values [321]. The other study, focused on temporal lobe epilepsy, also used a cut-off of 35 and GN but, this time, the geometric mean was used. In addition, they paid special attention to filtering data according to Amp Score and Cq Confidence values to ensure good quality Cq values [322]. However, none of them have referred to use specially designed analysis methods to yield the maximum and optimum information in CSF miRNA studies. One thing is clear, the use of 35 as cut-off is justified to obtain the maximum number of detected miRNAs as it could be observed in the previously mentioned CSF OpenArray studies, despite the recommendation of removing Cq values >28 by manufacturer to avoid stochastic results [323].

Therefore, the aim of this part was to describe the most suitable way to analyze data from TaqMan OpenArray Human Advanced microRNA panels in CSF samples before using them to further analyze MS samples. This was made by comparing the performance of different proposed methods in handling technical replicates, selecting curve quality conditions, handling missing data and selecting normalization method. Using that, the best approach to maximize the potential of CSF miRNA profiling studies was suggested.

Profiling miRNA studies using high-throughput platforms are not usually conducted in replicates due to the increased cost of the procedure and triplicates are reserved to posterior individual qPCR reactions in the validation phase [290].

DISCUSSION

However, the opportunity of running three measurements for the same sample in OpenArray was feasible in this doctoral thesis. As CSF presents higher Cq values than serum and replicate measurements variability in OpenArray increases with higher Cq values [304], one aim was to compare different acceptable Cq ranges for replicates measurements from a non-strict method to the recently calculated Cq range by de Ronde *et al.* A method including two different ranges depending on the Cq values of replicates was added, which was finally selected as it offered more analyzable miRNAs with low variability. This led us to the question of choosing whether to use replicas or not. We could observe that RQ distributions remained mostly homogenous between individual miRNA datasets and triplicates data, despite the discrepancy in significant differences. OpenArray is a platform that displays more biological than technical variability [319]. This highlights the need of posterior validation phases to assess statistical significance as variation in data from multiple biological replicates might not result in significant differences [324]. Sufficient number of samples in further validation cohorts might allow smaller experimental differences to be distinguishable, increasing the statistical significance of the experiment [277]. Running each CSF sample per triplicate in OpenArray plates during profiling phases would offer a wider and more robust range of data, despite not getting the statistical significance that needs to be required in validation phases.

Although it would be desirable to obtain a higher number of miRNAs to work with, there is evidence that CSF contains less number of miRNAs and in less quantity than other biofluids as serum or even tears [318]. As the same comparisons applied in CSF samples along the study were performed with serum samples, the different nature and characteristics of both biofluids in terms of miRNA content could be confirmed [301,318]. This was reflected in the fact that when analyzing quality and reliability of Cq curves, there were disagreement in miRNA detectability categories between methods in CSF datasets, what led us to choose a non-strict method. However, serum dataset did not differ in detectability

frequency among methods probably due to the high number of detectable miRNAs in serum that barely changed when shifting quality conditions. Furthermore, when comparing miRNA detectability frequency, it was observed that CSF dataset did not follow the distribution observed in serum samples.

High-throughput platforms as OpenArray might often offer data with some missing values that could be generated from technical factors other than biological reasons [278]. Regarding missing data, there is no consensus in qPCR studies and different approaches are used. Some studies support the need of these values to be properly imputed [325]. On one hand, Ronde *et al.* suggested a method combining multiple imputation and highest detected Cq value to handle missing data when analysing circulating miRNAs, showing the best accuracy in detecting a specific condition. However, their study was focused on plasma samples and differences in biological biofluids have been already demonstrated. On the other hand, a study performed by McCall *et al.* compared different methods of treating missing data and concluded that treating non-detects as missing data reduced bias whereas substituting missing data with the maximum PCR cycle introduces a great bias [326]. Three different approaches were compared and it was found that for CSF samples the best option is not replacing missing values at all.

An essential step in qPCR experiments is the normalization procedure, required before any comparison in miRNA concentrations between different samples and biological groups is performed [277]. It enables to control variations due to technical factors (sample collection and storage, miRNA extraction, miRNA quantification) and biological factors (amount of miRNAs, secretion intensity into body fluids, miRNA stability) [327]. GN is one of the normalization approaches that could be employed in large scale experiments such as OpenArray plates and it involves the mean expression value of all miRNAs [278,328]. Other normalization procedures as QN or RIN have also shown their robustness [329]. QN aim is to distribute the probe intensities for each array in a whole set equal [330]. RIN method tries to identify invariant miRNAs using the whole dataset [279]. In this

DISCUSSION

case, GN method presented less miRNA variability for CSF samples whereas the best choice for serum datasets was QN.

Finally, the reproducibility of the outcome of individual and triplicate plates was evaluated in section 4.2.7 and it should be highlighted the repeated observed tendency to have increased levels of miR-150-5p in CSF samples of RRMS. This is important as it would validate previous results from our group and other studies, which previously indicated elevated levels of this specific miRNAs in RRMS individuals [133,241]. Interestingly, this miRNA presents different patterns of expression between immune cells and biofluids, which might suggest its potential role in MS by supporting cell-to-cell communication [151].

In conclusion, a specific way to analyze CSF miRNA data to maximize the information obtained in OpenArray screening experiments has been proposed. The different nature of CSF, highlighting variations in miRNA content and quantity when compared with other biological fluid as serum was corroborated. The use of triplicates when possible is further encouraged, to maximize results on biological replicates and support the need of future validation phases in bigger cohorts.

5.3 STUDY OF THE CIRCULATING miRNA PROFILES IN PPMS PATIENTS

PPMS phenotype, characterized by sterile-associated damage, demyelination and disability from the onset, is presented by 15% of MS individuals [2]. Even if the pathological mechanisms causing tissue damage in both RRMS and PPMS overlap, some characteristics differ enormously. While focal inflammatory lesions with accumulation of T and B cells and BBB leakage is the main pathologic indicator of RRMS, the gradual accumulation of disability characteristic of PPMS individuals might be the result of diffuse immune mechanisms and neurodegeneration [87]. All current DMTs are largely only suitable for RRMS as they decrease relapse frequency and new lesions formation in MRI. They show little efficacy in PPMS, SPMS and later stages of RRMS and might have potentially serious side-effects. In

addition, DMTs are unable to prevent the progressive accumulation of permanent disability from neuronal damage and to induce neurorepair [331].

Deregulation of miRNAs has been observed in different inflammatory and degenerative neurologic diseases such as MS [332,333]. Due to their stability in different biological fluids and the fact that miRNA changes might be detected prior to their functional effect on protein expression, circulating miRNAs are considered promising valuable diagnostic and prognostic biomarkers [300]. It has been proposed a possible role of circulating miRNAs in cell-to-cell communication, so their function beyond biomarker is been examined [334].

Since Haghikia *et al.* published the first analysis of circulating miRNAs in the CSF of MS patients [240], a total of 11 MS studies studying miRNA expression in CSF samples have been reported. Four of them carried out a preliminary screening phase using high-throughput platforms as TLDA [133,241] or arrays [240,242], whereas the rest only analyzed the expression of specific individuals miRNAs. Three studies used CSF samples from PPMS and, while two of them only analyzed specific miRNAs [244,259], Haghikia *et al.* could not find any statistical change in PPMS probably due to the small size of the cohort (n=6) [240]. However, none of these CSF MS studies aimed to specifically uncover miRNA signatures in PPMS individuals. Therefore, we aimed to characterize for the first time a specific miRNA profile of PPMS patients compared to OND and RRMS in both CSF and serum samples using the cc-OA and fc-OA plates, respectively. A validation of the results obtained in this screening phase was further performed in a bigger cohort of samples by means of individual qPCR.

Some statistical significant differences in some clinical and radiological variables were observed. First, although we tried to match samples of similar ages among the three studied groups in screening phase, when increasing the cohort for the validation phase, RRMS group was statistically younger than PPMS and OND. It has already been established that the age at onset in PPMS is higher than the one

DISCUSSION

observed in RRMS [2]. For this reason, at least, we tried to get an OND cohort comparable to PPMS in terms of age to be able to avoid possible miRNA regulation due to aging. Second, EDSS was also found increased in PPMS. It has been described that PPMS might carry a worse prognosis than RRMS or SPMS [335], so this EDSS difference was expected. In addition, the probability of reaching EDSS of 3 or 4 was significantly influenced by the clinical phenotype, with PPMS patients reaching higher values earlier as observed in a comparative study between RRMS, SPMS and PPMS [336]. Third, PPMS group also presented a lower number of Gd+ lesions in MRI than RRMS. Disease activity in MS has been strongly associated with Gd+ lesions [337] and PPMS have a low rate of new lesion formation and the frequency of Gd+ lesions is usually less than the described in other MS phenotypes [338,339].

In this study, let-7b-5p and miR-143-3p were found downregulated in CSF samples of PPMS compared to OND. let-7b-5p has been previously found upregulated in peripheral blood of paediatric MS cases compared to healthy controls [340] and its expression changes during IFN treatment [341]. Regarding miR-143-3p, it was found downregulated in different studies focused on MS. First, its downregulation was evident in astrocytes from WM and active GM lesions [342]. In addition, decreased levels in CSF were also found in MS patients compared to controls in the profiling phase of a previous study of our group [133]. We couldn't find deregulated miRNAs that differentiate PPMS group from both RRMS and OND. On the contrary, miR-20a-5p and miR-320b in serum might assume that role as their levels were increased and decreased in PPMS, respectively. In addition, other changes in serum samples were observed in this study as miR-26a-5p levels were downregulated in PPMS versus RRMS whereas miR-142-5p was found upregulated in RRMS against OND.

There are two published studies whose aims were to associate miRNA expression in serum samples with MRI measures and phenotypes in MS [264,266]. Correlations between miR-142-5p, miR-148a-3p, miR-320b and miR-421 and

number of T2 lesions and/or Gd+ lesions have been also described. Only miR-142-5p levels were found associated with some radiological measure, T1:T2 ratio, in Regev's study [266].

PPMS could be further sub-classified into inflammatory or non-inflammatory according to clinical relapse or radiological activity (existence of Gd+ lesions or increased number of T2 lesions in follow-up MRIs) [80]. Using the PPMS cohort, miRNA profiles depending on this activity or not-activity were further studied filtering individuals according to radiological data and/or the presence of LS_OCMB. This last characteristic was included as LS_OCMB has been identified as a molecular marker of patients with worse disease courses [133,134]. miR-92b-3p showed a tendency to be upregulated in CSF and miR-103a-2-5p was downregulated in serum samples of inflammatory PPMS individuals.

In conclusion, this is the first study focused on describing miRNA profiles in CSF of PPMS individuals showing that let-7b-5p and miR-143-3p might differentiate PPMS from OND. In addition, other deregulated miRNAs in serum and according to the inflammatory status of PPMS have been proposed. The fact that the validation cohort of this study comprised samples coming from three different centers that strengthened the results with a global character should be highlighted. However, there are some limitations in our study. First, we were unable to find a CSF miRNA that distinguished PPMS from OND and RRMS. This might be due to the differences in age in this last group. Sample size should be increased and some other potential miRNAs should be analyzed in order to find one. Second, total RNA extracted from cell-free CSF was analyzed in this study instead of focusing in exosomes, small vesicles containing miRNAs that might provide information about their cellular origin [220]. It would be interesting to isolate exosomes in further studies and compare their miRNA content with these results. In addition, the inclusion of longitudinal samples of these PPMS individuals and RRMS, which some might have shifted to SPMS, would be a really enriching incorporation as valuable epigenetic information might be obtained regarding progression and

DISCUSSION

differences in subclinical forms. Despite the mentioned deficiencies, let-7b-3p and miR-143-3p are firm candidates to be studied in future works to unravel their potential biological role in PPMS.

5.4 RELATION OF THE CSF miRNA PROFILE OF MS INDIVIDUALS WITH THE miRNA SIGNATURE DURING DEMYELINATION AND REMYELINATION IN CEREBELLAR ORGANOTYPIC CULTURE MODEL

Primary demyelination, characterized by injury, breakdown and loss of myelin sheaths, is a pathological indicator, which distinguishes MS from other CNS diseases [79]. Demyelinated lesions can be partly or completely repaired by remyelination, although these processes are often disrupted in MS [343]. As mentioned before, all current DMTs are focused on modulating the immune response and are unable to prevent the accumulation of disability from neuronal damage and to induce neurorepair [331]. The study of remyelination, including elements that could act as inhibitors or accelerators, is important to develop new therapies [100]. The specific potential role of miRNAs in each cell type involved in the remyelination process has been recently discussed [343].

It is suggested that non-inflammatory forms of PPMS could reflect the primary disease process of MS without being masked by inflammatory reactions [331]. The use of *in vitro* and *ex vivo* models that accurately reflect the neurodegenerative event *per se* is vital to dissociate the demyelinating event from the complexities introduced by inflammatory mechanisms, as it could happen with some animal models as EAE [331]. Murine *ex vivo* organotypic brain culture is a model that mimicks the initial demyelinating event observed in PPMS, using sterile damage induced by LPC and independent of an inflammatory insult. Importantly, these cultures can be used to assess how the brain endogenously remyelinate after such insults and/or used to investigate therapeutic agents that can enhance and promote neurorepair [273].

In this doctoral thesis, a preliminary miRNA analysis in murine *ex vivo* organotypic brain culture during demyelination and remyelination and miRNA data from CSF of SAS, non-inflammatory PPMS and RRMS individuals were combined for the first time, joining basic research and clinical observations in order to move along in the knowledge of these processes

First, a comparative analysis of miRNA expression levels in murine organotypic tissue was made among the different conditions that the culture went through: normal myelination, demyelination after LPC insult and remyelination. We are really aware of the preliminary nature of this study but some interesting results could be observed as some deregulated miRNAs such as miR-142-3p, miR-143-3p, miR-146a-5p, miR-21-5p, miR-25-3p, miR-219a-5p or miR-335-5p have been previously found deregulated in MS brain lesions from patients [238,295,344,345]. Specifically, miR-219a-5p, which was upregulated in remyelination *vs* normal myelination, plays critical roles in oligodendrocyte precursor cells differentiation and remyelination [343], its delivery via extracellular vesicles has been proposed as a promising strategy to induce remyelination [346] and the use of miR-219a mimics has enhanced myelin restoration in MS animal models [346,347].

Second, as we searched for a miRNA reflecting the mechanism of MS pathology, the use of SAS as a control group to be compared with non-inflammatory PPMS and RRMS supposed an innovative approach to characterize the signature of demyelinating events [348]. Thus the deregulation of miR-320a and miR-1260a was observed. On the one hand, miR-320a, whose levels were increased in MS subjects, has been also found upregulated in active lesions and normal appearing WM [295,345]. In other biological material as B cells of MS individuals, its levels were decreased and its potential role in increasing BBB permeability and neurological disability has been proposed [349]. Another study remarked its deregulation between MS and healthy individuals [250]. On the other hand, miR-1260a has been found deregulated in inactive MS lesions and in GM subpial and leucocortical MS lesions [238].

DISCUSSION

Finally, the cross-analysis between *ex vivo* cultures and human CSF samples yielded some interesting results as it highlighted some miRNAs as miR-143-3p, miR-145-5p or miR-21-5p. miR-143-3p was one miRNA extremely highlighted all along this preliminary study. It was downregulated in tissue during remyelination and increased in RRMS group when compared with SAS individuals. Interestingly, miR-143-3p was one of the miRNAs that presented statistically decreased levels in CSF of PPMS vs OND in the previous study and has been found downregulated in different studies focused on MS as in astrocytes from WM and active GM lesions [342] and in CSF of RRMS patients [133]. Despite some discrepancies in the direction of the deregulation that might be due to the different source of miRNAs and diverse MS groups, this miRNA could be postulated to be further investigated in MS studies. Another interesting miRNA that should be mentioned is miR-21-5p as its levels were increased during demyelination and remyelination. Although statistical significant differences were not found in human samples analysis, Venn diagrams showed overlapping of increased levels in human samples and tissue. Increased levels of miR-21-5p in CSF of RRMS with Gd+lesions was also found and its role modulating T cell activation and apoptosis, Treg function and development, or Th17 differentiation has been described [350]. miR-145-5p, found upregulated in RRMS, showed overlapping enhanced levels between human CSF samples and tissue only during demyelination as its expression decreased in remyelination. Its increased levels have been described in different studies and biological materials: plasma [255,272] and leukocytes [307] and it might be used for monitoring the patients response to interferon- β therapy [306].

In conclusion, the comparative analysis between *ex vivo* models and human CSF samples might be a valuable approach to connect clinical and basic knowledge about miRNAs involved in demyelination, remyelination and neurorepair. Remyelination-promoting studies are usually restricted to studying remyelination and the miRNA analysis during demyelination allows to use the data as a continuum myelin break-down and repair as observed in the majority of MS

lesions and suggest potential remyelinating interventions taking into account the entire frame [87]. Despite the extremely preliminary nature of this study, its results might be interesting and worthy to replicate.

5.5 STUDY OF THE CIRCULATING miRNA SIGNATURE IN RIS INDIVIDUALS

Since 2009, when the term RIS was first introduced by Okuda [83], most of the studies have focused on describing risk factors associated with the clinical conversion to CDMS. Some other studies have analyzed other clinical parameters and biological molecules like OCGB, NF-L, CHI3L1 or progranulin [85,351,352] in order to establish predictor biomarkers of clinical conversion in RIS subjects. However, none of them has been focused on the miRNA profile when RIS diagnosis is established comparing between individuals who remain as RIS or finally convert to CDMS. The study presented herein brings in a differential circulating miRNA signature in those two groups, and describes some already established risk factors and predictor biomarkers of conversion in our cohort.

Some previous described risk factors for clinical conversion from RIS individuals into CDMS [351] did not show significant differences in this study. However, some aspects related to radiological, clinical and biochemical parameters should be highlighted. The number of T2 lesions was significantly increased in RIS-Conversion subjects compared to RIS-RIS group, and the presence of black holes might seem to be characteristic in those individuals who converted to CDMS. Despite being asymptomatic individuals, RIS-RIS group presented EDSS score above zero as observed in other studies in some individuals in the moment of RIS diagnosis [86,352]. In addition, the results presented in this study did not validate the role of NF-L and OCGB as predictors for RIS conversion [85], despite markedly showing the expected trend, probably due to the small size of the studied cohort.

DISCUSSION

Regarding circulating miRNA profiles, we have described deregulation of miR-144-3p, miR-448 and miR-653-3p in CSF samples, whereas miR-142-3p, miR-338-3p, miR-363-3p, miR-374b-5p, miR-424-5p and miR-483-3p levels were found deregulated in plasma. Due to the lack of a common and solid way of normalization as one of the most important limitation in this kind of studies [278], two different normalization strategies were used when analyzing plasma samples, as previously made by Wang-Renault et al [353] to strongly define a specific miRNA signature in this biological fluid. Some of the miRNAs found deregulated, according to the conversion status of RIS individuals, had been previously described in some MS studies or in the context of remyelination processes. miR-448 had been previously found upregulated in PBMCs and CSF of MS patients [261]. miR-338-3p is downregulated in inactive MS lesions [295] and involved in remyelination processes [347]. miR-363-3p also showed decreased levels in MS patients in several studies involving PBMCs and B lymphocytes [35,354,355]. However, miR-142-3p was upregulated in PBMCs of RRMS compared to healthy controls [356,357]. Although this deregulation is opposed to the one we found in plasma samples, this variation might be explained by the different source of biological material employed in the studies, as miRNAs can present different patterns of expression between tissues and biofluids [287,301]. This fact highlights the importance of studying miRNAs in specific cell types or biofluids to try to uncover the complex interactions between tissues.

Although the use of circulating miRNAs as biomarkers should not be confused with their potential regulatory functions inside the cells, the existing data provide the rationale for looking at the functionality of selected miRNAs. On the one hand, circulating miRNAs, specially those secreted in extracellular vesicles, might mediate communication between different tissues, regulating mRNA and protein expression in distal cells [358]. On the other hand, exosomes might be influenced by the tissue of origin and their effects in receptor cells might play an important role in different pathological conditions [220]. In this case, CSF, which is in direct

contact with the extracellular space of the brain, might mirror biochemical changes affecting the brain [359].

For these reasons, the functional roles of these deregulated miRNAs *in silico* was investigated. It has been suggested that RIS subjects could present a more beneficial response to the demyelinating insult than RRMS individuals and, an exceptional ability to repair this demyelinating event [360]. However, not all RIS subjects will develop a symptomatic demyelinating event and evolve toward CDMS [84]. Deregulated miRNA identified in this study are involved in different biological processes and pathways and it would be interesting studying their possible role in the clinical conversion process, beyond their possible prognostic role.

Some parts of miRNA fraction in biofluids could also be released due to the passive leakage of apoptosis or necrosis [216]. Different repositories containing expression profiles of miRNAs in tissue, primary cells and biofluids are available [287–289]. This information might be valuable in directing future studies towards specific cell lines or tissues as well as in confirming the presence of a certain miRNA in a biological fluid. Most of deregulated miRNAs in our study can be found in different types of immune cells such as natural killer, T and B cells whose roles in MS pathogenesis have been previously reported [361]. In addition, miR-338-3p and miR-374b-5p, two miRNAs deregulated in plasma samples, are highly expressed in brain [287]. These findings along with the target and pathway analyses previously discussed support the idea of directing future research towards a deeper knowledge of miRNA functionality.

This study has some limitations. The most important one is the small size of the studied cohort due to the limited number of RIS patients available at our centre. To partially counteract this, replicate measurements for miRNA analysis were used trying to increase accuracy and reduce technical variations in the process and employed two different normalization strategies in plasma samples data.

DISCUSSION

In conclusion, this exploratory study reports a signature pattern of circulating miRNAs in RIS individuals, differentiating those who finally converted to CDMS from those who remained as RIS. The preliminary results presented herein should be validated in independent and larger cohorts. In spite of not reaching statistical significance, the presence of black holes is proposed to be studied in future studies to confirm its prognostic role in conversion to MS in RIS individuals.

5.6 STUDY OF CIRCULATING miRNA PROFILES IN CSF OF RRMS PATIENTS

RRMS, initially diagnosed in 85% of MS patients, is the most common clinical phenotype and is associated with an inflammatory burden [362]. All current DMTs are mainly focused on modulating this immune response, which leads to a reduction on relapse frequency and new T2 MRI lesions [331]. At the same time, most of miRNA studies in MS have been carried out in this clinical phenotype [151]. However, miRNAs could be useful for more than just diagnosis and new questions regarding miRNAs and RRMS were explored in this doctoral thesis.

5.6.1 Comparison of CSF miRNA profiles in MS patients according to their ethnic origin

MS is a disease with a global distribution that presents a variable prevalence depending on the geographical areas. It has been established that there is a clear North-South gradient as the prevalence seems to increase with the distance from the equator [10]. While MS prevalence in Spain is 120 per 100,000 inhabitants, nearby countries from North-Africa as Morocco, Algeria or Tunisia present lower prevalences (20, 35 and 20 per 100,000 inhabitants, respectively) according to the Atlas of MS 2020 [5]. Therefore, MS prevalence has been reported to differ depending on race and ethnicity. However, some studies performed in America have shown that some minority populations have a higher incidence of MS and a more severe disease course compared with their ancestral countries of origin.

[363,364]. These differences might be due to environmental, genetic or, socioeconomic and cultural factors [365]. In addition, it is believed that age of migration could be also decisive in this regard [366].

Moving to Europe, there are three studies that should be highlighted. The first one was developed by Berg-Hansen *et al.* in Norway and it found that descendants from Pakistan immigrants presented an incidence rate similar to the one described in Norwegian population compared to their parents whose incidence was lower, which suggests that the early exposure to an environment might play a role in the risk of MS [367]. Sidhom *et al.* identified a remarked severity of the disease in NAs living in France, especially for the second generation [294]. However, another study carried out in France established that NA immigrants have a higher risk of disability than Europeans and NAs of second generation. This discrepancy was attributed to a small sample size and/or a biased cohorts of patients with more aggressive MS [368].

Some studies have suggested the role of miRNAs as epigenetic mechanisms to cause population differences observed for complex traits [369]. Some mRNA-miRNA pairs have been highlighted as differentially expressed by race in some conditions such as female hypertension [370]. For this reason, we proposed to analyze profile of circulating CSF miRNAs among individuals with RRMS based on their ethnic origin.

First, our studied cohort was divided in two sub-cohorts depending on their ethnic origin without taking into account the birth place. Regarding clinical variables, MS-NA presented a tendency to have higher number of T2 lesions in MRI than MS-E as well as increased levels of IgG anti-CMV. The presence of a high T2 lesion load have been recognized as early predictors for disease progression [371]. Although there are some inconsistencies regarding to the role of CMV infection in MS risk, some studies suggest that lower rates of CMV are linked to an increased MS risk. In this case, the increased levels of IgG anti-CMV in NA individuals was

DISCUSSION

observed, which presented more aggressive disease courses. However, other studies of CMV seropositive in multi-ethnic populations only found association of CMV and MS risk in Hispanics [372], what reinforces the need of further studies in this scope. Statistically significant lower levels of vitamin D were found in NA subjects, what might partly support this greater disease aggressiveness observed in NA individuals, as low vitamin D levels have been related to increased MS risk [38].

Second, miRNA differential expression profile between the two studied groups showed that miR-335-5p and miR-653-3p were statistically overexpressed in MS-NA compared to MS-E. Furthermore, miR-143-3p and miR-20a-5p presented a tendency to be downregulated and upregulated in MS-NA, respectively. In addition, miR-142-3p and miR-451a levels in CSF correlated with the number of T2 lesions, miR-143-3p and miR-335-5p with levels of vitamin D and, miR-21-5p levels were positively associated with EDSS.

As it has been claimed that people who migrate after a critical age (15 years old) are less susceptible to the new environmental risk factors for MS existing in the new location [373], another analysis sub-classifying MS-NA depending on their age at migration was performed. Interestingly, MS-NA (<15) presented a tendency to have higher number of Gd⁺ lesions in MRI than MS-NA (>15) that would agree with the remarked severity of MS observed for the second generation of NAs living in France [294]. miRNA analysis revealed that miR-145-5p, miR-150-5p, miR-335-5p and miR-653-3p showed significant differences among some of the three groups. Specifically, it should be highlighted that miR-150-5p showed statistically lower levels in MS-NA individuals who migrated older than 15 years old whereas its expression in the other two groups was similar between them. This miRNA has been previously related to MS in CSF [133,241] and its key role in modulating inflammatory responses has been widely recognized [374].

In conclusion, these results are the first description of miRNA signatures in CSF of RRMS individuals depending on their ethnic origin. However, there are some

important deficiencies in this study. This is a preliminary study consisting in a miRNA screening phase in small number of samples, especially in MS-NA sub-analysis. Further studies are needed to validate these results in a bigger cohort. It would be interesting to add more clinical, radiological, biochemical and genetic data as well as longitudinal samples to evaluate the epigenetic changes.

5.6.2 Comparison of CSF miRNA profiles in RRMS patients depending on age at disease onset

The average age of onset for RRMS is 32 years old [293]. However, individuals with early and late MS onset could be also diagnosed and each subgroup might present distinct features and characteristics that should be taken into account in their treatment [13]. Aging might be considered a risk factor for MS progression. Regarding the ability of remyelination, age has been proved to diminish this natural capability [14] and individuals of early onset are characterized by a slower rate of disease progression as they presented more plasticity to recover lesions in CNS [375]. In addition, late onset in RMMS has been associated with an earlier conversion to SPMS [376].

Aging not only affects the plasticity of CNS to remyelinate existing demyelinating lesions but also some changes in the immune system have been related to age [15]. There is no need to remark that RRMS presents a really important inflammatory aspect causing the relapses that are characterized by an infiltration of peripheral immune cells into CNS [377]. A phenomenon known as “immunosenescence” describes the changes observed in the immune system during the course of normal human aging. This functional decline and remodeling in cellular immune subsets might have significant impacts on the course of neuro-inflammatory conditions such as MS [378].

Different studies have proved the key role of miRNAs in regulating immune responses and processes and, interestingly, some of these miRNA expression

DISCUSSION

might be modulated during aging [379]. For this reason, the existence of a differential profile of circulating CSF miRNAs between individuals with RRMS depending on the age of disease onset was studied.

Our first approach was to compare miRNA levels among three categories depending on the age at RRMS onset: early (<25), normal (25-35) and late onset (>45). Unfortunately, this first approach did not yield promising results. Only let-7c-5p showed a tendency to be deregulated in some of the groups. let-7c-5p has been previously related to MS as it was found upregulated in inactive MS lesions [295]. An analysis to determine tissue and primary cells where this miRNA is expressed [287,288] was performed and it showed that let-7c-5p might be highly found in brain, spinal cord and neuronal stem cells, what makes its detection in CSF feasible. These results might suggest that there are no differentiated altered pathways among patients with early, normal or late MS onset.

miRNA signatures in extreme and opposed early and late onset were further compared, as they are more infrequent situations that might present atypical symptoms and uncertain outcomes [13]. While let-7c-5p and miR-448 might be downregulated in the younger group, miR-204-5p presented a higher expression in RRMS<25 than in RR>45.

On one hand, miR-204-5p is highly expressed in brain and spinal cord tissue samples, as occurred with let-7c-5p [287]. In addition, it has been previously related to MS as it was found upregulated in inactive WM MS lesions [295] and downregulated in hippocampal MS lesions [344]. On the other hand, miR-448 has been found upregulated in PBMCs and CSF of MS patients, positively correlating to disease severity. Th17 T cells lineage were the major source of miR-448 expression [261] and the role of these cells in the pathogenesis of MS has already been confirmed [380].

Therefore, this preliminary study only showed some potential miRNA deregulations among individuals with RRMS with early and late onset. These potential deregulated miRNAs in early and late onset might have a role in the ability to compensate for the development of the disease. It would be interesting to further study the role of let-7c-5p, miR-448 and miR-204-5p in the processes of compensation in order to delay disease onset.

5.6.3 Comparison of active lesions-enriched miRNAs in CSF according to the presence of Gd+ lesions in MRI

Several studies have analyzed miRNA expression in cell-free CSF [133,240,241], a biological fluid that could mirror events occurring in the CNS. However, none of them have checked their relationship with the presence of active MS lesions. The differential expression of miRNAs in CSF collected from MS patients could be a valuable indicator of CNS inflammation.

Junker *et al.* [295] reported a set of 28 miRNAs deregulated in brain tissue with active MS lesions. Our results confirmed the presence in the CSF of seven of the miRNAs previously reported as deregulated in active brain lesions (miR-21, miR-146a, miR-146b, miR-155, miR-223, miR-320 and miR-328). Moreover, miR-21, miR-146a and miR-146b were overexpressed in the CSF of Gd+ MS patients and also associated with radiological variables and clinical disability. This overexpression also agrees with the findings reported in active MS lesions, where these three miRNAs were upregulated when compared to normal WM [295]. It was also observed the correlation between miR-21, miR-146a and miR-146b and CSF NF-L levels, one of the most validated biomarkers for axonal damage [381], which supports the relation between these miRNAs and injury in the CNS.

Fenoglio *et al.* [382] found miR-21 and miR-146a/b overrepresented in PBMCs of RRMS patients compared to controls. They suggested that this upregulation was specific of the acute phase of MS and contribute to the differentiation and

DISCUSSION

regulation of CD4⁺ T cells, which are involved in the CNS inflammatory processes that take place in MS [297]. First, activated T lymphocytes migrate from the periphery into the CNS through the BBB. Then, CD4⁺ T cells contribute to maintain the inflammation within the CNS and cytotoxic CD8⁺ T cells can induce direct axonal damage [383]. However, regulatory T cells, which maintain immune self-tolerance by suppressing effector T cells, exert that control, in part, by the release of miRNA-containing exosomes as non-cell-autonomous gene silencing mechanism [384]. In addition, extracellular vesicles released by regulatory T cells are enriched in miR-21 and miR-146a [385].

These miRNAs have several roles in regulating T-cell biology. On the one hand, miR-21 may modulate T cell activation and apoptosis, regulatory T cell function and development, or Th17 differentiation [350]. On the other hand, miR-146a is thought to constitute an important negative regulator of the innate immune response [386] and controls IL17 production [387]. Remarkably, the expression of miR-146b is increased upon the presence of proinflammatory cytokines as IFN- γ [388]. Thus, an overexpression of these miRNAs might be reactive to the proinflammatory milieu in MS. In presence of CNS inflammatory processes miR-21, miR-146a and miR-146b could be highly expressed in order to counteract the harmful activity of other cells.

In silico pathway analysis underpins the relevance of these miRNAs in the acute phase of inflammation in the CNS of RRMS patients. Specifically, their target genes are involved in apoptosis, cell migration and proliferation, immune response and cytokine-mediated signalling. As previously mentioned, migration of T lymphocytes into the CNS is a prerequisite to tissue damage in MS, and all these biological processes are involved in the cascade of events that trigger brain lesions. The miRNA-target interaction analysis revealed that the three overexpressed miRNAs have common targeted genes: *IRAK1* and *EGFR* [389–393]. However, the *in silico* analysis of public datasets of miRNA and mRNA expression arrays showed that only *IRAK1* expression seemed to be negatively correlated mainly to

miR-146a and miR-146b levels. IRAK1 is a serine/threonine kinase associated with interleukin-1 receptor and Toll-like receptor signalling pathways that play a role in the innate immune response and exert an important influence in T helper differentiation and proliferation [394]. IRAK1-deficient mice are resistant to EAE [395], suggesting a critical role of this protein in autoimmune and inflammatory diseases. The use of IRAK1 inhibitors was tested to treat inflammatory diseases [396]. Thus, these *in silico* observations suggest that it would be interesting to study the modulation of *IRAK1* expression due to the overexpression of miR-21, miR-146a and miR-146b in the CSF in order to prove its role in controlling inflammation and re-establish the self-tolerance after an acute inflammatory event.

Finally, due to the invasiveness of the lumbar puncture, the detection of biomarkers in serum or plasma is the most appropriate option for monitoring disease progression. Although miR-21, miR-146a and miR-146b could be detected in plasma samples, no significant differences were found between Gd⁺ and Gd⁻ patients. Other groups also failed to correlate their CSF and plasma findings [241,322]. The poor correlation between CSF and plasma findings might suggest that CSF miRNA profile could provide different information not available in plasma.

In conclusion, overexpression of miR-21, miR-146a and miR-146b in cell-free CSF allowed to discriminate MS patients with Gd⁺ lesions in the MRI. All data point to the hypothesis that an overexpression of these miRNAs in CSF is induced to counteract the pro-inflammatory milieu in MS and they might be released into the CSF in an attempt to reduce the harmful damage into the brain. However, additional functional studies and analyses of larger cohorts are needed to validate these results and to elucidate the real role of these miRNAs in the context of MS.

DISCUSSION

5.7 STUDY OF CIRCULATING VIRUS-ENCODED miRNAs IN MS PATIENTS AND HEALTHY CONTROLS

EBV is an herpesvirus that is highly prevalent in human population, infecting more than 90% of people globally [20]. Despite being harmless in most cases of infection, EBV has been related to different malignancies [34]. EBV is considered an environmental MS risk factor, since EBV seropositivity is linked to the development of MS as different studies have demonstrated. In addition, the role of this virus in MS pathology and pathogenesis and, the immune response of MS patients to EBV, are other aspects that are being studied [397].

It has been shown that *in vitro* EBV infection was capable of influencing cellular miRNAs [398]. Moreover, the own viral genome encodes 44 miRNAs that regulate genes involved in different cellular processes such as cell apoptosis, antigen presentation and recognition or B cell transformation [34]. Some of these viral miRNAs, which have been mostly studied in EBV associated cancers, have been observed deregulated in other conditions including some autoimmune diseases as Sjögren's syndrome [399].

Some studies have studied the expression of EBV miRNAs in MS. *ebv-miR-BART7*, *ebv-miR-BART19-5p* and *ebv-miR-BART11-5p* were downregulated in B lymphocytes of untreated RRMS compared with controls in the study published by Sievers *et al.* [35]. Wang *et al.* found increased levels of *ebv-miR-BHRF1-2-5p* and *ebv-miR-BHRF1-3* in serum samples of RRMS patients compared with healthy controls associating their expression with EDSS scores [36]. In addition, the interaction between MS risk loci, EBV DNA copy number and viral miRNA expression in lymphoblastoid cell lines was studied and *ebv-miR-BART4-3p* and *ebv-miR-BART3-5p* were highly associated with the other studied variables [400].

From the total of seven studied miRNAs in this doctoral thesis, only expression levels of *ebv-miR-BART7-3p* were detected in our cohort. The other two miRNA

deregulated in Sievers' work couldn't be found. They used B lymphocytes to extract RNA and, it should be mentioned that the main reservoir for EBV is memory B cells [401]. However, Wang *et al.* analyzed circulating EBV miRNAs and there is also disagreement in the findings in both studies. On the one hand, the detection of the miRNAs they declared as existent in their samples failed in our cohort and, on the other hand, they analyzed all EBV encoded miRNAs and did not detect ebv-miR-BART7-3p. This lack of detection agreement might be due to two different aspects. First, there are two main EBV genotypes with perceivable geographical variation in their distribution [402]. New strains are subsequently reported from different origins and, even EBV variants could be detected in the same subject, which might affect disease induction and prognosis [403]. Second, the biological fluid was different in both studies and samples from serum and plasma could also show different miRNA concentration affecting the spectrum of extracellular miRNA in blood [231].

Statistically significant increased levels of IgG anti-EBNA1 in MS cohort respect OND group were observed. This overexpression is consistent with the results previously reported in other studies [404,405]. EBNA1 has an essential function in the replication and partitioning of EBV DNA during its latency stage [406].

Although decreased levels of ebv-miR-BART7-3p in plasma samples of MS were found, statistical differences in its expression with OND were not observed, unlike findings in Siever's study. On the one hand, they used B lymphocytes, the main reservoir for EBV [401], and different normalization method as they used spike-in controls. On the other hand, they observed this deregulation during the screening phase of their study and the validation of these results was not further mentioned.

Within MS group, a sub-classification between CIS and RRMS was made and, interestingly, ebv-miR-BART7-3p was upregulated in plasma samples of RRMS individuals. In addition, it was also observed that its expression was increased in those MS individuals who had suffered any relapse in two-year time frame since

DISCUSSION

sampling. These preliminary results might suggest the implication of ebv-miR-BART7-3p in greater activity in MS. The association of EBV infection and MS disease activity has been previously suggested as EBV serological data differences have been observed between subgroups and anti-EBNA1 IgG correlated to number of Gd+ and T2 lesions [31]. While plasma samples analyzed in our study belonged to MS patients who were not in relapse, Wang *et al.* found the deregulation of ebv-miR-BHRF1-2-5p and ebv-miR-BHRF1-3 and their association to EDSS scores in serum samples of RRMS patients at relapse. All this highlights the interest of expanding viral miRNA studies in MS using larger longitudinal cohorts including samples at relapse with available information regarding disease activity as radiological and clinical parameters. We increased our preliminary cohort with samples from other Neurology departments but, as we lacked this valuable information, we could not go further than analyzing expression between MS and OND without relating ebv-miR-BART7-3p to disease activity and progression.

One of the functions of ebv-miR-BART7-3p in cells is enhancing the proliferation of cancerous cells by affecting oncogenic pathways including the TGF- β signaling pathway [407] and its inhibition has reduced tumor growth in animal models [408]. TGF- β has been proposed as a promising option in MS treatment as this cytokine might control the growth and function of different cells implicated in MS and it could protect against relapses in EAE and MS [409].

In conclusion, overexpression of ebv-miR-BART7-3p was found in plasma samples of RRMS compared to CIS subjects and in those individuals further suffering any relapse in two-year time frame. It would be interesting to expand our study relating its expression to different clinical, radiological and genetic data and study EBV viral load as EBV DNA copy number has been associated with significantly more risk alleles for MS [400]. Thus, the technical conditions should be improved to increase viral miRNA detection and study the other 37 EBV miRNAs. To study B cells might be also suggested as Sievers *et al.* made as these EBV-infected B cells

could alter the immune system response [401] and relate viral and cellular miRNA expression.

5.8 GENERAL DISCUSSION

MS is a chronic inflammatory and neurodegenerative disease of the CNS that affects 47,000 people only in Spain [6], representing the most common non-traumatic neurological cause of disability in young individuals [5,11]. This disease has a great impact in the quality of life of patients as they might experience disability, fatigue and cognitive difficulties. These difficulties could affect their productivity at work in at least 72% of those MS individuals employed in Spain [410]. In addition, MS supposes a high cost in health systems. It has been estimated that total annual costs might vary between €20,600 and €68,700 for patient [410].

miRNA studies in MS have gained attention recently due to the new insights they can offer [151]. Although most studies have been focused on analyzing miRNA profiles in blood cells [151] or even in WM and GM lesions of MS patients [238], circulating miRNAs present lots of properties to be considered promising biomarkers [223,224]. However, heterogenous and conflicting results and the lack of replication between studies are one of the current challenges that need to be solved to fully exploit miRNA potential in this field [220]. In table 52, all results obtained throughout this doctoral thesis are summarized including correlations with clinical variables, changes observed in the preliminary *ex vivo* experiment and other already published studies describing some kind of deregulation in circulating miRNA levels in MS. Altogether, some miRNAs such as miR-21-5p, miR-20a-5p, miR-142-5p, miR-143-3p, miR-146a-5p and miR-448 might be highlighted and be presented as potential candidates to be studied in further MS studies as they appeared as deregulated in different sub-studies and other publications.

Table 52. Summary table of miRNA findings in this doctoral thesis.

Biological material	miRNA	Deregulation	Thesis sub-study	Other MS studies
CSF	let-7b-5p	DownR PPMS vs OND	4.3	Manna <i>et al</i> , 2018
	let-7c-5p	UpR RRMS>45	4.6.2	Regev <i>et al</i> , 2016; Kimura <i>et al</i> , 2018
	miR-20a-5p	DownR RRMS vs SAS, DownR MS-E vs MS-NA	4.4, 4.6.1	Perdaens <i>et al</i> , 2020
	miR-21-5p	UpR Gd+ / Pos correlation Gd+ lesion number & T2 lesion number & EDSS / UpR Dem vs Mye&Rem vs Mye	4.4, 4.6.3	Quintana <i>et al</i> , 2017; Perdaens <i>et al</i> , 2020
	miR-92b-3p	UpR Inflammatory PPMS vs non-inflammatory PPMS	4.3	
	miR-143-3p	DownR PPMS vs OND, UpR RRMS vs SAS, UpR MS-E vs MS-NA / Pos Correlation VitD levels / UpR Dem vs Rem, DownR Rem vs Mye	4.3, 4.4, 4.6.1	Regev <i>et al</i> , 2017
	miR-144-3p	UpR RIS-Conversion	4.5	
	miR-145-5p	UpR RRMS vs SAS	4.4	Søndergaard <i>et al</i> , 2013; Sharaf-Eldin <i>et al</i> , 2017; Hemond <i>et al</i> , 2019; Perdaens <i>et al</i> , 2020
	miR-146a	UpR Gd+ / Pos correlation Gd+ lesion number / UpR Dem vs Rem	4.4, 4.6.3	Zhang <i>et al</i> , 2014; Quintana <i>et al</i> , 2017; Manna <i>et al</i> , 2018; Perdaens <i>et al</i> , 2020
	miR-146b	UpR Gd+ / Pos Correlation NF-L levels in CSF & Gd+ lesion number	4.6.3	
	miR-204-5p	DownR RRMS>45	4.6.2	
	miR-320a	UpR RRMS&PPMS vs SAS	4.4	Regev <i>et al</i> , 2016; Regev <i>et al</i> , 2018
	miR-335-5p	DownR MS-E vs MS-NA / Neg Correlation VitD levels / DownR Rem vs Mye	4.4, 4.6.1	
	miR-448	UpR RIS-Conversion, DownR RRMS>45 / Pos Correlation T2 lesion number	4.5, 4.6.2	Wu <i>et al</i> , 2017
	miR-653-3p	UpR RIS-Conversion, DownR MS-E vs MS-NA	4.5, 4.6.1	
	miR-1260a	DownR RRMS&PPMS vs SAS	4.4	
	Plasma	miR-142-3p	DownR RIS-Conversion / UpR Dem vs Mye	4.4, 4.5
miR-338-3p		DownR RIS-Conversion	4.5	
miR-363-3p		DownR RIS-Conversion / Neg Correlation T2 lesion number	4.5	
miR-374b-5p		DownR RIS-Conversion	4.5	
miR-424-5p		DownR RIS-Conversion	4.5	
miR-483-3p		UpR RIS-Conversion / Pos Correlation T2 lesion number & CHI3L1 & NF-L levels in CSF	4.5	
Serum	miR-20a-5p	UpR PPMS vs OND	4.3	Perdaens <i>et al</i> , 2020
	miR-26a-5p	UpR RRMS vs PPMS / DownR Dem vs Mye	4.3, 4.4	Vistbakka <i>et al</i> , 2017; Manna <i>et al</i> , 2018
	miR-103a-2-5p	DownR Inflammatory PPMS vs non-inflammatory PPMS	4.3	
	miR-142-5p	UpR RRMS vs OND	4.3	Regev <i>et al</i> , 2017; Regev <i>et al</i> , 2018

CSF: cerebrospinal fluid; DownR: downregulated (red color); PPMS: primary progressive multiple sclerosis; OND: other neurological diseases; UpR: upregulated (green color); RRMS>45: RRMS individuals whose age at onset was above 45 years old; RRMS: relapsing-remitting multiple sclerosis; SAS: spinal anesthesia subjects; MS-E: MS individuals of European origin; MS-NA: MS individuals of North-African origin. Gd+: patients with gadolinium enhanced lesions; Pos correlation: positive correlation; Dem: demyelination; Mye: myelination; Rem: remyelination; VitD: vitamin D; RIS-Conversion: patients who converted to CIS or MS after five years of monitoring; NF-L: neurofilament light chain; Neg correlation: negative correlation; CHI3L1: chitinase 3 like-1.

There is no doubt that miRNAs will have an important role as recognized biomarkers in the future but, researchers should make a common effort to try to unify protocols to achieve greater replication of studies.

Beyond their role as biomarkers, miRNA studies in MS might also provide new concepts into disease pathology and therapeutic targets [151]. The etiology of MS is still unknown [1] and there are no useful DMTs for PPMS [411]. It has been proposed that remyelination therapies might limit the progressive degeneration and restore function [100]. Although the therapeutic research area is less advanced, some miRNA-based therapeutics are already in clinical trials and feedback on their potential is promising, e.g. Miravirsen and RG-101 for Hepatitis C or MRG-201 for fibrosis [412]. Specifically in MS, the therapeutic potential of the inhibition or overexpression of targets miRNAs such as miR-155, miR-326, miR-20a or miR-219a has already been explored in mouse models [151,346,347].

5.9 LIMITATIONS

One the major limitations in most miRNA studies, including this, is the small sample size, which is not enough to obtain robust results. In addition, most biological samples belong to specific geographic areas, which does not allow to rule out the influence of environmental and/or genetic factors on the results obtained. These two important limitations might be overcome by creating and using collaborative networks between research groups and countries.

5.10 FINAL CONSIDERATION

Finally, I would like to mention that a lot of authors have already clarified that one of the challenges that should be overcome is funding [220]. Gross domestic expenditure on research and development (GDERD) is a measure of the level of research and development (R&D) activity performed in a specific economy [413]. Data obtained from the Organisation for Economic Co-operation and Development show that Korea was by far the country with the highest GDERD in 2018, followed

DISCUSSION

by Japan, United States, China and the European Union (EU) [414]. The internal R&D spending increased 6.3% in 2018 in Spain, reaching 1.24% of GDERD [415]. This amount is far from those observed in other European and bordering countries, as it could be observed in Table 53. This could be attributable to the fact of having a lower number of researchers per 1,000 employees [416]. However, our country has witnessed a loss of research talent due to the economic crisis and the cutouts. Large researcher registries have shown that this decrease was balanced with an entrance during the years 2,000 and 2,010 but this equilibrium was altered and this situation has not been compensated yet [417]. For this reason, countries should promote R&D by improving researcher's conditions, supporting emerging groups and giving visibility to the vital function R&D has in society.

Table 53. Number of researchers and gross domestic expenditure on research and development per country in 2018.

Country	Researcher per 1,000 employed (2018)	% GDERD (2018)
Korea	15.326	4.528
Japan	9.882	3.275
United States	9.225	2.826
China	2.405	2.141
European Union	8.778	2.025
Sweden	14.777	3.321
Germany	9.669	3.130
France	10.900	2.193
Netherlands	10.255	2.164
United Kingdom	9.426	1.729
Italy	6.018	1.426
Portugal	9.697	1.355
Spain	7.071	1.243
Ireland	11.622	0.997

6. Conclusions

1. TaqMan® Advanced miRNA technology from Applied Biosystems™ is suitable for the study of miRNAs in CSF samples as long as an initial volume of 300 µl is used to extract RNA and 22 cycles of preamplification step are performed. The cc-OA plates could be valuable tools to describe miRNA profiles in different neurological diseases including MS due to its reproducibility, correlation with individual qPCR data and ability to detect a wide range of CSF-enriched miRNAs.
2. The suggested OpenArray data analysis for CSF samples implies the use of triplicate measurements whose maximum allowed Cq variation would be 0.7 between replicates for the Cq interval 15-28 or 0.9 in Cq interval 28-35. The selection of those miRNAs detected in at least 70% of the samples ensures the inclusion of amplification data with good quality. Replacement of missing data is not required and GN is assumed to be the proper method to normalize OpenArray Cq values and calculate RQ values.
3. The overall outcome of the study of miRNA signatures in PPMS shows the down-regulation of let-7b-5p and miR-143-3p levels in CSF samples of PPMS subjects compared to OND and, the up-regulation of miR-20a-5p in serum of PPMS against OND. At the same time, miR-26a-5p is down-regulated in PPMS compared to RRMS and miR-142-5p up-regulated in RRMS against OND in serum. In addition, miR-92b-3p and miR-103a-2-5p in CSF and serum samples respectively, might differentiate PPMS subjects according to their inflammatory activity.
4. Cross-analysis between *ex vivo* models and human CSF samples suggest miR-143-3p, miR-21-5p or miR-145-5p as candidates to be involved in the neurodegenerative process. Comparison between *ex vivo* demyelination and CSF samples of patients might be a valuable approach to propose new miRNAs involved in demyelination and remyelination.
5. The exploratory study involving RIS individuals reports a specific signature pattern of circulating miRNAs that might differentiate subjects according to their prospective conversion status to CDMS. Specifically, miR-144-3p, miR-448

CONCLUSIONS

and miR-653-3p are up-regulated in CSF in those individuals who finally converted to CDMS. Regarding plasma samples, miR-142-3p, miR-338-3p, miR-363-3p, miR-374b-5p and miR-424-5p are down-regulated while miR-483-3p is up-regulated in RIS-Conversion subjects.

6. RRMS patients might present differential levels of miRNAs in CSF depending on their ethnic origin. While miR-143-3p presents lower levels in CSF samples of MS-NA individuals, miR-20a-5p, miR-335-5p and miR-653-3p are up-regulated in these subjects. Different expression patterns are also found when subclassifying NA-MS patients according to the age at which they migrated to Europe.

7. The preliminary study of CSF miRNA in RRMS individuals depending on the age of disease onset shows no potential deregulation, which might suggest that the altered pathways are the same. Nevertheless, it would be interesting to further study the role of let-7c-5p, miR-448 and miR-204-5p in the processes of compensation in order to delay disease onset.

8. Overexpression of miR-21, miR-146a and miR-146b in CSF discriminates MS patients with Gd⁺ lesions in the MRI. *In silico* analysis might suggest that this overexpression could be due to an attempt to reduce the harmful damage into the brain.

9. Among the studied EBV miRNAs, ebv-miR-BART7-3p is the only viral miRNA detected in plasma samples from MS and OND individuals, whose expression does not vary between both groups. Within MS group, ebv-miR-BART7-3p was up-regulated in RRMS compared to CIS individuals and in subjects suffering from relapses in the two-year time frame since sampling.

10. Altogether, miR-21-5p, miR-20a-5p, miR-142-5p, miR-143-3p, miR-146a-5p and miR-448 are potential candidates to be studied in further MS studies as their deregulation has been manifested in different sub-studies.

7. References

REFERENCES

1. Thompson AJ, Baranzini SE, Geurts J, Hemmer B, Ciccarelli O. Multiple sclerosis. *Lancet*. 2018;391(10130):1622-1636. doi:10.1016/S0140-6736(18)30481-1
2. Moreno-Torres I, Sabín-Muñoz J, García-Merino A. CHAPTER 1: Multiple Sclerosis: Epidemiology, Genetics, Symptoms, and Unmet Needs. Emerging Drugs and Targets for Multiple Sclerosis. *Royal Society of Chemistry*; 2019:3-32. doi:10.1039/9781788016070-00001
3. Orrell RW. Multiple sclerosis: The history of a disease. *J R Soc Med*. 2005;98(6):289.
4. Omerhoca S, Yazici Akkas S, Kale Icen N. Multiple sclerosis: Diagnosis and Differential Diagnosis. *Arch Neuropsychiatry*. 2018;55(1):S1. doi:10.29399/npa.23418
5. Multiple Sclerosis International Federation. The Multiple Sclerosis International Federation, Atlas of MS, 3rd Edition.; 2020. <https://www.atlasofms.org/map/global/epidemiology/number-of-people-with-ms>. Accessed October 15, 2020.
6. Sociedad Española de Neurología. 8 de Diciembre: Día Nacional de La Esclerosis Múltiple. 2019.
7. European Multiple Sclerosis Platform. MS Barometer 2020. <http://www.emsp.org/wp-content/uploads/2021/03/MS-Barometer2020-Final-Full-Report-Web.pdf>. Accessed May 01, 2021.
8. Wallin MT, Culpepper WJ, Nichols E, et al. Global, regional, and national burden of multiple sclerosis 1990–2016: a systematic analysis for the Global Burden of Disease Study 2016. *Lancet Neurol*. 2019;18(3):269-285. doi:10.1016/S1474-4422(18)30443-5
9. Simpson S, Blizzard L, Otahal P, Van Der Mei I, Taylor B. Latitude is significantly associated with the prevalence of multiple sclerosis: A meta-analysis. *J Neurol Neurosurg Psychiatry*. 2011;82(10):1132-1141. doi:10.1136/jnnp.2011.240432
10. García-Estévez DA, Fraga-González C, Elvira Ramos-Pacho M, López-Díaz LM, Pardo-Parrado M, Prieto JM. The prevalence of multiple sclerosis in the city of Ourense, Galicia, in the north-west of the Iberian Peninsula. *Rev Neurol*. 2020;71(1):19-25. doi:10.33588/RN.7101.2019432
11. Hollen CW, Paz Soldán MM, Rinker JR, Spain RI. The Future of Progressive Multiple Sclerosis Therapies. *Fed Pract*. 2020;37(1):S43-S49.
12. Kobelt G, Thompson A, Berg J, Gannedahl M, Eriksson J. New insights into the burden and costs of multiple sclerosis in Europe. *Mult Scler*. 2017;23(8):1123-1136. doi:10.1177/1352458517694432
13. Mirmosayyeb O, Brand S, Barzegar M, et al. Clinical Characteristics and Disability Progression of Early- and Late-Onset Multiple Sclerosis Compared to Adult-Onset Multiple Sclerosis. *J Clin Med*. 2020;9(5):1326. doi:10.3390/jcm9051326
14. Neumann B, Segel M, Chalut KJ, Franklin RJM. Remyelination and ageing:

REFERENCES

- Reversing the ravages of time. *Mult Scler.* 2019;25(14):1835-1841. doi:10.1177/1352458519884006
15. Cunha LL, Perazzio SF, Azzi J, Cravedi P, Riella LV. Remodeling of the Immune Response With Aging: Immunosenescence and Its Potential Impact on COVID-19 Immune Response. *Front Immunol.* 2020;11:1748. doi:10.3389/fimmu.2020.01748
 16. Krysko KM, Graves JS, Dobson R, et al. Sex effects across the lifespan in women with multiple sclerosis. *Ther Adv Neurol Disord.* 2020;13. doi:10.1177/1756286420936166
 17. Angum F, Khan T, Kaler J, Siddiqui L, Hussain A. The Prevalence of Autoimmune Disorders in Women: A Narrative Review. *Cureus.* 2020;12(5). doi:10.7759/cureus.8094
 18. Ribbons KA, McElduff P, Boz C, et al. Male sex is independently associated with faster disability accumulation in relapse-onset MS but not in primary progressive MS. *PLoS One.* 2015;10(6). doi:10.1371/journal.pone.0122686
 19. Miller AE. Multiple Sclerosis: Where Will We Be in 2020? *Mt Sinai J Med.* 2011;78(2):268-279. doi:10.1002/msj.20242
 20. Burnard S, Lechner-Scott J, Scott RJ. EBV and MS: Major cause, minor contribution or red-herring? *Mult Scler Relat Disord.* 2017;16:24-30. doi:10.1016/j.msard.2017.06.002
 21. Fugl A, Andersen CL. Epstein-Barr virus and its association with disease - A review of relevance to general practice. *BMC Fam Pract.* 2019;20(1). doi:10.1186/s12875-019-0954-3
 22. Smatti MK, Al-Sadeq DW, Ali NH, Pintus G, Abou-Saleh H, Nasrallah GK. Epstein-barr virus epidemiology, serology, and genetic variability of LMP-1 oncogene among healthy population: An update. *Front Oncol.* 2018;8(JUN):211. doi:10.3389/fonc.2018.00211
 23. Ascherio A, Munger KL. Environmental risk factors for multiple sclerosis. Part I: The role of infection. *Ann Neurol.* 2007;61(4):288-299. doi:10.1002/ana.21117
 24. Dobson R, Kuhle J, Middeldorp J, Giovannoni G. Epstein-Barr-negative MS: A true phenomenon? *Neurol Neuroimmunol NeuroInflammation.* 2017;4(2):318. doi:10.1212/NXI.0000000000000318
 25. Ascherio A, Munger KL, Lennette ET, et al. Epstein-Barr virus antibodies and risk of multiple sclerosis: A prospective study. *J Am Med Assoc.* 2001;286(24):3083-3088. doi:10.1001/jama.286.24.3083
 26. Sundström P, Juto P, Wadell G, et al. An altered immune response to Epstein-Barr virus in multiple sclerosis: A prospective study. *Neurology.* 2004;62(12):2277-2282. doi:10.1212/01.WNL.0000130496.51156.D7

REFERENCES

27. DeLorenze GN, Munger KL, Lennette ET, Orentreich N, Vogelmann JH, Ascherio A. Epstein-Barr Virus and Multiple Sclerosis. *Arch Neurol.* 2006;63(6):839. doi:10.1001/archneur.63.6.noc50328
28. Levin LI, Munger KL, Rubertone M V., et al. Temporal relationship between elevation of Epstein-Barr virus antibody titers and initial onset of neurological symptoms in multiple sclerosis. *J Am Med Assoc.* 2005;293(20):2496-2500. doi:10.1001/jama.293.20.2496
29. Levin LI, Munger KL, O'Reilly EJ, Falk KI, Ascherio A. Primary infection with the Epstein-Barr virus and risk of multiple sclerosis. *Ann Neurol.* 2010;67(6):824-830. doi:10.1002/ana.21978
30. Munger KL, Levin LI, O'Reilly EJ, Falk KI, Ascherio A. Anti-Epstein-Barr virus antibodies as serological markers of multiple sclerosis: A prospective study among United States military personnel. *Mult Scler.* 2011;17(10):1185-1193. doi:10.1177/1352458511408991
31. Farrell RA, Antony D, Wall GR, et al. Humoral immune response to EBV in multiple sclerosis is associated with disease activity on MRI. *Neurology.* 2009;73(1):32-38. doi:10.1212/WNL.0b013e3181aa29fe
32. Handel AE, Williamson AJ, Disanto G, Handunnetthi L, Giovannoni G, Ramagopalan S V. An Updated Meta-Analysis of Risk of Multiple Sclerosis following Infectious Mononucleosis. *PLoS One.* 2010;5(9):e12496. doi:10.1371/journal.pone.0012496
33. Santpere G, Darre F, Blanco S, et al. Genome-wide analysis of wild-type Epstein-Barr virus genomes derived from healthy individuals of the 1000 Genomes Project. *Genome Biol Evol.* 2014;6(4):846-860. doi:10.1093/gbe/evu054
34. Hassani A, Khan G. Epstein-Barr virus and miRNAs: Partners in crime in the pathogenesis of multiple sclerosis? *Front Immunol.* 2019;10(APR):695. doi:10.3389/fimmu.2019.00695
35. Sievers C, Meira M, Hoffmann F, Fontoura P, Kappos L, Lindberg RLP. Altered microRNA expression in B lymphocytes in multiple sclerosis. Towards a better understanding of treatment effects. *Clin Immunol.* 2012;144(1):70-79. doi:10.1016/j.clim.2012.04.002
36. Wang YF, He DD, Liang HW, et al. The identification of up-regulated EBV-miR-BHRF1-2-5p targeting MALT1 and EBV-miR-BHRF1-3 in the circulation of patients with multiple sclerosis. *Clin Exp Immunol.* 2017;189(1):120-126. doi:10.1111/cei.12954
37. Kremmentsov DN, Asarian L, Fang Q, McGill MM, Teuscher C. Sex-specific Gene-by-Vitamin D interactions regulate susceptibility to central nervous system autoimmunity. *Front Immunol.* 2018;9(JUL):1622. doi:10.3389/fimmu.2018.01622
38. Munger KL, Levin LI, Hollis BW, Howard NS, Ascherio A. Serum 25-

REFERENCES

- hydroxyvitamin D levels and risk of multiple sclerosis. *J Am Med Assoc.* 2006;296(23):2832-2838. doi:10.1001/jama.296.23.2832
39. Smolders J, Menheere P, Kessels A, Damoiseaux J, Hupperts R. Association of vitamin D metabolite levels with relapse rate and disability in multiple sclerosis. *Mult Scler.* 2008;14(9):1220-1224. doi:10.1177/1352458508094399
40. Simpson S, Taylor B, Blizzard L, et al. Higher 25-hydroxyvitamin D is associated with lower relapse risk in multiple sclerosis. *Ann Neurol.* 2010;68(2):193-203. doi:10.1002/ana.22043
41. Mowry EM, Waubant E, McCulloch CE, et al. Vitamin D status predicts new brain magnetic resonance imaging activity in multiple sclerosis. *Ann Neurol.* 2012;72(2):234-240. doi:10.1002/ana.23591
42. Bjørnevik K, Riise T, Casetta I, et al. Sun exposure and multiple sclerosis risk in Norway and Italy: The EnvIMS study. *Mult Scler.* 2014;20(8):1042-1049. doi:10.1177/1352458513513968
43. Van Der Mei IAF, Dwyer t., Blizzard l., et al. Past exposure to sun, skin phenotype, and risk of multiple sclerosis: Case-control study. *BMJ.* 2003;327(7410):316. doi:10.1136/bmj.327.7410.316
44. Tremlett H, Zhu F, Ascherio A, Munger KL. Sun exposure over the life course and associations with multiple sclerosis. *Neurology.* 2018;90(14):E1191-E1199. doi:10.1212/WNL.0000000000005257
45. Hawkes CH. Smoking is a risk factor for multiple sclerosis: A metanalysis. *Mult Scler.* 2007;13(5):610-615. doi:10.1177/1352458506073501
46. O’Gorman C, Bukhari W, Todd A, Freeman S, Broadley SA. Smoking increases the risk of multiple sclerosis in Queensland, Australia. *J Clin Neurosci.* 2014;21(10):1730-1733. doi:10.1016/j.jocn.2014.01.009
47. Degelman ML, Herman KM. Smoking and multiple sclerosis: A systematic review and meta-analysis using the Bradford Hill criteria for causation. *Mult Scler Relat Disord.* 2017;17:207-216. doi:10.1016/j.msard.2017.07.020
48. Hernán MA, Jick SS, Logroscino G, Olek MJ, Ascherio A, Jick H. Cigarette smoking and the progression of multiple sclerosis. *Brain.* 2005;128(6):1461-1465. doi:10.1093/brain/awh471
49. O’Gorman CM, Broadley SA. Smoking increases the risk of progression in multiple sclerosis: A cohort study in Queensland, Australia. *J Neurol Sci.* 2016;370:219-223. doi:10.1016/j.jns.2016.09.057
50. Koch M, Van Harten A, Uyttenboogaart M, De Keyser J. Cigarette smoking and progression in multiple sclerosis. *Neurology.* 2007;69(15):1515-1520. doi:10.1212/01.wnl.0000277658.78381.db

REFERENCES

51. Nishanth K, Tariq E, Nzvere FP, Miqdad M, Cancarevic I. Role of Smoking in the Pathogenesis of Multiple Sclerosis: A Review Article. *Cureus*. 2020;12(8). doi:10.7759/cureus.9564
52. Gianfrancesco MA, Acuna B, Shen L, et al. Obesity during childhood and adolescence increases susceptibility to multiple sclerosis after accounting for established genetic and environmental risk factors. *Obes Res Clin Pract*. 2014;8(5):e435-e447. doi:10.1016/j.orcp.2014.01.002
53. Langer-Gould A, Brara SM, Beaver BE, Koebnick C. Childhood obesity and risk of pediatric multiple sclerosis and clinically isolated syndrome. *Neurology*. 2013;80(6):548-552. doi:10.1212/WNL.0b013e31828154f3
54. Hedström AK, Olsson T, Alfredsson L. High body mass index before age 20 is associated with increased risk for multiple sclerosis in both men and women. *Mult Scler J*. 2012;18(9):1334-1336. doi:10.1177/1352458512436596
55. Luciardi MC, Carrizo TR, Díaz EI, Áleman MN, Bazán MC, Abregú AV. Proinflammatory state in obese children. *Rev Chil Pediatr*. 2018;89(3):346-351. doi:10.4067/S0370-41062018005000501
56. Kantorová E, Kurča E, Čierny D, Dobrota D, Sivák Š. The Role of Over-Nutrition and Obesity in Multiple Sclerosis. Trending Topics in Multiple Sclerosis. *InTech*; 2016. doi:10.5772/63992
57. Schepici G, Silvestro S, Bramanti P, Mazzon E. The Gut Microbiota in Multiple Sclerosis: An Overview of Clinical Trials. *Cell Transplant*. 2019;28(12):1507-1527. doi:10.1177/0963689719873890
58. Kirby T, Ochoa-Repáraz J. The Gut Microbiome in Multiple Sclerosis: A Potential Therapeutic Avenue. *Med Sci*. 2018;6(3):69. doi:10.3390/medsci6030069
59. Chu F, Shi M, Lang Y, et al. Gut microbiota in multiple sclerosis and experimental autoimmune encephalomyelitis: current applications and future perspectives. *Mediators Inflamm*. 2018;2018. doi:10.1155/2018/8168717
60. Filippi M, Bar-Or A, Piehl F, et al. Multiple sclerosis. *Nat Rev Dis Prim*. 2018;4(1):1-27. doi:10.1038/s41572-018-0041-4
61. Tafti D, Ehsan M, Xixis KL. Multiple Sclerosis. *StatPearls Publishing*. 2020.
62. Patsopoulos NA, Baranzini SE, Santaniello A, et al. Multiple sclerosis genomic map implicates peripheral immune cells and microglia in susceptibility. *Science* (80-). 2019;365(6460). doi:10.1126/science.aav7188
63. Hafler DA, Compston A, Sawcer S, et al. Risk alleles for multiple sclerosis identified by a genomewide study. *N Engl J Med*. 2007;357(9):851-862. doi:10.1056/NEJMoa073493
64. De Jager PL, Jia X, Wang J, et al. Meta-analysis of genome scans and replication

REFERENCES

- identify CD6, IRF8 and TNFRSF1A as new multiple sclerosis susceptibility loci. *Nat Genet.* 2009;41(7):776-782. doi:10.1038/ng.401
65. Sawcer S, Hellenthal G, Pirinen M, et al. Genetic risk and a primary role for cell-mediated immune mechanisms in multiple sclerosis. *Nature.* 2011;476(7359):214-219. doi:10.1038/nature10251
66. Patsopoulos NA, Esposito F, Reischl J, et al. Genome-wide meta-analysis identifies novel multiple sclerosis susceptibility loci. *Ann Neurol.* 2011;70(6):897-912. doi:10.1002/ana.22609
67. Beecham AH, Patsopoulos NA, Xifara DK, et al. Analysis of immune-related loci identifies 48 new susceptibility variants for multiple sclerosis. *Nat Genet.* 2013;45(11):1353-1362. doi:10.1038/ng.2770
68. Patsopoulos NA, Barcellos LF, Hintzen RQ, et al. Fine-Mapping the Genetic Association of the Major Histocompatibility Complex in Multiple Sclerosis: HLA and Non-HLA Effects. Gibson G, ed. *PLoS Genet.* 2013;9(11):e1003926. doi:10.1371/journal.pgen.1003926
69. Moutsianas L, Jostins L, Beecham AH, et al. Class II HLA interactions modulate genetic risk for multiple sclerosis. *Nat Genet.* 2015;47(10):1107. doi: 10.1038/ng.3395
70. Multiple Sclerosis Genetics Consortium I, Mitrovič M, Patsopoulos NA, et al. Low-Frequency and Rare-Coding Variation Contributes to Multiple Sclerosis Risk. *Cell.* 2018;175:1679-1687.e7. doi:10.1016/j.cell.2018.09.049
71. Didonna A, Oksenberg JR. The genetics of multiple sclerosis - Chapter 1. Multiple Sclerosis: Perspectives in Treatment and Pathogenesis. *CRC Press.* 2017.
72. Olsson T, Barcellos LF, Alfredsson L. Interactions between genetic, lifestyle and environmental risk factors for multiple sclerosis. *Nat Rev Neurol.* 2016;13(1):26-36. doi:10.1038/nrneurol.2016.187
73. Lublin FD, Reingold SC, Cohen JA, et al. Defining the clinical course of multiple sclerosis: The 2013 revisions. *Neurology.* 2014;83(3):278-286. doi:10.1212/WNL.0000000000000560
74. Rommer PS, Ellenberger D, Hellwig K, et al. Relapsing and progressive MS: the sex-specific perspective. *Ther Adv Neurol Disord.* 2020;13. doi:10.1177/1756286420956495
75. Gross HJ, Watson C. Characteristics, burden of illness, and physical functioning of patients with relapsing-remitting and secondary progressive multiple sclerosis: A cross-sectional US survey. *Neuropsychiatr Dis Treat.* 2017;13:1349-1357. doi:10.2147/NDT.S132079
76. Li KX, Picheca L. Second-Line Therapy for Patients with Relapsing-Remitting Multiple Sclerosis: A Review of Guidelines. *Canadian Agency for Drugs and Technologies in Health.* 2019.

77. Frisch T, Elkjaer ML, Reynolds R, et al. Multiple Sclerosis Atlas: A Molecular Map of Brain Lesion Stages in Progressive Multiple Sclerosis. *Netw Syst Med.* 2020;3(1):122-129. doi:10.1089/nsm.2020.0006
78. Amatruda M, Petracca M, Wentling M, et al. Retrospective unbiased plasma lipidomic of progressive multiple sclerosis patients-identifies lipids discriminating those with faster clinical deterioration. *Sci Rep.* 2020;10(1). doi:10.1038/s41598-020-72654-8
79. Lublin FD, Reingold SC. Chapter 2 Clinical Features and Subtypes of Multiple Sclerosis. *Blue Books Pract Neurol.* 2003;27(C):13-20. doi:10.1016/S1877-3419(09)70031-5
80. Ciampi E, Uribe-San-Martin R, Cárcamo C, et al. Efficacy of andrographolide in not active progressive multiple sclerosis: a prospective exploratory double-blind, parallel-group, randomized, placebo-controlled trial. *BMC Neurol.* 2020;20:173. doi:10.1186/s12883-020-01745-w
81. Teixeira M, Seabra M, Carvalho L, et al. Clinically isolated syndrome, oligoclonal bands and multiple sclerosis. *Clin Exp Neuroimmunol.* 2020;11(1):33-39. doi:10.1111/cen3.12554
82. Grzegorski T, Losy J. What do we currently know about the clinically isolated syndrome suggestive of multiple sclerosis? An update. *Rev Neurosci.* 2020;31(3):335-349. doi:10.1515/revneuro-2019-0084
83. Okuda DT, Mowry EM, Beheshtian A, et al. Incidental MRI anomalies suggestive of multiple sclerosis: The radiologically isolated syndrome. *Neurology.* 2009;72(9):800-805. doi:10.1212/01.wnl.0000335764.14513.1a
84. Okuda DT. Radiologically Isolated Syndrome. *Neuroimaging Clin N Am.* 2017;27(2):267-275. doi:10.1016/j.nic.2016.12.008
85. Matute-Blanch C, Villar LM, Álvarez-Cermeño JC, et al. Neurofilament light chain and oligoclonal bands are prognostic biomarkers in radiologically isolated syndrome. *Brain.* 2018;141(4):1085-1093. doi:10.1093/brain/awy021
86. Okuda DT, Siva A, Kantarci O, et al. Radiologically Isolated Syndrome: 5-Year Risk for an Initial Clinical Event. Jacobson S, ed. *PLoS One.* 2014;9(3):e90509. doi:10.1371/journal.pone.0090509
87. Ontaneda D. Progressive multiple sclerosis. *Contin Lifelong Learn Neurol.* 2019;25(3):736-752. doi:10.1212/CON.0000000000000727
88. Popescu BFG, Pirko I, Lucchinetti CF. Pathology of multiple sclerosis: Where do we stand? *Contin Lifelong Learn Neurol.* 2013;19(4):901-921. doi:10.1212/01.CON.0000433291.23091.65
89. Dendrou CA, Fugger L, Friese MA. Immunopathology of multiple sclerosis. *Nat Rev Immunol.* 2015;15(9):545-558. doi:10.1038/nri3871

REFERENCES

90. Ontaneda D, Thompson AJ, Fox RJ, Cohen JA. Progressive multiple sclerosis: prospects for disease therapy, repair, and restoration of function. *Lancet*. 2017;389(10076):1357-1366. doi:10.1016/S0140-6736(16)31320-4
91. Lassmann H. Pathogenic mechanisms associated with different clinical courses of multiple sclerosis. *Front Immunol*. 2019;10(JAN). doi:10.3389/fimmu.2018.03116
92. Bothwell SW, Janigro D, Patabendige A. Cerebrospinal fluid dynamics and intracranial pressure elevation in neurological diseases. *Fluids Barriers CNS*. 2019;16(1). doi:10.1186/s12987-019-0129-6
93. Lassmann H, van Horssen J. Oxidative stress and its impact on neurons and glia in multiple sclerosis lesions. *Biochim Biophys Acta - Mol Basis Dis*. 2016;1862(3):506-510. doi:10.1016/j.bbadis.2015.09.018
94. Pegoretti V, Swanson KA, Bethea JR, Probert L, Eisel ULM, Fischer R. Inflammation and Oxidative Stress in Multiple Sclerosis: Consequences for Therapy Development. *Oxid Med Cell Longev*. 2020;2020. doi:10.1155/2020/7191080
95. de Barcelos IP, Troxell RM, Graves JS. Mitochondrial dysfunction and multiple sclerosis. *Biology (Basel)*. 2019;8(2). doi:10.3390/biology8020037
96. Shafaroudi MM, Zarei H, Shafaroudi AM, Karimi N, Abedini M. The Relationship between Glutamate and Multiple Sclerosis. *IBBJ*. 2018;4(1):1-13.
97. Waxman SG. Axonal conduction and injury in multiple sclerosis: The role of sodium channels. *Nat Rev Neurosci*. 2006;7(12):932-941. doi:10.1038/nrn2023
98. Su KG, Banker G, Bourdette D, Forte M. Axonal degeneration in multiple sclerosis: The mitochondrial hypothesis. *Curr Neurol Neurosci Rep*. 2009;9(5):411-417. doi:10.1007/s11910-009-0060-3
99. Baldassari LE, Feng J, Clayton BLL, et al. Developing therapeutic strategies to promote myelin repair in multiple sclerosis. *Expert Rev Neurother*. 2019;19(10):997-1013. doi:10.1080/14737175.2019.1632192
100. Franklin RJM, Ffrench-Constant C. Regenerating CNS myelin - From mechanisms to experimental medicines. *Nat Rev Neurosci*. 2017;18(12):753-769. doi:10.1038/nrn.2017.136
101. Thompson AJ, Banwell BL, Barkhof F, et al. Diagnosis of multiple sclerosis: 2017 revisions of the McDonald criteria. *Lancet Neurol*. 2018;17(2):162-173. doi:10.1016/S1474-4422(17)30470-2
102. Pandit L, Murthy JMK. Treatment of multiple sclerosis. *Ann Indian Acad Neurol*. 2011;14(1):S65. doi:10.4103/0972-2327.83094
103. Ontaneda D, Rae-Grant AD. Management of acute exacerbations in multiple sclerosis. *Ann Indian Acad Neurol*. 2009;12(4):264-272. doi:10.4103/0972-2327.58283
104. Correia JC, Airas L, Bartholome E, et al. Symptomatic therapy in multiple sclerosis:

- A review for a multimodal approach in clinical practice. *Ther Adv Neurol Disord.* 2011;4(3):139-168. doi:10.1177/1756285611403646
105. Shah P. Symptomatic management in multiple sclerosis. *Ann Indian Acad Neurol.* 2015;18(1):S35-S42. doi:10.4103/0972-2327.164827
 106. Saposnik G, Sotoca J, Sempere AP, et al. Therapeutic status quo in patients with relapsing-remitting multiple sclerosis: A sign of poor self-perception of their clinical status? *Mult Scler Relat Disord.* 2020;45. doi:10.1016/j.msard.2020.102354
 107. Ciotti JR, Valtcheva M V., Cross AH. Effects of MS disease-modifying therapies on responses to vaccinations: A review. *Mult Scler Relat Disord.* 2020;45. doi:10.1016/j.msard.2020.102439
 108. Tur C, Montalban X. Progressive MS trials: Lessons learned. *Mult Scler.* 2017;23(12):1583-1592. doi:10.1177/1352458517729460
 109. CIMA-Centro de información de medicamentos. <https://cima.aemps.es/cima/publico/home.html>. Accessed November 3, 2020.
 110. Lubetzki C, Zalc B, Williams A, Stadelmann C, Stankoff B. Remyelination in multiple sclerosis: from basic science to clinical translation. *Lancet Neurol.* 2020;19(8):678-688. doi:10.1016/S1474-4422(20)30140-X
 111. Cole KLH, Early JJ, Lyons DA. Drug discovery for remyelination and treatment of MS. *Glia.* 2017;65(10):1565-1589. doi:10.1002/glia.23166
 112. Bove RM, Green AJ. Remyelinating Pharmacotherapies in Multiple Sclerosis. *Neurotherapeutics.* 2017;14(4):894-904. doi:10.1007/s13311-017-0577-0
 113. FDA-NIH Biomarker Working Group. Glossary. August 2020. <https://www.ncbi.nlm.nih.gov/books/NBK338448/>. Accessed October 31, 2020.
 114. Califf RM. Biomarker definitions and their applications. *Exp Biol Med.* 2018;243(3):213-221. doi:10.1177/1535370217750088
 115. Gandhi R. MiRNA in multiple sclerosis: Search for novel biomarkers. *Mult Scler.* 2015;21(9):1095-1103. doi:10.1177/1352458515578771
 116. Housley WJ, Pitt D, Hafler DA. Biomarkers in multiple sclerosis. *Clin Immunol.* 2015;161(1):51-58. doi:10.1016/j.clim.2015.06.015
 117. Huff T, Tadi P, Varacallo M. Neuroanatomy, Cerebrospinal Fluid. *StatPearls Publishing.* 2019. <http://www.ncbi.nlm.nih.gov/pubmed/29262203>.
 118. Vernau W, Vernau KA, Sue Bailey C. Cerebrospinal Fluid. *Clinical Biochemistry of Domestic Animals.* Elsevier Inc. 2008:769-819. doi:10.1016/B978-0-12-370491-7.00026-X
 119. Telano LN, Baker S. Physiology, Cerebral Spinal Fluid (CSF). *StatPearls Publishing.* 2018.

REFERENCES

120. Krishnamurthy S, Li J. New concepts in the pathogenesis of hydrocephalus. *Transl Pediatr.* 2014;3(3):185-18594. doi:10.3978/j.issn.2224-4336.2014.07.02
121. Whish S, Dziegielewska KM, Møllgård K, et al. The inner csf-brain barrier: Developmentally controlled access to the brain via intercellular junctions. *Front Neurosci.* 2015;9(FEB). doi:10.3389/fnins.2015.00016
122. Khasawneh A, Garling R, Harris C. Cerebrospinal fluid circulation: What do we know and how do we know it? *Brain Circ.* 2018;4(1):14. doi:10.4103/bc.bc_3_18
123. Irani DN. Properties and Composition of Normal Cerebrospinal Fluid. *Cerebrospinal Fluid in Clinical Practice. Elsevier Inc.* 2009:69-89. doi:10.1016/B978-141602908-3.50013-3
124. Ziemssen T, Akgün K, Brück W. Molecular biomarkers in multiple sclerosis. *J Neuroinflammation.* 2019;16(1). doi:10.1186/s12974-019-1674-2
125. Sádaba MC, González Porqué P, Masjuan J, Alvarez-Cermeño JC, Bootello A, Villar LM. An ultrasensitive method for the detection of oligoclonal IgG bands. *J Immunol Methods.* 2004;284(1-2):141-145.
126. Tintore M, Rovira À, Río J, et al. Defining high, medium and low impact prognostic factors for developing multiple sclerosis. *Brain.* 2015;138(7):1863-1874. doi:10.1093/brain/awv105
127. Gasperi C, Salmen A, Antony G, et al. Association of Intrathecal Immunoglobulin G Synthesis with Disability Worsening in Multiple Sclerosis. *JAMA Neurology.* Vol 76. *American Medical Association.* 2019:841-849. doi:10.1001/jamaneurol.2019.0905
128. Toscano S, Patti F. CSF biomarkers in multiple sclerosis: beyond neuroinflammation. *Neuroimmunol Neuroinflammation.* 2020;2020. doi:10.20517/2347-8659.2020.12
129. Paul A, Comabella M, Gandhi R. Biomarkers in multiple sclerosis. *Cold Spring Harb Perspect Med.* 2019;9(3). doi:10.1101/cshperspect.a029058
130. Deisenhammer F, Zetterberg H, Fitzner B, Zettl UK. The cerebrospinal fluid in multiple sclerosis. *Front Immunol.* 2019;10(APR):726. doi:10.3389/fimmu.2019.00726
131. Lin J, Bettin P, Lee JK, Ho JK, Sadiq SA. Cerebrospinal fluid and serum JC virus antibody detection in multiple sclerosis patients treated with natalizumab. *J Neuroimmunol.* 2013;261(1-2):123-128. doi:10.1016/j.jneuroim.2013.05.009
132. Quintana E, Coll C, Salavedra-Pont J, et al. Cognitive impairment in early stages of multiple sclerosis is associated with high cerebrospinal fluid levels of chitinase 3-like 1 and neurofilament light chain. *Eur J Neurol.* 2018;25(9):1189-1191. doi:10.1111/ene.13687
133. Quintana E, Ortega FJ, Robles-Cedeño R, et al. miRNAs in cerebrospinal fluid identify patients with MS and specifically those with lipid-specific oligoclonal IgM

- bands. *Mult Scler*. 2017;23(13):1716-1726. doi:10.1177/1352458516684213
134. Thangarajh M, Gomez-Rial J, Hedström AK, et al. Lipid-specific immunoglobulin M in CSF predicts adverse long-term outcome in multiple sclerosis. *Mult Scler*. 2008;14(9):1208-1213. doi:10.1177/1352458508095729
135. Villar LM, Casanova B, Ouamara N, et al. Immunoglobulin M oligoclonal bands: Biomarker of targetable inflammation in primary progressive multiple sclerosis. *Ann Neurol*. 2014;76(2):231-240. doi:10.1002/ana.24190
136. Pfuhl C, Grittner U, Gieß RM, et al. Intrathecal IgM production is a strong risk factor for early conversion to multiple sclerosis. *Neurology*. 2019;93(15):e1439-e1451. doi:10.1212/WNL.00000000000008237
137. Huss A, Abdelhak A, Halbgebauer S, et al. Intrathecal immunoglobulin M production: A promising high-risk marker in clinically isolated syndrome patients. *Ann Neurol*. 2018;83(5):1032-1036. doi:10.1002/ana.25237
138. Durante L, Zaaraoui W, Rico A, et al. Intrathecal synthesis of IgM measured after a first demyelinating event suggestive of multiple sclerosis is associated with subsequent MRI brain lesion accrual. *Mult Scler*. 2012;18(5):587-591. doi:10.1177/1352458511424589
139. Klein A, Selter RC, Hapfelmeier A, et al. CSF parameters associated with early MRI activity in patients with MS. *Neurol Neuroimmunol NeuroInflammation*. 2019;6(4):573. doi:10.1212/NXI.0000000000000573
140. Fonderico M, Biagioli T, Lanzilao L, et al. Prognostic role of intrathecal IgM synthesis in multiple sclerosis: Results from a clinical series. *Mult Scler*. 2020. doi:10.1177/1352458520907913
141. Huang J, Khademi M, Fugger L, et al. Inflammation-related plasma and CSF biomarkers for multiple sclerosis. *Proc Natl Acad Sci U S A*. 2020;117(23):12952-12960. doi:10.5878/p6dc-8149
142. Kapoor R, Smith KE, Allegretta M, et al. Serum neurofilament light as a biomarker in progressive multiple sclerosis. *Neurology*. 2020;95(10):436-444. doi:10.1212/WNL.0000000000010346
143. Huynh JL, Casaccia P. Epigenetic mechanisms in multiple sclerosis: Implications for pathogenesis and treatment. *Lancet Neurol*. 2013;12(2):195-206. doi:10.1016/S1474-4422(12)70309-5
144. Tronick E, Hunter RG, Waddington, Dynamic systems, and epigenetics. *Front Behav Neurosci*. 2016;10(JUN):107. doi:10.3389/fnbeh.2016.00107
145. Ganesan A, Arimondo PB, Rots MG, Jeronimo C, Berdasco M. The timeline of epigenetic drug discovery: From reality to dreams. *Clin Epigenetics*. 2019;11(1). doi:10.1186/s13148-019-0776-0

REFERENCES

146. Koch MW, Metz LM, Kovalchuk O. Epigenetics and miRNAs in the diagnosis and treatment of multiple sclerosis. *Trends Mol Med.* 2013;19(1):23-30. doi:10.1016/j.molmed.2012.10.008
147. Zhou Y, Simpson S, Holloway AF, Charlesworth J, Van Der Mei I, Taylor B V. The potential role of epigenetic modifications in the heritability of multiple sclerosis. *Mult Scler.* 2014;20(2):135-140. doi:10.1177/1352458514520911
148. Aslani S, Jafari N, Javan MR, Karami J, Ahmadi M, Jafarnejad M. Epigenetic Modifications and Therapy in Multiple Sclerosis. *NeuroMolecular Med.* 2017;19(1):11-23. doi:10.1007/s12017-016-8422-x
149. Riggs AD. X inactivation, differentiation, and DNA methylation. *Cytogenet Genome Res.* 1975;14(1):9-25. doi:10.1159/000130315
150. Holliday R, Pugh J. DNA modification mechanisms and gene activity during development. *Science.* 1975;187(4173):226-232.
151. Piket E, Zheleznyakova GY, Kular L, Jagodic M. Small non-coding RNAs as important players, biomarkers and therapeutic targets in multiple sclerosis: A comprehensive overview. *J Autoimmun.* 2019;101:17-25. doi:10.1016/j.jaut.2019.04.002
152. Wei JW, Huang K, Yang C, Kang CS. Non-coding RNAs as regulators in epigenetics (Review). *Oncol Rep.* 2017;37(1):3-9. doi:10.3892/or.2016.5236
153. Han BW, Zamore PD. piRNAs. *CURBIO.* 2014;24:R730-R733. doi:10.1111/j.1748-7692.2011.00495.x
154. Ma Y, Liu Y, Jiang Z. CircRNAs: A new perspective of biomarkers in the nervous system. *Biomed Pharmacother.* 2020;128:110251. doi:10.1016/j.biopha.2020.110251
155. Zurawska A, Mycko MP, Selmaj KW. Circular RNAs as a novel layer of regulatory mechanism in multiple sclerosis. *J Neuroimmunol.* 2019;334:576971. doi:10.1016/j.jneuroim.2019.576971
156. Flores-Concha M, Oñate ÁA. Long Non-coding RNAs in the Regulation of the Immune Response and Trained Immunity. *Front Genet.* 2020;11:718. doi:10.3389/fgene.2020.00718
157. Bianchi M, Renzini A, Adamo S, Moresi V. Coordinated actions of microRNAs with other epigenetic factors regulate skeletal muscle development and adaptation. *Int J Mol Sci.* 2017;18(4). doi:10.3390/ijms18040840
158. ENCODE: Encyclopedia of DNA Elements - ENCODE. <https://www.encodeproject.org/>. Accessed October 26, 2020.
159. Roadmap Epigenomics Project - Data. <http://www.roadmapepigenomics.org/data/>. Accessed October 26, 2020.
160. Baranzini SE, Mudge J, van Velkinburgh JC, et al. Genome, epigenome and RNA

REFERENCES

- sequences of monozygotic twins discordant for multiple sclerosis. *Nature*. 2010;464(7293):1351-1356. doi:10.1038/nature08990
161. Souren NY, Gerdes LA, Lutsik P, et al. DNA methylation signatures of monozygotic twins clinically discordant for multiple sclerosis. *Nat Commun*. 2019;10(1). doi:10.1038/s41467-019-09984-3
 162. Huynh JL, Garg P, Thin TH, et al. Epigenome-wide differences in pathology-free regions of multiple sclerosis-affected brains. *Nat Neurosci*. 2014;17(1):121-130. doi:10.1038/nn.3588
 163. Chomyk AM, Volsko C, Tripathi A, et al. DNA methylation in demyelinated multiple sclerosis hippocampus. *Sci Rep*. 2017;7(1):1-10. doi:10.1038/s41598-017-08623-5
 164. Maltby VE, Graves MC, Lea RA, et al. Genome-wide DNA methylation profiling of CD8+ T cells shows a distinct epigenetic signature to CD4+ T cells in multiple sclerosis patients. *Clin Epigenetics*. 2015;7(1). doi:10.1186/s13148-015-0152-7
 165. Liggett T, Melnikov A, Tilwalli S, et al. Methylation patterns of cell-free plasma DNA in relapsing-remitting multiple sclerosis. *J Neurol Sci*. 2010;290(1-2):16-21. doi:10.1016/j.jns.2009.12.018
 166. Neven KY, Piola M, Angelici L, et al. Repetitive element hypermethylation in multiple sclerosis patients. *BMC Genet*. 2016;17(1):84. doi:10.1186/s12863-016-0395-0
 167. Pinto-Medel MJ, Oliver-Martos B, Urbaneja-Romero P, et al. Global methylation correlates with clinical status in multiple sclerosis patients in the first year of IFNbeta treatment. *Sci Rep*. 2017;7(1):1-9. doi:10.1038/s41598-017-09301-2
 168. Dunaeva M, Derksen M, Pruijn GJM. LINE-1 Hypermethylation in Serum Cell-Free DNA of Relapsing Remitting Multiple Sclerosis Patients. *Mol Neurobiol*. 2018;55(6):4681-4688. doi:10.1007/s12035-017-0679-z
 169. Castro K, Ntranos A, Amatruda M, et al. Body Mass Index in Multiple Sclerosis modulates ceramide-induced DNA methylation and disease course. *EBioMedicine*. 2019;43:392-410. doi:10.1016/j.ebiom.2019.03.087
 170. Ayuso T, Aznar P, Soriano L, et al. Vitamin D receptor gene is epigenetically altered and transcriptionally up-regulated in multiple sclerosis. *PLoS One*. 2017;12(3). doi:10.1371/journal.pone.0174726
 171. Field J, Fox A, Jordan MA, et al. Interleukin-2 receptor- α proximal promoter hypomethylation is associated with multiple sclerosis. *Genes Immun*. 2017;18(2):59-66. doi:10.1038/gene.2016.50
 172. Castro K, Casaccia P. Epigenetic modifications in brain and immune cells of multiple sclerosis patients. *Mult Scler*. 2018;24(1):69-74. doi:10.1177/1352458517737389

REFERENCES

173. Ruhrmann S, Ewing E, Piket E, et al. Hypermethylation of MIR21 in CD4+ T cells from patients with relapsing-remitting multiple sclerosis associates with lower miRNA-21 levels and concomitant up-regulation of its target genes. *Mult Scler.* 2018;24(10):1288-1300. doi:10.1177/1352458517721356
174. Ntranos A, Ntranos V, Bonnefil V, et al. Fumarates target the metabolic-epigenetic interplay of brain-homing T cells in multiple sclerosis. *Brain.* 2019;142(3):647-661. doi:10.1093/brain/awy344
175. He H, Hu Z, Xiao H, Zhou F, Yang B. The tale of histone modifications and its role in multiple sclerosis. *Hum Genomics.* 2018;12(1):1-12. doi:10.1186/s40246-018-0163-5
176. Pedre X, Mastronardi F, Bruck W, López-Rodas G, Kuhlmann T, Casaccia P. Changed histone acetylation patterns in normal-appearing white matter and early multiple sclerosis lesions. *J Neurosci.* 2011;31(9):3435-3445. doi:10.1523/JNEUROSCI.4507-10.2011
177. Lovett-Racke AE, Cravens PD, Gocke AR, Racke MK, Stüve O. Therapeutic potential of small interfering RNA for central nervous system diseases. *Arch Neurol.* 2005;62(12):1810-1813. doi:10.1001/archneur.62.12.1810
178. Wang X, Zheng X, Ma C, Zhao L. Role of TRIF small interference RNA (siRNA) in chronic experimental allergic encephalomyelitis (EAE). *Med Sci Monit.* 2015;21:2583-2587. doi:10.12659/MSM.894564
179. Kim KW. PIWI proteins and piRNAs in the nervous system. *Mol Cells.* 2019;42(12):828-835. doi:10.14348/molcells.2019.0241
180. Cardamone G, Paraboschi EM, Rimoldi V, Duga S, Soldà G, Asselta R. The characterization of GSDMB splicing and backsplicing profiles identifies novel isoforms and a circular RNA that are dysregulated in multiple sclerosis. *Int J Mol Sci.* 2017;18(3):576. doi:10.3390/ijms18030576
181. Iparraguirre L, Muñoz-Culla M, Prada-Luengo I, Castillo-Triviño T, Olascoaga J, Otaegui D. Circular RNA profiling reveals that circular RNAs from ANXA2 can be used as new biomarkers for multiple sclerosis. *Hum Mol Genet.* 2017;26(18):3564-3572. doi:10.1093/hmg/ddx243
182. Yang X, Wu Y, Zhang B, Ni B. Noncoding RNAs in multiple sclerosis. *Clin Epigenetics.* 2018;10(1). doi:10.1186/s13148-018-0586-9
183. Paraboschi EM, Cardamone G, Soldà G, Duga S, Asselta R. Interpreting Non-coding Genetic Variation in Multiple Sclerosis Genome-Wide Associated Regions. *Front Genet.* 2018;9:647. doi:10.3389/fgene.2018.00647
184. Cardamone G, Paraboschi EM, Soldà G, et al. Not only cancer: The long non-coding RNA MALAT1 affects the repertoire of alternatively spliced transcripts and circular RNAs in multiple sclerosis. *Hum Mol Genet.* 2019;28(9):1414-1428. doi:10.1093/hmg/ddy438

REFERENCES

185. Santoro M, Nociti V, Lucchini M, De Fino C, Losavio FA, Mirabella M. Expression Profile of Long Non-Coding RNAs in Serum of Patients with Multiple Sclerosis. *J Mol Neurosci*. 2016;59(1):18-23. doi:10.1007/s12031-016-0741-8
186. Zhang F, Gao C, Ma XF, et al. Expression Profile of Long Noncoding RNAs in Peripheral Blood Mononuclear Cells from Multiple Sclerosis Patients. *CNS Neurosci Ther*. 2016;22(4):298-305. doi:10.1111/cns.12498
187. Eftekharian MM, Ghafouri-Fard S, Soudyab M, et al. Expression Analysis of Long Non-coding RNAs in the Blood of Multiple Sclerosis Patients. *J Mol Neurosci*. 2017;63(3-4):333-341. doi:10.1007/s12031-017-0982-1
188. Gupta M, Martens K, Metz LM, De Koning J, Pfeffer G. Long noncoding RNAs associated with phenotypic severity in multiple sclerosis. *Mult Scler Relat Disord*. 2019;36:101407. doi:10.1016/j.msard.2019.101407
189. Bhaskaran M, Mohan M. MicroRNAs: History, Biogenesis, and Their Evolving Role in Animal Development and Disease. *Vet Pathol*. 2014;51(4):759-774. doi:10.1177/0300985813502820
190. Ryan B, Joilin G, Williams JM. Plasticity-related microRNA and their potential contribution to the maintenance of long-term potentiation. *Front Mol Neurosci*. 2015;8(FEB):1-17. doi:10.3389/fnmol.2015.00004
191. Sempere LF. Celebrating 25 years of microRNA research: From discovery to clinical application. *Int J Mol Sci*. 2019;20(8). doi:10.3390/ijms20081987
192. Dexheimer PJ, Cochella L. MicroRNAs: From Mechanism to Organism. *Front Cell Dev Biol*. 2020;8:409. doi:10.3389/fcell.2020.00409
193. Almeida MI, Reis RM, Calin GA. MicroRNA history: Discovery, recent applications, and next frontiers. *Mutat Res - Fundam Mol Mech Mutagen*. 2011;717(1-2):1-8. doi:10.1016/j.mrfmmm.2011.03.009
194. Lee RC, Feinbaum RL, Ambros V. The *C. elegans* heterochronic gene *lin-4* encodes small RNAs with antisense complementarity to *lin-14*. *Cell*. 1993;75(5):843-854. doi:10.1016/0092-8674(93)90529-Y
195. Wightman B, Ha I, Ruvkun G. Posttranscriptional regulation of the heterochronic gene *lin-14* by *lin-4* mediates temporal pattern formation in *C. elegans*. *Cell*. 1993;75(5):855-862. doi:10.1016/0092-8674(93)90530-4
196. Reinhart BJ, Slack FJ, Basson M, et al. The 21-nucleotide *let-7* RNA regulates developmental timing in *Caenorhabditis elegans*. *Nature*. 2000;403(6772):901-906. doi:10.1038/35002607
197. Slack FJ, Basson M, Liu Z, Ambros V, Horvitz HR, Ruvkun G. The *lin-41* RBCC gene acts in the *C. elegans* heterochronic pathway between the *let-7* regulatory RNA and the *LIN-29* transcription factor. *Mol Cell*. 2000;5(4):659-669. doi:10.1016/S1097-2765(00)80245-2

REFERENCES

198. Lee RC, Ambros V. An extensive class of small RNAs in *Caenorhabditis elegans*. *Science*. 2001;294(5543):862-864. doi:10.1126/science.1065329
199. Lagos-Quintana M, Rauhut R, Lendeckel W, Tuschl T. Identification of novel genes coding for small expressed RNAs. *Science*. 2001;294(5543):853-858. doi:10.1126/science.1064921
200. Pasquinelli AE, Reinhart BJ, Slack F, et al. Conservation of the sequence and temporal expression of *let-7* heterochronic regulatory RNA. *Nature*. 2000;408(6808):86-89. doi:10.1038/35040556
201. Griffiths-Jones S, Grocock RJ, van Dongen S, Bateman A, Enright AJ. miRBase: microRNA sequences, targets and gene nomenclature. *Nucleic Acids Res*. 2006;34:D140-D144. doi:10.1093/nar/gkj112
202. Kozomara A, Birgaoanu M, Griffiths-Jones S. MiRBase: From microRNA sequences to function. *Nucleic Acids Res*. 2019;47(D1):D155-D162. doi:10.1093/nar/gky1141
203. Matsuyama H, Suzuki HI. Systems and synthetic microRNA biology: From biogenesis to disease pathogenesis. *Int J Mol Sci*. 2020;21(1). doi:10.3390/ijms21010132
204. Lee Y, Ahn C, Han J, et al. The nuclear RNase III Drosha initiates microRNA processing. *Nature*. 2003;425(6956):415-419. doi:10.1038/nature01957
205. O'Brien J, Hayder H, Zayed Y, Peng C. Overview of microRNA biogenesis, mechanisms of actions, and circulation. *Front Endocrinol (Lausanne)*. 2018;9:402. doi:10.3389/fendo.2018.00402
206. Yi R, Qin Y, Macara IG, Cullen BR. Exportin-5 mediates the nuclear export of pre-microRNAs and short hairpin RNAs. *Genes Dev*. 2003;17(24):3011-3016. doi:10.1101/gad.1158803
207. Reichholf B, Herzog VA, Fasching N, Manzenreither RA, Sowemimo I, Ameres SL. Time-Resolved Small RNA Sequencing Unravels the Molecular Principles of MicroRNA Homeostasis. *Mol Cell*. 2019;75(4):756-768.e7. doi:10.1016/j.molcel.2019.06.018
208. Wahid F, Shehzad A, Khan T, Kim YY. MicroRNAs: Synthesis, mechanism, function, and recent clinical trials. *Biochim Biophys Acta - Mol Cell Res*. 2010;1803(11):1231-1243. doi:10.1016/j.bbamcr.2010.06.013
209. Gebert LFR, MacRae IJ. Regulation of microRNA function in animals. *Nat Rev Mol Cell Biol*. 2019;20(1):21-37. doi:10.1038/s41580-018-0045-7
210. Bartel DP. MicroRNAs: Target Recognition and Regulatory Functions. *Cell*. 2009;136(2):215-233. doi:10.1016/j.cell.2009.01.002
211. MacFarlane L-A, R. Murphy P. MicroRNA: Biogenesis, Function and Role in Cancer. *Curr Genomics*. 2010;11(7):537-561. doi:10.2174/138920210793175895

212. Xiao M, Li J, Li W, et al. MicroRNAs activate gene transcription epigenetically as an enhancer trigger. *RNA Biol.* 2017;14(10):1326-1334. doi:10.1080/15476286.2015.1112487
213. Jopling CL, Yi MK, Lancaster AM, Lemon SM, Sarnow P. Molecular biology: Modulation of hepatitis C virus RNA abundance by a liver-specific MicroRNA. *Science.* 2005;309(5740):1577-1581. doi:10.1126/science.1113329
214. Zhang L, Ding H, Zhang Y, Wang Y, Zhu W, Li P. Circulating MicroRNAs: Biogenesis and Clinical Significance in Acute Myocardial Infarction. *Front Physiol.* 2020;11:1088. doi:10.3389/fphys.2020.01088
215. Sohel MH. Extracellular/Circulating MicroRNAs: Release Mechanisms, Functions and Challenges. *Achiev Life Sci.* 2016;10(2):175-186. doi:10.1016/j.als.2016.11.007
216. Cui M, Wang H, Yao X, et al. Circulating MicroRNAs in Cancer: Potential and Challenge. *Front Genet.* 2019;10. doi:10.3389/fgene.2019.00626
217. Kacperska MJ, Walenczak J, Tomasik B. Plasmatic microRNA as potential biomarkers of multiple sclerosis: Literature review. *Adv Clin Exp Med.* 2016;25(4):775-779. doi:10.17219/acem/60098
218. Théry C, Witwer KW, Aikawa E, et al. Minimal information for studies of extracellular vesicles 2018 (MISEV2018): a position statement of the International Society for Extracellular Vesicles and update of the MISEV2014 guidelines. *J Extracell Vesicles.* 2018;7(1). doi:10.1080/20013078.2018.1535750
219. Battistelli M, Falcieri E. Apoptotic bodies: Particular extracellular vesicles involved in intercellular communication. *Biology (Basel).* 2020;9(1). doi:10.3390/biology9010021
220. Mycko MP, Baranzini SE. microRNA and exosome profiling in multiple sclerosis. *Mult Scler.* January 2020:135245851987930. doi:10.1177/1352458519879303
221. O'Brien K, Breyne K, Ughetto S, Laurent LC, Breakefield XO. RNA delivery by extracellular vesicles in mammalian cells and its applications. *Nat Rev Mol Cell Biol.* 2020;21(10):585-606. doi:10.1038/s41580-020-0251-y
222. Valadi H, Ekström K, Bossios A, Sjöstrand M, Lee JJ, Lötvall JO. Exosome-mediated transfer of mRNAs and microRNAs is a novel mechanism of genetic exchange between cells. *Nat Cell Biol.* 2007;9(6):654-659. doi:10.1038/ncb1596
223. Bär C, Thum T, De Gonzalo-Calvo D. Circulating miRNAs as mediators in cell-to-cell communication. *Epigenomics.* 2019;11(2):111-113. doi:10.2217/epi-2018-0183
224. Turchinovich A, Samatov TR, Tonevitsky AG, Burwinkel B. Circulating miRNAs: Cell-cell communication function? *Front Genet.* 2013;4. doi:10.3389/fgene.2013.00119
225. Ye J, Xu M, Tian X, Cai S, Zeng S. Research advances in the detection of miRNA. *J Pharm Anal.* 2019;9(4):217-226. doi:10.1016/j.jpha.2019.05.004

REFERENCES

226. Tam S, De Borja R, Tsao MS, Mcpherson JD. Robust global microRNA expression profiling using next-generation sequencing technologies. *Lab Investig.* 2014;94(3):350-358. doi:10.1038/labinvest.2013.157
227. Coenen-Stass AML, Magen I, Brooks T, et al. Evaluation of methodologies for microRNA biomarker detection by next generation sequencing. *RNA Biol.* 2018;15(8):1133-1145. doi:10.1080/15476286.2018.1514236
228. Tribolet L, Kerr E, Cowled C, et al. MicroRNA Biomarkers for Infectious Diseases: From Basic Research to Biosensing. *Front Microbiol.* 2020;11. doi:10.3389/fmicb.2020.01197
229. Poel D, Buffart TE, Oosterling-Jansen J, Verheul HMW, Voortman J. Evaluation of several methodological challenges in circulating miRNA qPCR studies in patients with head and neck cancer. *Exp Mol Med.* 2018;50(3):454. doi:10.1038/emm.2017.288
230. Moldovan L, Batte KE, Trgovcich J, Wisler J, Marsh CB, Piper M. Methodological challenges in utilizing miRNAs as circulating biomarkers. *J Cell Mol Med.* 2014;18(3):371-390. doi:10.1111/jcmm.12236
231. Wang K, Yuan Y, Cho J-H, McClarty S, Baxter D, Galas DJ. Comparing the MicroRNA Spectrum between Serum and Plasma. Ahuja SK, ed. *PLoS One.* 2012;7(7):e41561. doi:10.1371/journal.pone.0041561
232. Petzold A, Altintas A, Andreoni L, et al. Neurofilament ELISA validation. *J Immunol Methods.* 2010;352(1-2):23-31. doi:10.1016/j.jim.2009.09.014
233. Bargaje R, Hariharan M, Scaria V, Pillai B. Consensus miRNA expression profiles derived from interplatform normalization of microarray data. *RNA.* 2010;16(1):16-25. doi:10.1261/rna.1688110
234. Taylor SC, Nadeau K, Abbasi M, Lachance C, Nguyen M, Fenrich J. The Ultimate qPCR Experiment: Producing Publication Quality, Reproducible Data the First Time. *Trends Biotechnol.* 2019;37(7):761-774. doi:10.1016/j.tibtech.2018.12.002
235. Bustin S, Dhillon HS, Kirvell S, et al. Variability of the reverse transcription step: Practical implications. *Clin Chem.* 2015;61(1):202-212. doi:10.1373/clinchem.2014.230615
236. Ferlinz A, Miller C, Formosa R, Lee KY. Gene expression analysis of both mRNA and miRNA on the same TaqMan[®] Array Card: Development of a pancreatic tumor tissue classification methodology. *Methods.* 2013;59:174-178. doi:10.1016/j.jymeth.2012.09.014
237. Chen Y, Gelfond JAL, McManus LM, Shireman PK. Reproducibility of quantitative RT-PCR array in miRNA expression profiling and comparison with microarray analysis. *BMC Genomics.* 2009;10:407. doi:10.1186/1471-2164-10-407
238. Fritsche L, Teuber - Hanselmann S, Soub D, Harnisch K, Mairinger F, Junker A.

- MicroRNA profiles of MS gray matter lesions identify modulators of the synaptic protein synaptotagmin - 7. *Brain Pathol.* 2020;30(3):524-540. doi:10.1111/bpa.12800
239. Jagot F, Davoust N. Is it worth considering circulating microRNAs in multiple sclerosis? *Front Immunol.* 2016;7(APR):1. doi:10.3389/fimmu.2016.00129
240. Haghikia A, Haghikia A, Hellwig K, et al. Regulated microRNAs in the CSF of patients with multiple sclerosis: A case-control study. *Neurology.* 2012;79(22):2166-2170. doi:10.1212/WNL.0b013e3182759621
241. Bergman P, Piket E, Khademi M, et al. Circulating miR-150 in CSF is a novel candidate biomarker for multiple sclerosis. *Neurol Neuroimmunol Neuroinflammation.* 2016;3(3):e219. doi:10.1212/NXI.0000000000000219
242. Perdaens O, Dang HA, D'Auria L, van Pesch V. CSF microRNAs discriminate MS activity and share similarity to other neuroinflammatory disorders. *Neurol Neuroimmunol neuroinflammation.* 2020;7(2):673. doi:10.1212/NXI.0000000000000673
243. Ahlbrecht J, Martino F, Pul R, et al. Deregulation of microRNA-181c in cerebrospinal fluid of patients with clinically isolated syndrome is associated with early conversion to relapsing-remitting multiple sclerosis. *Mult Scler.* 2016;22(9):1202-1214. doi:10.1177/1352458515613641
244. Kramer S, Haghikia A, Bang C, et al. Elevated levels of miR-181c and miR-633 in the CSF of patients with MS: A validation study. *Neurol Neuroimmunol neuroinflammation.* 2019;6(6):e623. doi:10.1212/NXI.0000000000000623
245. Cortez MA, Welsh JW, Calin GA. Circulating MicroRNAs as noninvasive biomarkers in breast cancer. *Recent Results Cancer Res.* 2012;195:151-161. doi:10.1007/978-3-642-28160-0_13
246. Manna I, Iaccino E, Dattilo V, et al. Exosome-associated miRNA profile as a prognostic tool for therapy response monitoring in multiple sclerosis patients. *FASEB J.* 2018;32(8):4241-4246. doi:10.1096/fj.201701533R
247. Ebrahimkhani S, Vafae F, Young PE, et al. Exosomal microRNA signatures in multiple sclerosis reflect disease status. *Sci Rep.* 2017;7(1):14293. doi:10.1038/s41598-017-14301-3
248. Niwald M, Migdalska-Sęk M, Brzezińska-Lasota E, Miller E. Evaluation of Selected MicroRNAs Expression in Remission Phase of Multiple Sclerosis and Their Potential Link to Cognition, Depression, and Disability. *J Mol Neurosci.* 2017;63(3-4):275-282. doi:10.1007/s12031-017-0977-y
249. Zhang J, Cheng Y, Cui W, Li M, Li B, Guo L. MicroRNA-155 modulates Th1 and Th17 cell differentiation and is associated with multiple sclerosis and experimental autoimmune encephalomyelitis. *J Neuroimmunol.* 2014;266(1-2):56-63. doi:10.1016/j.jneuroim.2013.09.019

REFERENCES

250. Regev K, Healy BC, Paul A, et al. Identification of MS-specific serum miRNAs in an international multicenter study. *Neurol Neuroimmunol Neuroinflammation*. 2018;5(5):e491. doi:10.1212/NXI.0000000000000491
251. Regev K, Paul A, Healy B, et al. Comprehensive evaluation of serum microRNAs as biomarkers in multiple sclerosis. *Neurol Neuroimmunol NeuroInflammation*. 2016;3(5). doi:10.1212/NXI.0000000000000267
252. Fenoglio C, Ridolfi E, Cantoni C, et al. Decreased circulating miRNA levels in patients with primary progressive multiple sclerosis. *Mult Scler*. 2013;19(14):1938-1942. doi:10.1177/1352458513485654
253. Ridolfi E, Fenoglio C, Cantoni C, et al. Expression and genetic analysis of microRNAs involved in multiple sclerosis. *Int J Mol Sci*. 2013;14(3):4375-4384. doi:10.3390/ijms14034375
254. Sharaf-Eldin WE, Kishk NA, Gad YZ, et al. Extracellular miR-145, miR-223 and miR-326 expression signature allow for differential diagnosis of immune-mediated neuroinflammatory diseases. *J Neurol Sci*. 2017;383:188-198. doi:10.1016/j.jns.2017.11.014
255. Gandhi R, Healy B, Gholipour T, et al. Circulating MicroRNAs as biomarkers for disease staging in multiple sclerosis. *Ann Neurol*. 2013;73(6):729-740. doi:10.1002/ana.23880
256. Siegel SR, Mackenzie J, Chaplin G, Jablonski NG, Griffiths L. Circulating microRNAs involved in multiple sclerosis. *Mol Biol Rep*. 2012;39(5):6219-6225. doi:10.1007/s11033-011-1441-7
257. Kimura K, Hohjoh H, Fukuoka M, et al. Circulating exosomes suppress the induction of regulatory T cells via let-7i in multiple sclerosis. *Nat Commun*. 2018;9(1):1-14. doi:10.1038/s41467-017-02406-2
258. Kacperska MJ, Jastrzebski K, Tomasik B, Walenczak J, Konarska-Krol M, Glabinski A. Selected Extracellular microRNA as Potential Biomarkers of Multiple Sclerosis Activity – Preliminary Study. *J Mol Neurosci*. 2015;56(1):154-163. doi:10.1007/s12031-014-0476-3
259. Bruinsma IB, van Dijk M, Bridel C, et al. Regulator of oligodendrocyte maturation, miR-219, a potential biomarker for MS. *J Neuroinflammation*. 2017;14(1). doi:10.1186/s12974-017-1006-3
260. Liu Q, Gao Q, Zhang Y, Li Z, Mei X. MicroRNA-590 promotes pathogenic Th17 cell differentiation through targeting Tob1 and is associated with multiple sclerosis. *Biochem Biophys Res Commun*. 2017;493(2):901-908. doi:10.1016/j.bbrc.2017.09.123
261. Wu R, He Q, Chen H, et al. MicroRNA-448 promotes multiple sclerosis development through induction of Th17 response through targeting protein tyrosine phosphatase non-receptor type 2 (PTPN2). *Biochem Biophys Res Commun*.

- 2017;486(3):759-766. doi:10.1016/j.bbrc.2017.03.115
262. Mandolesi G, De Vito F, Musella A, et al. MiR-142-3p is a key regulator of IL-1 β -dependent synaptopathy in neuroinflammation. *J Neurosci*. 2017;37(3):546-561. doi:10.1523/JNEUROSCI.0851-16.2016
263. Lecca D, Marangon D, Coppolino GT, et al. MiR-125a-3p timely inhibits oligodendroglial maturation and is pathologically up-regulated in human multiple sclerosis. *Sci Rep*. 2016;6(1):1-12. doi:10.1038/srep34503
264. Hemond CC, Healy BC, Tauhid S, et al. MRI phenotypes in MS: Longitudinal changes and miRNA signatures. *Neurol Neuroimmunol NeuroInflammation*. 2019;6(2). doi:10.1212/NXI.0000000000000530
265. Vistbakka J, Sumelahti ML, Lehtimäki T, Elovaara I, Hagman S. Evaluation of serum miR-191-5p, miR-24-3p, miR-128-3p, and miR-376c-3 in multiple sclerosis patients. *Acta Neurol Scand*. 2018;138(2):130-136. doi:10.1111/ane.12921
266. Regev K, Healy BC, Khalid F, et al. Association between serum MicroRNAs and magnetic resonance imaging measures of multiple sclerosis severity. *JAMA Neurol*. 2017;74(3):275-285. doi:10.1001/jamaneurol.2016.5197
267. Selmaj I, Cichalewska M, Namiecinska M, et al. Global exosome transcriptome profiling reveals biomarkers for multiple sclerosis. *Ann Neurol*. 2017;81(5):703-717. doi:10.1002/ana.24931
268. Vistbakka J, Elovaara I, Lehtimäki T, Hagman S. Circulating microRNAs as biomarkers in progressive multiple sclerosis. *Mult Scler*. 2017;23(3):403-412. doi:10.1177/1352458516651141
269. Mancuso R, Hernis A, Agostini S, Rovaris M, Caputo D, Clerici M. MicroRNA-572 expression in multiple sclerosis patients with different patterns of clinical progression. *J Transl Med*. 2015;13(1):148. doi:10.1186/s12967-015-0504-2
270. Sáenz-Cuesta M, Alberro A, Muñoz-Culla M, et al. The first dose of fingolimod affects circulating extracellular vesicles in multiple sclerosis patients. *Int J Mol Sci*. 2018;19(8). doi:10.3390/ijms19082448
271. Giovannelli I, Martelli F, Repice A, Massacesi L, Azzi A, Giannecchini S. Detection of JCPyV microRNA in blood and urine samples of multiple sclerosis patients under natalizumab therapy. *J Neurovirol*. 2015;21(6):666-670. doi:10.1007/s13365-015-0325-3
272. Søndergaard HB, Hesse D, Krakauer M, Sørensen PS, Sellebjerg F. Differential microRNA expression in blood in multiple sclerosis. *Mult Scler*. 2013;19(14):1849-1857. doi:10.1177/1352458513490542
273. Zhang H, Jarjour AA, Boyd A, Williams A. Central nervous system remyelination in culture - A tool for multiple sclerosis research. *Exp Neurol*. 2011;230(1):138-148. doi:10.1016/j.expneurol.2011.04.009

REFERENCES

274. Thermo Fisher Scientific. TaqMan® Advanced MiRNA Assays Single-Tube Assays for Use with: TaqMan® Advanced MiRNA CDNA Synthesis Kit. 2016. Pub No. 100027897. Rev. C.
275. Thermo Fisher Scientific. TaqMan Advanced MiRNA Assays User Guide—TaqMan OpenArray Plates, Pub. No. MAN0016124, Rev. B.0.
276. Ortega FJ, Mercader JM, Catalan V, et al. Targeting the Circulating MicroRNA Signature of Obesity. *Clin Chem.* 2013;59(5):781-792. doi:10.1373/clinchem.2012.195776
277. Bustin SA, Benes V, Garson JA, et al. The MIQE guidelines: Minimum information for publication of quantitative real-time PCR experiments. *Clin Chem.* 2009;55(4):611-622. doi:10.1373/clinchem.2008.112797
278. Marabita F, de Candia P, Torri A, Tegnér J, Abrignani S, Rossi RL. Normalization of circulating microRNA expression data obtained by quantitative real-time RT-PCR. *Brief Bioinform.* 2016;17(2):204-212. doi:10.1093/bib/bbv056
279. Mar JC, Kimura Y, Schroder K, et al. Data-driven normalization strategies for high-throughput quantitative RT-PCR. *BMC Bioinformatics.* 2009;10. doi:10.1186/1471-2105-10-110
280. Andersen CL, Jensen JL, Ørntoft TF. Normalization of real-time quantitative reverse transcription-PCR data: A model-based variance estimation approach to identify genes suited for normalization, applied to bladder and colon cancer data sets. *Cancer Res.* 2004;64(15):5245-5250. doi:10.1158/0008-5472.CAN-04-0496
281. Vandesompele J, De Preter K, Pattyn F, et al. Accurate normalization of real-time quantitative RT-PCR data by geometric averaging of multiple internal control genes. *Genome Biol.* 2002;3(7). doi:10.1186/gb-2002-3-7-research0034
282. Rao X, Huang X, Zhou Z, Lin X. An improvement of the $2^{-\Delta\Delta CT}$ method for quantitative real-time polymerase chain reaction data analysis. *Biostat Bioinforma Biomath.* 2013;3(3):71-85.
283. Chou CH, Shrestha S, Yang CD, et al. miRTarBase update 2018: a resource for experimentally validated microRNA-target interactions. *Nucleic Acids Res.* 2018;46(D1):D296-D302. doi:10.1093/nar/gkx1067
284. Kuleshov M V., Jones MR, Rouillard AD, et al. Enrichr: a comprehensive gene set enrichment analysis web server 2016 update. *Nucleic Acids Res.* 2016;44(W1):W90-W97. doi:10.1093/nar/gkw377
285. Supek F, Bošnjak M, Škunca N, Šmuc T. REVIGO Summarizes and Visualizes Long Lists of Gene Ontology Terms. Gibas C, ed. *PLoS One.* 2011;6(7):e21800. doi:10.1371/journal.pone.0021800
286. Shannon P, Markiel A, Ozier O, et al. Cytoscape: A Software Environment for Integrated Models of Biomolecular Interaction Networks. *Genome Res.*

- 2003;13(11):2498-2504. doi:10.1101/gr.1239303
287. Ludwig N, Leidinger P, Becker K, et al. Distribution of miRNA Expression Across Human Tissues. *Nucleic Acids Res.* 2016;44(8):3865-3877. doi: 10.1093/nar/gkw116
288. Lizio M, Harshbarger J, Shimoji H, et al. Gateways to the FANTOM5 promoter level mammalian expression atlas. *Genome Biol.* 2015;16(1):22. doi:10.1186/s13059-014-0560-6
289. Murillo OD, Thistlethwaite W, Rozowsky J, et al. exRNA Atlas Analysis Reveals Distinct Extracellular RNA Cargo Types and Their Carriers Present across Human Biofluids. *Cell.* 2019;177(2):463-477.e15. doi:10.1016/j.cell.2019.02.018
290. de Ronde MWJ, Ruijter JM, Lanfear D, et al. Practical data handling pipeline improves performance of qPCR-based circulating miRNA measurements. *RNA.* 2017;23(5):811-821. doi:10.1261/rna.059063.116
291. Inada K, Okoshi Y, Cho-Isoda Y, et al. Endogenous reference RNAs for microRNA quantitation in formalin-fixed, paraffin-embedded lymph node tissue. *Sci Rep.* 2018;8(1). doi:10.1038/s41598-018-24338-7
292. Thermo Fisher Scientific. Applied Biosystems Standard Curve Analysis Module - User Guide. 2015. Pub. No. MAN0014819, Rev. B.0.
293. McKay KA, Kwan V, Duggan T, Tremlett H. Risk Factors Associated with the Onset of Relapsing-Remitting and Primary Progressive Multiple Sclerosis: A systematic Review. *Biomed Res Int.* 2015;2015(817238).
294. Sidhom Y, Maillart E, Du Montcel ST, et al. Fast multiple sclerosis progression in North Africans. *Neurology.* 2017;88(13):1218-1225. doi:10.1212/WNL.0000000000003762
295. Junker A, Krumbholz M, Eisele S, et al. MicroRNA profiling of multiple sclerosis lesions identifies modulators of the regulatory protein CD47. *Brain.* 2009;132(12):3342-3352. doi:10.1093/brain/awp300
296. Allantaz F, Cheng DT, Bergauer T, et al. Expression Profiling of Human Immune Cell Subsets Identifies miRNA-mRNA Regulatory Relationships Correlated with Cell Type Specific Expression. Schönbach C, ed. *PLoS One.* 2012;7(1):e29979. doi:10.1371/journal.pone.0029979
297. Sospedra M, Martin R. IMMUNOLOGY OF MULTIPLE SCLEROSIS. *Annu Rev Immunol.* 2005;23(1):683-747. doi:10.1146/annurev.immunol.23.021704.115707
298. Giovannoni G, Knappertz V, Steinerman JR, et al. A randomized, placebo-controlled, phase 2 trial of laquinimod in primary progressive multiple sclerosis. *Neurology.* 2020;95(8):e1027-e1040. doi:10.1212/WNL.0000000000010284
299. Kular L, Castelo-Branco G, Jagodic M. Epigenetics and multiple sclerosis. *Neuropsychiatric Disorders and Epigenetics. Elsevier Inc.* 2017:185-213.

REFERENCES

- doi:10.1016/B978-0-12-800226-1.00010-1
300. Stoicea N, Du A, Lakis CD, Tipton C, Arias-Morales CE, Bergese SD. The miRNA journey from theory to practice as a CNS biomarker. *Front Genet.* 2016;7(FEB):11. doi:10.3389/fgene.2016.00011
 301. Weber JA, Baxter DH, Zhang S, et al. The microRNA spectrum in 12 body fluids. *Clin Chem.* 2010;56(11):1733-1741. doi:10.1373/clinchem.2010.147405
 302. Wang WX, Fardo DW, Jicha GA, Nelson PT. A Customized Quantitative PCR MicroRNA Panel Provides a Technically Robust Context for Studying Neurodegenerative Disease Biomarkers and Indicates a High Correlation Between Cerebrospinal Fluid and Choroid Plexus MicroRNA Expression. *Mol Neurobiol.* 2017;54(10):8191-8202. doi:10.1007/s12035-016-0316-2
 303. Applied Biosystems. Applied Biosystems TaqMan ® Low Density Array SUBJECT: Running TaqMan ® Low Density Arrays on 7900HT Real-Time PCR Systems. 2006. User Bulletin.
 304. Farr RJ, Januszewski AS, Joglekar M V., et al. A comparative analysis of high-throughput platforms for validation of a circulating microRNA signature in diabetic retinopathy. *Sci Rep.* 2015;5. doi:10.1038/srep10375
 305. Thermo Fisher Scientific. TaqMan Advanced MiRNA Assays - superior performance for miRNA detection and quantification. 2016. Application note.
 306. Ehtesham N, Khorvash F, Kheirollahi M. miR-145 and miR20a-5p Potentially Mediate Pleiotropic Effects of Interferon-Beta Through Mitogen-Activated Protein Kinase Signaling Pathway in Multiple Sclerosis Patients. *J Mol Neurosci.* 2017;61(1):16-24. doi:10.1007/s12031-016-0851-3
 307. Magner WJ, Weinstock-Guttman B, Rho M, et al. Dicer and microRNA expression in multiple sclerosis and response to interferon therapy. *J Neuroimmunol.* 2016;292:68-78. doi:10.1016/j.jneuroim.2016.01.009
 308. Sheinerman K, Djukic A, Tsivinsky VG, Umansky SR. Brain-enriched microRNAs circulating in plasma as novel biomarkers for Rett syndrome. *PLoS One.* 2019;14(7). doi:10.1371/journal.pone.0218623
 309. Raihan O, Brishti A, Molla MR, et al. The Age-dependent Elevation of miR-335-3p Leads to Reduced Cholesterol and Impaired Memory in Brain. *Neuroscience.* 2018;390:160-173. doi:10.1016/j.neuroscience.2018.08.003
 310. Krishnan SundaramID V, Kumar Sampathkumar N, Massaad C, Grenier J. Optimal use of statistical methods to validate reference gene stability in longitudinal studies. *PLoS One.* 2019;14(7):e0219440. doi:10.1371/journal.pone.0219440
 311. Chan OYW, Keng BMH, Ling MHT. Correlation and variation-based method for identifying reference genes from large datasets. *Electron physician.* 2014;6(1):719-71927. doi:10.14661/2014.719-727

312. Shen Y, Li Y, Ye F, et al. Identification of miR-23a as a novel microRNA normalizer for relative quantification in human uterine cervical tissues. *Exp Mol Med.* 2011;43(6):358-366. doi:10.3858/emm.2011.43.6.039
313. Ma M, Dai J, Tang H, et al. MicroRNA-23a-3p inhibits mucosal melanoma growth and progression through targeting adenylate cyclase 1 and attenuating cAMP and MAPK pathways. *Theranostics.* 2019;9(4):945-960. doi:10.7150/thno.30516
314. Solayman MHM, Langae T, Patel A, et al. Identification of Suitable Endogenous Normalizers for qRT-PCR Analysis of Plasma microRNA Expression in Essential Hypertension. *Mol Biotechnol.* 2016;58(3):179-187. doi:10.1007/s12033-015-9912-z
315. Baraniskin A, Kuhnhen J, Schlegel U, et al. Identification of microRNAs in the cerebrospinal fluid as biomarker for the diagnosis of glioma. *Neuro Oncol.* 2012;14(1):29-33. doi:10.1093/neuonc/nor169
316. Sørensen SS, Nygaard A-B, Carlsen AL, Heegaard NHH, Bak M, Christensen T. Elevation of brain-enriched miRNAs in cerebrospinal fluid of patients with acute ischemic stroke. *Biomark Res.* 2017;5(1):24. doi:10.1186/s40364-017-0104-9
317. de Ronde MWJ, Ruijter JM, Moerland PD, Creemers EE, Pinto-Sietsma S-J. Study Design and qPCR Data Analysis Guidelines for Reliable Circulating miRNA Biomarker Experiments: A Review. *Clin Chem.* 2018;64(9):1308-1318. doi:10.1373/clinchem.2017.285288
318. Hulstaert E, Morlion A, Avila Cobos F, et al. Charting extracellular transcriptomes in The Human Biofluid RNA Atlas. *Cell Rep.* 2020;33(13):108552. doi:10.1016/j.celrep.2020.108552
319. Prokopec SD, Watson JD, Waggott DM, et al. Systematic evaluation of medium-throughput mRNA abundance platforms. *RNA.* 2013;19(1):51-62. doi:10.1261/rna.034710.112
320. Denk J, Boelmans K, Siegismund C, Lassner D, Arlt S, Jahn H. MicroRNA profiling of CSF reveals potential biomarkers to detect Alzheimer's disease. *PLoS One.* 2015;10(5). doi:10.1371/journal.pone.0126423
321. Akers JC, Hua W, Li H, et al. A cerebrospinal fluid microRNA signature as biomarker for glioblastoma. *Oncotarget.* 2017;8(40):68769-68779. doi:10.18632/oncotarget.18332
322. Raoof R, Jimenez-Mateos EM, Bauer S, et al. Cerebrospinal fluid microRNAs are potential biomarkers of temporal lobe epilepsy and status epilepticus. *Sci Rep.* 2017;7(1):3328. doi:10.1038/s41598-017-02969-6
323. Thermo Fisher Scientific. Crt , a Relative Threshold Method for QPCR Data Analysis on the QuantStudio 12K Flex System with OpenArray Technology. 2016. Application note.
324. Willems E, Leyns L, Vandesompele J. Standardization of real-time PCR gene

REFERENCES

- expression data from independent biological replicates. *Anal Biochem.* 2008;379(1):127-129. doi:10.1016/j.ab.2008.04.036
325. Yang Y, Xu Z, Song D. Missing value imputation for microRNA expression data by using a GO-based similarity measure. *BMC Bioinformatics.* 2016;17(1):10. doi:10.1186/s12859-015-0853-0
326. McCall MN, McMurray HR, Land H, Almudevar A. On non-detects in qPCR data. *Bioinformatics.* 2014;30(16):2310-2316. doi:10.1093/bioinformatics/btu239
327. Kopkova A, Sana J, Fadrus P, Slaby O. Cerebrospinal fluid microRNAs as diagnostic biomarkers in brain tumors. *Clin Chem Lab Med.* 2018;56(6).
328. Faraldi M, Gomarasca M, Sansoni V, Perego S, Banfi G, Lombardi G. Normalization strategies differently affect circulating miRNA profile associated with the training status. *Sci Rep.* 2019;9(1):1-13. doi:10.1038/s41598-019-38505-x
329. Pradervand S, Weber J, Thomas J, et al. Impact of normalization on miRNA microarray expression profiling. *RNA.* 2009;15(3):493-501. doi:10.1261/rna.1295509
330. Bolstad BM, Irizarry RA, Åstrand M, Speed TP. A comparison of normalization methods for high density oligonucleotide array data based on variance and bias. *Bioinformatics.* 2003;19(2):185-193. doi:10.1093/bioinformatics/19.2.185
331. Stys PK, Zamponi GW, Van Minnen J, Geurts JJG. Will the real multiple sclerosis please stand up? *Nat Rev Neurosci.* 2012;13(7):507-514. doi:10.1038/nrn3275
332. Juźwik CA, S. Drake S, Zhang Y, et al. microRNA dysregulation in neurodegenerative diseases: A systematic review. *Prog Neurobiol.* 2019;182. doi:10.1016/j.pneurobio.2019.101664
333. Slota JA, Booth SA. MicroRNAs in neuroinflammation: Implications in disease pathogenesis, biomarker discovery and therapeutic applications. *Non-coding RNA.* 2019;5(2). doi:10.3390/ncrna5020035
334. Meinel E, Meister G. MicroRNAs in the CSF macro-advance in MS? *Neurology.* 2012;79(22):2162-2163. doi:10.1212/WNL.0b013e31827597d1
335. Soldán MMP, Novotna M, Zeid NA, et al. Relapses and disability accumulation in progressive multiple sclerosis. *Neurology.* 2015;84(1):81-88. doi:10.1212/WNL.0000000000001094
336. Sola P, Mandrioli J, Simone AM, et al. Primary progressive versus relapsing-onset multiple sclerosis: presence and prognostic value of cerebrospinal fluid oligoclonal IgM. *Mult Scler.* 2011;17(3):303-311. doi:10.1177/1352458510386996
337. Rovira A, Auger C, Alonso J. Magnetic resonance monitoring of lesion evolution in multiple sclerosis. *Ther Adv Neurol Disord.* 2013;6(5):298-310. doi:10.1177/1756285613484079
338. Thompson AJ, Kermode AG, Wicks D, et al. Major differences in the dynamics of

- primary and secondary progressive multiple sclerosis. *Ann Neurol.* 1991;29(1):53-62. doi:10.1002/ana.410290111
339. Ingle GT, Thompson AJ, Miller DH. Magnetic resonance imaging in primary progressive multiple sclerosis. *J Rehabil Res Dev.* 2002;39(2):261-272.
340. Liguori M, Nuzziello N, Licciulli F, et al. Combined microRNA and mRNA expression analysis in pediatric multiple sclerosis: an integrated approach to uncover novel pathogenic mechanisms of the disease. *Hum Mol Genet.* 2018;27(1):66-79. doi:10.1093/hmg/ddx385
341. Hecker M, Thamilarasan M, Koczan D, et al. MicroRNA Expression Changes during Interferon-Beta Treatment in the Peripheral Blood of Multiple Sclerosis Patients. *Int J Mol Sci.* 2013;14(8):16087-16110. doi:10.3390/ijms140816087
342. Rao VTS, Fuh SC, Karamchandani JR, et al. Astrocytes in the pathogenesis of multiple sclerosis: An in situ microRNA study. *J Neuropathol Exp Neurol.* 2019;78(12):1130-1146. doi:10.1093/jnen/nlz098
343. Duffy CP, McCoy CE. The Role of MicroRNAs in Repair Processes in Multiple Sclerosis. *Cells.* 2020;9(7). doi:10.3390/cells9071711
344. Dutta R, Chang A, Doud MK, et al. Demyelination causes synaptic alterations in hippocampi from multiple sclerosis patients. *Ann Neurol.* 2011;69(3):445-454. doi:10.1002/ana.22337
345. Noorbakhsh F, Ellestad KK, Maingat F, et al. Impaired neurosteroid synthesis in multiple sclerosis. *Brain.* 2011;134(9):2703-2721. doi:10.1093/brain/awr200
346. Osorio-Querejeta I, Carregal-Romero S, Ayerdi-Izquierdo A, et al. MiR-219a-5p enriched extracellular vesicles induce OPC differentiation and EAE improvement more efficiently than liposomes and polymeric nanoparticles. *Pharmaceutics.* 2020;12(2). doi:10.3390/pharmaceutics12020186
347. Wang H, Moyano AL, Ma ZZ, et al. miR-219 Cooperates with miR-338 in Myelination and Promotes Myelin Repair in the CNS. *Dev Cell.* 2017;40(6):566-582.e5. doi:10.1016/j.devcel.2017.03.001
348. Teunissen C, Menge T, Altintas A, et al. Consensus definitions and application guidelines for control groups in cerebrospinal fluid biomarker studies in multiple sclerosis. *Mult Scler.* 2013;19(13):1802-1809. doi:10.1177/1352458513488232
349. Aung LL, Mouradian MM, Dhib-Jalbut S, Balashov KE. MMP-9 expression is increased in B lymphocytes during multiple sclerosis exacerbation and is regulated by microRNA-320a. *J Neuroimmunol.* 2015;278:185-189. doi:10.1016/j.jneuroim.2014.11.004
350. Wang S, Wan X, Ruan Q. The MicroRNA-21 in Autoimmune Diseases. *Int J Mol Sci.* 2016;17(6). doi:10.3390/ijms17060864

REFERENCES

351. Thouvenot E, Hinsinger G, Demattei C, et al. Cerebrospinal fluid chitinase-3-like protein 1 level is not an independent predictive factor for the risk of clinical conversion in radiologically isolated syndrome. *Mult Scler.* March 2018;135245851876704. doi:10.1177/1352458518767043
352. Pawlitzki M, Sweeney-Reed CM, Bittner D, et al. CSF-Progranulin and Neurofilament Light Chain Levels in Patients With Radiologically Isolated Syndrome-Sign of Inflammation. *Front Neurol.* 2018;9:1075. doi:10.3389/fneur.2018.01075
353. Wang-Renault S-F, Boudaoud S, Nocturne G, et al. Deregulation of microRNA expression in purified T and B lymphocytes from patients with primary Sjögren's syndrome. *Ann Rheum Dis.* 2018;77(1):133-140. doi:10.1136/annrheumdis-2017-211417
354. Yang D, Wang WZ, Zhang XM, et al. MicroRNA expression aberration in chinese patients with relapsing remitting multiple sclerosis. *J Mol Neurosci.* 2014;52(1):131-137. doi:10.1007/s12031-013-0138-x
355. Martinelli-Boneschi F, Fenoglio C, Brambilla P, et al. MicroRNA and mRNA expression profile screening in multiple sclerosis patients to unravel novel pathogenic steps and identify potential biomarkers. *Neurosci Lett.* 2012;508(1):4-8. doi:10.1016/j.neulet.2011.11.006
356. Keller A, Leidinger P, Lange J, et al. Multiple Sclerosis: MicroRNA Expression Profiles Accurately Differentiate Patients with Relapsing-Remitting Disease from Healthy Controls. Martin DP, ed. *PLoS One.* 2009;4(10):e7440. doi:10.1371/journal.pone.0007440
357. Waschbisch A, Atiya M, Linker RA, Potapov S, Schwab S, Derfuss T. Glatiramer acetate treatment normalizes deregulated microRNA expression in relapsing remitting multiple sclerosis. *PLoS One.* 2011;6(9):1-5. doi:10.1371/journal.pone.0024604
358. Mori MA, Ludwig RG, Garcia-Martin R, Brandā BB, Kahn CR. Extracellular miRNAs: From Biomarkers to Mediators of Physiology and Disease. *Cell Metab.* 2019. doi:10.1016/j.cmet.2019.07.011
359. Anoop A, Singh PK, Jacob RS, Maji SK. CSF Biomarkers for Alzheimer's Disease Diagnosis. *Int J Alzheimers Dis.* 2010;2010. doi:10.4061/2010/606802
360. De Stefano N, Stromillo ML, Rossi F, et al. Improving the Characterization of Radiologically Isolated Syndrome Suggestive of Multiple Sclerosis. Kleinschnitz C, ed. *PLoS One.* 2011;6(4):e19452. doi:10.1371/journal.pone.0019452
361. Høglund RA, Maghazachi AA. Multiple sclerosis and the role of immune cells. *World J Exp Med.* 2014;4(3):27. doi:10.5493/wjem.v4.i3.27
362. Hurwitz BJ. The diagnosis of multiple sclerosis and the clinical subtypes. *Ann Indian*

- Acad Neurol.* 2009;12(4):226-230. doi:10.4103/0972-2327.58276
363. Khan O, Williams MJ, Amezcua L, Javed A, Larsen KE, Smrtka JM. Multiple sclerosis in US minority populations: Clinical practice insights. *Neurol Clin Pract.* 2015;5(2):132-142. doi:10.1212/CPJ.0000000000000112
364. Aurenção JCK, Vasconcelos CCF, Thuler LCS, Alvarenga RMP. Incapacidade e progressão em pacientes afrodescendentes com esclerose múltipla. *Arq Neuropsiquiatr.* 2016;74(10):836-841. doi:10.1590/0004-282X20160118
365. Ventura RE, Antezana AO, Bacon T, Kister I. Hispanic Americans and African Americans with multiple sclerosis have more severe disease course than Caucasian Americans. *Mult Scler.* 2017;23(11):1554-1557. doi:10.1177/1352458516679894
366. Cabre P. Migration and multiple sclerosis: The French West Indies experience. *J Neurol Sci.* 2007;262(1-2):117-121. doi:10.1016/j.jns.2007.06.044
367. Berg-Hansen P, Moen SM, Sandvik L, et al. Prevalence of multiple sclerosis among immigrants in Norway. *Mult Scler.* 2015;21(6):695-702. doi:10.1177/1352458514554055
368. Nardin C, Latarche C, Soudant M, et al. Generational changes in multiple sclerosis phenotype in North African immigrants in France: A population-based observational study. *PLoS One.* 2018;13(3). doi:10.1371/journal.pone.0194115
369. Huang RS, Gamazon ER, Ziliak D, et al. Population differences in microRNA expression and biological implications. *RNA Biol.* 2011;8(4):692. doi:10.4161/rna.8.4.16029
370. Dluzen DF, Noren Hooten N, Zhang Y, et al. Racial differences in microRNA and gene expression in hypertensive women. *Sci Rep.* 2016;6. doi:10.1038/srep35815
371. Iacobaeus E, Arrambide G, Amato MP, et al. Aggressive multiple sclerosis (1): Towards a definition of the phenotype. *Mult Scler.* 2020;26(9):1031-1044. doi:10.1177/1352458520925369
372. Amezcua L, McCauley JL. Race and ethnicity on MS presentation and disease course. *Mult Scler.* 2020;26(5):561-567. doi:10.1177/1352458519887328
373. Gale CR, Martyn CN. Migrant studies in multiple sclerosis. *Prog Neurobiol.* 1995;47(4-5):425-448.
374. Sang W, Wang Y, Zhang C, et al. MiR-150 impairs inflammatory cytokine production by targeting ARRB-after blocking CD28/B7 costimulatory pathway. *Immunol Lett.* 2016;172:1-10. doi:10.1016/j.imlet.2015.11.001
375. Simone IL, Carrara D, Tortorella C, et al. Course and prognosis in early-onset MS: Comparison with adult-onset forms. *Neurology.* 2002;59(12):1922-1928. doi:10.1212/01.WNL.0000036907.37650.8E
376. Tutuncu M, Tang J, Zeid NA, et al. Onset of progressive phase is an age-dependent

REFERENCES

- clinical milestone in multiple sclerosis. *Mult Scler J*. 2013;19(2):188-198. doi:10.1177/1352458512451510
377. Ruiz F, Vigne S, Pot C. Resolution of inflammation during multiple sclerosis. *Semin Immunopathol*. 2019;41(6):711-726. doi:10.1007/s00281-019-00765-0
378. Grebenciucova E, Berger JR. Immunosenescence: the Role of Aging in the Predisposition to Neuro-Infectious Complications Arising from the Treatment of Multiple Sclerosis. *Curr Neurol Neurosci Rep*. 2017;17(8). doi:10.1007/s11910-017-0771-9
379. Olivieri F, Procopio AD, Montgomery RR. Effect of aging on microRNAs and regulation of pathogen recognition receptors. *Curr Opin Immunol*. 2014;29(1):29-37. doi:10.1016/j.coi.2014.03.006
380. Capone A, Bianco M, Ruocco G, et al. Distinct Expression of Inflammatory Features in T Helper 17 Cells from Multiple Sclerosis Patients. *Cells*. 2019;8(6):533. doi:10.3390/cells8060533
381. Villar LM, Picón C, Costa-Frossard L, et al. Cerebrospinal fluid immunological biomarkers associated with axonal damage in multiple sclerosis. *Eur J Neurol*. 2015;22(8):1169-1175. doi:10.1111/ene.12579
382. Fenoglio C, Cantoni C, De Riz M, et al. Expression and genetic analysis of miRNAs involved in CD4+ cell activation in patients with multiple sclerosis. *Neurosci Lett*. 2011;504(1):9-12. doi:10.1016/j.neulet.2011.08.021
383. Peeters LM, Vanheusden M, Somers V, et al. Cytotoxic CD4+ T Cells Drive Multiple Sclerosis Progression. *Front Immunol*. 2017;8:1160. doi:10.3389/fimmu.2017.01160
384. Okoye IS, Coomes SM, Pelly VS, et al. MicroRNA-Containing T-Regulatory-Cell-Derived Exosomes Suppress Pathogenic T Helper 1 Cells. *Immunity*. 2014;41(1):89-103. doi:10.1016/j.immuni.2014.05.019
385. Torri A, Carpi D, Bulgheroni E, et al. Extracellular MicroRNA Signature of Human Helper T Cell Subsets in Health and Autoimmunity. *J Biol Chem*. 2017;292(7):2903-2915. doi:10.1074/jbc.M116.769893
386. de Faria O, Moore CS, Kennedy TE, Antel JP, Bar-Or A, Dhaunchak AS. MicroRNA dysregulation in multiple sclerosis. *Front Genet*. 2013;3(JAN):1-6. doi:10.3389/fgene.2012.00311
387. Ma X, Zhou J, Zhong Y, et al. Expression, Regulation and Function of MicroRNAs in Multiple Sclerosis. *Int J Med Sci*. 2014;11(8):810-818. doi:10.7150/ijms.8647
388. Kutty RK, Nagineni CN, Samuel W, et al. Differential regulation of microRNA-146a and microRNA-146b-5p in human retinal pigment epithelial cells by interleukin-1 β , tumor necrosis factor- α , and interferon- γ . *Mol Vis*. 2013;19:737-750. <http://www.ncbi.nlm.nih.gov/pubmed/23592910>. Accessed July 12, 2018.

389. Chen Y, Chen J, Wang H, et al. HCV-Induced miR-21 Contributes to Evasion of Host Immune System by Targeting MyD88 and IRAK1. *PLoS Pathog.* 2013;9(4):e1003248. doi:10.1371/journal.ppat.1003248
390. Xie Y-F, Shu R, Jiang S-Y, Liu D-L, Ni J, Zhang X-L. MicroRNA-146 inhibits pro-inflammatory cytokine secretion through IL-1 receptor-associated kinase 1 in human gingival fibroblasts. *J Inflamm.* 2013;10(1):20. doi:10.1186/1476-9255-10-20
391. Zhou X, Ren Y, Moore L, et al. Downregulation of miR-21 inhibits EGFR pathway and suppresses the growth of human glioblastoma cells independent of PTEN status. *Lab Investig.* 2010;90(2):144-155. doi:10.1038/labinvest.2009.126
392. Xu B, Wang N, Wang X, et al. MiR-146a suppresses tumor growth and progression by targeting EGFR pathway and in a p-ERK-dependent manner in castration-resistant prostate cancer. *Prostate.* 2012;72(11):1171-1178. doi:10.1002/pros.22466
393. CAI J, XU L, CAI Z, WANG J, ZHOU B, HU H. MicroRNA-146b-5p inhibits the growth of gallbladder carcinoma by targeting epidermal growth factor receptor. *Mol Med Rep.* 2015;12(1):1549-1555. doi:10.3892/mmr.2015.3461
394. Heiseke AF, Jeuk BH, Markota A, et al. IRAK1 Drives Intestinal Inflammation by Promoting the Generation of Effector Th Cells with Optimal Gut-Homing Capacity. *J Immunol.* 2015;195(12):5787-5794. doi:10.4049/jimmunol.1501874
395. Deng C, Radu C, Diab A, et al. IL-1 Receptor-Associated Kinase 1 Regulates Susceptibility to Organ-Specific Autoimmunity. *J Immunol.* 2017;170:2833-2842. doi:10.4049/jimmunol.170.6.2833
396. Hossen MJ, Yang WS, Kim D, Aravinthan A, Kim JH, Cho JY. Thymoquinone: An IRAK1 inhibitor with in vivo and in vitro anti-inflammatory activities. *Sci Rep.* 2017;7(June 2016):1-12. doi:10.1038/srep42995
397. Fernández-Menéndez S, Fernández-Morán M, Fernández-Vega I, Pérez-Álvarez A, Villafani-Echazú J. Epstein-Barr virus and multiple sclerosis. from evidence to therapeutic strategies. *J Neurol Sci.* 2016;361:213-219. doi:10.1016/j.jns.2016.01.013
398. Anastasiadou E, Garg N, Bigi R, et al. Epstein-Barr virus infection induces miR-21 in terminally differentiated malignant B cells. *Int J Cancer.* 2015;137(6):1491-1497. doi:10.1002/ijc.29489
399. Gallo A, Jang SI, Ong HL, et al. Targeting the Ca²⁺ + Sensor STIM1 by Exosomal Transfer of Ebv-miR-BART13-3p is Associated with Sjögren's Syndrome. *EBioMedicine.* 2016;10:216-226. doi:10.1016/j.ebiom.2016.06.041
400. Afrasiabi A, Parnell GP, Swaminathan S, Stewart GJ, Booth DR. The interaction of Multiple Sclerosis risk loci with Epstein-Barr virus phenotypes implicates the virus in pathogenesis. *Sci Rep.* 2020;10(1):1-11. doi:10.1038/s41598-019-55850-z
401. Márquez AC, Horwitz MS. The role of latently infected B cells in CNS autoimmunity. *Front Immunol.* 2015;6(OCT). doi:10.3389/fimmu.2015.00544

REFERENCES

402. Hjalgrim H, Friborg J, Melbye M. The epidemiology of EBV and its association with malignant disease. *Human Herpesviruses: Biology, Therapy, and Immunoprophylaxis*. Cambridge University Press. 2007:929-959. doi:10.1017/CBO9780511545313.054
403. Smatti MK, Yassine HM, AbuOdeh R, et al. Prevalence and molecular profiling of Epstein Barr virus (EBV) among healthy blood donors from different nationalities in Qatar. Pagano JS, ed. *PLoS One*. 2017;12(12):e0189033. doi:10.1371/journal.pone.0189033
404. Kreft KL, Van Nierop GP, Scherbeijn SMJ, Janssen M, Verjans GMGM, Hintzen RQ. Elevated EBNA-1 IgG in MS is associated with genetic MS risk variants. *Neurol Neuroimmunol NeuroInflammation*. 2017;4(6):406. doi:10.1212/NXI.0000000000000406
405. Pfuhl C, Oechtering J, Rasche L, et al. Association of serum Epstein-Barr nuclear antigen-1 antibodies and intrathecal immunoglobulin synthesis in early multiple sclerosis. *J Neuroimmunol*. 2015;285:156-160. doi:10.1016/j.jneuroim.2015.06.012
406. Saridakis V, Sheng Y, Sarkari F, et al. Structure of the p53 binding domain of HAUSP/USP7 bound to epstein-barr nuclear antigen 1: Implications for EBV-mediated immortalization. *Mol Cell*. 2005;18(1):25-36. doi:10.1016/j.molcel.2005.02.029
407. Wang M, Gu B, Chen X, Wang Y, Li P, Wang K. The Function and Therapeutic Potential of Epstein-Barr Virus-Encoded MicroRNAs in Cancer. *Mol Ther Nucleic Acids*. 2019;17:657-668. doi:10.1016/j.omtn.2019.07.002
408. Cai L, Li J, Zhang X, et al. Gold nano-particles (AuNPs) carrying anti-EBV-miR-BART7-3p inhibit growth of EBV-positive nasopharyngeal carcinoma. *Oncotarget*. 2015;6(10):7838-7850. doi:10.18632/oncotarget.3046
409. Mirshafiey A, Mohsenzadegan M. TGF- β as a promising option in the treatment of multiple sclerosis. *Neuropharmacology*. 2009;56(6-7):929-936. doi:10.1016/j.neuropharm.2009.02.007
410. Oreja-Guevara C, Kobelt G, Berg J, Capsa D, Eriksson J. New insights into the burden and costs of multiple sclerosis in Europe: Results for Spain. *Mult Scler*. 2017;23(2_suppl):166-178. doi:10.1177/1352458517708672
411. Hauser SL, Chan JR, Oksenberg JR. Multiple sclerosis: Prospects and promise. *Ann Neurol*. 2013;74(3):317-327. doi:10.1002/ana.24009
412. Bonneau E, Neveu B, Kostantin E, Tsongalis GJ, De Guire V. How close are miRNAs from clinical practice? A perspective on the diagnostic and therapeutic market. *EJIFCC*. 2019;30(2):114-127.
413. The EU in the world - research and development - Statistics Explained. https://ec.europa.eu/eurostat/statistics-explained/index.php?title=The_EU_in_the_world_-_research_and_development.

Accessed November 20, 2020.

414. OECD. Gross domestic spending on R&D (indicator). doi:10.1787/d8b068b4-en
415. Instituto Nacional de Estadística. Estadística Sobre Actividades de I+D. Año 2018. Datos Definitivos.; 2019.
416. OECD. Researchers (indicator). doi:10.1787/20ddfb0f-en
417. Bohannon J, Doran K. Introducing ORCID. *Science*. 2017;356(6339):691-692. doi:10.1126/science.356.6339.691

8. Annex I

List of selected miRNA assays included in TaqMan™ OpenArray™ Human Advanced microRNA panels.

miRNA	Assay code	MS-associated miRNA	Brain-enriched miRNA	CSF-detectable miRNA	Potential normalizer	Negative control
ath-miR-159a	478411					X
let-7a-5p	478575	X		X		
let-7b-3p	478221			X		
let-7b-5p	478576			X		
let-7c-5p	478577		X	X		
let-7e-5p	478579	X		X		
let-7f-2-3p	477843			X		
let-7f-5p	478578	X		X		
let-7g-5p	478580	X	X	X		
let-7i-5p	478375			X		
miR-1-3p	477820	X		X		
miR-9-5p	478214		X	X		
miR-9-3p	478211			X		
miR-10a-5p	479241			X		
miR-10b-5p	478494			X		
miR-15a-5p	477858	X		X		
miR-15b-5p	478313	X		X		
miR-17-5p	478447			X	X	
miR-19a-3p	479228	X		X		
miR-19b-3p	478264	X		X		
miR-20a-5p	478586	X		X		
miR-21-5p	477975	X		X		
miR-22-3p	477985	X		X		
miR-23a-3p	478532	X	X	X		
miR-23b-3p	478602			X		
miR-24-3p	477992	X		X	X	
miR-25-3p	477994	X		X		
miR-26a-5p	477995	X		X		
miR-26b-5p	478418			X		
miR-27a-3p	478384	X		X		
miR-27b-3p	478270	X		X		
miR-27b-5p	478789			X		
miR-28-5p	478000			X		
miR-29a-3p	478587		X	X		
miR-29c-5p	478005			X		
miR-30a-3p	478273	X		X		
miR-30c-1-3p	479412			X		
miR-30c-2-3p	479401			X		
miR-30c-5p	478008			X		

ANNEX I

miR-30d-5p	478606			X		
miR-30e-3p	478388			X		
miR-31-5p	478015	X		X		
miR-32-5p	478026			X		
miR-34a-3p	478047			X		
miR-34a-5p	478048	X		X		
miR-34b-5p	478050			X		
miR-34b-3p	478049			X		
miR-34c-3p	478051			X		
miR-34c-5p	478052			X		
miR-92a-3p	477827			X		
miR-92b-3p	477823			X		
miR-93-5p	478210	X		X		
miR-99a-3p	479224			X		
miR-99b-5p	478343			X		
miR-100-3p	478619			X		
miR-100-5p	478224			X		
miR-101-3p	477863		X	X		
miR-103a-3p	478253			X	X	
miR-103a-2-5p	477864			X		
miR-106b-3p	477866			X		
miR-106b-5p	478412	X		X		
miR-107	478254		X	X		
miR-122-5p	477855			X		
miR-124-3p	477879		X	X		
miR-125a-5p	477884		X	X		
miR-125a-3p	477883			X		
miR-125b-5p	477885	X	X	X		
miR-126-5p	477888			X		
miR-127-3p	477889			X		
miR-128-3p	477892	X	X	X		
miR-129-2-3p	478544			X		
miR-130a-3p	477851			X		
miR-132-3p	477900	X	X	X		
miR-133a-3p	478511			X		
miR-133b	480871			X		
miR-135a-5p	478581		X	X		
miR-137	477904		X	X		
miR-142-3p	477910	X		X		
miR-142-5p	477911			X		
miR-143-3p	477912			X		
miR-144-3p	477913	X		X		
miR-145-3p	477915			X		
miR-145-5p	477916	X		X		
miR-146a-5p	478399	X		X		

miR-146b-5p	478513	X		X		
miR-148a-3p	477814	X		X		
miR-148b-3p	477824			X		
miR-150-5p	477918	X		X		
miR-151a-3p	477919			X		
miR-151a-5p	478505			X		
miR-153-3p	477922		X	X		
miR-155-5p	477927	X		X		
miR-181a-5p	477857	X	X	X		
miR-181b-5p	478583			X		
miR-181c-5p	477934	X		X		
miR-181d-5p	479517			X		
miR-183-3p	477936		X	X		
miR-185-5p	477939			X		
miR-186-5p	477940	X		X	X	
miR-190a-5p	478358		X	X		
miR-191-3p	477951			X		
miR-191-5p	477952			X	X	
miR-193a-5p	477954	X		X		
miR-194-5p	477956			X		
miR-195-5p	477957			X		
miR-196a-5p	478230			X		
miR-199a-3p	477961			X		
miR-199a-5p	478231			X		
miR-200c-3p	478351			X		
miR-203a-3p	478316			X		
miR-204-5p	478491			X		
miR-205-5p	477967			X		
miR-206	477968			X		
miR-210-3p	477970			X		
miR-211-5p	478507			X		
miR-216a-5p	477976			X		
miR-218-5p	477977			X		
miR-219a-5p	477980		X	X		
miR-221-3p	477981			X		
miR-222-3p	477982			X		
miR-223-3p	477983	X		X		
miR-302b-3p	478591			X		
miR-302d-3p	478237			X		
miR-320a	478594	X		X		
miR-320b	478588			X		
miR-323a-3p	477853		X	X		
miR-325	478025			X		
miR-326	478027	X		X		
miR-328-3p	478028			X		

ANNEX I

miR-335-5p	478324		X	X		
miR-338-3p	478037		X	X		
miR-339-5p	478040			X		
miR-342-3p	478043			X		
miR-361-3p	478055			X		
miR-361-5p	478056			X		
miR-363-3p	478060			X		
miR-369-3p	478067			X		
miR-369-5p	478068			X		
miR-373-3p	478363			X		
miR-374b-5p	478389			X		
miR-375	478074			X		
miR-376a-3p	478240			X		
miR-376c-3p	478459	X		X		
miR-378a-3p	478349			X		
miR-378a-5p	478076			X		
miR-383-5p	478079		X	X		
miR-410-3p	478085			X		
miR-411-5p	478086		X	X		
miR-412-3p	478087			X		
miR-423-5p	478090			X		
miR-424-5p	478092			X		
miR-425-5p	478094			X		
miR-448	478105			X		
miR-449a	478561			X		
miR-449b-5p	479528			X		
miR-450b-3p	478913			X		
miR-450b-5p	478914			X		
miR-451a	478107	X		X		
miR-452-3p	478917			X		
miR-452-5p	478109			X		
miR-454-3p	478329	X		X		
miR-455-3p	478112			X		
miR-483-3p	478122			X		
miR-483-5p	478432			X		
miR-484	478308	X		X		
miR-486-5p	478128			X		
miR-487a-3p	477826			X		
miR-489-3p	478130			X		
miR-490-3p	478131			X		
miR-497-5p	478138	X		X		
miR-501-3p	478350			X		
miR-502-3p	478348			X		
miR-505-3p	478145			X		
miR-513a-5p	479483			X		

miR-515-3p	478976			X		
miR-516b-5p	478979			X		
miR-518d-3p	479393			X		
miR-518e-3p	479408			X		
miR-518f-3p	478984			X		
miR-520h	479499			X		
miR-523-3p	478994			X		
miR-524-3p	479338			X		
miR-525-3p	478995			X		
miR-532-3p	478336			X		
miR-532-5p	478151			X		
miR-548d-5p	480870			X		
miR-548e-3p	478362			X		
miR-548k	479374			X		
miR-548n	479024			X		
miR-551a	478158			X		
miR-570-3p	479053			X		
miR-576-3p	478164			X		
miR-583	479065			X		
miR-593-5p	479077			X		
miR-615-3p	478175			X		
miR-628-3p	478181			X		
miR-633	479115	X		X		
miR-642a-5p	479121			X		
miR-645	478188			X		
miR-652-3p	478189			X		
miR-653-3p	479134			X		
miR-656-3p	479137			X		
miR-660-5p	478192	X		X		
miR-664a-3p	478193	X		X		
miR-770-5p	479178			X		
miR-876-3p	479186			X		
miR-885-5p	478207			X		
miR-937-3p	479212			X		
miR-939-5p	478245	X		X		
miR-1247-5p	477882			X		
miR-1249-3p	478654			X		
miR-1260a	478476			X		
miR-1264	478670			X		
miR-1292-5p	478691			X		
miR-1298-5p	479452			X		
miR-1911-5p	479583		X	X		

9. Annex II

RESEARCH

Open Access



Analysis of miRNA signatures in CSF identifies upregulation of miR-21 and miR-146a/b in patients with multiple sclerosis and active lesions

María Muñoz-San Martín¹ , Gemma Reverter¹ , Rene Robles-Cedeño^{1,2,3} , Maria Buxó⁴ , Francisco José Ortega⁵ , Imma Gómez¹, Jordi Tomàs-Roig¹ , Naiara Celarain¹, Luisa María Villar^{2,6} , Hector Perkal¹, José Manuel Fernández-Real^{3,5} , Ester Quintana^{1,2,3*†} and Lluís Ramió-Torrentà^{1,2,3*†}

Abstract

Background: MicroRNAs (miRNAs) have been reported as deregulated in active brain lesions derived from patients with multiple sclerosis (MS). In there, these post-transcriptional regulators may elicit very important effects but proper identification of miRNA candidates as potential biomarkers and/or therapeutic targets is scarcely available.

Objective: The aim of the study was to detect the presence of a set of candidate miRNAs in cell-free cerebrospinal fluid (CSF) and to determine their association with gadolinium-enhancing (Gd+) lesions in order to assess their value as biomarkers of MS activity.

Methods: Assessment of 28 miRNA candidates in cell-free CSF collected from 46 patients with MS (26 Gd+ and 20 Gd- patients) was performed by TaqMan assays and qPCR. Variations in their relative abundance were analyzed by the Mann-Whitney *U* test and further evaluated by receiver operating characteristic (ROC) analysis. Signaling pathways and biological functions of miRNAs were analyzed using bioinformatic tools (miRTarBase, Enrichr, REVIGO, and Cytoscape softwares).

Results: Seven out of 28 miRNA candidates were detected in at least 75% of CSF samples. Consistent increase of miR-21 and miR-146a/b was found in Gd+ MS patients. This increase was in parallel to the number of Gd+ lesions and neurofilament light chain (NF-L) levels. Gene Ontology enrichment analysis revealed that the target genes of these miRNAs are involved in biological processes of key relevance such as apoptosis, cell migration and proliferation, and in cytokine-mediated signaling pathways.

Conclusion: Levels of miR-21 and miR-146a/b in cell-free CSF may represent valuable biomarkers to identify patients with active MS lesions.

Keywords: Active lesions, Epigenetics, Gadolinium positive (Gd+), Inflammation, miRNAs, Multiple sclerosis

* Correspondence: equintana@idibgi.org; llramio@idibgi.org

†Ester Quintana and Lluís Ramió-Torrentà contributed equally as principal investigators.

¹Neuroimmunology and Multiple Sclerosis Unit, Neurology Department, Dr. Josep Trueta University Hospital, Girona Biomedical Research Institute (IDIBGI), Girona, Spain

Full list of author information is available at the end of the article



Introduction

Multiple sclerosis (MS) is an immune-mediated disease of the central nervous system (CNS) characterized by inflammation, demyelination, and neurodegeneration. Inflammation of the white and gray matter tissues in the CNS are responsible for MS lesions, which are an evidence of the nerve cell damage produced in the brain or spinal cord [1, 2]. Disease activity in MS is strongly linked to the formation of new lesions that could be detected as a focal area of contrast enhancement on T1-weighted images obtained after gadolinium injection (Gd+) [3].

MicroRNAs (miRNAs) are small non-coding single-stranded RNA molecules with the ability to regulate gene expression at the post-transcriptional level by binding to target messenger RNAs, leading to their degradation or translational repression [4]. miRNAs may control many biological processes in health and disease including neurologic disorders such as MS [5]. Several studies in MS have analyzed the role or profile of miRNAs in different tissues including peripheral blood mononuclear cells (PBMCs) [6], CD4+ cells [7], and MS brain lesions [8]. They can be also released extracellularly into body fluids such as plasma or cerebrospinal fluid (CSF), where they remain stable [9–12].

CSF is in direct contact with the extracellular space of the brain and can mirror biochemical changes affecting the brain [13]. Recently, some studies have evaluated the presence of miRNAs in CSF and their usefulness as potential biomarkers of MS [14–16].

This study aims to test the presence of a set of deregulated miRNAs, previously found in active MS lesions from brain biopsies [8], in cell-free CSF of MS patients, and to study their association with the presence of gadolinium-enhancing (Gd+) lesions to assess their value as biomarkers of new MS lesion formation.

Patients and methods

Study design and patients

Patients included in this study were recruited at the Girona Neuroimmunology and Multiple Sclerosis Unit of Dr. Josep Trueta University Hospital (Girona, Spain) and in the Immunology and Neurology Departments of Ramón y Cajal University Hospital (Madrid, Spain). A sample of 46 relapse-onset MS patients over 18 years old was included. Twenty-six MS patients showed Gd+ lesions in their magnetic resonance imaging (MRI) (Gd+), whereas 20 patients were not characterized by this clinical output (Gd-). CSF and plasma samples were collected at the diagnosis of the disease. MRI acquisition was made within 30 days from the sample collection. All patients were naïve of disease-modifying drugs. Demographic data including sex ratio and age, as well as clinical and radiological outputs, are depicted in Table 1. The Ethics Committee and the Committee for Clinical Investigation from Dr. Josep Trueta University Hospital approved the protocol employed in this study. All participants signed a written informed consent.

Table 1 Demographic data of the study cohort

	Gd- (n = 20)	Gd+ (n = 26)	p value
Age (mean ± SD)	31.15 ± 10.37	36.15 ± 8.65	0.081
Sex (male/female)			0.818
Male	6 (30.00%)	7 (26.92%)	
Female	14 (70.00%)	19 (73.08%)	
EDSS at sampling (median, Q1–Q2)	2 (1–2.5)	2 (1.5–2.13)	0.819
OCGB (N/P)			0.432
Negative	1 (5.26%)	0 (0.00%)	
Positive	18 (94.74%)	25 (100.00%)	
LS_OCMB (N/P)			0.393
Negative	14 (73.68%)	16 (61.54%)	
Positive	5 (26.32%)	10 (38.46%)	
T2 lesions			0.004
< 9 lesions	12 (66.67%)	4 (16.67%)	
10–20 lesions	5 (27.78%)	10 (41.67%)	
21–50 lesions	1 (5.56%)	8 (33.33%)	
51–100 lesions	0 (0.00%)	2 (8.33%)	

Gd- patients without gadolinium-enhanced lesions, Gd+ patients with gadolinium-enhanced lesions; SD standard deviation, OCGB oligoclonal IgG bands; N/P negative/positive, LS_OCMB lipid-specific oligoclonal IgM bands

Samples

Following consensus conditions for CSF and plasma collection and biobanking, CSF was centrifuged immediately after a lumbar puncture at 400×g for 15 min to obtain cell-free CSF. Plasma was collected in EDTA tubes and centrifuged at 2000×g for 10 min. Cell-free CSF and plasma aliquots were stored at −80 °C until RNA extraction [17].

Analysis of circulating miRNAs

Circulating RNA extraction and purification

Total RNA was extracted from CSF or plasma using mirVana PARIS Isolation Kit (Applied Biosystems) according to the manufacturer's instructions. In brief, 300 µl of sample was mixed with an equal volume of 2× Denaturing solution. Spike-in cel-miR-39 and cel-miR-54 exogenous miRNAs were added to check the quality of the extraction. Then, the same volume of acid-phenol:chloroform was added. After centrifugation (17,000×g, 10 min, 19 °C), the upper aqueous phase was recovered and mixed with 100% ethanol. After being placed into a filter cartridge, three washing steps were performed. Total RNA was eluted with 40 µl of nuclease-free water.

Circulating miRNA RT and preamplification

We used a fixed volume of 3 µl of total purified for the reverse transcription (RT). A set of 754 miRNAs were processed in CSF samples, using TaqMan miRNA Reverse Transcription Kit and Multiplex RT Assays (Human pool sets A and B) (Applied Biosystems) as previously described [18]. For RNA isolated from plasma samples, we used custom RT primer pool directed to the miRNAs identified as altered in CSF following the appropriate protocol. Each protocol has demonstrated sensitivity, specificity as well as repeatable and accurate results [19]. RT products for both CSF and plasma were then preamplified by means of TaqMan PreAmp Master Mix and/or Megaplex PreAmp Primers (Human pool sets A and B) (Applied Biosystems), or by custom preamplification primer pool, respectively. Preamplification step is mandatory before real-time PCR (RT-PCR) reaction when analytical sensitivity is the utmost importance and the sample is limiting [18].

Analysis of individual miRNAs with TaqMan hydrolysis probes

To study the presence of circulating miRNA candidates, the preamplification product was diluted (1:50 for CSF and 1:200 for plasma) and quantified with Individual TaqMan hydrolysis probes (Applied Biosystems). Individual gene expression was assessed by RT-PCR using the Light-Cycler® 480 System (Roche Molecular Biochemicals) and triplicates for each sample were performed. Expression values in CSF were normalized using

miR-17 as previously described [16]. Whereas plasma levels were normalized using the mean value of miR-17, miR-191, miR-103, and miR-186.

Targets and pathway analyses

Experimentally validated targets for differentially expressed miRNAs were retrieved from miRTarBase [20]. Those genes which validation was made by western blot, reporter assay and/or qPCR were introduced in Enrichr to explore the gene ontology (GO) biological processes [21]. Associated GO terms were clustered according to their relatedness using REVIGO [22] after removing redundant terms. A microRNA-target interaction network was performed using Cytoscape software [23].

NF-L quantification

Levels of neurofilament light chain (NF-L) in CSF of 25 patients were measured by ELISA (UmanDiagnostics, Umea, Sweden) at the Ramón y Cajal University Hospital (Madrid, Spain) according to the manufacturer's instructions.

Microarray data analysis

We downloaded publically available gene expression datasets, containing normalized data, from a study which contains gene and miRNA expression levels from human immune cell subsets [24]. We wanted to study the possible interaction between our deregulated miRNAs and their shared targets in silico. The datasets were included in the SuperSeries GSE28492.

Statistical analysis

Demographic, clinical, radiological, and normalized mRNA levels data were reported as follows: categorical variables were shown as frequencies and percentages while continuous variables were represented by mean ± standard deviation (SD) or median (quartiles). Normal distribution of a data set was assessed with normal Q-Q plots and the Shapiro-Wilk test. Statistical differences were determined using Student's *t* test and Mann-Whitney *U* test in the case of quantitative variables while chi-square test or Fisher's exact test for categorical ones. Correlation analysis of normalized miRNA levels and clinical/radiological/biochemical data were estimated by Spearman's Rho (r_s). Receiver operating characteristic (ROC) analysis was conducted to determine the ability of miRNA levels to discriminate between patients with Gd+ and Gd− lesions. Area under the curve (AUC), 95% confidence interval (95% CI), and the optimal cut-off values using Youden's index were determined. The sensitivity, specificity, and positive and negative likelihood ratios (LR+ and LR−, respectively) were also calculated. In addition, a ROC curve for combined miRNAs was calculated via logistic analysis. All analyses were two-

tailed and the significance level was set to 0.05. Statistical analyses were performed in Statistical Package for the Social Sciences (SPSS) version 25.0 (IBM SPSS Statistics for Windows, NY, USA) and R 3.4.3 using pROC package [25]. Figures were built with GraphPad PRISM v.5.

Results

Detection of miRNAs in CSF

Forty-six MS patients (71.7% women) with a mean age and standard deviation of 33.98 ± 9.66 were studied. Gd+ lesions were present in 56.5% of the subjects. No differences were observed for either sex distribution or age between Gd- and Gd+ patients (Table 1). Seven of 28 miRNAs reported as deregulated in active MS lesions (9) were detected in at least 75% of CSF samples, assessed in triplicate by Ct values lower than 37 (miR-155, miR-223, miR-21, miR-320, miR-328, miR-146a, and miR-146b). A group of five miRNAs was present in less than 75% of samples (miR-34a, miR-130a, miR-214, miR-27a, and miR-656) while the others show very low expression measures or were undetected (Additional file 1: Table S1).

Differential miRNA values in CSF of MS patients with Gd+ lesions

Differential expression of the seven miRNAs detected in at least 75% of the CSF samples was tested to compare Gd- and Gd+ patients. Increased expression of miR-21, miR-146a, and miR-146b was found in Gd+ patients (Table 2 and Fig. 1). ROC curves were performed to determine the potential discriminatory capacity provided by each single miRNA present in cell-free CSF for detecting brain acute inflammatory activity. miR-21, miR-146a, and miR-146b presented AUC values of 0.703, 0.728, and 0.712, respectively, which support a valuable discriminatory indicator to differentiate Gd- from Gd+ patients. Logistic regression analysis was performed to evaluate the discriminatory ability of selected miRNAs combination. Variables were dichotomized according to

Table 2 Differential miRNA expression between groups in CSF

	Gd- (n = 20)		Gd+ (n = 26)		p value
	Median	Q1-Q3	Median	Q1-Q3	
miR-21	0.014	0.010–0.022	0.029	0.013–0.052	0.024
miR-146a	0.065	0.031–0.136	0.135	0.082–0.239	0.016
miR-146b	0.008	0.002–0.020	0.021	0.012–0.052	0.030
miR-155	0.007	0.002–0.016	0.011	0.006–0.019	0.163
miR-223	0.066	0.043–0.328	0.124	0.088–0.226	0.232
miR-320	0.038	0.010–0.048	0.042	0.026–0.087	0.271
miR-328	0.007	0.003–0.012	0.011	0.005–0.026	0.143

Gd- patients without gadolinium-enhanced lesions, Gd+ patients with gadolinium-enhanced lesions; Q1–Q3 first quartile–third quartile

cut-off values deduced from ROC analysis (AUC = 0.867) (Table 3, Additional file 1: Figure S1).

Correlation between deregulated miRNAs and CSF NF-L levels

Differential expression of NF-L levels was tested to compare Gd- and Gd+ subjects (data not shown). Increased expression of NF-L was found in CSF of Gd+ patients (median Gd- = 462.5 ng/L vs median Gd+ = 1116.0 ng/L; $p = 0.010$).

We also studied the correlation between CSF deregulated miRNA levels and NF-L levels (Fig. 2). The expression of miR-146b was strongly positively correlated with NF-L ($r_s = 0.682$ and $p = 0.001$) while miR-21 and miR-146a showed a moderate relationship ($r_s = 0.374$ and $p = 0.086$, $r_s = 0.400$ and $p = 0.090$, respectively). NF-L levels also presented strong correlation with number of Gd+ lesions ($r_s = 0.620$ and $p = 0.001$) (Fig. 2).

Association of CSF miRNA expression with radiological and clinical variables

Levels of miR-21, miR-146a, and miR-146b in CSF positively correlated with the number of Gd+ lesions. In addition, the expression of miR-21 and miR-155 mirrored the number of lesions in T2 weighted images. Finally, miR-21 was also associated with the basal expanded disability status scale (EDSS) score (Table 4).

Target and pathway analysis of miR-21, miR-146a, and miR-146b

Experimentally validated human molecules with strong evidence for being targets for miR-21, miR-146a, and miR-146b were retrieved from miRTarBase (Additional file 1: Table S2) and then, uploaded to Enrichr to explore the GO biological processes. Clustered GO terms revealed that miRNAs target genes were involved in distinct biological processes such as apoptosis, cell migration, and proliferation and cytokine-mediated signaling pathways (Fig. 3a). The miRNA-target interaction network showed interleukin receptor-associated kinase 1 (*IRAK1*) and epidermal growth factor receptor (*EGFR*) as shared targets for the three deregulated miRNAs (Fig. 3b).

Correlation analysis of miRNAs and mRNA expression in in silico datasets

In order to evaluate the possible interaction between miR-21, miR-146a and miR-146b, and their shared targets *IRAK1* and *EGFR*, we used the normalized publicly available datasets GSE28487 (miRNA expression) and GSE28490 (mRNA expression) belonging to the Super-Series GSE28492 from GEO [24]. We made correlation analysis between normalized miRNA levels and *IRAK1* and *EGFR* mRNA levels in the whole set of studied

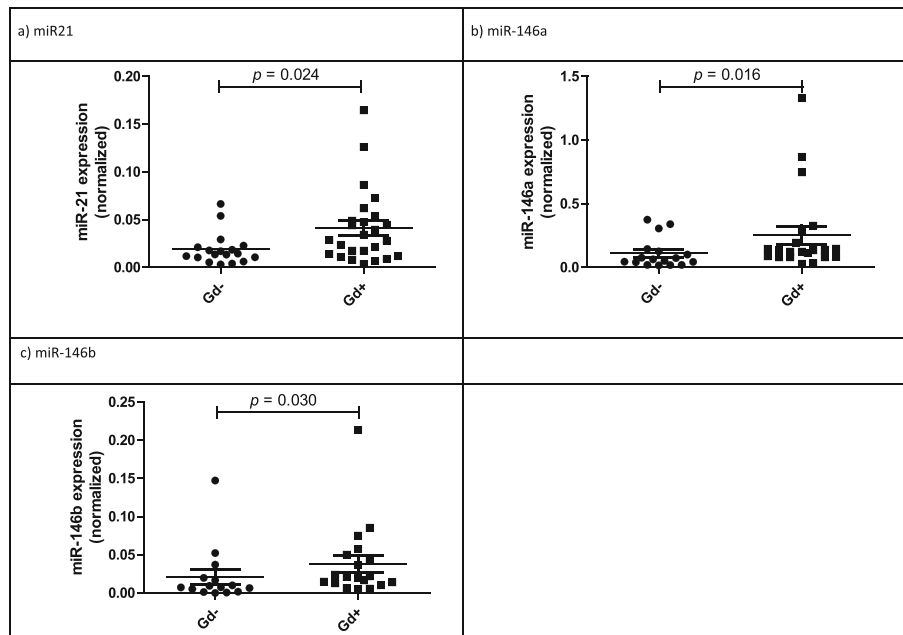


Fig. 1 Differentially expressed miRNAs. Dot plots for normalized value of **a** miR-21, **b** miR-146a, and **c** miR-146b in patients according to the presence of Gd+ lesions in the brain. The line indicates the median and Mann-Whitney *U* test was used to determine statistical differences between groups

immune cells. We found that *IRAK1* was strongly negatively correlated to miR-146a and miR-146b expression ($r_s = -0.670$ and $r_s = -0.635$, respectively), while the relation with miR-21 did not reach statistical significance. However, the expression of *EGFR* was not correlated to the expression of these miRNAs (Additional file 1: Figure S2).

Plasma expression of miR-21, miR-146a, and miR-146b

Circulating miRNAs from plasma samples of 30 patients included in the CSF study (13 Gd- and 17 Gd+ patients) were extracted and quantified by RT-PCR. Differential expression analysis of miRNAs in plasma based on Gd- or Gd+ status revealed no significant differences for the three deregulated miRNAs in CSF (Additional file 1: Table S3). Furthermore, no significant correlation between CSF and plasma miRNA levels was found, with the exception of miR-146b ($r_s = -0.398$ and $p = 0.049$) (Additional file 1: Figure S3). Moreover, no association was observed between plasma miRNA levels and number of Gd+ lesions. Only plasma level of miR-146a

showed a positive correlation with EDSS ($r_s = 0.383$ and $p = 0.037$)

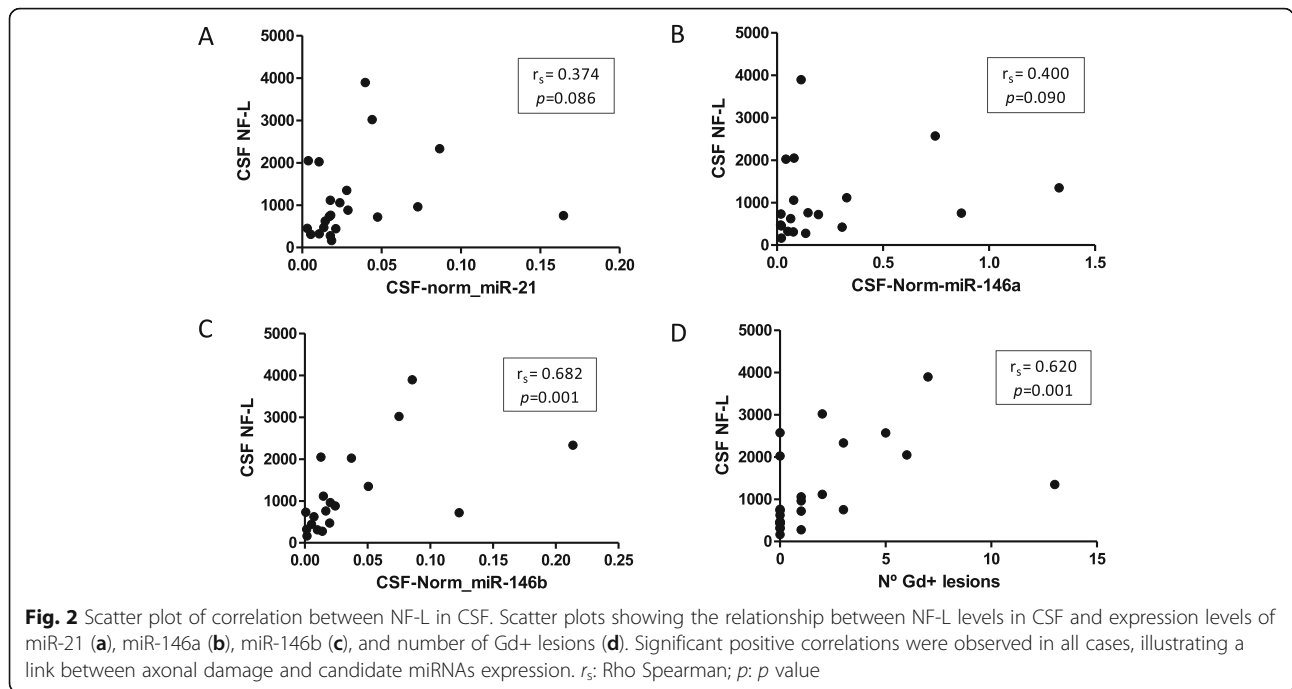
Discussion

Circulating miRNAs are being widely studied as potential biomarkers of diagnosis and prognosis in different diseases due to their stability and the ease to be measured in tissues and biological fluids [26]. Most of these studies are related to cancer research and have demonstrated the ability of circulating miRNAs as a new and reliable diagnosis and prognosis biomarker to detect and identify different cancer [27–29]. Recent studies elucidate the role of miRNAs in neurodegenerative diseases, such as MS, and their capacity to predict disease subtype with a high degree of accuracy [30, 31], as well as, response to a specific treatment [32]. Several studies have analyzed miRNA expression in cell-free CSF [14–16], a biological fluid that could mirror events occurring in the CNS. However, none of them have checked their relationship with the presence of active MS lesions. We hypothesized that the differential expression of miRNAs in

Table 3 Capacity of selected miRNAs to detect inflammatory activity in CNS

	AUC	95% CI	Sensitivity (%)	Specificity (%)	LR+	LR-
miR-21	0.703	0.543–0.863	60.00	77.78	2.70	0.51
miR-146a	0.728	0.553–0.904	90.48	64.71	2.56	0.15
miR-146b	0.712	0.531–0.894	81.82	66.67	2.45	0.27
miR-21 + miR-146a + miR-146b	0.867	0.736–0.997	94.12	69.23	3.06	0.08

AUC area under curve, CI confidence interval, LR+ positive likelihood ratio, LR- negative likelihood ratio



CSF collected from MS patients could be a valuable indicator of CNS inflammation.

Junker et al. [8] reported a set of 28 miRNAs deregulated in brain tissue with active MS lesions. Our results confirmed the presence in the CSF of seven of the miRNAs previously reported as deregulated in active brain lesions (miR-21, miR-146a, miR-146b, miR-155, miR-

223, miR-320, and miR-328). Moreover, miR-21, miR-146a, and miR-146b were overexpressed in the CSF of Gd+ MS patients and also associated with radiological variables and clinical disability. This overexpression also agrees with the findings reported in active MS lesions, where these three miRNAs were upregulated when compared to normal white matter [8]. We also have observed

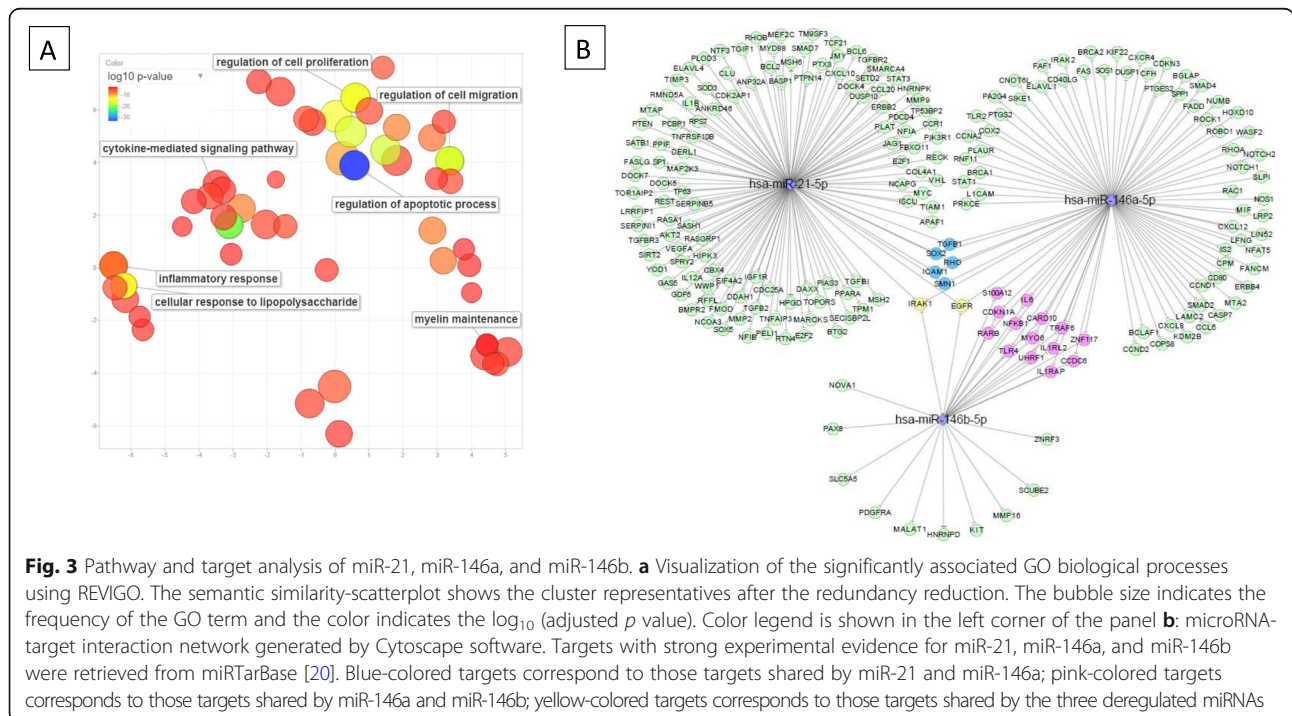


Table 4 Correlations between radiological and clinical data with miRNAs expression

	No. of Gd+ lesions		No. of T2 lesions		Basal EDSS	
	r_p	p value	r_p	p value	r_p	p value
miR-21	0.379	0.015	0.377	0.017	0.440	0.003
miR-146a	0.463	0.004	0.125	0.474	0.030	0.856
miR-146b	0.349	0.040	0.004	0.984	-0.299	0.072
miR-155	0.270	0.077	0.308	0.047	-0.010	0.949
miR-223	0.159	0.309	0.113	0.481	0.249	0.099
miR-320	0.187	0.243	0.035	0.831	0.035	0.825
miR-238	0.298	0.073	0.213	0.211	-0.089	0.592

r_s Spearman's Rho coefficient

a correlation between miR-21, miR-146a and miR-146b, and CSF NF-L levels, one of the most validate biomarkers for axonal damage [33], what supports the relation between these miRNAs and injury in the CNS.

Fenoglio et al. [34] found miR-21 and miR-146a/b over-represented in PBMCs of relapsing-remitting MS patients compared to controls. They suggested that this upregulation was specific to the acute phase of MS and contribute to the differentiation and regulation of CD4+ T cells, which are involved in the CNS inflammatory processes that take place in MS [35]. First, activated T lymphocytes migrate from the periphery into the CNS through the blood-brain barrier. Then, CD4+ T cells contribute to maintain the inflammation within the CNS and cytotoxic CD8+ T cells can induce direct axonal damage [36]. However, regulatory T cells (T reg), which maintain immune self-tolerance by suppressing effector T cells, exert that control, in part, by the release of miRNA-containing exosomes as non-cell-autonomous gene silencing mechanism [37]. In addition, extracellular vesicles released by Treg cells are enriched in miR-21 and miR-146a [38].

These miRNAs have several roles in regulating T cell biology. miR-21 may modulate T cell activation and apoptosis, Treg function and development, or Th17 differentiation [39]. On the other hand, miR-146a is thought to constitute an important negative regulator of the innate immune response [40] and controls IL17 production [41]. Remarkably, the expression of miR-146b is increased upon the presence of proinflammatory cytokines as IFN- γ [42]. Thus, we could speculate that an overexpression of these miRNAs might be reactive to the proinflammatory milieu in MS. In the presence of CNS inflammatory processes miR-21, miR-146a and miR-146b could be highly expressed in order to counteract the harmful activity of other cells.

In silico pathway analysis underpins the relevance of these miRNAs in the acute phase of inflammation in the CNS of RRMS patients. Specifically, their target genes are involved in apoptosis, cell migration and proliferation,

immune response, and cytokine-mediated signaling. As previously mentioned, migration of T lymphocytes into the CNS is a prerequisite to tissue damage in MS, and all these biological processes are involved in the cascade of events that trigger brain lesions. The miRNA-target interaction analysis revealed that the three overexpressed miRNAs have common targeted genes *IRAK1* and *EGFR* [43–47]. However, the in silico analysis of public datasets of miRNA and mRNA expression arrays showed that only *IRAK1* expression seemed to be negatively correlated with miR-146a and miR-146b levels mainly. *IRAK1* is a serine/threonine kinase associated with interleukin-1 receptor (IL-1R) and Toll-like receptor (TLR) signaling pathways that play a role in the innate immune response and exert an important influence in T helper differentiation and proliferation [48]. *IRAK1*-deficient mice are resistant to experimentally induced autoimmune encephalomyelitis [49], suggesting a critical role of this protein in autoimmune and inflammatory diseases. The use of *IRAK1* inhibitors was tested to treat inflammatory diseases [50]. Thus, even though the levels of circulating miRNAs do not necessarily reflect deregulation in cells and that the use of circulating miRNAs as biomarkers should not be confounded with their potential regulatory functions inside the cells, these in silico observations suggest that it would be interesting to study the modulation of *IRAK1* expression due to the overexpression of miR-21, miR-146a, and miR-146b in the CSF in order to prove its role in controlling inflammation and re-establish the self-tolerance after an acute inflammatory event.

Finally, due to the invasiveness of the lumbar puncture, the detection of biomarkers in serum or plasma is the most appropriate option for monitoring disease progression. Although we were able to detect miR-21, miR-146a, and miR-146b in plasma samples, we found no significant differences between Gd+ and Gd- patients. Other groups also failed to correlate their CSF and plasma findings [15, 51]. The poor correlation between CSF and plasma findings might suggest that CSF miRNA profile could provide different information not available in plasma.

Conclusions

In conclusion, overexpression of miR-21, miR-146a, and miR-146b in cell-free CSF were able to discriminate MS patients with Gd+ lesions in the MRI. All data point to the hypothesis that an overexpression of these miRNAs in CSF is induced to counteract the pro-inflammatory milieu in MS, and they might be released into the CSF in an attempt to reduce the harmful damage into the brain. However, additional functional studies and analyses of larger cohorts are needed to validate these results and to elucidate the real role of these miRNAs in the context of MS.

Supplementary information

Supplementary information accompanies this paper at <https://doi.org/10.1186/s12974-019-1590-5>.

Additional file 1: Table S1. List of 28 analyzed miRNAs and percentage of detection for each miRNAs in CSF. **Table S2.** Validated targets for miR-21-5p, miR-146a-5p and miR-146b-5p from miRTarBase. **Table S3.** Differential miRNA expression between groups in plasma. **Figure S1.** TITL: Receiver Operating Characteristics (ROC) analysis of individual (a-c) and combined (d) CSF miR-21, miR-146a and miR-146b to discriminate inflammatory activity. **Figure S2.** Correlation analysis of deregulated miRNAs and candidate targets mRNA expression in publicly available dataset. miRNA and mRNA expression profile of GSE28487 and GSE28490, respectively from Gene Expression Omnibus (GEO) DataSets (<https://www.ncbi.nlm.nih.gov/gds/>) was obtained. Scatter plots of correlations between up-regulated miRNAs in CSF (miR-21, miR-146a and miR-146b) and their shared target genes (*IRAK1* and *EGFR*) were presented. r_s : Rho Spearman; p : p value. **Figure S3.** Correlation of normalized Ct between CSF and plasma for (a) miR-21, (b) miR-146a and (c) miR-146b. Scatter plots showing the relationship between CSF and plasma levels for the deregulated miRNAs. r_s : Rho Spearman; p : p value.

Abbreviations

95% CI: 95% confidence interval; AUC: Area under the curve; CNS: Central nervous system; CSF: Cerebrospinal fluid; EDSS: Expanded disability status scale; *EGFR*: Epidermal growth factor receptor; Gd⁻: Non-gadolinium-enhancing; Gd⁺: Gadolinium-enhancing; GO: Gene ontology; IL-1R: Interleukin-1 receptor; *IRAK1*: Interleukin receptor-associated kinase 1; LR: Likelihood ratio; miRNAs: MicroRNAs; MRI: Magnetic resonance imaging; MS: Multiple sclerosis; PBMCs: Peripheral blood mononuclear cells; ROC: Receiver operating characteristic; RT: Reverse transcription; RT-PCR: Real-time PCR; SD: Standard deviation; SPSS: Statistical Package for the Social Sciences; TLR: Toll-like receptor

Acknowledgements

We want to particularly acknowledge the patients and the IDIBGI Biobank (Biobanc IDIBGI, B. 0000872), integrated in the Spanish National Biobank Network, for their collaboration.

Authors' contributions

RR-C, FJO, JMF-R, EQ, and LLR-T contributed to the concept and study design. MM-SM, GR, IG, JT-R, NC, HP, and EQ contributed to miRNAs studies, data acquisition, and analysis. RR-C, LMV, HP, EQ, and LLR-T contributed to patients and clinical data, analysis, and interpretation of the data. MM-SM, MB, FJO, JT-R, LMV, JMF-R, EQ, and LLR-T contributed to the drafting of the manuscript and figures. All authors read and approved the final manuscript.

Funding

The author(s) disclosed receipt of the following financial support for the research, authorship, and/or publication of this article: this study was supported by a grant from the Instituto Carlos III-Spanish Government (PI13/01782) and by a grant from Fundación Genzyme (2015). M. M.-S.M. was supported by a FI-DGR 2016 from AGAUR. J. T.-R was supported by Deutsche Forschungsgemeinschaft fellowship [Grant TO 977/1-1]. N. C. was supported by IFUdG2017 fellowship from Universitat de Girona.

Availability of data and materials

Please contact the corresponding author for datasets requests.

Ethics approval and consent to participate

The study was approved by the corresponding local ethics committee, and all participants provided informed consent.

Consent for publication

Not applicable.

Competing interests

The authors declare that they have no competing interests.

Author details

¹Neuroimmunology and Multiple Sclerosis Unit, Neurology Department, Dr. Josep Trueta University Hospital, Girona Biomedical Research Institute (IDIBGI), Girona, Spain. ²REEM. Red Española de Esclerosis Múltiple, Madrid, Spain. ³Medical Sciences Department, Faculty of Medicine, University of Girona, Girona, Spain. ⁴Girona Biomedical Research Institute (IDIBGI), Girona, Spain. ⁵Department of Diabetes, Endocrinology and Nutrition, Girona Biomedical Research Institute (IDIBGI), Girona, Spain. ⁶Immunology Department, Hospital Ramón y Cajal, IRYCIS, Madrid, Spain.

Received: 24 December 2018 Accepted: 20 September 2019

Published online: 14 November 2019

References

- Confavreux C, Vukusic S, Moreau T, Adeleine P. Relapses and progression of disability in multiple sclerosis. *N Engl J Med*. 2000;343:1430–8. <https://doi.org/10.1056/NEJM200011163432001>.
- Frohman EM, Racke MK, Raine CS. Multiple sclerosis — the plaque and its pathogenesis. *N Engl J Med*. 2006;354:942–55. <https://doi.org/10.1056/NEJMra052130>.
- Rovira A, Auger C, Alonso J. Magnetic resonance monitoring of lesion evolution in multiple sclerosis. *Ther Adv Neurol Disord*. 2013;6:298–310. <https://doi.org/10.1177/1756285613484079>.
- Mendell JT, Olson EN. MicroRNAs in stress signaling and human disease. *Cell*. 2012;148:1172–87. <https://doi.org/10.1016/j.cell.2012.02.005>.
- Junker A, Hohlfeld R, Meinl E. The emerging role of microRNAs in multiple sclerosis. *Nat Rev Neurol*. 2011;7:56–9. <https://doi.org/10.1038/nrneuro.2010.179>.
- Otaegui D, Baranzini SE, Armañanzas R, Calvo B, Muñoz-Culla M, Khankhanian P, Inza I, Lozano JA, Castillo-Triviño T, Asensio A, Olaskoaga J, de Munain AL. Differential micro RNA expression in PBMC from multiple sclerosis patients. *PLoS One*. 2009;4:e6309. <https://doi.org/10.1371/journal.pone.0006309>.
- Lindberg RLP, Hoffmann F, Mehling M, Kuhle J, Kappos L. Altered expression of miR-17-5p in CD4⁺ lymphocytes of relapsing-remitting multiple sclerosis patients. *Eur J Immunol*. 2010;40:888–98. <https://doi.org/10.1002/eji.200940032>.
- Junker A, Krumbholz M, Eisele S, Mohan H, Augstein F, Bittner R, Lassmann H, Wekerle H, Hohlfeld R, Meinl E. MicroRNA profiling of multiple sclerosis lesions identifies modulators of the regulatory protein CD47. *Brain*. 2009;132:3342–52. <https://doi.org/10.1093/brain/awp300>.
- Gilad S, Meiri E, Yogev Y, Benjamin S, Lebanony D, Yerushalmi N, Benjamin H, Kushnir M, Cholak H, Melamed N, Bentwich Z, Hod M, Goren Y, Chajut A. Serum MicroRNAs are promising novel biomarkers. *PLoS One*. 2008;3:e3148. <https://doi.org/10.1371/journal.pone.0003148>.
- Cogswell JP, Ward J, Taylor IA, Waters M, Shi Y, Cannon B, Kelnar K, Kempainen J, Brown D, Chen C, Prinjha RK, Richardson JC, Saunders AM, Roses AD, Richards CA. Identification of miRNA changes in Alzheimer's disease brain and CSF yields putative biomarkers and insights into disease pathways. *J Alzheimers Dis*. 2008;14:27–41. <http://www.ncbi.nlm.nih.gov/pubmed/18525125> (Accessed 12 July 2018).
- Gandhi R, Healy B, Gholipour T, Egorova S, Musallam A, Hussain MS, Nejad P, Patel B, Hei H, Khoury S, Quintana F, Kivisakk P, Chitnis T, Weiner HL. Circulating MicroRNAs as biomarkers for disease staging in multiple sclerosis. *Ann Neurol*. 2013;73:729–40. <https://doi.org/10.1002/ana.23880>.
- Zhang J, Cheng Y, Cui W, Li M, Li B, Guo L. MicroRNA-155 modulates Th1 and Th17 cell differentiation and is associated with multiple sclerosis and experimental autoimmune encephalomyelitis. *J Neuroimmunol*. 2014;266:56–63. <https://doi.org/10.1016/j.jneuroim.2013.09.019>.
- Anoop A, Singh PK, Jacob RS, Maji SK. CSF Biomarkers for Alzheimer's Disease Diagnosis. *Int J Alzheimers Dis*. 2010;2010. <https://doi.org/10.4061/2010/606802>.
- Haghikia A, Haghikia A, Hellwig K, Baraniskin A, Holzmann A, Decard BF, Thum T, Gold R. Regulated microRNAs in the CSF of patients with multiple sclerosis: a case-control study. *Neurology*. 2012;79:2166–70. <https://doi.org/10.1212/WNL.0b013e3182759621>.
- Bergman P, Piket E, Khademi M, James T, Brundin L, Olsson T, Piehl F, Jagodic M. Circulating miR-150 in CSF is a novel candidate biomarker for multiple sclerosis. *Neurol Neuroimmunol Neuroinflamm*. 2016;3:e219. <https://doi.org/10.1212/NXI.0000000000000219>.
- Quintana E, Ortega FJ, Robles-Cedeño R, Villar ML, Buxó M, Mercader JM, Alvarez-Cermeño JC, Pueyo N, Perkal H, Fernández-Real JM, Ramió-Torrentà

- L. miRNAs in cerebrospinal fluid identify patients with MS and specifically those with lipid-specific oligoclonal IgM bands. *Mult Scler J.* 2017;23:1716–26. <https://doi.org/10.1177/1352458516684213>.
17. Teunissen CE, Petzold A, Bennett JL, Berven FS, Brundin L, Comabella M, Franciotta D, Frederiksen JL, Fleming JO, Furlan R, Hintzen RQ, Hughes SG, Johnson MH, Krasulova E, Kuhle J, Magnone MC, Rajda C, Rejdak K, Schmidt HK, van Pesch V, Waubant E, Wolf C, Giovannoni G, Hemmer B, Tumani H, Deisenhammer F. A consensus protocol for the standardization of cerebrospinal fluid collection and biobanking. *Neurology.* 2009;73:1914–22. <https://doi.org/10.1212/WNL.0b013e3181c47cc2>.
 18. Ortega FJ, Mercader JM, Catalan V, Moreno-Navarrete JM, Pueyo N, Sabater M, Gomez-Ambrosi J, Anglada R, Fernandez-Formoso JA, Ricart W, Fruhbeck G, Fernandez-Real JM. Targeting the circulating MicroRNA signature of obesity. *Clin Chem.* 2013;59:781–92. <https://doi.org/10.1373/clinchem.2012.195776>.
 19. Le Carré J, Lamon S, Léger B. Validation of a multiplex reverse transcription and pre-amplification method using TaqMan[®] MicroRNA assays. *Front Genet.* 2014;5:413. <https://doi.org/10.3389/fgene.2014.00413>.
 20. Chou CH, Shrestha S, Yang CD, Chang NW, Lin YL, Liao KW, Huang WC, Sun TH, Tu SJ, Lee WH, Chiew MY, Tai CS, Wei TY, Tsai TR, Huang HT, Wang CY, Wu HY, Ho SY, Chen PR, Chuang CH, Hsieh PJ, Wu YS, Chen WL, Li MJ, Wu YC, Huang XY, Ng FL, Buddhakosai W, Huang PC, Lan KC, Huang CY, Weng SL, Cheng YN, Liang C, Hsu WL, Huang HD. miRTarBase update 2018: a resource for experimentally validated microRNA-target interactions. *Nucleic Acids Res.* 2018;46:D296–302. <https://doi.org/10.1093/nar/gkx1067>.
 21. Kuleshov MV, Jones MR, Rouillard AD, Fernandez NF, Duan Q, Wang Z, Koplev S, Jenkins SL, Jagodnik KM, Lachmann A, McDermott MG, Monteiro CD, Gundersen GW, Ma'ayan A. Enrichr: a comprehensive gene set enrichment analysis web server 2016 update. *Nucleic Acids Res.* 2016;44:W90–7. <https://doi.org/10.1093/nar/gkw377>.
 22. Supek F, Bošnjak M, Škunca N, Šmuc T. REVIGO summarizes and visualizes long lists of gene ontology terms. *PLoS One.* 2011;6:e21800. <https://doi.org/10.1371/journal.pone.0021800>.
 23. Shannon P, Markiel A, Ozier O, Baliga NS, Wang JT, Ramage D, Amin N, Schwikowski B, Ideker T. Cytoscape: a software environment for integrated models of biomolecular interaction networks. *Genome Res.* 2003;13:2498–504. <https://doi.org/10.1101/gr.1239303>.
 24. Allantaz F, Cheng DT, Bergauer T, Ravindran P, Rossier MF, Ebeling M, Badi L, Reis B, Bitter H, D'Asaro M, Chiappe A, Sridhar S, Pacheco GD, Burczynski ME, Hochstrasser D, Vonderscher J, Matthes T. Expression profiling of human immune cell subsets identifies miRNA-mRNA regulatory relationships correlated with cell type specific expression. *PLoS One.* 2012;7:e29979. <https://doi.org/10.1371/journal.pone.0029979>.
 25. Robin X, Turck N, Hainard A, Tiberti N, Lisacek F, Sanchez J-C, Müller M. pROC: an open-source package for R and S+ to analyze and compare ROC curves. *BMC Bioinformatics.* 2011;12:77. <https://doi.org/10.1186/1471-2105-12-77>.
 26. Zampetaki A, Willeit P, Drozdov I, Kiechl S, Mayr M. Profiling of circulating microRNAs: from single biomarkers to re-wired networks. *Cardiovasc Res.* 2012;93:555–62. <https://doi.org/10.1093/cvr/cvr266>.
 27. Moshiri F, Salvi A, Gramantieri L, Sangiovanni A, Guerriero P, De Petro G, Bassi C, Lupini L, Sattari A, Cheung D, Veneziano D, Nigita G, Shankaraiah RC, Portolani N, Carcoforo P, Fornari F, Bolondi L, Frassoldati A, Sabbioni S, Colombo M, Croce CM, Negrini M. Circulating miR-106b-3p, miR-101-3p and miR-1246 as diagnostic biomarkers of hepatocellular carcinoma. *Oncotarget.* 2018;9:15350–64. <https://doi.org/10.18632/oncotarget.24601>.
 28. Cui X, Li Z, Zhao Y, Song A, Shi Y, Hai X, Zhu W. Breast cancer identification via modeling of peripherally circulating miRNAs. *PeerJ.* 2018;6:e4551. <https://doi.org/10.7717/peerj.4551>.
 29. Drusco A, Fadda P, Nigita G, Fassan M, Bottoni A, Gardiman M, Sacchi D, Calore F, Carosi M, Antenucci A, Casini B, Kelani H, Pescarmona E, Di Leva G, Zanesi N, Berger M, Croce C. Circulating MicroRNAs predict survival of patients with tumors of glial origin. *EBioMedicine.* 2018;30:105–12. <https://doi.org/10.1016/j.ebiom.2018.03.022>.
 30. Ebrahimkhani S, Vafaee F, Young PE, Hur SSS, Hawke S, Devenney E, Beadnall H, Barnett MH, Suter CM, Buckland ME. Exosomal microRNA signatures in multiple sclerosis reflect disease status. *Sci Rep.* 2017;7:14293. <https://doi.org/10.1038/s41598-017-14301-3>.
 31. Vistbakka J, Elovaara I, Lehtimäki T, Hagman S. Circulating microRNAs as biomarkers in progressive multiple sclerosis. *Mult Scler J.* 2017;23:403–12. <https://doi.org/10.1177/1352458516651141>.
 32. Fenoglio C, De Riz M, Pietroboni AM, Calvi A, Serpente M, Cioffi SMG, Arcaro M, Oldoni E, Scarpini E, Galimberti D. Effect of fingolimod treatment on circulating miR-15b, miR23a and miR-223 levels in patients with multiple sclerosis. *J Neuroimmunol.* 2016;299:81–3. <https://doi.org/10.1016/j.jneuroim.2016.08.017>.
 33. Villar LM, Picón C, Costa-Frossard L, Alenda R, García-Caldentey J, Espiño M, Muriel A, Álvarez-Cermeño JC. Cerebrospinal fluid immunological biomarkers associated with axonal damage in multiple sclerosis. *Eur J Neurol.* 2015;22:1169–75. <https://doi.org/10.1111/ene.12579>.
 34. Fenoglio C, Cantoni C, De Riz M, Ridolfi E, Cortini F, Serpente M, Villa C, Comi C, Monaco F, Mellesi L, Valzelli S, Bresolin N, Galimberti D, Scarpini E. Expression and genetic analysis of miRNAs involved in CD4+ cell activation in patients with multiple sclerosis. *Neurosci Lett.* 2011;504:9–12. <https://doi.org/10.1016/j.neulet.2011.08.021>.
 35. Sospedra M, Martin R. Immunology of multiple sclerosis. *Annu Rev Immunol.* 2005;23:683–747. <https://doi.org/10.1146/annurev.immunol.23.021704.115707>.
 36. Peeters LM, Vanheusden M, Somers V, Van Wijmeersch B, Stinissen P, Broux B, Hellings N. Cytotoxic CD4+ T cells drive multiple sclerosis progression. *Front Immunol.* 2017;8:1160. <https://doi.org/10.3389/fimmu.2017.01160>.
 37. Okoye IS, Coomes SM, Pelly VS, Czieso S, Papayannopoulos V, Tolmachova T, Seabra MC, Wilson MS. MicroRNA-containing T-regulatory-cell-derived Exosomes suppress pathogenic T helper 1 cells. *Immunity.* 2014;41:89–103. <https://doi.org/10.1016/j.immuni.2014.05.019>.
 38. Torri A, Carpi D, Bulgheroni E, Crosti M-C, Moro M, Guarini P, Rossi RL, Rossetti G, Di Vizio D, Hoxha M, Bollati V, Gagliani C, Tacchetti C, Paroni M, Geginat J, Corti L, Venegoni L, Berti E, Pagani M, Matarese G, Abbrignani S, de Candia P. Extracellular MicroRNA Signature of Human Helper T Cell Subsets in Health and Autoimmunity. *J Biol Chem.* 2017;292:2903–15. <https://doi.org/10.1074/jbc.M116.769893>.
 39. Wang S, Wan X, Ruan Q. The microRNA-21 in autoimmune diseases. *Int J Mol Sci.* 2016;17. <https://doi.org/10.3390/ijms17060864>.
 40. de Faria O, Moore CS, Kennedy TE, Antel JP, Bar-Or A, Dhaunchak AS. MicroRNA dysregulation in multiple sclerosis. *Front Genet.* 2013;3:1–6. <https://doi.org/10.3389/fgene.2012.00311>.
 41. Ma X, Zhou J, Zhong Y, Jiang L, Mu P, Li Y, Singh N, Nagarkatti M, Nagarkatti P. Expression, regulation and function of microRNAs in multiple sclerosis. *Int J Med Sci.* 2014;11:810–8. <https://doi.org/10.7150/ijms.8647>.
 42. Kutty RK, Nagineni CN, Samuel W, Vijayarathna C, Jaworski C, Duncan T, Cameron JE, Flemington EK, Hooks JJ, Redmond TM. Differential regulation of microRNA-146a and microRNA-146b-5p in human retinal pigment epithelial cells by interleukin-1 β , tumor necrosis factor- α , and interferon- γ . *Mol Vis.* 2013;19:737–50. <http://www.ncbi.nlm.nih.gov/pubmed/23592910> (Accessed 12 July 2018).
 43. Chen Y, Chen J, Wang H, Shi J, Wu K, Liu S, Liu Y, Wu J. HCV-induced miR-21 contributes to evasion of host immune system by targeting MyD88 and IRAK1. *PLoS Pathog.* 2013;9:e1003248. <https://doi.org/10.1371/journal.ppat.1003248>.
 44. Xie Y-F, Shu R, Jiang S-Y, Liu D-L, Ni J, Zhang X-L. MicroRNA-146 inhibits pro-inflammatory cytokine secretion through IL-1 receptor-associated kinase 1 in human gingival fibroblasts. *J Inflamm.* 2013;10:20. <https://doi.org/10.1186/1476-9255-10-20>.
 45. Zhou X, Ren Y, Moore L, Mei M, You Y, Xu P, Wang B, Wang G, Jia Z, Pu P, Zhang W, Kang C. Downregulation of miR-21 inhibits EGFR pathway and suppresses the growth of human glioblastoma cells independent of PTEN status. *Lab Invest.* 2010;90:144–55. <https://doi.org/10.1038/abinvest.2009.126>.
 46. Xu B, Wang N, Wang X, Tong N, Shao N, Tao J, Li P, Niu X, Feng N, Zhang L, Hua L, Wang Z, Chen M. MiR-146a suppresses tumor growth and progression by targeting EGFR pathway and in a p-ERK-dependent manner in castration-resistant prostate cancer. *Prostate.* 2012;72:1171–8. <https://doi.org/10.1002/pros.22466>.
 47. Cai J, Xu L, Cai Z, Wang J, Zhou B, Hu H. MicroRNA-146b-5p inhibits the growth of gallbladder carcinoma by targeting epidermal growth factor receptor. *Mol Med Rep.* 2015;12:1549–55. <https://doi.org/10.3892/mmr.2015.3461>.
 48. Heiseke AF, Jeuk BH, Markota A, Straub T, Lehr H-A, Reindl W, Krug AB. IRAK1 drives intestinal inflammation by promoting the generation of effector Th cells with optimal gut-homing capacity. *J Immunol.* 2015;195:5787–94. <https://doi.org/10.4049/jimmunol.1501874>.
 49. Deng C, Radu C, Diab A, Tsen MF, Hussain R, Cowdery JS, Racke MK, Thomas JA. IL-1 receptor-associated kinase 1 regulates susceptibility to organ-specific autoimmunity. *J Immunol Ref.* 2017;170:2833–42. <https://doi.org/10.4049/jimmunol.170.6.2833>.

50. Hossen MJ, Yang WS, Kim D, Aravinthan A, Kim JH, Cho JY. Thymoquinone: an IRAK1 inhibitor with in vivo and in vitro anti-inflammatory activities. *Sci Rep.* 2017;7:1–12. <https://doi.org/10.1038/srep42995>.
51. Raouf R, Jimenez-Mateos EM, Bauer S, Tackenberg B, Rosenow F, Lang J, Onugoren MD, Hamer H, Huchtemann T, Körtvélyessy P, Connolly NMC, Pfeiffer S, Prehn JHM, Farrell MA, O'Brien DF, Henshall DC, Mooney C. Cerebrospinal fluid microRNAs are potential biomarkers of temporal lobe epilepsy and status epilepticus. *Sci Rep.* 2017;7:3328. <https://doi.org/10.1038/s41598-017-02969-6>.

Publisher's Note

Springer Nature remains neutral with regard to jurisdictional claims in published maps and institutional affiliations.

Ready to submit your research? Choose BMC and benefit from:

- fast, convenient online submission
- thorough peer review by experienced researchers in your field
- rapid publication on acceptance
- support for research data, including large and complex data types
- gold Open Access which fosters wider collaboration and increased citations
- maximum visibility for your research: over 100M website views per year









At BMC, research is always in progress.

Learn more biomedcentral.com/submissions





Radiologically isolated syndrome: targeting miRNAs as prognostic biomarkers

María Muñoz-San Martín¹ , Sandra Torras¹, René Robles-Cedeño^{2,3,4} , Maria Buxó⁵ ,
Imma Gomez¹, Clara Matute-Blanch⁶ , Manuel Comabella^{3,6} , Luisa María Villar^{3,7} ,
Héctor Perkal², Ester Quintana^{*,†,1,3,4}  & Lluís Ramió-Torrentà^{**,†,2,3,4} 

¹Neurodegeneration & Neuroinflammation Group, Girona Biomedical Research Institute (IDIBGI), 17190 Salt, Spain

²Department of Neurology, Girona Neuroimmunology & Multiple Sclerosis Unit, Dr. Josep Trueta University Hospital & Santa Caterina Hospital, Girona/Salt-Spain; Neurodegeneration & Neuroinflammation Group, Girona Biomedical Research Institute (IDIBGI), 17190 Salt, Spain

³REEM, Red Española de Esclerosis Múltiple

⁴Department of Medical Sciences, Faculty of Medicine, University of Girona, 17190 Girona, Spain

⁵Girona Biomedical Research Institute (IDIBGI), 17190 Salt, Spain

⁶Servei de Neurologia-Neuroimmunologia, Centre d'Esclerosi Múltiple de Catalunya (Cemcat), Institut de Recerca Vall d'Hebron (VHIR), Hospital Universitari Vall d'Hebron, Universitat Autònoma de Barcelona, 08035 Barcelona, Spain

⁷Department of Immunology, Hospital Ramón y Cajal, IRYCIS, 28034 Madrid, Spain

*Author for correspondence: Tel.: +34 872987087; equintana@idibgi.org

**Author for correspondence: Tel.: +34 872987087; llramio@idibgi.org

†Authors contributed equally

Aim: Some clinical and biological characteristics have been described as prognostic factors for clinical conversion into clinically definite multiple sclerosis in radiologically isolated syndrome (RIS) population. The aim of this study was to assess signatures of circulating miRNAs in those patients according to their conversion status after 5 years of follow-up. **Patients & methods:** OpenArray plates assessing 216 miRNA candidates were run in 15 RIS patients, and their relative abundances were analyzed. **Results:** A specific profile of deregulated circulating miRNAs (miR-144-3p, miR-448 and miR-653-3p in cerebrospinal fluid and miR-142-3p, miR-338-3p, miR-363-3p, miR-374b-5p, miR-424-5p, miR-483-3p in plasma) differentiated individuals who remained as RIS after 5 years of follow-up. **Conclusion:** Circulating miRNAs might be used as prognostic biomarkers for RIS patients.

First draft submitted: 28 April 2020; Accepted for publication: 4 October 2020; Published online: 00 December 2020

Keywords: miRNAs • multiple sclerosis • neurofilament light chain • prognostic biomarker • radiologically isolated syndrome

The incidental radiological finding of white matter lesions suggestive of multiple sclerosis (MS) in asymptomatic individuals is known as 'radiologically isolated syndrome' (RIS), a term first introduced by Okuda *et al.* in 2009 [1]. These RIS individuals are followed by means of neuroimaging surveillance and clinical follow-up [1] and approximately a third of subjects could develop a symptomatic demyelinating event and evolve toward clinically definite MS (CDMS) in 5 years [2].

Some elements have been described as risk factors for clinical conversion into CDMS in RIS population: younger age, male sex and presence of spinal cord lesions [3]. Other clinical parameters and biological molecules like oligoclonal bands (OCB) and neurofilament light chain (NF-L) have also been added as predictors biomarkers of clinical conversion in RIS subjects [4].

miRNAs are small noncoding RNA molecules with the ability to regulate gene expression controlling many biological processes [5]. Circulating miRNAs in serum, plasma or cerebrospinal fluid (CSF) might present valuable potential as biomarkers in different diseases. Specifically, several studies have supported their utility in MS predicting disease subtype or response to a specific treatment [6–9]. None of these studies have been focused on analyzing possible miRNA signature in RIS population.

Table 1. Demographic, clinical, radiological and genetic data of the studied cohort.

Baseline characteristics	Whole group	RIS-RIS	RIS-Conversion	p-value
n	15	8	7	
Sex				0.077
Male	4 (26.7)	4 (50.0)	0 (0.0)	
Female	11 (73.3)	4 (50.0)	7 (100.0)	
Age	38.0 (32.0–48.5)	38.5 (33.0–52.0)	37.0 (29.0–43.0)	0.336
Time of follow-up (years)	6.5 (5.8–6.5)	6.5 (5.3–7.0)	6.5 (6.0–6.5)	1.000
EDSS	1.50 (1.00–2.00)	1.25 (0.50–1.75)	1.50 (1.25–2.25)	0.232
Vitamin D				0.592
<20 ng/ml	8 (57.1)	5 (71.4)	3 (42.9)	
>20 ng/ml	6 (42.9)	2 (28.6)	4 (57.1)	
OCGB				0.200
Absence	3 (20.0)	3 (37.5)	0 (0.0)	
Presence	12 (80.0)	5 (62.5)	7 (100.0)	
Index IgG	0.749 (0.583–1.736)	0.634 (0.567–0.986)	1.779 (1.502–1.811)	0.127
T2 lesions	13.5 (9.0–28.0)	9.5 (4.5–19.5)	27.0 (12.0–31.0)	0.043
Gd+ lesions				1.000
Absence	12 (85.7)	7 (87.5)	5 (83.3)	
Presence	2 (14.3)	1 (12.5)	1 (16.7)	
Spinal cord lesions	0.0 (0.0–2.0)	0.0 (0.0–0.5)	2.0 (1.0–2.0)	0.230
Black holes				0.055
Absence	11 (78.6)	8 (100.0)	3 (50.0)	
Presence	3 (21.4)	0 (0.0)	3 (50.0)	
Atrophy				1.000
Absence	13 (92.9)	7 (87.5)	6 (100.0)	
Presence	1 (7.1)	1 (12.5)	0 (0.0)	
HLA-DRB1*15:01 or *03				0.315
Absence	7 (46.7)	5 (62.5)	2 (28.6)	
Presence	8 (53.3)	3 (37.5)	5 (71.4)	
CHI3L1 (ng/ml)	183.256 (122.485–219.874)	158.873 (113.094–210.824)	215.218 (175.367–252.844)	0.435
NF-L (pg/ml)	258.177 (177.907–615.137)	204.572 (103.626–480.788)	615.137 (258.177–857.226)	0.171

RIS-RIS: Individuals who remained as RIS after 5 years of monitoring; RIS-Conversion: Individuals who converted to CIS or MS after 5 years of monitoring; Categorical variables were shown as absolute and relative frequencies and their statistical differences were determined by the Fisher's exact test. Continuous variables were presented by median and Q1–Q3: First quartile–Third quartile and their statistical differences were determined by the Mann–Whitney U test.
CIS: Clinically isolated syndrome; EDSS: Expanded disability status scale; Gd+: Gadolinium enhanced; MS: Multiple sclerosis; n: Number of sample; OCGB: Oligoclonal IgG bands; RIS: Radiologically isolated syndrome.

The principal aim of this study was to assess the prognostic role of miRNA profiles in CSF and plasma for conversion to clinically isolated syndrome (CIS) or to MS in RIS patients. Additionally, other radiological, clinical and biological variables were studied in our RIS cohort.

Patients & methods

Study design & patients

15 patients diagnosed with RIS following the 2009 Okuda *et al.*'s criteria [1], were recruited at the Girona Neuroimmunology and Multiple Sclerosis Unit of Dr. Josep Trueta University Hospital (Girona, Spain). The inclusion criteria were over than 18 years old and availability of biological samples during RIS diagnosis. After a 5-year follow-up, seven patients converted to CIS or MS (RIS-Conversion), while eight remained as RIS (RIS-RIS). Conversion was defined as the occurrence of neurological symptoms, increase of number of lesions and/or disability [4].

Demographic data including sex and age, time of follow-up, as well as clinical, genetic and radiological outputs are depicted in Table 1. Clinical data and MRI acquisition and analysis were obtained and interpreted by specialized neurologists and radiologists, respectively. Specifically, T1-3D, T2/DP 2D, FLAIR (2D and 3D), and T1

postgadolinium sequences were used to obtain MRI parameters. The Ethics Committee and the Committee for Clinical Investigation from Dr. Josep Trueta University Hospital approved the protocol employed in this study. All participants signed a written informed consent.

Biological samples

CSF was centrifuged immediately after lumbar puncture at 400 *g* for 15 min to precipitate cells and obtain cell-free CSF. Plasma, buffy coat and serum were collected after centrifuging blood at 2000 *g* for 10 min. Cell-free CSF, plasma, buffy coat and serum aliquots were stored at -80°C until RNA or DNA extraction or biochemical quantifications.

Laboratory procedures

OCB detection

Serum and CSF IgG were quantified by nephelometry using an Immage 800 nephelometer (Beckman Coulter, Nyon, Switzerland). IgG bands were analyzed by isoelectric focusing and immunoblotting as previously described [10]. Antibody RRID: 109-055-003.

HLA-DRB1 allele detection

DNA was extracted from frozen buffy coat using QIAamp DNA Mini Kit (QIAGEN, Madrid, Spain). Allelic assay for this gene was made by PCR amplification and subsequent hybridization with sequence-specific oligonucleotide probes (PCR-SSO) (Diagnostica Longwood, Catalog number: 628925, 2017; Zaragoza, Spain). Control DNA from well genetic-characterized patients for *HLA-DRB1* was included in each assay. *HLA-DRB1*15:01* genotyping was confirmed by sequencing with specific primers.

Vitamin D quantification

Levels of 25-OH vitamin D were assessed by electro-chemiluminescence (Elecsys Total Vitamin D, Catalog number: 05894913190, 2015; Roche Diagnostics, Basel, Switzerland) and classified into two ranges 0–20 or more than 20 ng/ml.

CHI3L1 & NF-L quantification

Levels of CHI3L1 in CSF were studied by ELISA (MicroVue YKL-40 EIA Kit, Quidel, Catalog number: 8020; CA, USA) at the Cemcat (Barcelona, Spain) and NF-L levels were also measured by ELISA (Uman Diagnostics, Catalog number: 10-7001 CE; Umea, Sweden) at the Ramón y Cajal Hospital (Madrid, Spain) according to the manufacturers' instructions.

Analysis of circulating miRNAs

Circulating RNA extraction & purification

Circulating RNA from cell-free CSF and plasma was extracted using mirVana PARIS Isolation Kit (Applied Biosystems, Catalog number: AM1556, 2018; CA, USA) according to manufacturer's instructions and our previous experience [8]. Briefly, 300 µl of sample was mixed with the same volume of 2x Denaturing solution. To assure the quality of the extraction process, spike-in cel-miR-39 and cel-miR-54 exogenous miRNAs were added at this point. Then, the same volume of acid-phenol:chloroform was added. After centrifugation (17,000 *g*, 10 min, 19°C), the upper aqueous phase was recovered, mixed with 100% ethanol and placed into a filter cartridge. After the washing procedures suggested by the manufacturer, total RNA was eluted with 40 µl of nuclease-free water.

Circulating miRNA retrotranscription & preamplification

We used 2 µl of RNA eluate for the preparation of miRNA cDNA using TaqMan Advanced miRNA cDNA Synthesis Kit (Applied Biosystems, Catalog number: A28007, 2018; Warrington, United Kingdom). Briefly, after the addition of a poly(A) tail and adaptor following the manufacturer's instructions, a reverse transcription reaction and miRNA amplification reaction were performed. The preamplification step is usually needed before real-time PCR (RT-PCR) analysis when analytical sensitivity is of the utmost importance or the sample size is small [11].

Circulating miRNA profiling

Custom OpenArray plates (selected miRNA list could be shared under request) containing 216 TaqMan Advanced miRNA assays (Applied Biosystems, Catalog number: A33469, 2018) were used for miRNA profiling in cell-free CSF and plasma samples per triplicate after assuring extraction quality with spike-in and some endogenous miRNAs. RT-PCR was carried out using QuantStudio 12K Flex Real-Time PCR System (Applied BioSystems).

Analysis of OpenArray plates

OpenArray data were first filtered according to 'AmpScore' and/or 'CqConfidence' values (1.1 and 0.6 for plasma and 0.75 and 0.45 for CSF) provided by the Relative Quantification module in the Thermo Fisher Cloud, ensuring good quality detection. All samples were run in triplicate and the maximal acceptable range for those measurements were dependent on the mean Ct value [12]. To remove variation due to technical or biological sources, we used global normalization method instead of spike-in normalization approach [13]. This method employs the mean expression value of all miRNAs, for both CSF and plasma miRNA profiling [14]. Plasma levels were also normalized using the mean value of the most stable endogenous miRNAs miR-20a, miR-103a and miR-191, according to the Relative Quantification module in the Thermo Fisher Cloud. Delta Ct method was used to calculate the relative expression.

Targets, pathways & cellular/tissue-enriched sources analyses

Validated targets for selected differentially expressed miRNAs in CSF were obtained from miRTarBase [15]. Those targets were filtered according to the validation method (western blot, reporter assay and/or qPCR) and introduced in Enrichr to explore the gene ontology (GO) biological processes [16]. Associated GO terms were clustered according to their relatedness using REVIGO [17] after removing redundant terms.

Different repositories containing expression profiles of miRNAs in tissue, primary cells and biofluids have been used to study potential tissue and cellular sources of miRNAs [18–20].

Statistical analysis

Demographic, clinical, genetic and radiological data were reported as follows: categorical variables were shown as absolute and relative frequencies while continuous variables were represented by median (quartiles). Statistical differences were determined by the Mann–Whitney U test in the case of quantitative variables while the Fisher's exact test for categorical ones. All analyses were two-tailed and the significance level was set to 0.05. Due to the preliminary nature of the study, as well as the small size of the cohort, multiple comparisons corrections were not employed. Statistical analyses were performed in Statistical Package for the Social Sciences version 25.0 (IBM SPSS Statistics for Windows, NY, USA). Figures were built using GraphPad PRISM v.5 (GraphPad Software, CA, USA).

All variables were measured by experimenters blind to clinical data.

Results

Clinical characteristics of the RIS patients

This was a longitudinal exploratory study comprising 15 patients with RIS (73.3% women) with a median age of 38 years. Conversion was observed in seven patients (100% women), while eight patients remained as RIS (50% women). No significant differences were observed in sex or age between RIS–RIS and RIS–Conversion individuals. Clinical, radiological and genetic data collected close to the sample extraction date, as well as levels of Vitamin D, one of the environmental risk factors in MS, did not reveal any differences between both groups either, except for an increased number of T2 lesions in the RIS–Conversion group (RIS–RIS median = 9.5 lesions vs RIS–Conversion median = 27.0 lesions; $p = 0.043$). Although the presence of black holes in MRI did not reach statistical significance ($p = 0.055$), it was observed in 50.0% of RIS–Conversion patients versus 0% of RIS–RIS patients. All these data are depicted in Table 1.

CHI3L1 & NF-L levels in CSF

CHI3L1 and NF-L levels were tested to compare RIS–RIS and RIS–Conversion subjects. No changes in CHI3L1 and NF-L levels were observed (CHI3L1: RIS–RIS median = 158.873 ng/ml vs RIS–Conversion median = 215.218 ng/ml, $p = 0.435$; NF-L: RIS–RIS median = 204.572 pg/ml vs RIS–Conversion median = 615.137 pg/ml, $p = 0.171$; respectively) (Table 1).

A strong correlation was observed between CSF levels of CHI3L1 and NF-L ($r_s = 0.852$, $p < 0.001$). Further association analyses between CHI3L1, NF-L and radiological variables revealed a correlation only between NF-L

Table 2. Differential miRNA expression between groups in cerebrospinal fluid samples.

	Global normalization				p-value
	RIS-RIS (n = 7)		RIS-Conversion (n = 5)		
	Median	Q1-Q3	Median	Q1-Q3	
miR-144-3p	0.405	0.308–0.409	1.082	0.827–1.036	0.016
miR-448	0.086	0.071–0.109	0.307	0.252–0.536	0.005
miR-653-3p	0.271	0.233–0.299	0.421	0.403–0.609	0.030

RIS-RIS: Individuals who remained as RIS after 5 years of monitoring; RIS-Conversion: Individuals who converted to CIS or MS after 5 years of monitoring. Statistical differences were determined by the Mann-Whitney U test.
CIS: Clinically isolated syndrome; MS: Multiple sclerosis; n: Number of sample; Q1-Q3: First quartile-Third quartile; RIS: Radiologically isolated syndrome.

Table 3. Differential miRNA expression between groups in plasma samples.

	Global normalization			Endogenous normalization		
	RIS-RIS (n = 8)	RIS-Conversion (n = 7)	p-value	RIS-RIS (n = 8)	RIS-Conversion (n = 7)	p-value
	Median (Q1-Q3)	Median (Q1-Q3)		Median (Q1-Q3)	Median (Q1-Q3)	
miR-142-3p	8.783 (7.695–9.991)	4.893 (3.760–6.882)	0.029	1.504 (1.357–1.955)	0.872 (0.765–1.152)	0.004
miR-338-3p	0.120 (0.083–0.134)	0.051 (0.035–0.069)	0.014	0.020 (0.013–0.024)	0.009 (0.007–0.011)	0.021
miR-363-3p	0.392 (0.261–0.505)	0.139 (0.098–0.247)	0.030	0.060 (0.056–0.074)	0.027 (0.017–0.050)	0.045
miR-374b-5p	0.473 (0.310–0.601)	0.176 (0.138–0.316)	0.029	0.083 (0.065–0.094)	0.033 (0.026–0.056)	0.029
miR-424-5p	0.189 (0.179–0.249)	0.076 (0.050–0.110)	0.002	0.040 (0.028–0.048)	0.014 (0.010–0.020)	0.006
miR-483-3p	0.053 (0.045–0.061)	0.089 (0.079–0.220)	0.009	0.011 (0.006–0.013)	0.018 (0.015–0.044)	0.030

RIS-RIS: Patients who remained as RIS after 5 years of monitoring; RIS-Conversion: Patients who converted to CIS or MS after 5 years of monitoring. Statistical differences were determined by the Mann-Whitney U test.
CIS: Clinically isolated syndrome; MS: Multiple sclerosis; n: Number of sample; Q1-Q3: First quartile-Third quartile; RIS: Radiologically isolated syndrome.

and number of T2 lesions, and a tendency between NF-L and Gd+ (gadolinium-enhanced) lesions ($r_s = 0.600$ and $p = 0.030$; $r_s = 0.498$ and $p = 0.083$; respectively).

miRNA profile in CSF

12 patients with available CSF were analyzed for the screening of circulating miRNAs in cell-free CSF. We found that 124 of 216 analyzed miRNAs were detected fulfilling the established criteria of detection quality but only 15 miRNAs were present in at least 50% of samples according to the expected lower miRNA detection in CSF.

Three of the selected miRNAs presented differential expression in RIS-RIS and RIS-Conversion patients. miR-144-3p, miR-448 and miR-653-3p were upregulated in the RIS-Conversion group (Table 2 & Figure 1).

miRNA profile in plasma

Samples of all RIS-RIS and RIS-Conversion patients were used for the screening of circulating miRNAs in plasma. We found that 130 miRNAs were detected in at least 50% of plasma samples satisfying the same criteria of quality mentioned earlier.

We used two different normalization strategies and the differential expression between groups was studied in both cases (Table 3). On the one hand, we applied global normalization that uses the mean value of all detectable miRNAs as normalizer value. On the other hand, we used the mean value of miR-20a, miR-103a and miR-191, as they were the most stable miRNAs provided by the Relative Quantification module in the Thermo Fisher Cloud. Six miRNAs were significantly deregulated ($p < 0.050$) with both normalization strategies. miR-142-3p, miR-338-3p, miR-363-3p, miR-374b-5p and miR-424-5p were downregulated, while miR-483-3p was upregulated (Table 3 & Figure 2) in RIS-Conversion patients.

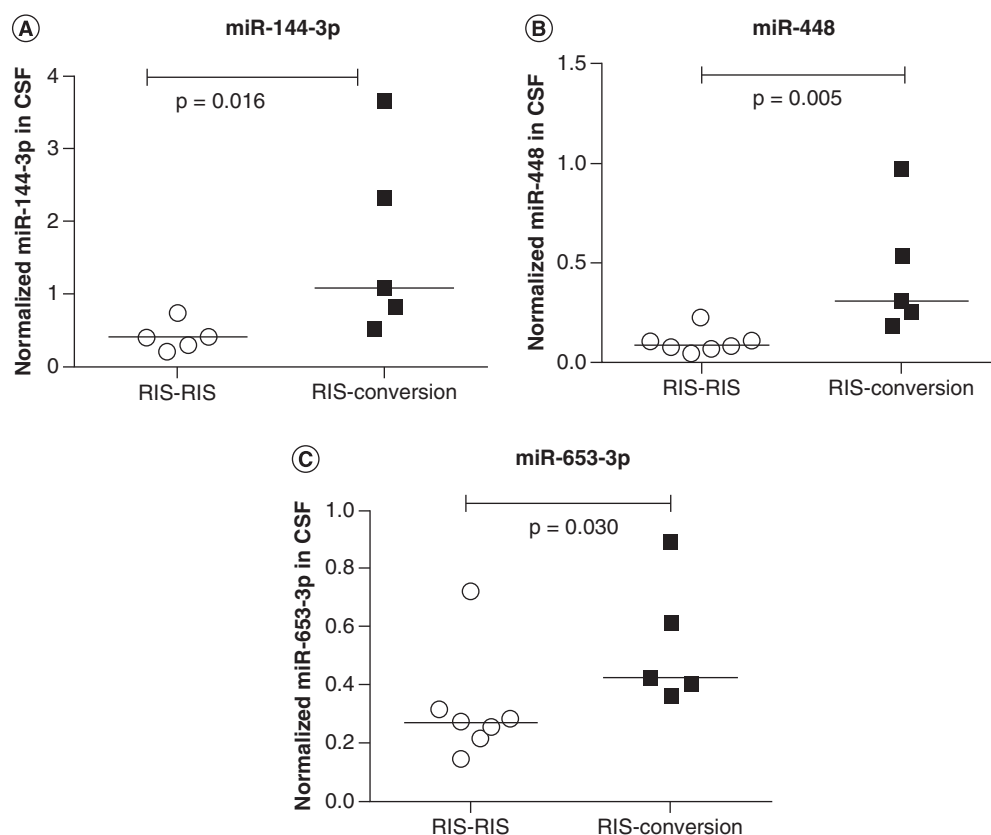


Figure 1. Differentially expressed miRNAs in cerebrospinal fluid. Dot plots for normalized value of (A) miR-144-3p, (B) miR-448 and (C) miR-653-3p in CSF samples according to the conversion status. Global normalization data were used in the figure. The dot indicates one sample and the line indicates the median. The Mann–Whitney U test was used to determine statistical differences between groups.

RIS–RIS: Individuals who remained as RIS after 5 years of monitoring; RIS–Conversion: Individuals who converted to CIS or MS after 5 years of monitoring.

CSF: Cerebrospinal fluid.

Targets, pathways & cellular/tissue-enriched sources analysis of selected miRNAs

Experimentally validated human targets for all deregulated miRNAs were retrieved from miRTarBase. Enrichr was used to determine the GO biological processes where strongly validated targets for deregulated CSF and plasma miRNAs were involved (Supplementary Tables 1 & 2). Clustered GO terms revealed that target genes for CSF-deregulated miRNAs were involved in distinct biological processes related to cell adhesion and migration or cytokine-mediated signaling pathways (Figure 3A). Regarding plasma-deregulated miRNAs targets, cellular processes involving cytokine stimulus and adherens junction organization were highlighted, among others (Figure 3B).

Potential miRNA's source studies showed high expressions of most deregulated miRNAs in natural killer, T or B cells, as well as in brain.

Association of miRNA levels with CSF biochemical & radiological variables

We studied the correlation between all deregulated miRNA levels and number of T2 lesions in MRI as a radiological variable, CHI3L1 and NF-L levels in CSF. The expression of miR-448 in CSF positively correlated with the number of T2 lesions. In plasma, whereas miR-363-3p only had a negative correlation with T2 lesions, miR-483-3p levels were positively associated with number of T2 lesions, CHI3L1 and NF-L levels (Supplementary Table 3).

Discussion

Since 2009, when the term RIS was first introduced by Okuda *et al.* [1], most of the studies focused on this entity, have defined the term or have described risk factors associated to the clinical conversion to CDMS. Some other studies have analyzed other clinical parameters and biological molecules like OCB, NF-L, CHI3L1 or progranulin [3,4,21]

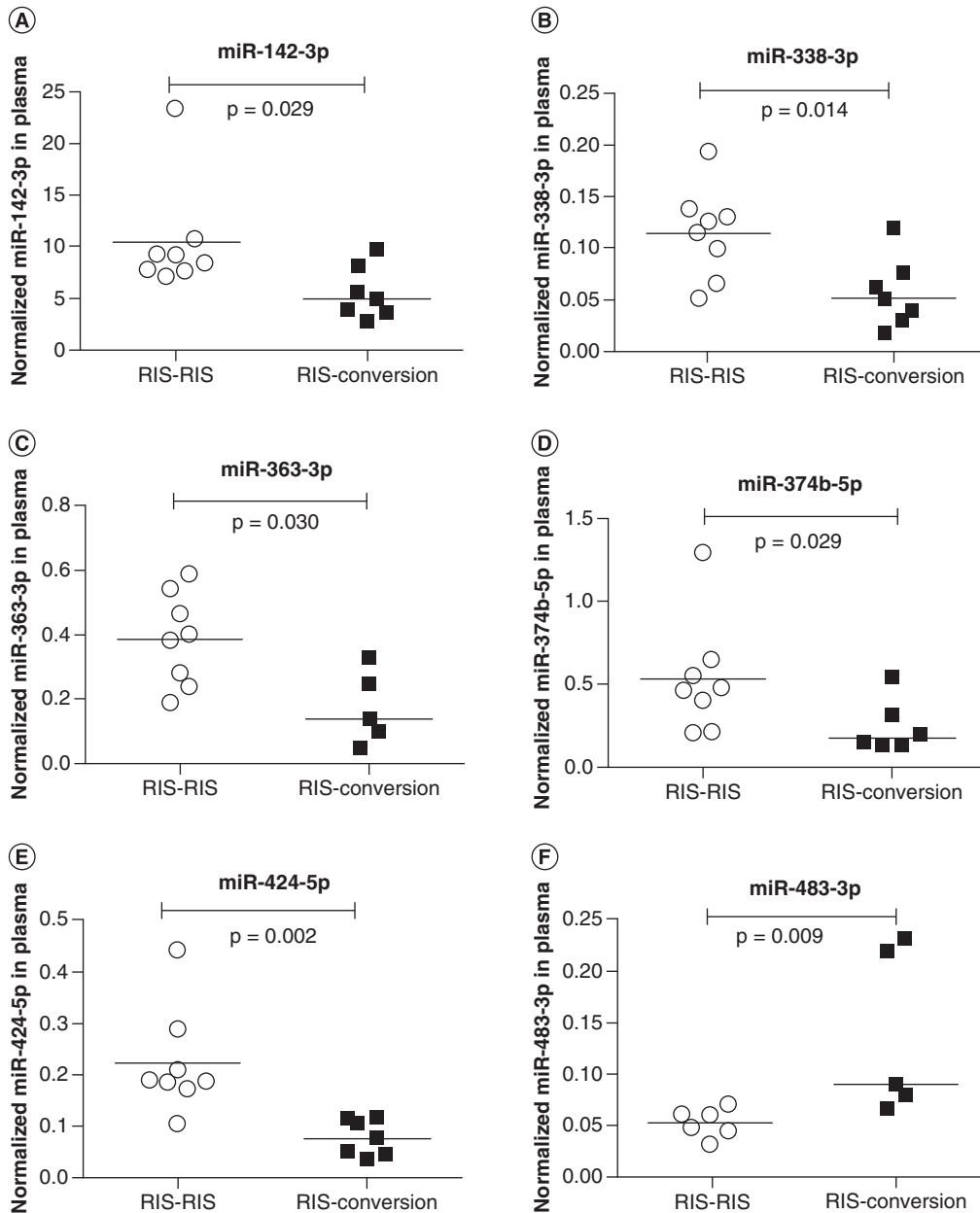


Figure 2. Differentially expressed miRNAs in plasma. Dot plots for normalized value of (A) miR-142-3p, (B) miR-338-3p, (C) miR-363-3p, (D) miR-374b-5p, (E) miR-424-5p and (F) miR-483-3p in plasma samples according to the conversion status. Global normalization data were used in the figure. The dot indicates one sample and the line indicates the median. The Mann–Whitney U test was used to determine statistical differences between groups. RIS–RIS: Patients who remained as RIS after 5 years of monitoring; RIS–Conversion: Patients who converted to CIS or MS after 5 years of monitoring.

in order to establish predictor biomarkers of clinical conversion in RIS subjects. However, none of them has been focused on the miRNA profile when RIS diagnosis is established comparing between individuals who remain as RIS or finally convert to CDMS. The study presented herein brings in a differential circulating miRNA signature in those two groups, and describes some already established risk factors and predictor biomarkers of conversion in our cohort.

Some previous described risk factors for clinical conversion into CDMS in RIS individuals [3] did not show significant differences in this study. However, we would like to highlight some aspects related to radiological, clinical and biochemical parameters. We found that the number of T2 lesions was significantly increased in RIS–Conversion

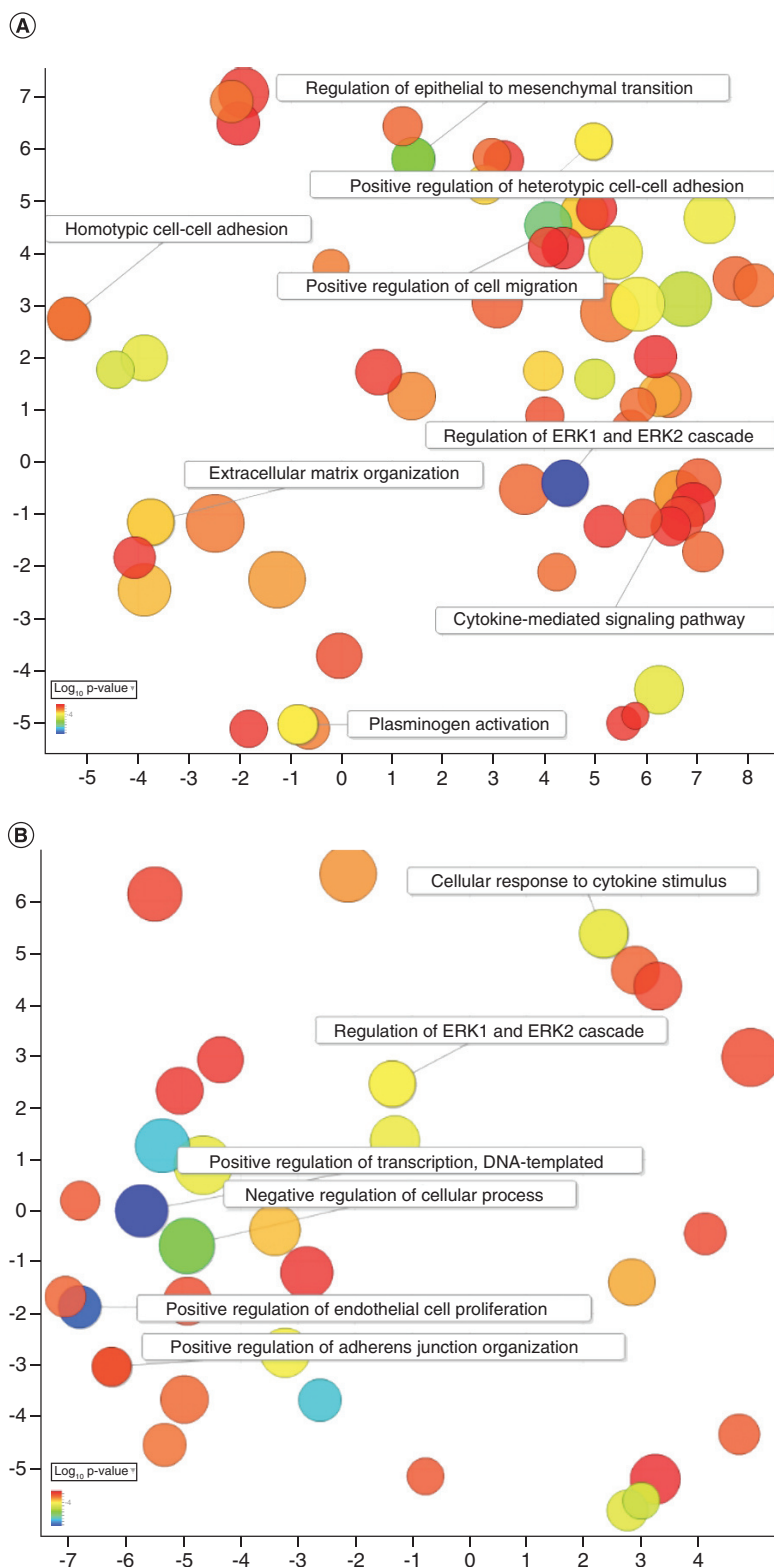


Figure 3. Visualization of the significantly associated gene ontology biological processes using REVIGO. Visualization of the significantly associated GO biological processes in CSF (A) and plasma (B) using REVIGO. The semantic similarity scatterplot shows the cluster representatives after the redundancy reduction. The bubble size indicates the frequency of the GO term and the color indicates the \log_{10} (adjusted p-value). Color legend is shown in the right corner of the figure. CSF: Cerebrospinal fluid; GO: Gene ontology.

subjects compared with RIS–RIS group, and the presence of black holes might seem to be characteristic in those individuals who converted to CDMS. Despite being asymptomatic individuals, RIS–RIS group presented EDSS score above zero as observed in other studies in some individuals in the moment of RIS diagnosis [21,22]. In addition, the results presented in this study did not validate the role of NF-L and OCB as predictors for RIS conversion [4], despite markedly showing the expected trend, probably due to the small size of the studied cohort.

miRNAs are noncoding RNA molecules that regulate gene expression at the post-transcriptional level [5]. Due to their presence and stability in biological fluids such as plasma or CSF [23], their potential role as biomarkers in MS has been previously investigated [8,23,24]. Circulating miRNAs studies should face some preanalytical and analytical challenges [25] and one of the most important limitation is the lack of a common and solid way of normalization [13]. To avoid this, we used two different normalization strategies when analyzing plasma samples, as previously made by Wang-Renault *et al.* [26]. So, we could define a specific miRNA signature in plasma relying in those miRNAs significantly deregulated by both methods. Due to the small size of the RIS cohort and the preliminary nature of the study, multiple comparisons corrections were not employed in this study to avoid missing some interesting miRNAs. However, this might lead to false-positives results, so this type of corrections will be employed in future validation studies [27]. Some of the miRNAs we have found deregulated according to the conversion status of RIS individuals had been previously described in some MS studies or in the context of remyelination processes. miR-448 had been previously found upregulated in peripheral blood mononuclear cells (PBMCs) and CSF of MS patients [28]. miR-338-3p is downregulated in inactive MS lesions [29] and involved in remyelination processes [30]. miR-363-3p also showed decreased levels in MS patients in several studies involving PBMCs and B lymphocytes [31–33]. However, miR-142-3p was upregulated in PBMCs of relapsing-remitting MS compared with healthy controls [34,35]. Although this deregulation is opposed to the one we found in plasma samples, this variation might be explained by the different source of biological material employed in the studies, as miRNAs can present different patterns of expression between tissues and biofluids [18,36]. For this reason, we focused our study on miRNA expression in both biofluids separately as CSF might present a miRNA profile formed by more homogenous biological sources than plasma's, which might be altered by systemic conditions [37]. This fact highlights the importance of studying miRNAs in specific cell types or biofluids to try to uncover the complex interactions between tissues.

Although the use of circulating miRNAs as biomarkers should not be confounded with their cellular functions regulating gene expression, there are published studies establishing the justification to investigate the functionality of selected miRNAs. On the one hand, circulating miRNAs can be transported from donor to recipient cells, showing a new mechanism of cell-to-cell communication [38]. Concretely, Zhang *et al.* [39] demonstrated that miRNAs could be selectively packaged into extracellular vesicles and then transferred to recipient cells in which they can regulate mRNA and protein expression. On the other hand, exosomes might be influenced by the tissue of origin and their effects in receptor cells might play an important role in different pathological conditions [40]. In this case, studying CSF might reflect some biochemical changes that occur in the brain under pathological conditions due to its direct contact with the extracellular space of the brain [37].

For these reasons, we decided to investigate the functional roles of these deregulated miRNAs *in silico*. It has been suggested that RIS subjects could present a more beneficial response to the demyelinating insult than relapsing-remitting MS individuals and, an exceptional ability to repair this demyelinating event [41]. However, not all RIS subjects will develop a symptomatic demyelinating event and evolve toward CDMS [2]. Some deregulated miRNAs identified in this study are involved in different biological processes and pathways and it would be interesting studying their possible role in the clinical conversion process, beyond their possible prognostic role.

Some parts of miRNA fraction in biofluids could also be released due to the passive leakage of apoptosis or necrosis [42]. Different repositories containing expression profiles of miRNAs in tissue, primary cells and biofluids are available [18–20]. This information might be valuable in directing future studies toward specific cell lines or tissues as well as in confirming the presence of a certain miRNA in a biological fluid. Most of deregulated miRNAs in our study can be found in different types of immune cells such as natural killer, T and B cells whose roles in MS pathogenesis have been previously reported [43]. In addition, miR-338-3p and miR-374b-5p, two miRNAs deregulated in plasma samples, are highly expressed in brain [18]. These findings along with the target and pathway analyses previously discussed support the idea of directing future research toward a deeper knowledge of miRNA functionality.

This study has some limitations. The most important one is the small size of the studied cohort due to the limited number of RIS patients available at our center. To partially counteract this, we used replicate measurements

for miRNA analysis trying to increase accuracy and reduce technical variations in the process and employed two different normalization strategies in plasma samples data.

Conclusion

This exploratory study reports a signature pattern of circulating miRNAs in RIS individuals, differentiating those who finally converted to CDMS from those who remained as RIS. Specifically, miR-144-3p, miR-448 and miR-653-3p were deregulated in CSF and, miR-142-3p, miR-338-3p, miR-363-3p, miR-374b-5p and miR-424-5p were deregulated in plasma samples. *In silico* analyses concerning the biological processes in which these miRNAs are involved and their cellular or tissular origin might suggest a potential interest in studying miRNA functionality in immune cells in further studies.

Future perspective

The preliminary results presented herein should be validated in independent and larger cohorts. In spite of not reaching statistical significance, we propose to study the presence of black holes in future studies to confirm its prognostic role in conversion to MS in RIS individuals.

Summary points

- An increased number of T2 lesions was observed in the radiologically isolated syndrome (RIS)-Conversion group.
- The presence of black holes was only present in the RIS-Conversion group.
- No changes in CHI3L1 and NF-L levels in cerebrospinal fluid (CSF) were observed between both groups, although RIS-conversion group presented higher levels.
- miR-144-3p, miR-448 and miR-653-3p were upregulated in CSF in the RIS-Conversion group.
- miR-142-3p, miR-338-3p, miR-363-3p, miR-374b-5p and miR-424-5p were downregulated in plasma samples in RIS-Conversion patients.
- miR-483-3p was upregulated in plasma of RIS-Conversion patients.
- Target genes for deregulated miRNAs were involved in cell adhesion and migration, adherens junction organization and cytokine-mediated signaling pathways.
- The expression of miR-448 in CSF positively correlated with the number of T2 lesions. miR-363-3p in plasma was negatively correlated to the number of T2 lesions.
- Plasma levels of miR-483-3p were positively associated with number of T2 lesions, CHI3L1 and NF-L levels.

Supplementary data

To view the supplementary data that accompany this paper please visit the journal website at: www.futuremedicine.com/doi/suppl/10.2217/epi-2020-0172

Author contributions

M Muñoz-San Martín participated in the design and conceptualization of the study, the analysis or interpretation of the data and drafting or revising the manuscript for intellectual content. S Torras participated in the analysis or interpretation of the data. R Robles-Cedeño participated in the design and conceptualization of the study, acquisition of data and revising the manuscript for intellectual content. M Buxó participated in the analysis or interpretation of the data and revision of the manuscript for intellectual content. I Gomez participated in the acquisition of data and the analysis or interpretation of the data. C Matute-Blanch participated in the acquisition of data and the analysis or interpretation of the data and and revision of the manuscript for intellectual content. M Comabella participated in the analysis or interpretation of the data and drafting or revising the manuscript for intellectual content. LM Villar participated in the analysis or interpretation of the data and drafting or revising the manuscript for intellectual content. H Perkal participated in the design and conceptualization of the study and played a major role in the acquisition of data. E Quintana participated in the design and conceptualization of the study, the analysis or interpretation of the data and drafting or revising the manuscript for intellectual content. LI Ramió-Torrentà participated in the design and conceptualization of the study, interpretation of the data, drafting or revising the manuscript for intellectual content and played a major role in acquisition of data.

Acknowledgments

The authors particularly acknowledge the patients and the IDIBGI Biobank (Biobanc IDIBGI, B. 0000872), integrated in the Spanish National Biobank Network, for their collaboration.

Financial & competing interests disclosure

This study was supported by a grant from the Instituto Carlos III – Spanish Government (PI13/01782) and by a grant from Fundación 2000 (2015). M. Muñoz-San Martín was supported by a FI-DGR 2016 from AGAUR. The authors have no other relevant affiliations or financial involvement with any organization or entity with a financial interest in or financial conflict with the subject matter or materials discussed in the manuscript apart from those disclosed.

No writing assistance was utilized in the production of this manuscript.

Ethical conduct of research

The authors state that they have obtained appropriate institutional review board approval or have followed the principles outlined in the Declaration of Helsinki for all human or animal experimental investigations. In addition, for investigations involving human subjects, informed consent has been obtained from the participants involved.

References

Papers of special note have been highlighted as: ● of interest

- Okuda DT, Mowry EM, Beheshtian A *et al.* Incidental MRI anomalies suggestive of multiple sclerosis: the radiologically isolated syndrome. *Neurology* 72(9), 800–805 (2009).
- **It described for the first time the term ‘radiologically isolated syndrome’ (RIS).**
- Okuda DT. Radiologically isolated syndrome. *Neuroimaging Clin. N. Am.* 27(2), 267–275 (2017).
- **It highlighted the rate of clinical conversion in RIS individuals after 5 years of follow-up.**
- Thouvenot E, Hinsinger G, Demattei C *et al.* Cerebrospinal fluid chitinase-3-like protein 1 level is not an independent predictive factor for the risk of clinical conversion in radiologically isolated syndrome. *Mult Scler* 25(5),669–677 (2019).
- Matute-Blanch C, Villar LM, Álvarez-Cermeño JC *et al.* Neurofilament light chain and oligoclonal bands are prognostic biomarkers in radiologically isolated syndrome. *Brain* 141(4), 1085–1093 (2018).
- **It described the prognostic role of neurofilament light chain and oligoclonal bands in the conversion of individuals diagnosed with RIS.**
- Mendell JT, Olson EN. MicroRNAs in stress signaling and human disease. *Cell* 148(6), 1172–1187 (2012).
- Ebrahimkhani S, Vafaee F, Young PE *et al.* Exosomal microRNA signatures in multiple sclerosis reflect disease status. *Sci. Rep.* 7(1), 14293 (2017).
- Vistbakka J, Elovaara I, Lehtimäki T, Hagman S. Circulating microRNAs as biomarkers in progressive multiple sclerosis. *Mult. Scler. J.* 23(3), 403–412 (2017).
- Quintana E, Ortega FJ, Robles-Cedeño R *et al.* miRNAs in cerebrospinal fluid identify patients with MS and specifically those with lipid-specific oligoclonal IgM bands. *Mult. Scler. J.* 23(13), 1716–1726 (2017).
- **It presented results of miRNAs dysregulation in multiple sclerosis patients in cerebrospinal fluid, showing the potential of this biofluid.**
- Fenoglio C, De Riz M, Pietroboni AM *et al.* Effect of fingolimod treatment on circulating miR-15b, miR23a and miR-223 levels in patients with multiple sclerosis. *J. Neuroimmunol.* 299, 81–83 (2016).
- Sádaba MC, González Porqué P, Masjuan J, Alvarez-Cermeño JC, Bootello A, Villar LM. An ultrasensitive method for the detection of oligoclonal IgG bands. *J. Immunol. Methods* 284(1–2), 141–145 (2004).
- Ortega FJ, Mercader JM, Catalan V *et al.* Targeting the circulating microRNA signature of obesity. *Clin. Chem.* 59(5), 781–792 (2013).
- de Ronde MWJ, Ruijter JM, Lanfear D *et al.* Practical data handling pipeline improves performance of qPCR-based circulating miRNA measurements. *RNA* 23(5), 811–821 (2017).
- Marabita F, de Candia P, Torri A, Tegnér J, Abrignani S, Rossi RL. Normalization of circulating microRNA expression data obtained by quantitative real-time RT-PCR. *Brief. Bioinform.* 17(2), 204–212 (2016).
- Mestdagh P, Van Vlierberghe P, De Weer A *et al.* A novel and universal method for microRNA RT-qPCR data normalization. *Genome Biol.* 10(6), R64 (2009).
- Chou CH, Shrestha S, Yang CD *et al.* miRTarBase update 2018: a resource for experimentally validated microRNA-target interactions. *Nucleic Acids Res.* 46(D1), D296–D302 (2018).
- Kuleshov MV, Jones MR, Rouillard AD *et al.* Enrichr: a comprehensive gene set enrichment analysis web server 2016 update. *Nucleic Acids Res.* 44(W1), W90–W97 (2016).
- Supek F, Bošnjak M, Škunca N, Šmuc T. REVIGO summarizes and visualizes long lists of gene ontology terms. *PLoS ONE* 6(7), e21800 (2011).
- Ludwig N, Leidinger P, Becker K *et al.* Distribution of miRNA expression across human tissues - PubMed. *Nucleic Acids Res.* 44(8), 3865–3877 (2016).

- 19 Lizio M, Harshbarger J, Shimoji H *et al.* Gateways to the FANTOM5 promoter level mammalian expression atlas. *Genome Biol.* 16(1), 22 (2015).
- 20 Murillo OD, Thistlethwaite W, Rozowsky J *et al.* exRNA atlas analysis reveals distinct extracellular RNA Cargo types and their carriers present across human biofluids. *Cell* 177(2), 463–477.e15 (2019).
- 21 Pawlitzki M, Sweeney-Reed CM, Bittner D *et al.* CSF-progranulin and neurofilament light chain levels in patients with radiologically isolated syndrome-sign of inflammation. *Front. Neurol.* 9, 1075 (2018).
- 22 Okuda DT, Siva A, Kantarci O *et al.* Radiologically isolated syndrome: 5-year risk for an initial clinical event. *PLoS ONE* 9(3), e90509 (2014).
- 23 Gandhi R, Healy B, Gholipour T *et al.* Circulating MicroRNAs as biomarkers for disease staging in multiple sclerosis. *Ann. Neurol.* 73(6), 729–740 (2013).
- 24 Siegel SR, Mackenzie J, Chaplin G, Jablonski NG, Griffiths L. Circulating microRNAs involved in multiple sclerosis. *Mol. Biol. Rep.* 39(5), 6219–6225 (2012).
- 25 McDonald JS, Milosevic D, Reddi HV, Grebe SK, Algeciras-Schimnich A. Analysis of circulating MicroRNA: preanalytical and analytical challenges. *Clin. Chem.* 57(6), 833–840 (2011).
- 26 Wang-Renault S-F, Boudaoud S, Nocturne G *et al.* Deregulation of microRNA expression in purified T and B lymphocytes from patients with primary Sjögren's syndrome. *Ann. Rheum. Dis.* 77(1), 133–140 (2018).
- 27 Columb MO, Atkinson MS. Statistical analysis: sample size and power estimations. *BJA Education* 16(5), 159–161 (2016).
- 28 Wu R, He Q, Chen H *et al.* MicroRNA-448 promotes multiple sclerosis development through induction of Th17 response through targeting protein tyrosine phosphatase non-receptor type 2 (PTPN2). *Biochem. Biophys. Res. Commun.* 486(3), 759–766 (2017).
- 29 Junker A, Krumbholz M, Eisele S *et al.* MicroRNA profiling of multiple sclerosis lesions identifies modulators of the regulatory protein CD47. *Brain* 132(12), 3342–3352 (2009).
- 30 Wang H, Moyano AL, Ma ZZ *et al.* miR-219 Cooperates with miR-338 in myelination and promotes myelin repair in the CNS. *Dev. Cell* 40(6), 566–582.e5 (2017).
- 31 Yang D, Wang WZ, Zhang XM *et al.* MicroRNA expression aberration in Chinese patients with relapsing remitting multiple sclerosis. *J. Mol. Neurosci.* 52(1), 131–137 (2014).
- 32 Martinelli-Boneschi F, Fenoglio C, Brambilla P *et al.* MicroRNA and mRNA expression profile screening in multiple sclerosis patients to unravel novel pathogenic steps and identify potential biomarkers. *Neurosci. Lett.* 508(1), 4–8 (2012).
- 33 Sievers C, Meira M, Hoffmann F, Fontoura P, Kappos L, Lindberg RLP. Altered microRNA expression in B lymphocytes in multiple sclerosis. Towards a better understanding of treatment effects. *Clin. Immunol.* 144(1), 70–79 (2012).
- 34 Keller A, Leidinger P, Lange J *et al.* Multiple sclerosis: microRNA expression profiles accurately differentiate patients with relapsing-remitting disease from healthy controls. *PLoS ONE* 4(10), e7440 (2009).
- 35 Waschbisch A, Atiyya M, Linker RA, Potapov S, Schwab S, Derfuss T. Glatiramer acetate treatment normalizes deregulated microRNA expression in relapsing remitting multiple sclerosis. *PLoS ONE* 6(9), 1–5 (2011).
- 36 Weber JA, Baxter DH, Zhang S *et al.* The microRNA spectrum in 12 body fluids. *Clin. Chem.* 56(11), 1733–1741 (2010).
- 37 Anoop A, Singh PK, Jacob RS, Maji SK. CSF biomarkers for Alzheimer's disease diagnosis. *Int. J. Alzheimers. Dis.* 2010, 606802 (2010).
- 38 Valadi H, Ekström K, Bossios A, Sjöstrand M, Lee JJ, Lötvall JO. Exosome-mediated transfer of mRNAs and microRNAs is a novel mechanism of genetic exchange between cells. *Nat. Cell Biol.* 9(6), 654–659 (2007).
- 39 Zhang Y, Liu D, Chen X *et al.* Secreted monocytic miR-150 enhances targeted endothelial cell migration. *Mol. Cell* 39(1), 133–144 (2010).
- 40 Mycko MP, Baranzini SE. microRNA and exosome profiling in multiple sclerosis. *Mult. Scler. J.* 26(5), 599–604 (2020).
- 41 De Stefano N, Stromillo ML, Rossi F *et al.* Improving the characterization of radiologically isolated syndrome suggestive of multiple sclerosis. *PLoS ONE* 6(4), e19452 (2011).
- **It suggested that RIS subjects could present a more beneficial response to a demyelinating insult than relapsing-remitting multiple sclerosis patients.**
- 42 Cui M, Wang H, Yao X *et al.* Circulating microRNAs in cancer: potential and challenge. *Front. Genet.* 10, 626 (2019).
- 43 Höglund RA, Maghazachi AA. Multiple sclerosis and the role of immune cells. *World J. Exp. Med.* 4(3), 27 (2014).